HYDRO-CLIMATOLOGICAL TREND ANALYSIS AND INFLUENCES ON THE DISCHARGE IN THE ELK RIVER WATERSHED, SOUTHEAST BRITISH COLUMBIA

by

Kristina Simone Anderson

BSc., University of Northern British Columbia, 1999

THESIS SUBMITTED IN PARTIAL FULFILLMENT OF
THE REQUIREMENTS FOR THE DEGREE OF
MASTER OF SCIENCE
IN
NATURAL RESOURCES AND ENVIRONMENTAL STUDIES
(ENVIRONMENTAL SCIENCE)

UNIVERSITY OF NORTHERN BRITISH COLUMBIA

August 2016

Abstract

Hydro-climatological modelling in mountainous environments is difficult due to topographic and climatic variability. Therefore, observed data (1970-2009) were used to assess trends in the Elk River watershed, a region experiencing growth of its open-pit coal mining industry. The Mann-Kendall trend test identified a decrease in snow throughout the watershed, small increase in rain, and overall decrease in northern precipitation. Moreover, mid-basin increase in temperature was detected. An increase in the Fording River winter discharge, counteracted the summer decrease in total watershed discharge from 1970-1989. Linear modelling identified baseflow, precipitation, and atmospheric teleconnection patterns as strong discharge drivers; whereas, the double mass curve identified a precipitation and discharge relationship change starting after 2007. Unfortunately, efforts to incorporate the Soil Water Assessment Tool proved unsuccessful for this watershed. Overall, these hydro-climatological trends were not as synchronized as expected likely due to other variables, such as watershed buffering capabilities and/or land-cover change.

Table of Contents

List of Tables

List of Figures

Glossary

Definitions

Calendar Year: January 1 to December 31

Land Cover: The matter that is covering the earth's surface. This includes both anthropogenic cover (such as buildings, pavement, agricultural fields, etc.) and natural cover (such as forests, water, bare rock, ice, etc.).

Land Use: Anthropogenic activities occurring on the lands surface, often with the intention to obtain benefit from the land resources; such as built environments (i.e. cities), industry (i.e. open-pit mining), linear corridors (i.e. roads) as well as semi-natural environments (i.e. managed forests, lawns, and gardens).

Water Year: October 1 to September 30

{XXXX}: R software packages are identified in the curly brackets

Acronyms

α: alpha

AO: Arctic Oscillation

BF: Baseflow

cms: cubic metres per second

Crk: Creek

CV: Coefficient of variation

Disch: Discharge

EC or ECCC: Environment and Climate Change Canada

Elev: Elevation

ENSO: El Niño/Southern Oscillation

ERW: Elk River Watershed

Freq: Frequency

GAM: Generalized Additive Model

GAMM: Generalized Additive Mixed Model

GLM: Generalized Linear Model

GLMM: Generalized Linear Mixed Model

GLS: Generalized Least Squares

IQR: Interquartile Range

KDE: Kernel Density Estimation

Lat.: Latitude (°N)

LM: Linear Model

Long.: Longitude (°W)

LULC: Land use land cover

masl: metres above sea level

MK: Mann-Kendall

NP: North Pacific pattern

NSR: Non statistically relevant

PDO: Pacific Decadal Oscillation

POR: Period of Record

Precip or Prcp: Precipitation

Q: Discharge

SD: Standard Deviation

SR: Statistically relevant

SWAT: Soil Water Assessment Tool

SWE: Snow Water Equivalent

τ: *tau* (Kendall)

Teck: Teck Coal Limited

Temp: Temperature

TS: Theil Sen slope estimator

μ: mean

WSC: Water Survey of Canada

Yrs: years

Water Survey of Canada hydrometric monitoring stations

002: WSC station 08NK002

005: WSC station 08NK005

016: WSC station 08NK016

018: WSC station 08NK018

021: WSC station 08NK021

022: WSC station 08NK022

027: WSC station 08NK027

Environment and Climate Change Canada climate monitoring stations

282: ECCC station 1153282

402: ECCC station 1155402

630: ECCC station 1157630

653: ECCC station 1152653

670: ECCC station 1152670

690: ECCC station 1150690

850: ECCC station 1152850

898: ECCC station 1152898

899: ECCC station 1152899

915: ECCC station 1151915

Acknowledgements

"The journey of a thousand miles begins with one step"

Lao Tzu

The support I have received over the years from so many has been remarkable. I am forever grateful for the many long conversations, continued strength, and patience as I try yet another approach to find the answers. My friends and family have stood by me through it all, stepping in when the chips were down and there to celebrate as things improved. A special thank you to Adam, Adrian, Ali, Andria, Anne, Becky, Claire, Daniel, Don, Donna, Faye, Gretchen, John, Kim, Leanne, Marie-Claire, Marnie, Michael, Michele, Melanie, Naomi, Nicola, Paddy, Spence, Tara, Tammy, Tiffany, and of course Kianna, Gabby and Sadie.

I remain ever indebted to my supervisor Dr. Phil Owens, and my committee members Dr. Stephen Déry and Dr. John Rex. Your guidance, knowledge and enthusiasm has been inspiring; strengthening my desire to continue learning and exchanging knowledge.

As a recipient of the Pacific Leaders Scholarship for Public Servants, I am grateful to the B.C. provincial government for providing the financial support for my tuition and books during my time as a Master's student.

1 Introduction

The hydrological impacts due to changes in climate as well as land use and land cover (LULC) have been reported worldwide. A good defense against possible ecological degradation and negative health outcomes associated with these hydrological impacts, is a proactive approach based on current understanding of what has happened and forecasting future effects (Palmer, et al., 2008). This research provides the foundation for a proactive management approach for the Elk River watershed (ERW) by identifying current hydro-climatological trends and hydrological influences.

The hydrological shifts arising from climatological and LULC changes can vary both in space and time. Moreover, the climate and discharge in mountainous regions can be more difficult to model partly due to the presence of micro-climates and watershed response variability associated with changes in topography and elevation (Brahney, 2014). In general, temperature and precipitation changes can affect the timing of peak flows and water quantity (Maidment, 1993; Ward & Trimble, 2004; Jones, 2011; Hatcher & Jones, 2013) as well as the frequency and volume of extreme events (Katz & Brown, 1992; Schaeffer, Selten, & Opsteegh, 2005). Land cover change can affect water retention, snow accumulation and snow melt; in turn, affecting both the timing and volume of the regional discharge (Dingman, 2002; Ward & Trimble, 2004). To complicate matters, the hydrological response from a change in climate and/or LULC may not become immediately apparent due to the watershed's natural buffering capability, sometimes the response can take years to manifest. Should this be the case, once

the response has become visible, it could take years of persistent effort to lessen the negative response (Fleckenstein, Anderson, Fogg, & Mount, 2004; Chhabr & Geist, 2006).

Why should a change in climate or LULC affect how watershed management planning is conducted? As Zhang et al. (2000) outline, even the slightest changes in climate can have a large effect on our surroundings. When increased urbanization, river channel constriction and water requirements are all present in one area, the cumulative effects are amplified and can affect the ecological integrity and buffering capabilities of the hydrological systems (Poff, et al., 1997; Palmer, et al., 2008; Owrangi, Lannigan, & Simonovic, 2014). The potential for an increase in the occurrence of extreme events is high (Canada, 2010), with many areas in the world experiencing water shortages (Palmer, et al., 2008), including parts of British Columbia (BC) (Schnorbus & Rodenhuis, 2010; Zwiers, Schnorbus, & Maruszeczka, 2011; Owrangi, Lannigan, & Simonovic, 2014). In the summer of 2015, BC experienced a drought affecting most of the province. For the Kootenay region, this low-water event was due to a combination of early snowmelt and reduced spring rains, which impacted community drinking water systems, water allocation allotments, fisheries, agriculture, industry, tourism, and with the reduced surface water presence, the area exhibited an increased potential for forest fires. This event was in stark contrast to the flood of 2013 in the East Kootenay region where the Elk River discharge was reported to be a >1:200 year event (Northwest Hydraulic Consultants Ltd., 2006) resulting in extensive flooding, evacuations and property damage. Understanding changes in the climatic patterns, the natural buffering mechanisms within the ERW, and how the discharge volume and frequency is affected, helps support informed policy making for water resources.

The province of BC has made a large step forward with the enactment of the *Water Sustainability Act*, allowing for the provincial monitoring and regulation of groundwater[1] and required consideration of environmental flows (Hatfield, Lewis, & Ohlson, 2003) for all permitting decisions. The ability of a drainage basin to store water (a.k.a. groundwater) is often a strong component of the buffer capabilities of that watershed. A surface water river system will often fluctuate between functioning as a gaining system (water provided from the groundwater source to recharge the surface water source) and a losing system (water provided from the surface water source to recharge the groundwater source), a process that supports the year-round presence of water in many of the streams in BC. If the groundwater source is reduced and not adequately replenished – which could occur from groundwater pumping, hardening of the river channels and land disturbance – the buffering capabilities of the stream could be affected (Fleckenstein, Anderson, Fogg, & Mount, 2004). Hydro-climatological trend analysis allows for the review of associated variables, how the variables are changing over time, and how one variable (i.e. climate) might be influencing the other (i.e. discharge). No change in the discharge levels during a period of change in climate variable could be interpreted as the discharge continues to be controlled by the buffering capabilities of the watershed[2]. Whereas, a change in the discharge may indicate that the change has exceeded the limits of the watershed's buffering capabilities designed to naturally lessen the effects from the change. Understanding the stream's ability to buffer for environmental changes (climate

[1] Having the capacity to understand the groundwater pressures in a region is an important component towards the regulator's ability to understand the implications of current and/or future effects on the region's water quantity and quality.

[2] When the presence of LULC change is not producing a hydrological response that is counteracting the hydrological response resulting from the change in climate.

and/or LULC) can enable society to minimize the destructive effects from extreme hydrological events. This information could help determine whether a dam should be constructed on one river rather than another, where the constricting of river channels would have a reduced effect on the stream's processes, and the quantity of water withdrawal that can occur from both surface and groundwater sources before the environmental flows are affected. Moreover, understanding where the threshold is with regards to a watershed's natural buffering capacity is an important component for understanding potential effects associated with proposed LULC and climate change.

1.1 Columbia Basin and the Elk River Watershed

Over the past 50 years, the ERW has undergone many changes in LULC tied both to mining and forestry (Schreier, 2012; Hansen, et al., 2013; Lemly, 2014; Godkin, 2015). Two communities, Sparwood and Elkford, were established in the last 45 years to support the growing number of coal mine employees. Due to the mountainous nature of this watershed, the communities are situated in the valley close to the Elk River, and the ERW's largest community, Fernie, has been partially constructed below the Elk River's 1:200 year flood level (Northwest Hydraulic Consultants Ltd., 2006). There are a number of open-pit mine expansions both in the planning and construction stages located in the northern half of the ERW (Katay, 2014).

Recently, the ERW has become an area of keen interest for a variety of reasons: (i) water quality concerns associated with a high selenium release from coal mining; (ii) proposed and approved coal mine expansions; and (iii) the 2013 high water event that caused significant

flooding in the valley. In July of 2012, Teck Resources Limited[3] (Teck) and the Ktunaxa Nation Council initiated the first multi-stakeholder workshop focused on investigating the cumulative effects from disturbances within the ERW, thus beginning the Elk Valley Cumulative Effects Management Framework (CEMF). In light of water quality concerns, on April 15, 2013, a Ministerial Order No. M113 was issued to Teck under Section 89 *Environmental Management Act* (Lake, 2013) requiring Teck to prepare an "Elk Valley Area Based Management Plan" (Teck Coal Ltd, 2013) prior to the authorization of any further mine expansions. By the fall of 2014, the BC Ministry of Forests, Lands and Natural Resource Operations (MFLNRO) took over leadership of the CEMF, which now involves 14 groups including First Nations, government, municipalities, forestry companies, mining companies, and non-governmental organizations. CEMF's objective is to find a sustainable solution towards resource management in the ERW. The McMaster University Watershed Hydrology Group, under support from Teck, is currently examining the influence of surface coal mining on the hydrological systems within the ERW (Shatilla, 2013; Wellen, Shatilla, & Carey, 2015). The desire to understand the effects and interaction of both anthropogenic and natural events on the ERW has become an important focus for many (Teck Coal Ltd, 2013; Wellen, Shatilla, & Carey, 2015); and for the local Elk Valley residents, people's livelihoods depend on it.

There have been a number of hydrological reviews completed in the ERW over the years (Obedkoff, 1985; Coulson & Obedkoff, 1998; Northwest Hydraulic Consultants Ltd., 2006; Brahney, 2014). Moreover, there have been numerous reports on the expected climate change for the Columbia Basin (Jost & Weber, 2012; Murdock & Soble, 2013; Brahney, 2014), the

[3] There have been a few official names for the mining industry currently being managed by Teck over the past 20 years which include: Elk Valley Coal, Teck Cominco, Teck Resources Limited and Teck Coal Limited.

effects of climate change on the streamflow (Jones, 2011; Hatcher & Jones, 2013) and land use change in the Columbia Basin (Matheussen, Kirschbaum, Goodman, O'Donnell, & Lettenmaier, 2000; VanShaar, Haddeland, & Lettenmaier, 2002; Lemly, 2014; Wellen, Shatilla, & Carey, 2015). The Columbia Basin Trust engaged the University of British Columbia Okanagan (UBCO) to: (i) complete a hydrological assessment of the Columbia Basin; (ii) undertake an in-depth examination of the state of the Columbia Basin's water quantity and quality; (iii) identify knowledge gaps; and (iv) provide recommendations for future undertakings (Brahney, 2014). Through this research Brahney (2014) corroborates the findings of an overall increase in temperature (>1.0°C) in the last 100 years in the Columbia Basin and a shift in the snow/rain ratio, with more rain falling than snow. The Pacific Decadal Oscillation (PDO) and El Niño Southern Oscillation (ENSO) proved to be important influences on the Columbia Basin's hydro-climatological components, as is often found to be the case in the Rocky Mountain region (Schoennagel, Veblen, Romme, Sibold, & Cook, 2005; Wei & Zhang, 2010). Groundwater information was found to be lacking for the Columbia Basin, so findings consisted of general statements of the groundwater's importance with regards to water temperature and sustaining the stream's baseflow; however, findings did show that the groundwater contributions were generally small and most important during the late summer and winter periods. With the forecasted change in climate, it is suspected that there will be an increase in the ecological role that groundwater plays. Additionally, a lack of information was identified for the mountainous and higher elevation regions, again culminating in an inability to form definite conclusions.

1.2 Regional Hydro-Climatological Changes

Hydro-climatological change has been identified locally, regionally, nationally and globally (Schindler, 2001; Schnorbus & Rodenhuis, 2010; Floury, Delattre, Ormerod, & Souchon, 2012). A change in discharge is predicted for all river systems in Canadian populated areas based on recognized climate projection modelling and anthropogenic activities (Palmer, et al., 2008; Canada, 2010). Over the past century, North American streams have shown an earlier shift in the timing of freshet and centre volume of flow (Burn 1994, Brahney 2014). The increase in high (flooding) and low (drought) hydrological extreme events have been observed in many parts of Canada, although the pattern is often inconsistent as they are affected by localized events and influenced from shifting hydrological processes (Canada, 2010). Climate and hydrological changes have been identified for BC throughout the past half century, as well as a warmer and wetter climate throughout Canada (Zhang, Harvey, Hogg, & Yuzyk, 2001; Schnorbus & Rodenhuis, 2010), an increase in discharge during the winter in the northern basins (Burn, Abdul Aziz, & Pietroniro, 2004) and a reduction in ice and glacial coverage (Rodenhuis, Bennett, Werner, Murdock, & Bronaugh, 2007; Canada, 2010). An average temperature increase of ~ 0.7°C in BC, as identified between 1990 and 2000, has resulted in both economic and ecological effects (Hamann & Wang, 2006). The environment's natural ability to cushion the effects on the discharge from these climatic changes, described in Section 1.1 as buffering, can be lost as the magnitude of the change increases and compounds. This compound, or cumulative effect, can be felt in a watershed that is experiencing both LULC and climate change.

In the Columbia Basin, southern BC, there has been an increase in temperature of 1.2°C to 2.0°C over the past 100 years (Brahney, 2014). In other regions of BC, negative temperature trends have been recorded, likely a result of the influence from atmospheric teleconnection patterns (Rodenhuis, Bennett, Werner, Murdock, & Bronaugh, 2007). A loss of snowpack and glacial coverage has been observed over the past century, as well as the spring runoff has been occurring 10 to 30 days earlier in snow-dominated watersheds (Rodenhuis, Bennett, Werner, Murdock, & Bronaugh, 2007). Throughout BC, the mean annual discharge has decreased in watersheds located at lower elevations, and in those that have lost their glacial influence; futhermore, a decrease in the minimum daily average discharge has been reported (Rodenhuis, Bennett, Werner, Murdock, & Bronaugh, 2007). Climatic studies within the Columbia Basin and Kootenay Boundary region report that an increase in air temperature and precipitation should be expected (Jost & Weber, 2012; Murdock & Soble, 2013) and by the 2050s the region is expected to see an increase, based on normalized conditions, from 0.8°C to 3.5°C in the winter and 1.9°C to 5.0°C in the summer period regardless of the model or emission scenario used (Zwiers, Schnorbus, & Maruszeczka, 2011). In the same region, a projected incease in precipitation is also expected by 2050 (compared to climate normals from 1971-2000) of 1% to 9% (Murdock & Spittlehouse, 2011). Based on median normals from 1961 to 1990, an increase in the discharge for the upper Columbia River basin is forecased to be between 3% to 19% (median normals for 2041 to 2070) based on the location and drainage size of the individual streams (Zwiers, Schnorbus, & Maruszeczka, 2011). Other studies project (by 2050) a reduction of discharge from 10% to 25% during the dry season (Rodenhuis, Bennett, Werner, Murdock, & Bronaugh, 2007). In addition, it is projected that the Upper Columbia region will experience higher late autumn and winter flows, earlier spring freshet, higher

discharge during spring and early summer, followed by a reduction in the discharge (compared to current mean levels) during the late summer and early autumn periods (Brahney, 2014).

The effects of LULC change has the ability to considerably affect streamflow. The loss of vegetation, such as by fire or logging, often results in an increase in snow accumulation, increase in peak flows and decrease in evapotranspiration (Matheussen, Kirschbaum, Goodman, O'Donnell, & Lettenmaier, 2000). Due to a strong forest presence in the headwaters of the Columbia Basin, it is anticiptated that should the vegetation cover continue to be reduced while increasing impermeable surfaces, the hydrological response would likely manifest as an earlier spring freshet, increased freshet magnitude and earlier onset of summer low flows within the next century. Thresholds associated with vegetation loss and its affects on the hydrological response is outlined in Stednick (1996), while Blöschl et al. (2007) describe the impact on the discharge by chatchment size of both land use land cover change and climate change.

1.3 Research Focus and Relevance

In support of the recent considerations regarding cumulative effects in the northeast corner of the Columbia Basin, efforts to improve our understanding of the historical, present and future environmental parameter trends and influences are needed (Brahney, 2014). Along with recent authorized open-pit mine expansions in the Fording River watershed, and additional mine expansions applications in review, understanding the buffer capabilities, implications and effects from climate and LULC change in the ERW provides tools in support of a sustainable and comprehensive management resource plan.

There are many processes involved when considering the effects of climate and LULC change on local hydrological systems, and many questions remain to be answered (DeFries & Eshleman, 2004; Hundecha & Bardossy, 2004; Tong, Sun, Ranatunga, He, & Yang, 2012; Schilling, et al., 2013; Wang, Yang, Wang, Xu, & Xue, 2014). The involvement of hydrological modelling and experimental watersheds has assisted significantly in understanding the effects of natural events, vegetative cover and hydrological processes (DeFries & Eshleman, 2004). Blösch et al. (2007) reference two approached to addressing hydrological impacts from climate and LULC change: (1) modelling and (2) trend analysis. It is anticipated that when these two methods are used together, a more comprehensive analysis can be established. This research is located in a nival mountainous regime, in a mostly forested watershed of the Columbia River Basin, an important transboundary watershed with considerable LULC change forecasted for the area (Katay, 2014).

Identifying the trends and variables contributing to water quantity (discharge) allows for a better ability to predict and prepare for extreme water events, development and water use requirements. The relationships between the hydrological and climatological parameters can provide the scientific baseline towards developing adaptive and area management practices in a defensible and sustainable manner. This research relies on 10 climate monitoring stations and seven discharge monitoring stations in the ERW (Figure A-1). Focus has been placed on three Water Survey of Canada discharge monitoring stations (referred to as discharge research stations) and two Environment and Climate Change Canada (EC) climate stations (referred to as climate research stations) in the ERW (Figure A-2) for in-depth hydro-climatological

analysis. Attention has been placed on analyzing periodic influences on the local discharge, identifying what variables are most influential on the discharge, and forecasting the stream discharge based on the projected change in climate and LULC over the next eight decades. There are many variables that could influence stream discharge, and this research will focus on the climatic parameters from the climate research stations, with consideration of other influences. It is anticipated that the methodologies and insights outlined in this research can be transferred to other similar watersheds throughout the Columbia Basin and elsewhere.

1.4 Research Questions

1) Is there a trend in discharge, precipitation and temperature over the past 40 years in the mid to upper portion of the ERW?
2) If there is a trend in discharge, can this trend be correlated to the climatic (precipitation and temperature) trends? Which climatic parameters have the most influence on the discharge? What other factors might influence the discharge in the ERW?
3) What will be the effect on the Elk River discharge of anticipated LULC[4] change and/or climate change[5] over the next 80 years? Is there a threshold for land cover change given a set of climate scenarios? Does this differ based on the location within the watershed?

[4] LULC based on location and estimates outlined by Katay (2014), within boundaries of the mine's authorized areas.
[5] Based on Regional Climate Model estimates outlined by PCIC (Murdock & Spittlehouse, 2011).

To address the aforementioned questions in the form of testable hypotheses, the following statements were developed:

1) H_O = There is no trend in discharge from the discharge research stations from 1970 to 2009.

   H_A = There is a trend in discharge from any or all of the discharge research stations from 1970 to 2009.

   H_O = There is no trend in precipitation from the climate research stations from 1970 to 2009.

   H_A = There is a trend in precipitation from either of the climate research stations from 1970 to 2009.

   H_O = There is no trend in temperature from the climate research stations from 1970 to 2009.

   H_A = There is a trend in temperature from either of the climate research stations from 1970 to 2009.

2) H_O = There is no correlation between the trend in discharge and the climate parameter trends for either precipitation or temperature.

   H_A = There is a correlation between the trend in discharge and the climate parameter trends for either precipitation and/or temperature.

3) H_O = There will be no change in discharge due to LULC and climate change over the next 80 years.

   H_A = There will be a change in discharge due to LULC and climate change over the next 80 years.

   H_O = There will be no change in discharge due to LULC over the next 80 years.

   H_A = There will be a change in discharge due to LULC over the next 80 years.

   H_O = There will be no change in discharge due to climate change over the next 80 years.

   H_A = There will be a change in discharge due to climate change over the next 80 years.

The Mann-Kendall trend analysis and associated Theil Sen slope estimator were used to answer question 1. Question 2 was addressed through a variety of methodologies that included analysis based on parametric and non-parametric correlation, generalized linear models and double mass curves. The hydrological model Soil Water Assessment Tool (SWAT) was applied to address question 3. In the course of answering question 3, it became apparent that SWAT was not able to effectively model the ERW, possibly due to the difficulty of modelling in a mountainous watershed compounded by the fact that ERW is largely forested and located in a snow-dominated region. Consequently, this research project was adjusted to focus on questions 1 and 2, examining the hydrological and climatological trends in the mid to upper portion of the ERW from 1970 to 2009 and the influence of the climatic variables on the discharge. However, the limited outcome of the SWAT modelling exercise is still presented

and discussed, as there are useful lessons to be learnt. Further investigation into appropriate model options is encouraged.

2 Literature Review

This Chapter will describe the techniques used to address the research questions identified in Section 1.4. A review of select hydro-climatological assessment tools, which includes a review of the Soil Water Assessment Tool (SWAT) hydrological model, is provided below.

2.1 Hydro-Climatological Assessment Tools

2.1.1 Trend Analysis

Trend analysis on hydrometric and climatological time series data has been the focus of many research projects and is ever adjusting as new information is discovered. The Mann-Kendall analysis is a well-used technique for monotonic trend determination in hydrological research, because there are a reduced number of assumptions to meet compared to the parametric (i.e. linear regression) options (Zhang & Zwiers, 2004; Déry, Hernandez-Henriquez, Owens, Parkes, & Petticrew, 2012; Brahney, 2014). With these trend analysis options, serial correlation must be removed prior to the analysis, otherwise the potential of a type I error (i.e. false positives) increases significantly (Helsel & Hirsch, 2002; Zhang & Zwiers, 2004). Autocorrelation (also known as serial correlation) occurs when a data value shows a likeness between itself and a lagged version of itself over repetitive time periods within a time series; a common occurrence in climatic and hydrological time series data. There are two frequently used pre-whitening techniques to address this auto correlation: (1) Yue, Pilon, Phinney and Cavadias (2002) and (2) Zhang, Vincent, Hogg and Niitsoo (2000), referred to herein as the Yue et al. (2002) and Zhang et al. (2000) approaches, respectively. The Pacific Climate Impacts Consortium (PCIC) built the R package {zyp} (Bronaugh & Werner, 2013) to support

trend analysis using the Mann-Kendall and Theil Sen slope estimator for climatic and hydrological time series data. Meeting the need to remove serial correlation (lag-1) from the dataset, {zyp} has been coded to pre-whiten the data prior to running the Mann-Kendall test and associated Theil Sen estimator using either the Yue et al. (2002) or Zhang et al. (2000) approaches.

The Yue et al. (2002) and Zhang et al. (2000) approaches differ slightly, with the Yue et al. (2002) first testing for a trend using the Theil Sen analysis. If no trend is found then no further pre-whitening or trend analysis is computed. If a trend is found then the time series is de-trended, and auto-regression (AR) 1 is performed on the outputs. The dataset is de-trended first since pre-whitening without first removing the linear trend, such as in the Monte Carlo procedure, can influence the Mann-Kendall statistic. The Mann-Kendall is then calculated on the residuals. The Zhang et al. (2000) approach removes the trend and tests for serial correlation. If serial correlation exists, the Zhang et al. (2000) approach pre-whitens the data repeatedly until the slope estimates and the AR in two passes is <1%. Once the serial correlation has been removed, the Mann-Kendall test and associated Theil Sen slope estimator are applied.

The debate continues with regards to whether pre-whitening can increase the potential of a type II error (i.e. false reduction of trend presence) when used on larger data sets (Yue & Wang, 2002; Bayazit & Onoz, 2007; Blain, 2013). Reviewing the claim that pre-whitening large datasets prior to using the Mann-Kendall trend test may in fact reduce the power or sensitivity of the test, Zhang and Zwiers (2004) agreed that pre-whitening reduced the significance of a

trend. However, they also cautioned against using the Mann-Kendall test on serially correlated data of any size. Bayazit and Onoz (2007) investigated the point where the benefit outweighs the negative effects of pre-whitening on serially correlated data prior to trend analysis, and vice versa. They found that trend analysis on datasets showing a (i) very low coefficient of variation, (ii) obvious slope trend and (iii) a large sample size appears to be negatively influenced (also known as type II errors) by the pre-whitening process. However, for datasets where the test does not have a high power, the pre-whitening process is necessary to reduce the potential of type I errors, which is of higher concern for this type of data series than the potential of type II errors developing from the pre-whitening process. Removing the serial correlation through other means such as adjusting timelines (annual means), transforming the data or calculating a moving average can remove the presence of serial correlation thereby eliminating the need for pre-whitening. However, these procedures also change the details of the data set, so the outputs would be adjusted accordingly.

2.1.2 Linear Models

"Essentially, all models are wrong, but some are useful."

George Box, British mathematician and statistician

The use of linear models (LM) allows for the interpretation of explanatory variables on a response variable. The many variations of the LM include: generalized linear models (GLM), generalized additive models (GAM), generalized least square (GLS), generalized linear mixed models (GLMM) and generalized additive mixed models (GAMM). These models are designed to accommodate different types of datasets such as count data, time series, non-

normal distribution, nested data, temporal correlation, spatial correlation, heterogeneity, random effects and/or repeated measurements (Zuur, Ieno, Walker, Saveliev, & Smith, 2009). These models are designed to include components (such as correlation structures, random effects) that are impossible to include in simple linear regression models. The advantage of using a GLS over the ordinary least squares (OLS) estimator is that the GLS has the ability to manage different parameter record lengths, variation among sample sites and cross correlation. The LM supports the basic multiple regression with a response variable showing normal distribution. The GLS model builds off of the LM, allowing correlated structures, which accounts for the existence of autocorrelation and heterogeneity, yet still relying on the normal distribution of the response variable.

Often there is a hesitation in using linear regression analysis with hydrological and climatological data due to the apparent difficulty for these datasets to meet the linear regression assumptions. Zuur et al. (2007) outline tools to apply different variations of GLM to these data type, along with interpreting the outputs to ensure that the residuals have met the regression assumptions. Hydrological analysis using the GLS and GLMs has been more often associated with the assessment of high flows, extreme events, quantiles and climatic influences on discharge (Griffis & Stedinger, 2007; Floury, Delattre, Ormerod, & Souchon, 2012). Floury et al. (2012) chose to rely on trend analysis and GLMs for their multi-parametric study designed to assess the varying influences associated with a declining discharge and increasing water temperature in the Loire River, France. First looking at the climatic and hydrological trends, a GLM was then used to determine the influence of land management, climate variability and other environmental factors on the river.

2.1.3 Frequency Analysis

Magnitude and frequency analysis has been an established component in climate research as this type of analysis looks at both the location and scale parameters of the climate variables, including the shape of the distribution (Katz R. W., 1993). It has been shown that relying on time series trend analysis alone can provide the researcher with a limited view of the broad changes occurring in a watershed when the discharge may be influenced by LULC change and/or climatic variability (Schaeffer, Selten, & Opsteegh, 2005; Green & Alila, 2012). Monitoring changes in extreme events - intensity, frequency, volume - provides essential information for identifying climate changes, rather than deriving the analysis from computations based on the means (Katz & Brown, 1992). The frequency of extreme events can be compared/explained more closely by the change in the variability of the event (scale parameter), which becomes proportionally greater as the extreme event increases in magnitude, than by the overall average change of the station's annual mean (location parameter). This can also be explained by the change in the standard deviation, which would change as the frequency and magnitude of extreme low and high events are increased. The occurrence of extreme events can cause a change to the local environment, including mass flooding, bedload movement, channel relocation, erosion, accretion and avulsions. The change can happen quickly, or take years to manifest. The slight change in a mean annual value may not coincide with the changes resulting from significant variability in the extreme events. Lessening the effects from extreme events is equally as important; understanding the hydrograph characteristics, such as the shape of the rising and falling limbs, location of the peak, is necessary to understand the cause and associated costs (Schaeffer, Selten, & Opsteegh, 2005; Coulthard, Smith, & Meko, 2016). As it is often the occurrence of extreme events that cause

society and environmental concerns, it is important to gain a clear understanding of changing to the frequency and/or magnitude of these events so that we can enhance our land and natural resource management decisions.

2.2 SWAT Model Review

A hydrological model can be designed to simulate many hydrological characteristics including infiltration, evapotranspiration, interception, snowmelt, groundwater flow, overland flow and stream flow. Models can be used to predict[6] or forecast[7] the hydrological information. There have been many different hydrological models designed throughout the world and these can be categorized based on their temporal representation, simulation basis, method of solution, etc. For individual groupings within these categories refer to Dingman (2002). Spatial representation is another common model category, it refers to whether the model is lumped or distributed. A lumped model represents the watershed as one point, so the soils, land cover and topography would consist of only one type. A distributed model breaks down the watershed into sub-basins and hydrologic response unit (HRU) categories and each HRU has its own classification for soils, vegetation, land cover and topography. Since the distributed model is capable of incorporating many diverse watershed characteristics it can provide the user with a more detailed response (Carpenter & Georgakakos, 2006; Beckers, et al., 2009; Beckers, Smerdon, & Wilson, 2009). However, many watersheds lack the input data required for a distributed model and without detailed input data, the additional complexity of this model is no longer of any value.

[6] A model used to predict the hydrological information would be providing data for a period greater than 1 day into the future.
[7] A model used to forecast the hydrological information would be providing data within approximately a 24 hour period.

Selecting a model to use for a research project is influenced by many different factors including: cost, technical support, availability, field of specialty, input variables, outputs, etc. The basis for choosing one model over another varies for each project and researcher. The criteria for model functionality in this research were:

- Outputs supporting the hydrological requirements of the project;
- Data collected were able to support the model input requirements;
- Capability of accepting differing LULC information within the sub-basins;
- Suitability for mountainous environments;
- Inclusion of a snow/glacier component;
- Strong technical support system; and
- Open source.

The hydrological model SWAT (Soil Water Assessment Tool) met most of the aforementioned criteria, and was chosen to be used in support of research question 3, outlined in Section 1.4. The following provides a brief description of the model, areas of use, field of specialty and identified limitations.

The SWAT model is a semi-distributed model that has been classified as highly complex by Beckers, Smerdon and Wilson (2009). SWAT is designed to predict what impacts may occur from environmental and anthropogenic activities on the water, sediment and agricultural chemical yields within a watershed (Gassman, Reyes, Green, & Arnold, 2007).

To improve on accuracy, the SWAT model separates the watershed into sub-watersheds and further into homogeneous parcels (i.e. HRUs) containing the same land use and soil characteristics. SWAT supports shallow groundwater movement in both directions, but considers that the water recharging deep aquifers will not resurface during the life of the model, so this component was not included in the model calculations. SWAT can simulate the following hydrologic processes: canopy storage, surface runoff, infiltration, evapotranspiration, lateral flow, tile drainage, redistribution of water within the soil profile, return flows, recharge by seepage from surface water bodies, ponds, tributary channels and consumptive use through pumping (Arnold, et al., 2012). SWAT differentiates between annual and perennial vegetation, using a single plant growth model to simulate vegetation growth and allows each HRU to be defined within a separate management practice.

The inputs required for the SWAT model include: daily precipitation, maximum and minimum air temperature, solar radiation, wind speed and relative humidity, digital elevation models, soils, and land cover. The outputs consist of: full hydrograph, annual yield, peak flow, low flow, snow water equivalent (snow cover), evapotranspiration, water balance (for soil columns and/or basin), soil moisture, infiltration, water table depth, overland flow, shallow subsurface flow, groundwater flow (baseflow), basin total runoff, soil erosion, sediment fluxes, nutrient fluxes, and water quality (Beckers, Smerdon, & Wilson, 2009). SWAT is capable of simulating nutrient cycling, sediment yield and pesticide movement through land-water systems. Based on Neitsch et al. (2005) SWAT is best suited for gradual terrain with a strong groundwater support to the water systems and forested landscapes. In response to the reputation that SWAT may not be strong in mountainous and glacial terrain, researchers have

worked at testing its capabilities within these types of environments, finding that through calibration this model proved to work effectively in these environments (Rahman, et al., 2012; Shope, et al., 2014).

The limitations of the SWAT model include the fact that it is not designed to interpret rain-on-snow events, and road hydrology, and does not have a glacier component. It is semi-distributed, rather than distributed, so the HRU process can eliminate small details, such as wetlands or riparian buffers, within its boundaries as the dominant characteristics will be used for the model calculations. This is a standard limitation with all semi-distributed models. In addition, there have been some reported concerns with how the model represents discharge during baseflow periods (Krysanova & Arnold, 2008). Despite these restrictions, it was selected as the model to use in this research because the limitations appeared to be largely manageable through the calibration process. There is a strong water withdrawal component allowing for multiple water withdrawals, and set up and calibration support was available at UNBC.

3 Study Area

3.1 Introduction

In the 1870s a coal seam was discovered in the Crowsnest pass[8]. The first mine was producing coal by the late 1890s followed closely by the construction of the Canadian Pacific Railway and a flourishing forestry industry. In April 1904, a major fire devastated the forests, and a second fire, in 1908 engulfed much of the City of Fernie. The City of Fernie was rebuilt within two years and supported a population of 6,000[9]. The coal industry remains a backbone of the Elk Valley's economy to this day, with the two communities Sparwood and Elkford[10] being developed in support of the mining. In the late 1960s, tourism started to gain some momentum with the building of the Fernie ski hill and by 1998 it had doubled in size due to a substantial increase in tourism. Fernie now has over 300,000 visitors to the local ski regions every winter.

3.1.1 Site Characterization

The Elk River is 220 km long and is located in southeastern BC. The ERW is located in the transnational Columbia River Basin (CRB), specifically in the southeast corner of the Canadian side of the CRB (Figure 3-1). The Canadian portion of the CRB is 101,000 km^2, which constitutes ~ 15% of the entire CRB land mass at 674,000 km^2 (Carver, 2013). Incorporating a significant portion of the CRB headwaters, the Canadian portion supplies 40% of the runoff for the Columbia River system (Columbia Basin Trust, 2013). As a result, what

[8] The historical information for the town of Fernie was sourced from the Fernie Museum (Fernie Museum, nd).
[9] Based on the 2011 Census, the population of Fernie is 4,811.
[10] Based on the 2011 Census, the population of Sparwood is 4,200, and the population of Elkford is 2,523.

happens in these headwaters can have a large effect on the entire basin, and is thus of considerable regional, national and international interest and importance.

The Canadian portion of the Rocky Mountains is classified into four ranges: Border, Kootenay Pass, Continental and Hart. The Elk River drainage is located within the Continental Ranges and the Border Range to the south, feeding into the Rocky Mountain Trench. The Rocky Mountains consist mostly of sedimentary and metamorphic rock, predominantly limestone, quartzites, schists and slates. Located between latitude 48.915° N and 50.591°N, and longitude 115.219°W and 114.569°W, the ERW covers ~4,500 km^2 with an elevation range from 745 m at Lake Koocanusa to 3,450 m at the top of Mount Joffre (Figure A-3); a mean watershed elevation of 1790 m (SD = 382 m). An overview of the ERW with the mountainous topography of BC to the west and the flatter topography of Alberta to the east is shown in Figure 3-2. The ERW extends across the US-Canada border and just to the west of the Flathead River drainage, a designated heritage site by UNESCO (United Nations Educational, Scientific and Cultural Organization) World Heritage Committee in 2010.

Figure 3-1. The Columbia River Basin; area highlighted in red identifies the location of the Elk River Watershed.

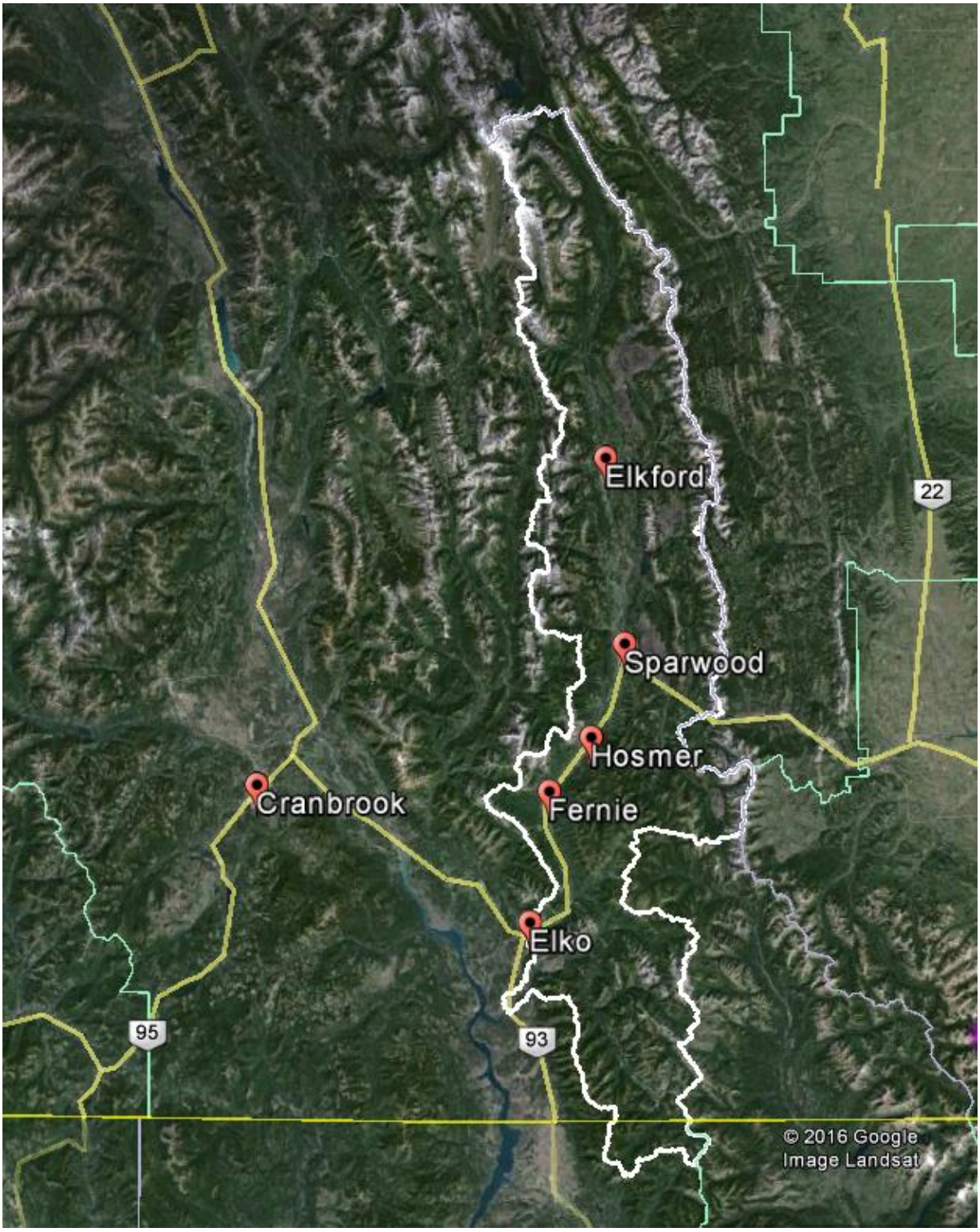

Figure 3-2. Overview of the Elk River Watershed (white boundary) and the local communities. The yellow lines represent main highways in the region. Google Earth image 2016.

The Elk River valley is orientated in a north – south direction with rugged mountains on either side; resulting in the tendency towards an east and, slightly more prominent, west aspects throughout the watershed (Figures A-4 and A-5). The majority of the slope angles are between 15° and 35°, with a mean watershed slope angle of 22.5° (Figure A-6). Based on the BC Provincial government mapping layers, there is approximately 10.5 km^2 of glacial coverage located in the most northern region (Figure A-2). The four largest glaciers in the watershed include Petain and Castelnau Glacier (5.0 km^2), Abruzzi Glacier (2.6 km^2) and Elk Glacier (1.0 km^2). In addition, 3.3 km^2 of land is covered by icefields. There are five main tributaries to the Elk River, from north to south: Fording River, Michel Creek, Coal Creek, Lizard Creek and Wigwam River. Obedkoff (1985) identified a north/south climatological (precipitation) division located between the Michel and Coal Creek systems. The precipitation for the northern portion of the watershed[11] varies between ~510-700 mm yr^{-1}, based on precipitation data from 1970 to 2009, with the amount of precipitation higher on the west side of the mountains compared to the east side, as well as an increase in precipitation as the elevation increases. The middle zone of the watershed shows a higher precipitation, averaging between 1020-1330 mm yr^{-1}. Farther south, away from the influence of the steep mountains, the mean total annual precipitation is reduced, such that at the mouth of the Elk River the average precipitation ranges from 500-650 mm yr^{-1}. The influence of glacial melt on discharge can vary significantly. A 2-5% glacial coverage in a BC watershed can result in high flows continuing through the summer and early autumn period (Eaton & Moore, 2010), while Prasch et al. (2013) showed that a 1% glacial coverage contributed 0.1-5% (increase) to the stream discharge for a 3,000 km^2 watershed in the Himalayas. With the proportion of glacial coverage

[11] This is based off of the 1st and 3rd quartile for the annual precipitation.

reaching 0.24% in the ERW, it is suspected that the influence on the entire Elk watershed may be small, while Brahney (2014) suggests that the input of glacial melt waters into the streams within the CRB has now peaked and is declining.

The land cover in the ERW has been affected by both natural and anthropogenic causes. In 1968 the ERW saw a change in the coal extraction process from underground mining (mine shafts) to surficial mining (open-pits) (Katay, 2014). Open-pit mining is a process where the rock is removed from the mountain until the coal seam has been exposed, then extracted. The rehabilitation of the site includes returning rock to the excavated area and re-establishing a vegetated surface. Accordingly, throughout the life of an open-pit mine, the land cover would change significantly during the extraction portion of the activity, with the anticipation that it would be returned to a vegetated state afterwards. Figure A-7 provides an estimation of the forested land cover change upstream from the Fernie discharge monitoring station (08NK002) from 2000 to 2013. During this time, there was approximately 25 km^2 of forest lost per year, with 7 km^2 of forest gained per year. The following information is a summary of the change in the forest cover findings separated by discharge research station's drainage basin from 2000 to 2013 (Table 3-1):

Table 3-1. Change in forest cover in the research drainage basins in the Elk River Watershed from 2000 - 2013.

Drainage Basin	Forested area lost (%)	Forested area gained (%)	Change (%)
08NK002	11	3	8
08NK016	10	4	6
08NK018	12	3	9

A reduction of forest cover of less than 20% within a watershed often does not result in an observable hydrological response (Stednick, 1996). With a range of forest cover change from 6% to 9% from 2000 – 2013, it is unlikely that this 13 year change will have resulted in an observable hydrological response. However, the above referenced 13 year time period does not represent the entire 40 year study period, so cumulative impact from LULC on the hydrological response within the ERW is still a possibility. Furthermore, as Blöschl et al. (2007) identify, the impact associated with LULC change lessens as the watershed (catchment) size increases.

3.2 Local Weather Patterns

The Pacific frontal storms have the largest influence on the weather patterns, with most of the storms from orographic lifting over the mountain peaks, often producing low intensity but long duration storms (Figure 3-3). Late spring and early summer often experience synoptic scale storms[12] that are associated with cold low pressure systems producing heavy rainfall; the spring rains that are anticipated every year. During the summer and autumn, there is a shift to local convective storms that provide the precipitation from southerly continental systems (Obedkoff, 1985) and the typical summer/early autumn thunderstorms (Wuerthner, 2001). This is a snow dominated (nival) watershed, defined as having a spring snowmelt freshet level of > 50% of the annual streamflow occurring between April and July (Regonda, Rajagopalan, Clark, & Pitlick, 2005). With a shift to a warmer climate, increased evapotranspiration and a reduction of precipitation in the form of snow will likely result (Brahney, 2014).

[12] Synoptic scale are storms also defined as large scale of the order of 1000 km or more. Most high and low pressure areas seen on weather maps such as surface weather analyzes are synoptic scale systems.

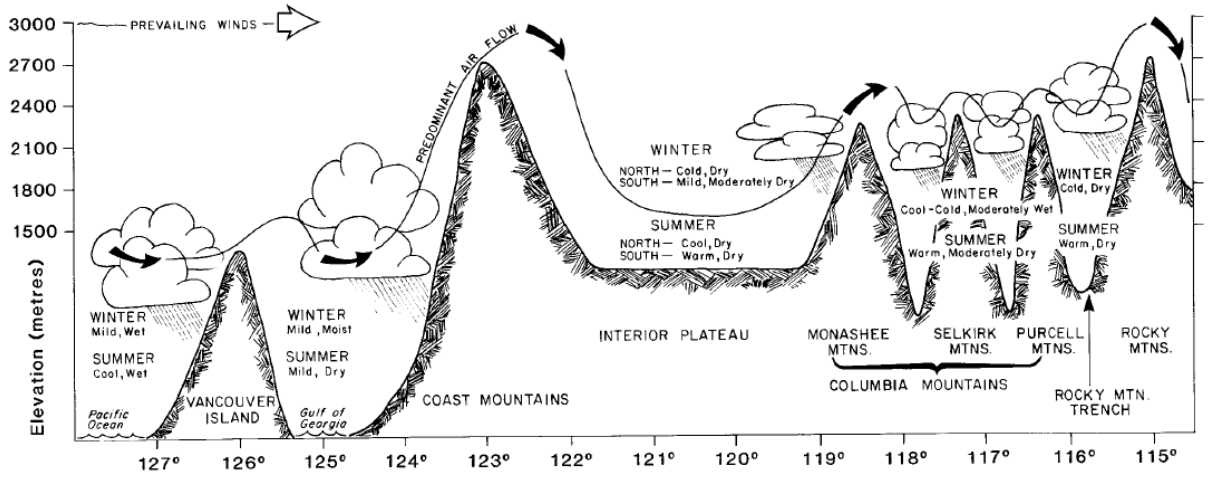

Figure 3-3. Prevailing wind model for British Columbia, comparing latitude (x axis) to elevation above sea level (y axis) (Chilton, 1981).

3.3 Hydro-Climatological Data for the Elk River Watershed

The hydrological (discharge) and climatological monitoring stations within the ERW are managed by a variety of agencies (privately, provincially and/or federally) with the data used in this research sourced from public access sites. A map showing the data monitoring stations outlined below in the ERW can be found in Figures A-1 and A-2. Table 3-2 provides a location description for each source used in this research. Note, reference to hydrometric monitoring stations and/or hydrology analysis refers to water quantity assessment only and not water quality; the analysis of water quality was outside the scope of this research.

Table 3-2. Data sources within the Elk River Watershed.

Data Type	Manager	Website/Location
Pacific Climate Impacts Consortium	University of Victoria	http://www.pacificclimate.org/
Environment and Climate Change Canada	Federal	http://climate.weather.gc.ca/
ClimateBC	UBC*	http://www.climatewna.com/
Water Survey of Canada	Federal	http://www.ec.gc.ca/rhc-wsc/
River Forecast Centre	Provincial	http://bcrfc.env.gov.bc.ca/data/
Wells Database	Provincial	https://a100.gov.bc.ca/pub/wells/public/indexreports.jsp
Geospatial Data	Federal	www.geogratis.ca
Aquifers	Provincial	https://a100.gov.bc.ca/pub/wells/public/common/aquifer_report.jsp
Research Branch MFLNRO (Alexandre Bevington)	Provincial	Information request in person

*University of British Columbia

3.3.1 Climate Monitoring Stations

A list of the Environment and Climate Change Canada (ECCC) climate stations in and around the ERW is included in Figure A-1, with the longest climate record located close to Fernie. The ECCC climate station 1152850 (Fernie) has been active since 1914 consisting of approximately 90 years of data, with nine years missing from 1953-1962. Climate stations used for the descriptive statistics included those with the most intact datasets and combined

they provided good coverage of the watershed. Table 3-3 provides a list of climate stations used for the descriptive statistical analysis.

Table 3-3. Climate monitoring stations included in descriptive analysis of the Elk River Watershed. ECCC: Environment and Climate Change Canada; WFM: Wildfire Management Branch.

Name	Stn. No.	Manager	POR*	Frequency	Elevation (m)
Fording Clode	1152898	ECCC	1976-2000	daily	2100
Fording	1152899	ECCC	1970-2011	daily	1585
Round Prairie	788	WFM	2001-2015	hourly	1647
Elkford	1152653	ECCC	1972-1993	daily	1370
Natal Harmer Ridge	1155402	ECCC	1971-2000	daily	1889.8
Sparwood	1157630	ECCC	1980-2014	daily	1136.7
Corbin	1151915	ECCC	1977-2000	daily	1572
Fernie	1152850	ECCC	1913-2011	daily	1001
Elko	1152670	ECCC	1923-1995	daily	931
Baynes	1150690	ECCC	1986-2011	daily	792
Grasmere	1153282	ECCC	1962-2000	daily	868.7

* POR: Period of Record

Unfortunately, there was a substantial amount of missing data at some of the climate stations throughout the region, with only a few stations active from 1970 – 2009. The two climate stations showing the highest percentage of available data during this period were chosen for the inferential statistical analysis: EC1152899 (subsequently referred to as EC899) and EC1152850 (subsequently referred to as EC850). Both of these stations are managed by

ECCC, and collectively they provide adequate climate (precipitation) coverage for research within the upper portion of the ERW based on the World Meteorological Organization (WMO) recommendations of a precipitation station every 100-250 km^2 (Brahney, 2014). EC850 provides climate information for the centre of the watershed (situated close to Fernie); approximately 75 km north, EC899 provides climate information for the northern portion of the watershed, situated close to the Fording Mine (Figure A-2). Analysis was based on period of record using meteorological parameters: rain (mm), snow (mm), precipitation (mm), minimum temperature (°C) and maximum temperature (°C).

3.3.2 Discharge Monitoring Stations

Water Survey of Canada (WSC) is a national organization that manages and disseminates standardized hydrometric data (discharge and level) for public use. Table 3-4 outlines the WSC hydrometric stations within the ERW; six on the Elk River and six on its tributaries. Stations with less than five years of data were not included. The stations have been listed in Table 3-4 from the most northerly station, Elk River below Weary Creek, to the most southerly station, Elk River at Phillips.

Table 3-4. List of Water Survey of Canada hydrometric stations within the Elk River Watershed; (a) stations on the Elk River; and (b) stations on tributaries to the Elk River.

Location on Elk River	Stn. Number	Stn. ID used in report*	Latitude (°N)	Longitude (°W)	POR Yrs	From	To
Below Weary	08NK027	Disch027	50.3825	114.9219	15	1982	1996
At Natal	08NK016	Disch016	49.8661	114.8683	67	1950	2016
At Fernie	08NK002	Disch002	49.5100	115.0714	52	1925	2016
At Stanley	08NK012	------	49.3117	115.0511	26	1944	1969
At Elko	08NK001	------	49.2806	115.0986	27	1914	1965
At Phillips	08NK005	Disch005	49.2150	115.1106	73	1924	1996

*only stations included in the analysis are identified in this column

Stream Name	Stn. Number	Stn. ID used in report*	Latitude (°N)	Longitude (°W)	POR Yrs	From	To
Line Creek	08NK022	Disch022	49.8914	114.8333	44	1971	2014
Fording River	08NK018	Disch018	49.8942	114.8647	47	1970	2016
Fording River	08NK021	Disch021	50.2014	114.8825	24	1971	1995
Grave Creek	08NK019	------	49.8433	114.8600	30	1970	1999
Michel Creek	08NK020	------	49.7303	114.8567	27	1970	1996
Hosmer Creek	08NK026	------	49.5842	114.9539	36	1981	2016

*only stations included in the analysis are identified in this column

Station 08NK005 (Elk River at Phillips) is a regulated system due to a BC Hydro dam located on the Elk River at Elko (~18 km from the station[13]). Construction was completed on the dam

[13] Based on stream measurement from Google Earth.

in 1925 by the East Kootenay Power Company, and sold to BC Hydro in 1968. Currently the Elko Dam can produce up to 12 MW of power with a licensed flow capacity of 25.5 $m^3 s^{-1}$. During the 2013 Elk River flood (Figure 3-4), with instantaneous discharge readings of >1000 $m^3 s^{-1}$, preparations were being made in the event of a dam failure; a situation that was avoided as the discharge levels dropped rapidly once the rain event ended.

1. 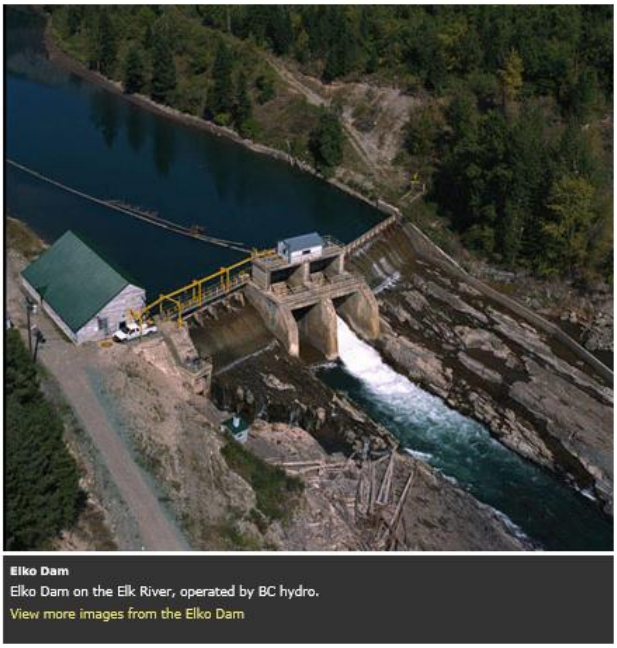

2. 

Figure 3-4. BC Hydro Run of the River dam on the Elk River at Elko, BC.

Photo 1: Photo credit:www.virtualmuseum.ca/sgc- $m^3 s^{-1}$/expositions-exhibitions/hydro/en/dams/?action=elko

Photo 2. Photo credit: Ministry of Forests, Lands and Natural Resource Operations – Water Division dated June 22, 2013.

The stations used in the inferential statistical analysis (08NK002, 08NK016 and 08NK018) were chosen based on the timing of their period of record and location. The station at Natal (08NK016) is located in the top third of the watershed, and ~45 km downstream from there is the Fernie station (08NK002), located in the middle of the watershed. Station 08NK018 on

the Fording River is located ~ 3.8 km upstream of 08NK016 (Natal), with the Fording River entering into the Elk River ~ 2 km upstream of 08NK016 (Natal). All three stations have >40 years of data, which is recommended to process flood analysis, as well as preferred when processing many of the necessary statistical analysis being used in this research (Northwest Hydraulic Consultants Ltd., 2006).

3.3.3 Snow Monitoring Stations

The BC provincial River Forecast Centre (RFC), a division of MFLNRO, monitors and runs the snow survey network in BC. Within this network are two types of monitoring: manual (with a snow course) and automated (using a snow pillow). For more information on either of these two systems refer to the RFC website shown in Table 3-2. Within the ERW there are two manual stations (2C16 and 2C07) and one automated snow pillow (2C09Q) (Figure 3-5 and Table 3-5). The parameters used at these sites included: snow depth (cm), snow water equivalency (mm) and snow density (%).

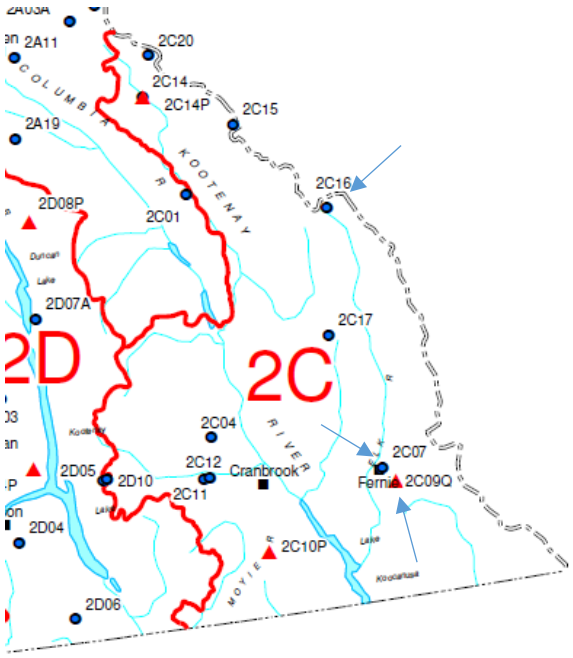

Figure 3-5. River Forecast Centre snow monitoring stations (blue arrows) in the Elk River Watershed. The location of the manual snow stations are identified by blue dots, and the automated snow stations by red triangles.

Table 3-5. Snow monitoring data stations located within the Elk River Watershed.

Name	Stn. No	Type	POR	Freq.	Elev. (m)	Lat. (°N)	Long. (°W)
Mount Joffre	2C16	Manual	1970-2015	month	1763	50.53	115.12
Thunder Creek*	2C17	Manual	1969-2015	month	2062	50.03	115.25
Fernie East	2C07	Manual	1951-2015	month	1213	49.50	115.33
Morrissey Ridge	2C09P	Auto	1979-1983	day	1860	49.45	114.97
Morrissey Ridge	2C09Q	Auto	1983-2008	day	1860	49.45	114.97

*Thunder Creek is located close to but outside of the ERW.

3.3.4 Groundwater

There are no deep groundwater level data publicly available for the ERW. With minimal aquifer information currently identified (Figure A-8), deep groundwater information is often estimated through access to the groundwater well information for the region (Figure A-9). With a provincial regulatory system that only started regulating groundwater in February 2016, it was determined that, for this research, the publicly available deep groundwater information is insufficient to support a defendable analysis. However, stream baseflow has been described as the groundwater contribution to the stream flow (Rumsey, Miller, Susong, Tillman, & Anning, 2015). When estimating baseflow without the use of tracers or markers, one can calculate baseflow based on the stream discharge reading, addressed in this research using the Lynn – Horlick method (as described in Section 4.7.1). Zomlot et al. (2015) compared the baseflow calculation for 15 streams, using the Web-based Hydrograph Analysis Tool (WHAT), with known groundwater contribution to the channel; it was determined that the baseflow calculation was a good approximation of the groundwater influence at these 15 locations. Baseflow has been included in this analysis, although findings associated with the baseflow component need to be treated with caution since, as stated above, in this research baseflow has been determined based on an equation correlated with the stream discharge.

3.4 Summary

The ERW lies in the headwaters of the CRB, in southeastern BC. Given its transboundary nature and environmental and socio-economic significance, there is much interest and concern associated with changes in the hydrology of the ERW and larger CRB as a function of changes in climate and LULC. The mountainous nature of the ERW can result in large fluctuations in

climate and hydrological response throughout its four seasons. With a warming climate shift over the past 100 years, reports of hydrological and other environmental changes have already been reported. As there are several hydrological and climate monitoring stations in the ERW, it is possible to examine changes in hydro-climate conditions over time.

4 Methods of Analysis

4.1 Introduction

This chapter will review the main statistical techniques used in this research project for analysis of both hydrometric (discharge) and climatological (temperature and precipitation) parameters to address research questions 1 and 2 (see Section 1.4). Research question 3 (see Section 1.4) was to be addressed using the SWAT model.

For this research, the statistical software systems used comprised of R (R Core Team, 2015), HEC-SSP (Hydrologic Engineering Center – Statistical Software Package) and Microsoft Excel. The main R packages used, in alphabetical order, included: {car} (Fox & Weisberg, 2011), {dplyr} (Wickham & Francois, 2015), {Hmisc} (Harrell Jr & Dupont), {hydrostats} (Bond, 2015), {hydroTSM} (Zambrano-Bigiarini, 2014), {Kendall} (McLeod, 2011), {lfstat} (Koffler, Gauster, & Laaha, 2015), {nlme} (Pineiro, Bates, DebRoy, Sarkar, & Team, 2016), {OpenAir} (Carslaw & Ropkins, openair: Open-Source Tools for the Analysis of Air Pollution Data, 2016), {VIM} (Templ, Alfons, Kowarik, & Prantner, 2015), {xts} (Ryan & Ulrich, 2014) and {zyp} (Bronaugh & Werner, 2013). Note that the aforementioned packages often activate other packages to support their functioning; however, these associated packages have not been identified but can be found through the main package documentation. The hydrological engineering software used is from the U.S. Army Corps of Engineers. Additional information regarding this tool can be found at the website: http://www.hec.usace.army.mil/software/hec-ssp/.

To answer the research questions, this project examines 40 years of historical data for the ERW broken down into: (1) descriptive statistics and (2) inferential statistics. The descriptive statistics were completed on seven discharge stations and 10 climate stations. Many of the discharge and climate stations show large periods of no information during the 40 year research period. As a result, the inferential statistics were completed on a subset of the stations, which included three discharge stations and two climate stations. Figure A-1 provides a map of the watershed outlining the location of all monitoring stations, and Figure A-2 outlines the stations used for the inferential statistics.

Descriptive statistics were computed using daily data, while incorporating monthly and annual means[14] where appropriate. The trend analysis was performed on a monthly, seasonal and annual time period. Discharge frequency analysis was completed using daily and monthly mean data, with instantaneous flows used for high flow analysis. Statistical analysis consists of both parametric and non-parametric tests.

4.2 Parametric Tests

The preference is to use both parametric and non-parametric tests where possible, as each techniques offers specific insights on the same data. The Pearson's r (r), and associated coefficient of determination (R^2) are two parametric tests used often in this type of research. There are many assumptions (outlined below) associated with a parametric test, which can prove difficult at times to meet with climate and hydrological data, and in these cases non-parametric tests are relied on as they require fewer assumptions.

[14] For discharge and temperature the monthly mean and annual mean was used. For precipitation the monthly sum and annual sum was used.

4.2.1 Linear Regression

Where linear regression is used in this research, the R^2 is reported (Equation 4-1 and Equation 4-2). The Pearson's r value, also referred to as the linear correlation coefficient, describes the strength and direction of the linear correlation between the variables. Whereas, the R^2 value provides information on the strength or ability of the linear regression to explain the variance of the data, so it provides the strength of how well a variable can be used to predict the outcome of a 2nd variable. However, even when the assumptions have been met, care must be taken when using R^2 as the only method to determine a relationship, since sole reliance on the computer's regression model has proven to be ineffective (Helsel & Hirsch, 2002). Graphing has been used in conjunction with the R^2 value when examining the relationship of two variables.

Required assumptions for linear regression analysis *(Zuur, Ieno, & Smith, 2007)*:

1. Normality: the data must show a normal distribution;
2. Homogeneity: the spread of data need to be consistent at each X value, this is accomplished by testing the spread of the residual data;
3. Fixed X: The independent (explanatory) variable is not random, one can determine the exact value of X with no associated noise;
4. Independence of variable: No serial correlation (auto correlation) is permitted.

Equation 4-1. Pearson's r

$$r = \frac{1}{n-1}\sum_{i=1}^{n}\left(\frac{x_i - \bar{x}}{s_x}\right)\left(\frac{y_i - \bar{y}}{s_y}\right)$$

n: number of sample points

s_x and s_y : standard deviation for x and standard deviation for y

$\bar{x}$ and $\bar{y}$: mean of x and mean of y

Equation 4-2. Coefficient of determination

$$R^2 = 1 - \frac{SS_{res}}{SS_{tot}}$$

SS_{res}: sum of squares of residuals, also called the residual sum of squares

SS_{tot}: total sum of squares

Throughout this research, if deemed relevant, findings are reported even though they may show a R^2 value < 0.1. As parametric tests are tied to the interpretation of the mean values, outliers can significantly affect the outputs. The use of graphing supports the visual interpretation of the analysis and provides information regarding potential effects from outliers. The R^2 interpretation (Table 4-1) is based on Sebok (2014).

Table 4-1. Linear regression correlation strength based on the associated R^2 value (Sebok, 2014).

R^2 value	Correlation measurement
< 0.10	No relationship
0.10 - 0.25	Weak relationship
0.26 - 0.50	Moderate relationship
> 0.50	Strong relationship

It is often assumed that hydrometric and climate time series should not be analyzed using linear regression due to the difficulty meeting the linear assumptions. As will be discussed later in this chapter, Zuur, Ieno and Smith (2007) provide tools that make linear regression analysis accessible to this form of data.

4.3 Accuracy of Results

A variety of tools have been developed to assess the accuracy of the results. These include setting the significance level (alpha), confidence level and reporting on the standard of error.

4.3.1 Significance Level

The significance level, p (probability) value, was set at alpha (α) = 0.05 for the majority of analysis, with the exception of the trend analysis where results were also reported at α = 0.1. To ensure detection of the trends, it was determined that reporting for both 5% and 10% significance levels was important[15].

4.3.2 Confidence Level

The confidence level (Cl) represents the probability that the true value of the population is located within its upper and lower boundaries. The Cl used throughout this research was set at 0.95, which represents the range of values to have a 95% chance to adequately represent the true parameter value.

[15] Setting the significance level at α = 0.1 increases the potential of Type I errors; however, it also decreases the potential of Type II errors, so a better chance at ensuring trend detection.

Equation 4-3. Confidence level

$$Cl = 1 - \alpha$$

Cl = confidence level

α = alpha (set at 0.05 or 0.1 for this research)

4.4 Missing Values

There was no infilling of data incorporated in the analysis. This was done to avoid introducing other sources of uncertainty (i.e. undue noise) in the statistical analysis and estimation of trends. Similar to the boundaries outlined by Zhang and Yang (2004), monthly mean or total values were calculated when the month contained ≥ 90% available data, and annual values were calculated for those years showing ≥ 95% available data. This is slightly different than Zhang and Yang (2004) who calculated annual values based on years that had ≥ 95.9% available data (Keggenhoff, Elizbarashvili, Amiri-Farahani, & King, 2014). A "not available" (NA) place holder was inserted for the months and/or years that did not meet the above outlined data availability criteria. As a result, some of the datasets used for the various analyzes contain periods showing no data (as outlined in Section 5.2).

To address potential concerns with relying on only observed data, the modelled data from ClimateBC (Wang, Hamann, Spittlehouse, & Carroll, 2016) were downloaded and compared with the associated observed data. The ClimateBC modelled data provide monthly temperatures (minimum, mean and maximum) and total (sum) monthly precipitation values. To compare against the observed data, the data were downloaded from ClimateBC using the same coordinates and elevation as the ECCC climate stations No. 1152899 and No.1152850;

the ClimateBC stations were labelled CBC899 and CBC850 respectively. A comparison between the observed and modelled data was achieved by means of linear correlation.

4.5 Descriptive Statistics

Similar to the research described in Burford, Déry and Holmes (2009) and Machiwal and Jha (2012), the descriptive statistics for the discharge and temperature data were computed using the observed daily data, which consists of: the mean, absolute maximum, absolute minimum, standard deviation (SD), median, coefficient of variation (CV) and interquartile range (IQR). The same descriptive statistics were calculated for the precipitation data, but the source of the data used for the computation was a total (sum) monthly and total annual value. Both the classic (mean based analysis) and robust (median based analysis) measures provide important information when forming land management decisions when planning for both the average (mean), most common (median) and extreme hydrological and climatological events (Machiwal & Jha, 2012).

Monthly, seasonal and annual findings were reported throughout this research. The seasonal distribution followed Burford et al. (2009) with three months included in each season: winter (December, January and February), spring (March, April and May), summer (June, July, August) and autumn (September, October and November). The summer period contains both the freshet (June) and low flow (August) periods, so monthly analyzes were completed to ensure that high and low flow information was properly represented.

4.5.1 Runoff per Unit Area

The runoff per unit area allows for the comparison of different discharge stations regardless of watershed area. This is calculated by dividing the mean discharge ($m^3\ s^{-1}$) by the gauged area (km^2).

4.5.2 Coefficient of Variation

Coefficient of variation (CV) is a measure of dispersion and is expressed as the standard deviation (SD) divided by the mean (μ). This value has been reported below as a percentage, as it is dimensionless value. As a result, it is very useful when comparing data sets from different units or time periods.

Equation 4-4. Coefficient of variation

$$CV = \frac{SD}{\mu} * 100\%$$

CV = coefficient of variation

SD = standard deviation

μ = mean

4.5.3 Interquartile Range

Interquartile Range (IQR) is the measure of spread around the median rather than the mean. This tool is used regularly as a method to gain a general understanding of the normal spread of the data. The minimum and maximum values are identified, as well as any outliers that are outside of the general range of values. The median, 25th and 75th percentile is indicated on the graph. The IQR is commonly displayed with the use of a box plot as shown in Figure 4-1.

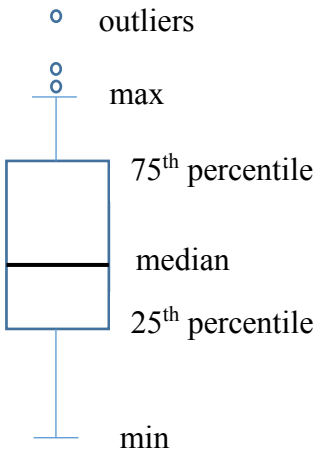

Figure 4-1. Description of the interquartile range output.

4.5.4 Mean Annual Catchment Runoff

The mean annual catchment runoff (mm yr^{-1}) describes the amount of water that is available over the catchment area based on the discharge station's mean annual flow. This calculated value is compared to the local observed precipitation value. This value depicts the amount of water over the catchment, which would be equivalent to that station's mean annual flow. If this is higher than the accumulated precipitation, it is expected that other water sources (e.g., groundwater, water inputs) are contributing to the annual flow; alternatively, evapotranspiration, groundwater storage and/or water use result in the precipitation value being higher than the catchment runoff. The equation that is used to calculate this is (Centre for Ecology and Hydrology, 2016):

Equation 4-5. Catchment Runoff

$$runoff\ (mm) = \frac{\mu\ flow\ (m^3\ s^{-1}) * 86.4\ (mm\ day^{-1}) * n}{catchment\ area\ (km^2)}$$

n = number of days for analysis (i.e. day)

Note: The constant number 86.4 is based on converting mm to meters and seconds to a 24 hour period: 86400 (s day^{-1}) * 0.001 (mm m^{-1}) = 86.4

$$\textit{Annual runoff (mm)} = \mu \textit{ flow } (m^3 s^{-1}) * 86.4 \textit{ (mm day}^{-1}) * 365 \textit{ (day) / catchment area } (km^2)$$

$$\textit{Daily runoff (mm)} = \mu \textit{ flow } (m^3 s^{-1}) * 86.4 \textit{ (mm day}^{-1}) * 1 \textit{ (day) / catchment area } (km^2)$$

4.6 Inferential Statistics

4.6.1 Trend Analysis

Trend analysis is an important tool when analyzing hydrometric and climatic data. Trend tests examine whether there is an overall change in the response of the dependent variable to the independent variable. Helsel and Hirsch (2002) have provided a detailed list of different trend analyzes often used for hydrological assessments.

Daily trend analysis was completed for extreme event information. The Mann-Kendall test (outlined below) was used to identify trend presence; if found to be present, the trend strength was then determined using the Theil Sen slope estimator. The significance level, *p* (probability) value, was set at alpha = 0.05 so all results from the Mann-Kendall trend analysis and Theil Sen assessment were considered statistically relevant if their associated two-sided *p* value was ≤ 0.05. Results showing a *p* value between 0.1 and 0.05 (alpha = 0.1) were also reported, but considered less significant. Analysis presenting a *p* value >0.1 indicate no statistically significant trend. The 95% Cl interval is reported alongside both the monotonic and non-monotonic trend outputs. To ensure a complete understanding of potential discharge trends, both statistically and non-statistically relevant trends were reported when deemed appropriate.

Trend analysis, smoothing trend line and non-parametric analysis, were calculated based on monthly, seasonal, annual and the full research period. As outlined above, only monthly periods with ≥ 90% available data, and annual periods with ≥ 95% of available data were used. Trend analysis was completed on three hydrometric (discharge) stations and two climate stations (precipitation and temperature), located in the central (discharge: 08NK002 and climate: 1152850) and northern (discharge: 08NK016 & 08NK018, and climate: 1152899) portion of the ERW (Figure A-2). Trend analysis was completed over a 40 year period from 1970 to 2009. This time period was chosen as it is within 10 years of the development of two northern communities in the ERW, covers a period of increased coal mining activities, and starts just after the 1968 switch from underground to open-pit coal mining (Katay, 2014). The research period ends shortly before the high water event in 2013 as there were monitoring equipment malfunctions during this event.

4.6.2 Smoothing Trend

While there are a number of options for producing a smooth trend line, this research took advantage of the Generalized Additive Model (GAM) and Locally Weighted Scatterplot Smooth (LOWESS).

A smoothing trend, provided through a GAM is used to visually estimate both monotonic[16] and non-monotonic trends[17], also providing information of trend changes throughout the

[16] A monotonic trend describes a relationship where the Y variable increases (positive trend) or decreases (negative trend) based on the X variable. This trend does not need to be linear; however, cannot be cyclic or U-shaped (both examples of non-monotonic trends).

[17] A non-monotonic trend is a state when the Y variable is related to the X variable in a pattern that fluctuates between a positive relationship (Y increases as X increases) and negative relationship (Y decreases as X increases) such as a cyclic or U-shaped relationship.

research period. The graphs associated with the smoothing trend are obtained using the function "smoothTrend" in the R package {Open Air} (Carslaw & Ropkins, openair - An R Package for Air Quality Data Analysis, 2012; Carslaw & Ropkins, openair: Open-Source Tools for the Analysis of Air Pollution Data, 2016) and is presented with the associated 95% Cl. This non-monotonic approach was conducted using monthly mean and annual mean values over the 40 year period. For monthly mean smoothing trend estimations, the seasonal trend was removed prior to reporting the overall trend. The seasonal trend is removed through the LOWESS regression procedure.

LOWESS[18] is a non-parametric regression that provides a robust means of describing a data pattern, assuming neither linearity nor normality of residuals (Helsel & Hirsch, 2002). Both LOWESS and LOESS work from classical regression methods (i.e. linear and least squares regression) and are designed to fit segments of the data rather than the full dataset. Using the LOWESS fitted value ($\widehat{Y}$), the equation for the residuals (R) is $R = Y - \widehat{Y}$. LOWESS is used in the R {stats} function "decompose" and "stl" that breaks down the time series into three parts: seasonal trend, trend and the irregular components (random and/or residuals).

4.6.3 Mann-Kendall

The Mann-Kendall is a commonly used non-parametric test for monotonic trend analysis (Robson, Bardossy, Jones, & Kundzewicz, 2000; Burn & Hag Elnur, Detection of Hydrologic Trends and Variability, 2002; Déry, Hernandez-Henriquez, Owens, Parkes, & Petticrew,

[18] LOESS (LOcal regrESSion) is an updated version of LOWESS. LOESS curve is derived from weighted quadratic least squares regression, whereas LOWESS curve allows only one predictor and is derived from the weighted linear least squares regression. However, the two are often interpreted as the same process.

2012). Déry et al. (2011) recommend using the Mann-Kendall equation to determine trend, followed by the Theil Sen slope estimator (outlined below) to determine the intensity of the trend. This non-parametric test is used to determine if the median (central value) is changing over time. The benefit of a Mann-Kendall test for trend is that:

- Data do not need to be normally distributed,
- Not strongly affected by outliers,
- Can be used when missing data are present, and
- Can be used with irregular monitoring periods.

The assumptions that need to be met to use the Mann-Kendall trend analysis include:

- There is no serial correlation in the data,
- The data are not influenced by seasonal effects[19],
- Distribution spread must remain constant, and
- It is recommended that there are, at minimum, six full cycles of data being analyzed.

The Mann-Kendall analysis examines if the Y (dependent) variable either increases or decreases monotonically based on the X (independent) variable, such that the regression slope coefficient is significantly different than zero (Helsel & Hirsch, 2002). In the case of this research, the X value is time. Based on this definition, the Mann-Kendall analysis hypothesis test at significance level (α) of 0.05, can be described as (Helsel & Hirsch, 2002):

[19] This can be accounted for by either ensuring the data are not affected by seasonality, or use data from the same season for analysis. https://sites.google.com/site/davidsstatistics/home/mann-kendall-trend

H_0: Prob $[Y_j > Y_i] = 0.5$, where time $T_j > T_i$

H_1: Prob $[Y_j > Y_i] \neq 0.5$ (2 – sided test)

Y = the dependent variable, and

T = the independent variable (time)

The outputs, and associated explanations, from the Mann-Kendall analysis include (Equation 4-6):

(i) *p* value: probability that the observed results will agree with H_0

(ii) Kendall *tau* coefficient (τ): strength of power, from -1 (strong negative correlation) to 1 (strong positive correlation). A value of zero represents no correlation.

Equation 4-6. Mann-Kendall

$$-1 \leq \tau \leq 1 \qquad \tau = S/D$$

(iii) S = Kendall Score that indicates the trend presence

$$S=\sum\_\{i<j\} (sign(x[j]-x[i])*sign(y[j]-y[i]))$$

S expressed in words equates too:

S = (number of concordant pairs) – (number of discordant pairs)

(iv) D = denominator

$$D = n (n-1)/2$$

As discussed in Section 2.1.1, a main concern for using the Mann-Kendall analysis on time series data is to ensure there is no serial correlation or seasonality of the data for the reported *p* values to be correct (Helsel & Hirsch, 2002). For this research the Mann-Kendall, Theil Sen

slope estimator and autocorrelation adjustment (see Section 4.6.4 and 4.6.5) were calculated using the R statistics package {zyp}. As a comparison, and for data sources where the serial correlation has been eliminated, the R package {OpenAir} function "TheilSen" was used, which produces a presence/absence of a trend, Theil Sen slope estimator value and associated 95% CI.

4.6.4 Theil Sen Slope Estimator

The Theil Sen slope estimator analysis is a non-parametric tool used to estimate the trend value (trend magnitude) once a trend has been identified by the Mann-Kendall analysis. This method estimates the slope of a straight line, using all data pairs available in the dataset; with the reported Theil Sen slope being the median of all of these calculated slope pairs. Basing the calculation on the median, the Theil Sen method remains minimally affected by the presence of outliers; thereby, a useful tool for hydrometric and climate data analysis. It should be noted that the 95% CI shown for the Theil Sen slope estimator calculation are computed based on the distribution of the slope of each pair of data points, rather than the methodology identified earlier, the standard least-squares regression, which uses the standard error calculation to determine the confidence level.

4.6.5 Autocorrelation and De-trending

The R package {zyp} supports two methodologies to remove autocorrelation from serial correlation data. This research has relied on the Zhang et al. (2000) approach to address all incidences of autocorrelation. Presence of autocorrelation and partial autocorrelation were determined through the use of the R package {stats} function "acf".

4.6.6 Generalized Models

Generalized linear models (GLMs) and generalized additive models (GAMs) determine the relationship(s) of explanatory variable(s) on a response variable (see Section 2.1.2). This research takes advantage of the linear model to determine the importance of different environmental variables on the discharge in the ERW.

There are two main purposes for using a model: descriptive (explanatory) or predictive. The descriptive modelling explains what is happening now; how the explanatory variable(s) are affecting the response variable. This is a useful tool for examining which parameters have the stronger influence on the response variable; which in turn, provide insights towards changing the response variable output. The predictive model is designed to calculate the response variable outcome based on the current influences shown by the explanatory variables. This is a tool for determining the future response variable output should the explanatory variables influence on the response variable remain the same; so for forecasting or predicting how the past may have looked. Two mechanisms used in support of finding the parsimonious model include the coefficient of determination (preference towards the descriptive model approach) and Akaike Information Criterion (preference towards the predictive model approach). A model that is attempting to explain a phenomenon within the data (e.g., descriptive model) can support a higher amount of serial correlation present in the explanatory variables as the goal of this type of model is to maximize the amount of variation explained in the response variable (i.e. the R^2 value). For a predictive model, serial correlation between the explanatory variables

should be minimized as serial correlation will increase the standard errors of the coefficients, making them difficult to interpret, which can result in a type II error.

Assumptions associated with GLMs match those outlined in the linear regression section of this chapter. The effects of violating these assumptions are outlined in Zuur et al. (2009); by understanding the implications of violating specific assumptions, a determination can be made as to whether there is still value in the model output should this be the case. It is through the interpretation of the model that it will be determined whether or not it provides sufficient useful information in response to the question. The models described below are ordered from basic to more complicated.

1. LM: needs normal distribution of residuals and homogeneity of variance.
2. GLM: a form of linear regression that also requires the residuals to be normally distributed and the variance to be homogeneous, but can account for spatial and temporal autocorrelation. GLMs allow the user to define the distribution family of the response variable, allowing greater flexibility for response variables that are not normally distributed.
3. GLS: are a specialized (nested) form of GLM for which the family distribution of the response variable is set to Gaussian (normal). The coefficient of determination (R^2) can be determined using a GLS that provides a measure of goodness of fit.
4. GAM: are for models where relationships between response and explanatory variables are not linear, and for which the data cannot be transformed to be linear. Like GLM, the user is allowed to define the distribution family of the response family and can account for spatial and temporal autocorrelation.

5. GLMM: same as the GLM but incorporates random effects/structures to account for nested designs.
6. GAMM: same as the GAM but incorporates random effects/structures to account for nested designs.

The following four steps (Zuur, Ieno, Walker, Saveliev, & Smith, 2009) have been used for setting up and analyzing the data, in response to the second research question (see Section 1.4). Each model will be written using the discharge as the response variable, and the explanatory variables will be a combination of precipitation, temperature, atmospheric indices (see Section 4.8.1), and baseflow. Two parsimonious models will be reported, one with and one without the explanatory variable baseflow. Baseflow shows a strong relationship with the discharge (response variable) since the calculation for baseflow, described above, includes the discharge reading. The baseflow was included in the model as a means to account for the groundwater contributions to the discharge (gaining system where groundwater is recharging the stream); however, without the ability to distinguish the proportion of shallow subsurface, deep groundwater and overland flow contributions to the baseflow, there is large uncertainty regarding this variable's contribution.

Below outlines the process for determining which explanatory variables are most influential on the response variable, based on a GLM descriptive model analysis.

I. Detailed data exploration
    a. Determine response variable distribution type to decide what type of family distribution to specify in the model.

b. Identify if outliers are present in the explanatory and response variables.

c. Plot the response variable against the explanatory variables to assess whether a linear relationship may exist; consequently, whether a GLM or GAM is more appropriate.

d. Correlation present between explanatory variables (multicollinearity) is identified when a strong relationship ($R^2 > 0.50$) is present. However, this analysis follows a descriptive model approach

    i. Explanatory variables showing serial correlation were not eliminated from the model selection.

II. Model Selection

a. All explanatory variables are standardized so the mean is zero with a standard deviation of one.

b. The model structure starts showing all explanatory variables, than the removal of the non-significant explanatory variables until the model with the highest R^2 is established.

c. If the diagnostic plots show the presence of outliers, a model with and without the outliers is produced. Models were derived both including the station's baseflow and excluding the station's baseflow.

d. The AIC is used to focus the model structure; ultimately the model with the highest R^2 value is the parsimonious model for this purpose.

III. Model Validation

a. To meet linear model assumptions, residuals need to show normality, no autocorrelation (i.e. show independence), homogeneity of variance, and no clear patterns.

b. Plot residuals versus fitted values to verify if there is a presence of pattern's, if a pattern exists this would suggest lack of linearity, wrong specification of family distribution, or other problems with the model (e.g., that important explanatory variables are missing).

c. Q-Q plot[20] to test for residual normality

d. Plot residuals against each explanatory variable to verify homogeneity of variance.

e. Use a correlogram to confirm the independence of the residuals (i.e. absence of autocorrelation).

IV. Model Interpretation

a. If outliers exist in the dataset, then four models will be derived in each category (shown below) based on the highest R^2 value. All models that meet the assumptions will be reported.

    i. Model using dataset that includes the outliers, including the baseflow

    ii. Model using dataset that includes the outliers, excluding the baseflow

    iii. Model using dataset that does not includes the outliers, including the baseflow

[20] A Q-Q plot is the quantiles of the first data set plotted against the quantiles of the second data set. If the data show a straight line then the residuals are considered having a normal distribution.

iv. Model using dataset that does not includes the outliers, excluding the baseflow

b. Explanatory variable significance is identified for both significance level 0.05 and 0.1.

c. When the preferred model does not include a correlation structure, the GLS model strength is determined by accessing the R^2 of the same model configuration, however using a linear model analysis. An R^2 value of 0.30 means that the model explains 30% of the variance in the response variable. A pseudo R^2 value is to be calculated when a GLS with correlated structure is identified as the strongest model. Although not required for this research, information on calculating a pseudo R^2 value for GLS models can be found in Griffis and Stedinger (2007) who also provide an analysis on the use of GLS models in hydrological assessments.

d. Is the chosen model a good fit for these data? When the residuals do not show a normal distribution, it is recommended that further research occurs to determine if another model type would be more appropriate.

e. Has independence been confirmed?

4.6.7 Double Mass Curves

Double mass curves allow one to observe if changes are occurring between two data records, such as a change in instrumentation or surrounding conditions. For this research, the double mass curve was used to assess changes in the streamflow based on precipitation. Zhang and Wei (2012) identify climate and/or LULC as the two most common influences to the

hydrological systems in a forested watershed. Analysis was conducted from 1970 to 2013 (44 years); the additional four years were added to this analysis as change was suspected at the end of the 2009 period. The R statistical program {lfstats}, function "dmcurve" was used in support of this analysis. The double mass curve was calculated by comparing daily and monthly cumulative precipitation with the associated cumulative discharge. For any pairs where one value was not available, the other value was removed from the calculation.

4.7 Frequency Analysis

Frequency analysis provides another approach of analyzing hydrometric data, providing temporal information and analysis of extreme events. This examination is crucial for assessing extreme events and supporting decision for land and water management. A number of different frequency analysis reports were computed that included: baseflow analysis, low flow indices, temporal and quantitative measure of extreme events and the timing of freshet.

4.7.1 Base Flow Calculations

Baseflow discharge calculations were completed using the R statistical package {hydrostats} (Bond, 2015), {lfstats} (Koffler, Gauster, & Laaha, 2015) and HEC-SSP. The {hydrostats} uses the Lyne-Hollick (LH) baseflow filter to calculate the baseflow. The LH baseflow filter (Lyne & Hollick, 1979) is a widely used digital filtering method for baseflow separation. Determining the baseflow volume within a stream, supports the ability to assess whether there has been a change over time for this parameter, and provides a means to estimate glacial water inputs by comparing the warm (summer) and cool (winter) baseflow periods.

4.7.2 Volume Frequency Analysis

The intensity and duration of instantaneous peak, maximum and minimum annual flows can offer insights to changes occurring within a watershed, which may or may not be reflective in the means annual flow. Low flow was analyzed with the HEC-SSP program over the 40 year period. Examination of the multi-year hydrograph for each station outlined the necessity for conducting low flow analysis in the ERW based on the water year (October 1 to September 30) rather than over the calendar year (January 1 to December 31). The low flow periods occur during the winter and summer months, so the break in the year must happen outside of this time period. Volume frequency analysis and timing of minimum discharge were calculated and linear regression was used to determine if a trend was present.

High flow analysis was conducted using two programs: duration of events was analyzed using R package {hydrostats}; and, the timing of extreme events and volume frequency analysis was analyzed using HEC-SSP. Analysis was conducted over the 40 year period, based on the calendar year. There were two freshet timing options used to identify the start of freshet. These included the methodology from (1) Zhang, Harvey, Hogg and Yuzyk (2001) and (2) Burn, Abdul Aziz and Pietroniro (2004). Burn (1994) determined the date when 50% of the water year volume was achieved. This approach allows for the incorporation of rain-on-snow events in the total volume estimation, focusing on the snow melt process rather than the spring rains. Burn (1994) felt that by relying on a sharp increase in discharge to determine a trend in flows, this could result in counting spring rain events rather than the snow melt response. A summary of these three approaches is outlined below:

(1) The date when the increase in streamflow over four days is greater than the average from that year from January to July (Zhang, Harvey, Hogg, & Yuzyk, 2001).

(2) The date on which the flow magnitude exceeded 1.5 times the average of the flow magnitude for the preceding 16 days (Burn, Abdul Aziz, & Pietroniro, 2004).

(3) The Julian/calendar day for when 50% of the water year (October 1 to September 30) is equalled or exceeded (Burn, 1994). This methodology allows for the incorporation of rain-on-snow events into the volume of water, rather than identifying spikes in the discharge (common approach for determining freshet), which could be attributed to a one-time rain-on-snow event.

4.8 Additional Considerations

4.8.1 Atmospheric Teleconnection Patterns

The four atmospheric teleconnection patterns that were examined for this research included: El Niño Southern Oscillation (ENSO), North Pacific pattern (NP), Pacific Decadal Oscillation (PDO) and the Arctic Oscillation (AO) index. Information regarding description and common period of influence for all four teleconnection patterns can be obtained from the Climate Diagnostics Center (CDC) of the National Oceanic and Atmospheric Administration (NOAA) website: www.cdc.noaa.gov/ClimateIndices. Brahney (2014) outlines the difficulty of teasing out the effects from the different atmospheric teleconnection patterns, as many of them are intertwined and influence each other. To determine definitively which atmospheric indices is affecting a specific watershed can be very difficult. Each teleconnection pattern was compared with the discharge and snow water equivalent (SWE) from the RFC stations, and statistical correlation was determined using the Mann-Kendall test; pre-whitening was not required for

this dataset. Graphing was used to support the specific indices findings. When correlating the atmospheric indices with the snow data, the previous month's atmospheric indices was used for the correlation as the snow data were collected the first of each month at the manual stations[21].

4.8.2 Water Inputs and Withdrawals

Water inputs and water withdrawals were not included in the assessments due to lack of available and precise data. Water withdrawal information is obtained from the BC water licencing database. This information refers to the total amount of water that is licenced for removal, and is not necessarily the quantity of water that is actually removed by the licensee. As a result, there is no way to know if the quantity of water authorized through the Provincial water licences system is in fact being removed from the stream. As a result, this information was not included in the analysis.

There is no publicly available information addressing water inputs into the stream channels. In theory, there are many activities that could be contributing water to the streams, such as: shallow groundwater runoff and overland flow associated with irrigation; water release from sewage lagoons; water release from sediment ponds; and water release from industrial/commercial activities, to name a few. Further investigation into quantifying these water inputs and withdrawals is recommended as this has the potential of influencing the discharge outputs and therefore may prove to be a missing component from the analysis.

[21] As an example, the January atmospheric indices was compared with the February's snow data.

4.9 Summary

The different analysis techniques for hydrological and climatological data are numerous; with trend and frequency analysis providing valuable information in support of natural resource land management decisions. Research question 1 (see Section 1.4) will be addressed using non-parametric trend analysis, Mann-Kendall and associated Theil Sen slope estimator. Research question 2 is complimentary to research question 1, as it will provide greater detail on the influences of the different parameters on the stream discharge, and was assessed using GLS and double mass curves. Research question 3 was attempted using the SWAT hydrological model. Understanding the past events and current conditions (research questions 1 and 2) allows for the effective forecasting of future scenarios (research question 3).

5 Results and Discussion: hydro-climatological trend analysis in the Elk River Watershed

5.1 Introduction

This chapter will address whether there are discharge, precipitation and temperature trends over the past 40 years in the northern half of the ERW so as to address research question 1 as identified in Chapter 1. Addressing the potential hydro-climatological trends will provide the basis for responding to research question 2, which is outlined in Chapter 6.

Trend analysis was completed for both (i) non-monotonic trends, alternating between a GAM and LOWESS analysis to develop a smoothing line, and (ii) monotonic trends using the Mann-Kendall (MK) test with associated Theil Sen (TS) slope estimator. Trends were assessed using mean monthly and mean annual data. Four stations on the Elk River and three tributary stations were analyzed to determine if a trend was present over the 40 year research period (1970-2009). As outlined in Chapter 4, a more comprehensive trend analysis was completed on three discharge stations 08NK002, 08NK016 and 08NK018, and two climate stations EC899 and EC850 (precipitation and temperature). These five stations will be referred to as the "research stations" throughout this thesis.

5.2 Data Availability

Analysis was completed using the monthly and annual time period based on the respective 90% and 95% data requirement as described in Section 4.4. Incomplete data records and/or missing data are common when working with publicly available data sources for extended

research periods, and this proved to be the case for both the climatological and hydrological data in the ERW. The percentage of available discharge data per stations is presented in Table 5-1, with Figure B-1 showing the available data from 1970 to 2013.

Table 5-1. Proportion of available discharge data per Water Survey of Canada station over the 40 year (1970 to 2009) study period. Rivers are ordered from north (top) to south (bottom).

Station Number (Stream)	Proportion of data available from 1970 to 2009
Disch027 (Elk River)	36%
Disch016 (Elk River)	100%
Disch002 (Elk River)	100%
Disch005 (Elk River)	67%
Tributaries to the Elk River	
Disch021 (Fording River)	59%
Disch018 (Fording River)	100%
Disch022 (Line Creek)	97%

Many of the climate stations in the ERW show a high percentage of missing data (Figures B-2 to B-4). The two stations showing the longest period of record within this 40 year study period are EC899 and EC850. Based on the 90% monthly and 95% annual thresholds, Table 5-2 provides the percentage of precipitation[22] data available for 10 climate stations in the ERW, which ranges from 18% to 96%. Table 5-3 summarizes the available data for the discharge and climate research stations. The monthly period shows a higher percentage of available data (92-100%) compared to the annual period (68-100%); as a result, more emphasis has been

[22] The climate parameter "precipitation" was used as a representation of the stations data availability. The percentage of data available for each parameter at a station may not be the same; however, they are similar.

placed on the monthly data analysis. When comparing stations, time periods were used that maximized the number of comparable years of data as well as time periods of sufficient length to provide conclusive findings.

Table 5-2. Percentage of available precipitation data by month and annual assessment per Environment and Climate Change Canada station from 1970 to 2009.

Station No.	898	899	653	402	630	915	850	670	690	282
month count	114	434	185	203	336	175	459	228	267	244
month %	24	90	39	42	70	36	96	48	56	51
annual count	7	28	12	9	27	8	30	14	16	12
annual %	18	70	30	23	68	20	75	35	40	30

Table 5-3. Available data, annual and monthly, from 1970 to 2009 (40 year/480 months study period) by research station.

	Annual period (threshold = 95%)	Annual (%)	Monthly period (threshold = 90%)	Monthly (%)
Discharge				
08NK018	40	100	480	100
08NK016	40	100	480	100
08NK002	40	100	480	100
Climate				
EC899 Temp Mean	30	75	432	90
EC899Temp Max	31	78	441	92
EC899Temp Min	30	75	433	90
EC899 Precipitation	28	70	434	90
EC899 Rain	27	68	434	90
EC899 Snow	28	70	432	90
EC850 Temp Mean	31	78	454	95
EC850 Temp Max	31	78	459	96
EC850 Temp Min	31	78	454	95
EC850 Precipitation	30	75	459	96
EC850 Rain	30	75	459	96
EC850 Snow	31	78	460	96

5.2.1 ClimateBC comparison

Comparing monthly mean observed data with the data modelled by ClimateBC[23] (Wang, Hamann, Spittlehouse, & Carroll, 2016) shows that at alpha = 0.05 the ClimateBC model is

[23] Description of the ClimateBC stations can be found in Section 4.4.

able to adequately represent temperature in the ERW (Figure B-5), showing R^2 values of 0.97 (CBC 899 compared with EC899) and 0.99 (CBC850 compared with EC850). However, the modelled precipitation is less precise, with R^2 values of 0.46 (CBC899 compared with EC899) and 0.43 (CBC850 compared with EC850) as shown in Figure B-5. Similar to findings obtained during the regionalization process, discussed below, the ability to model temperature in the ERW appears to be more accurate when compared to modelling precipitation data. This was also noticed in the Global Weather model, as will be discussed in Section 7.2. Due to the moderate linear relationship between the observed and modelled precipitation values, more research to understand this discrepancy should be considered before using the ClimateBC precipitation data in place of field observations.

5.3 Discharge

Streamflow in the ERW follows a nival regime pattern: baseflow throughout the winter months, increasing flows (freshet) during the spring period, and decreasing flows during the summer and autumn periods as the stream returns to the winter baseflow. A statistical summary of the four Elk River stations and three tributary stations provides a foundation for the evaluation of both monotonic and non-monotonic discharge trend analyzes. The annual hydrograph showing the three discharge research stations from 1970 to 2013 is available in Figure C-1.

5.3.1 Descriptive Statistics

During the 1995 freshet the Elk River experienced very high flows that resulted in some damage to a few WSC monitoring stations. In light of this damage, stations 08NK027 (Weary)

and 08NK005 (Phillips) were discontinued, ending their period of record in 1996. Descriptive statistics are provided for all of the ERW discharge stations, as well as associated tributaries (Table 5-4); this information provides insight into the functioning of this medium-sized watershed, the range in discharge and how this changes per location from the headwaters (northern point) to Lake Koocanusa (southern point).

As is expected, the mean discharge is positively correlated to that station's drainage basin area. The tributaries show the highest range of variability around the mean (CV) that could be a reflection of LULC variation in the area[24]. As the mean discharge varies greatly based on the area of the basin, a preferred method to compare the tributaries with the stations on the Elk River is through the discharge/unit area calculation, and a range of 0.01 to 0.02 $m^3 km^{-2}$ is identified for both the Elk River and the tributaries. The period of record for the three sites with the highest mean runoff, all end in the mid-1990s (Table 5-4), have different drainage areas, variation in stream size and due to their locations, experience slightly different climate conditions. It is for these reasons, that it is assumed this shortened period of record has, in some way, contributed to this increase in the mean runoff. Based on a similar calculation, the discharge per unit area shows a similar pattern as the runoff mean, and the stations with the period of record ending in the mid-1990s show the highest values.

[24] LULC variation is suspected to explain the large CV for the tributaries, as the stations are receiving similar climatic inputs and the variation does not appear to be related to the site's drainage area.

Table 5-4. Daily (top) and annual (bottom) hydrometric statistics from 1970 to 2009.

WSC Station	Stn. elev. (masl)	μ daily Q ($m^3 s^{-1}$)	Max daily Q ($m^3 s^{-1}$)	Min daily Q ($m^3 s^{-1}$)	SD ($m^3 s^{-1}$)	CV (%)	Q per unit area ($m^3 s^{-1} km^{-2}$)
08NK027	1552	6.68	75.0	0.46	8.56	128.05	0.020
08NK016	1199	25.10	333.0	2.58	31.72	126.41	0.014
08NK002	1000	46.93	642.0	5.80	57.54	122.61	0.015
08NK005	784	74.34	1020.0	7.65	92.66	124.64	0.017
08NK021	1677	1.82	59.7	0.09	3.09	169.60	0.018
08NK018	1230	7.94	155.0	0.67	11.22	141.29	0.013
08NK022	1286	2.10	46.7	0.24	2.96	140.81	0.015

WSC Station	Yrs	Lat (°N)	Long (°W)	Basin area (km^2)	Q ($km^3 yr^{-1}$)		CV (%)	Runoff mean ($mm yr^{-1}$)
					Mean	SD		
08NK027	14	50.3825	114.922	334	0.21	0.03	14.2	630.3
08NK016	40	49.8661	114.868	1840	0.79	0.17	21.5	430.4
08NK002	40	49.5100	115.071	3090	1.48	0.35	23.7	479.3
08NK005	26	49.2150	115.111	4450	2.31	0.54	23.4	518.6
08NK021	22	50.2014	114.883	104	0.06	0.02	34.8	552.5
08NK018	40	49.8942	114.865	621	0.25	0.06	25.1	403.5
08NK022	38	49.8914	114.833	138	0.07	0.02	25.6	477.3

The seasonal averages for the three discharge research stations, and corresponding standard deviation is shown in Table 5-5 with associated runoff calculations available in Table 5-6. This was used to calculate the percentage of change observed in the monotonic trend analysis.

Table 5-5. Seasonal averages for the discharge research stations from 1970 to 2009 based on the calendar year. The percentage of the seasonal flow based on the annual flow is shown in brackets.

I.D.	Annual Q ($m^3 s^{-1}$)	Winter Q ($m^3 s^{-1}$)	Spring Q ($m^3 s^{-1}$)	Summer Q ($m^3 s^{-1}$)	Autumn Q ($m^3 s^{-1}$)
08NK002					
μ	46.83	13.99 (30%)	56.60 (121%)	93.03 (199%)	23.69 (51%)
SD	51.89	4.77	50.03	66.02	8.91
08NK016					
μ	25.04	6.24 (25%)	25.14 (100%)	55.57 (222%)	13.20 (53%)
SD	28.86	1.68	25.02	35.53	4.86
08NK018					
μ	7.93	2.11 (27%)	9.30 (117%)	16.44 (207%)	3.85 (49%)
SD	9.86	0.69	9.24	13.32	1.50

Table 5-6. Seasonal discharge calculated per unit area for the discharge research stations; 1970 to 2009.

I.D.	Basin (km^2)	Annual μ ($m^3 s^{-1} km^{-2}$)	Winter μ ($m^3 s^{-1} km^{-2}$)	Spring μ ($m^3 s^{-1} km^{-2}$)	Summer μ ($m^3 s^{-1} km^{-2}$)	Autumn μ ($m^3 s^{-1} km^{-2}$)
08NK002	3090	0.015	0.005	0.018	0.030	0.008
08NK016	1840	0.014	0.003	0.014	0.030	0.007
08NK018	1677	0.005	0.001	0.006	0.010	0.002

The IQR for the discharge monitoring stations in the ERW demonstrates the spread between the 25th to 75th quartile of each station over the full period of record (Figures 5-1 and C-2). The volume of discharge is statistically different between each station, with the southern stations showing the highest volume.

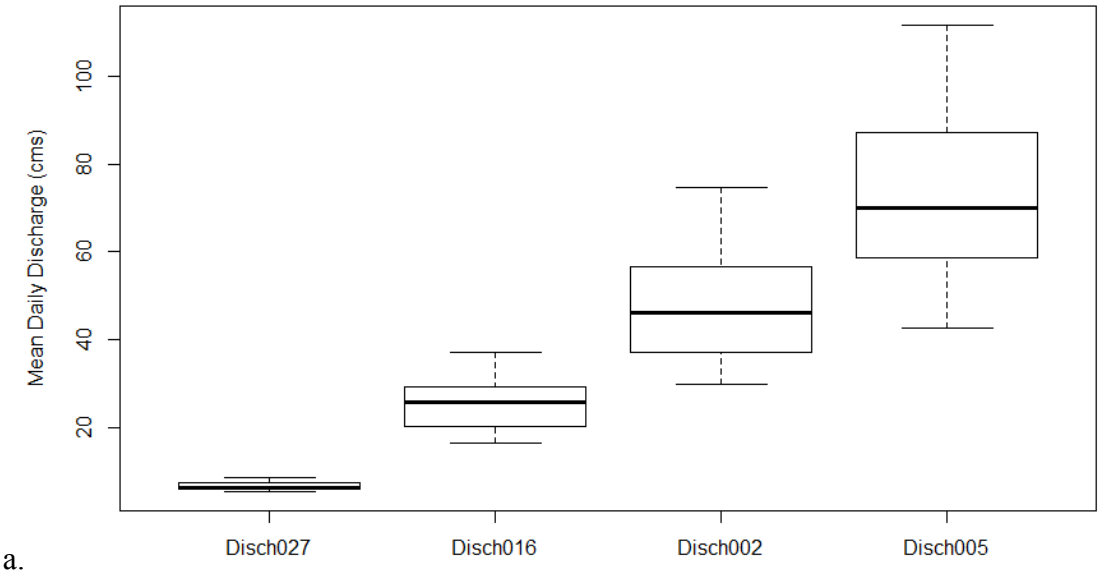

a.

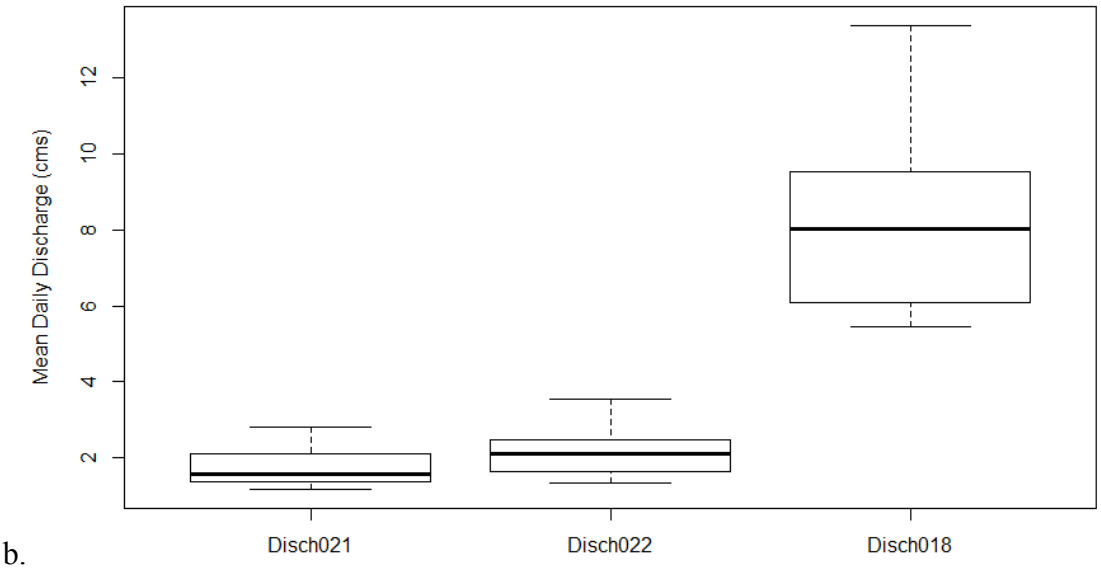

b.

Figure 5-1. Annual mean discharge for the Water Survey of Canada stations on the (a) Elk River, and (b) tributaries to the Elk River from 1970 to 1996[25]*. Plot interpretation defined in Section 4.5.3.*

As is common in a snow-dominated watershed, there is predictable variation in the discharge levels over a calendar year. The baseflow, rising limb, peak and receding limb are clearly

[25] The date range has been reduced to support comparison with stations containing a shorter period of record.

demonstrated in the IQR monthly spread for the three research discharge stations: 08NK002 in Figure 5-2, and 08NK016 and 08NK018 in Figures C-3 and C-4. The periodic spikes and fluctuations from January to December over the 40 year period can be observed in the associated station's hydrograph displayed in two forms (1) Figure C-1 (1970 – 2013) and (2) Figures C-5 and C-6 (1970 – 2009), where each year has been overlaid on the other, separated by station.

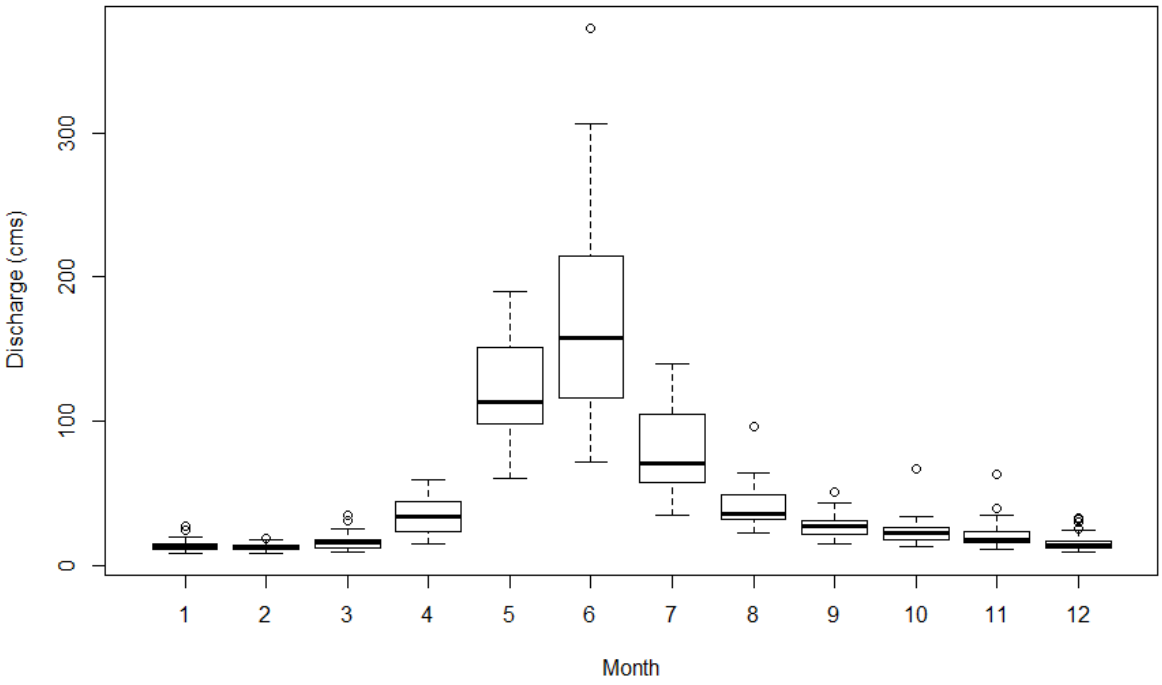

Figure 5-2. Interquartile range by monthly mean discharge for station 08NK002 from 1970 to 2009. Plot interpretation defined in Section 4.5.3. Graph is based on calendar months: January = 1 and December = 12.

Similar to the discharge per unit area expressed in Table 5-4, Figure 5-3 shows the monthly discharge for all stations normalized to the associated station's mean discharge. The time period for Figure 5-3 has been reduced to 26 years to accommodate the shortened period of record for station 08NK005 and 08NK027. Each normalized plot (Figures 5-3 to 5-5) displays

the associated 95% Cl for each measurement as a coloured box representing the colour of that station. If a neighbouring station's discharge is located outside of the 95% Cl limit of the first station's discharge, then the discharge from the two stations are considered to be statistically different. Factors that can affect/shape both the storm and annual hydrograph include the watershed's soil type and geomorphology, soil moisture, vegetation type, canopy moisture, drainage density, weather and climate, and human activities (Winkler, et al., 2010) The four Elk River stations all show a similar configuration for the rising limb (starts in March), peak (June) and falling limb (July to October) with baseflow dominating in the winter months (Figure 5-3). The difference between stations is tied to the slope of the rising and receding limbs, and the relative maximum and minimum discharge levels. Any or all of these streamflow components have been known to shift in response to changes in the explanatory variables, such as climate or LULC. This process demonstrates that, on average, the southern Elk River stations (08NK002 and 08NK005) are showing a gentler rising limb slope compared to the northern counterparts; conversely, the southern stations show a steeper receding limb. The two more northern stations (08NK016 and 08NK027) both show a lower baseflow level and higher peak flow compared to their southern counterparts. The normalized plot for the three research discharge stations (Figure 5-4) indicates that the Fording River station (08NK018) does not follow the same aforementioned pattern observed by the Elk River stations (08NK002 and 08NK016). Fording River shows a shift towards a steeper rising limb and higher relative peak discharge than the Elk River stations with a steeper receding limb. The Fording River station (08NK018) has the smallest drainage basin area of the three stations, and is located downstream of the active surface coal mining sites; consequently, both the

smaller basin size and changing land cover may contribute to this change in the discharge pattern.

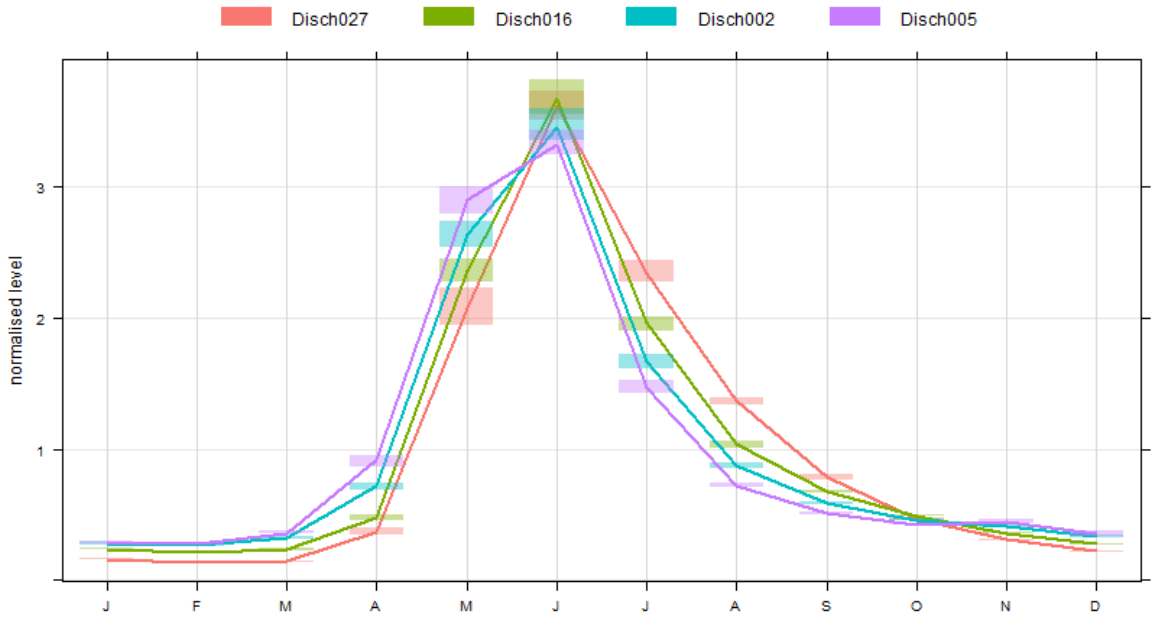

Figure 5-3. Normalized mean monthly discharge data for four Elk River monitoring stations from 1970 to 1995. The coloured boxes represent the 95% confidence interval.

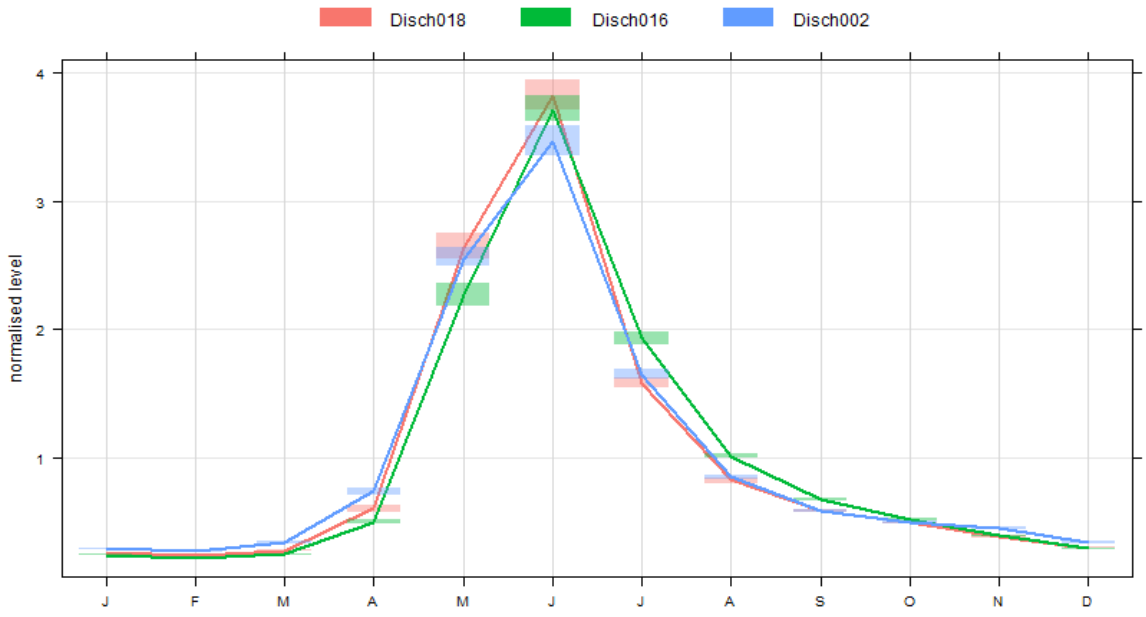

Figure 5-4. Normalized plot from 1970-2009 for the three reference discharge stations. The coloured boxes represent the 95% confidence interval.

The normalized plots were assessed by decade for the three discharge research stations to determine if the above mentioned pattern remained consistent. Based on a 95% CI (Figure 5-5), the highest discharge occurred at the Fording River station (08NK018) in the 1970s; by the 1980s, the Natal station (08NK016) shows the highest comparative peak discharge yet substantially lower than the previous decade, whereas by the 2000s Fernie (08NK002) has the lowest comparative peak discharge. These findings are supported in Table C-1 that shows mean discharge values per decade per station, verifying the statistical difference between stations and decades. The rising and receding limbs follow a similar slope pattern throughout the different decades.

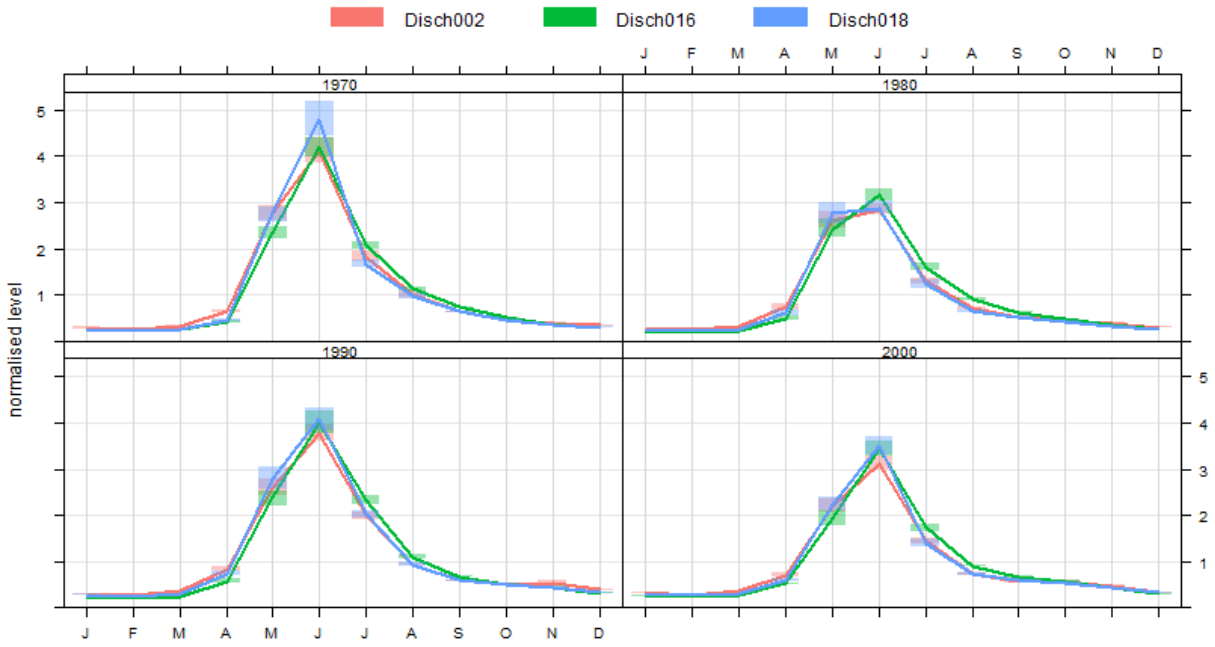

Figure 5-5. Normalized mean discharge plots by decade for stations 08NK002, 08NK016 and 08NK018.

Based on the 95% Cl, determined by decade, the discharge volume appears to be fluctuating over a two decade period; a statistically relevant decrease in discharge for all three stations from 1970 to the end of the 1980s, and again from 1990 to the end of the 2000s. Due to the

cyclic nature of this finding, it may be tied to a climatic pattern that occurs over a two decade period, such as the PDO (see Section 6.2).

Based on regionalization of the discharge stations (Figures C-7 and C-8), there is a strong positive correlation between the discharge at the four Elk River stations and the catchment basin size (R^2 = 0.99; p = 0.007), and an equally strong positive correlation between the discharge and station elevation (R^2 = 0.95; p = 0.024).

5.3.2 Trend Analysis

As can be expected with hydrometric time series data, auto correlation is present for discharge data at a mean daily and mean monthly time period when analysis was completed on a full year period. Trend analysis that was completed using data from this time period was pre-whitened. Annual mean discharge, and mean monthly data analysis per month is not serially correlated, so does not require pre-whitening prior to applying the MK trend analysis.

5.3.2.1 Non-monotonic Trends

Non-monotonic trend estimation was completed for the three discharge research stations: 08NK002, 08NK016 and 08NK018. A smoothing trend line was produced for the 40 year period using monthly mean data (Figure C-9) and annual mean data (Figure 5-6). Both stations 08NK002 and 08NK018 show a cyclic (wave) pattern in the monthly mean and annual mean analysis, peaking in the early 1970s and early to mid-1990s, while showing troughs in the mid-1980s and 2000s. Station 08NK016 shows a similar monthly pattern, with a straight line produced when assessing the change based on the annual mean values (Figure 5-6).

a.

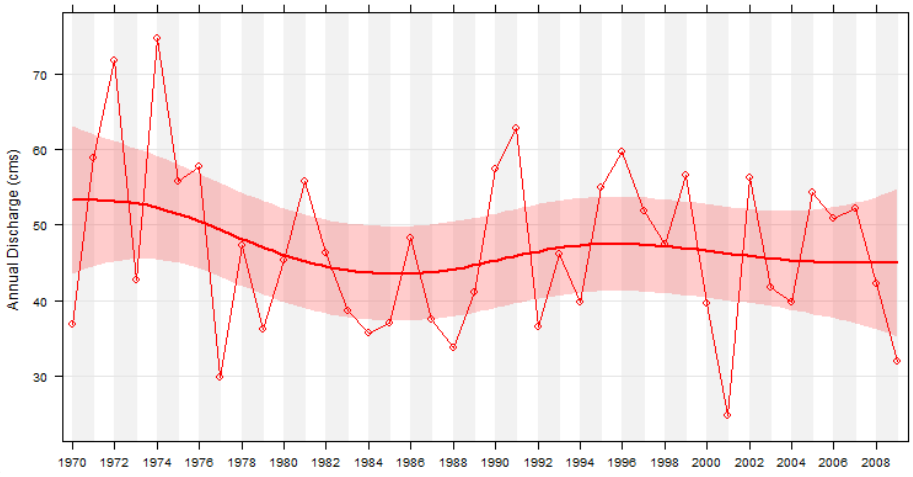

b.

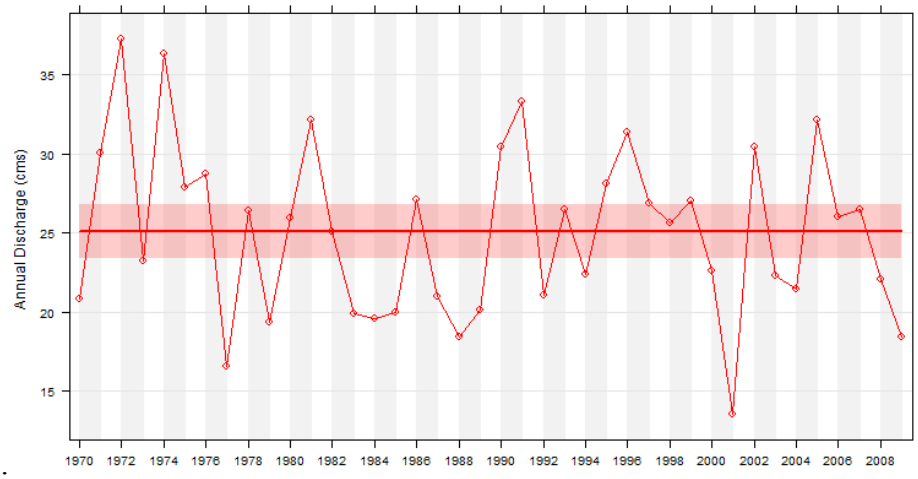

c.

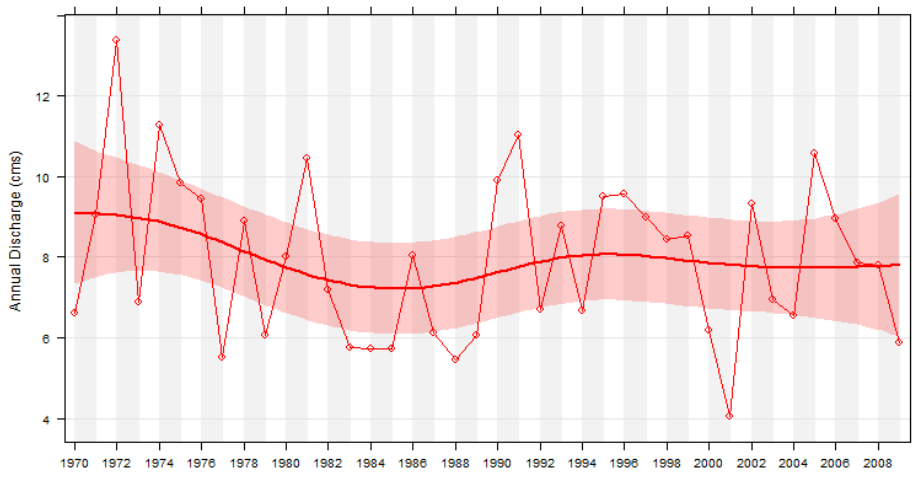

Figure 5-6. Non-monotonic trend analysis based on the annual mean for (a) 08NK002, (b) 08NK016, and (c) 08NK018 from 1970 to 2009. The pink band represents the 95% Cl range.

The mean non-monotonic trend for the 40 year period by month shows a linear relationship at 08NK002 for nine months of the year, 08NK016 for eight months of the year and 08NK018 for six months of the year (Figures C-10 to C-12). Table 5-7 outlines the change in the different stations by season, with the seasonal pattern at the most southerly station showing a different trend shape compared to the two northern stations (Figure C-13).

Table 5-7. Seasonal trends over the 40 year research period from 1970 to 2009.

Station	Winter (DJF)	Spring (MAM)	Summer (JJA)	Autumn (SON)
08NK002	Linear	Linear	Cyclic	Cyclic
08NK016	Cyclic	Linear	Linear	Linear
08NK018	Cyclic	Linear	Linear	Linear

The standard deviation for the three stations shows a linear pattern for 08NK002 and 08NK016 (the two research stations on the Elk River), whereas a cyclic pattern is observed for 08NK018 (Fording River), which has a pattern that is similar to the station's discharge pattern (Figure C-14). The cyclic versus linear pattern is consistent across the three stations in the spring; however varies between the northern stations (08NK016 and 08NK018) and southern station (08NK002). The cyclic versus linear pattern could be connected to the seasonal influence from the atmospheric teleconnection patterns on this watershed. The southern station is located within a band of high precipitation potential, as will be explained below. There is no change in the relative annual mean variability as determined based on the standard deviation for the three stations.

5.3.2.2 Monotonic Trends

Monotonic trend analysis was completed for the 40 year research period (1970 - 2009) on seven stations in the ERW (four on the Elk River, and three on tributaries to the Elk River). Trends were assessed for the seven stations mean monthly discharge and the mean annual discharge (Table C-2). There was generally a lack of significant trends with only two of a possible 14 showing a change. Station 08NK022 showed an increase of the mean monthly discharge of 0.2 $m^3 s^{-1}$ over the 40 year period ($p = 0.043$); and station 08NK027 showed an increase of the mean annual discharge of 2.77 $m^3 s^{-1}$ ($p = 0.033$) from 1970 to 1996 (26 years). A more detailed trend analysis was completed on the three discharge research stations: 08NK002, 08NK016 and 08NK018.

Trend assessment by annual mean and monthly mean discharge

Trend assessment determined from the annual mean discharge by decade over the 40 year period did not show any monotonic trend presences at $\alpha = 0.01$ (Figure C-15) either with or without the data pre-whitened prior to the trend analysis. In addition, no trend was observed for the full 40 year research period either using the mean monthly discharge data or the mean annual discharge data.

Season (mean monthly data)

Analysis of seasonal trends using mean monthly data shows no monotonic trends at $\alpha = 0.01$ for either of the two Elk River stations: 08NK002 and 08NK016 (Figure 5-7). The Fording River station (08NK018) has a statistically relevant monotonic positive trend ($\alpha = 0.1$) for autumn of 0.2 $m^3 s^{-1}$ over 40 years ($p = 0.050$) and a positive trend in the winter of 0.1 $m^3 s^{-1}$

over 40 years (p = 0.073). This translates to an increase in discharge at station 08NK018 of 5.2% during the autumn and 4.7% during the winter period. Pre-whitening was conducted in this analysis. Table C-3 provides the Theil Sen slope estimator results for all months, seasons and full year analysis based on the mean monthly discharge.

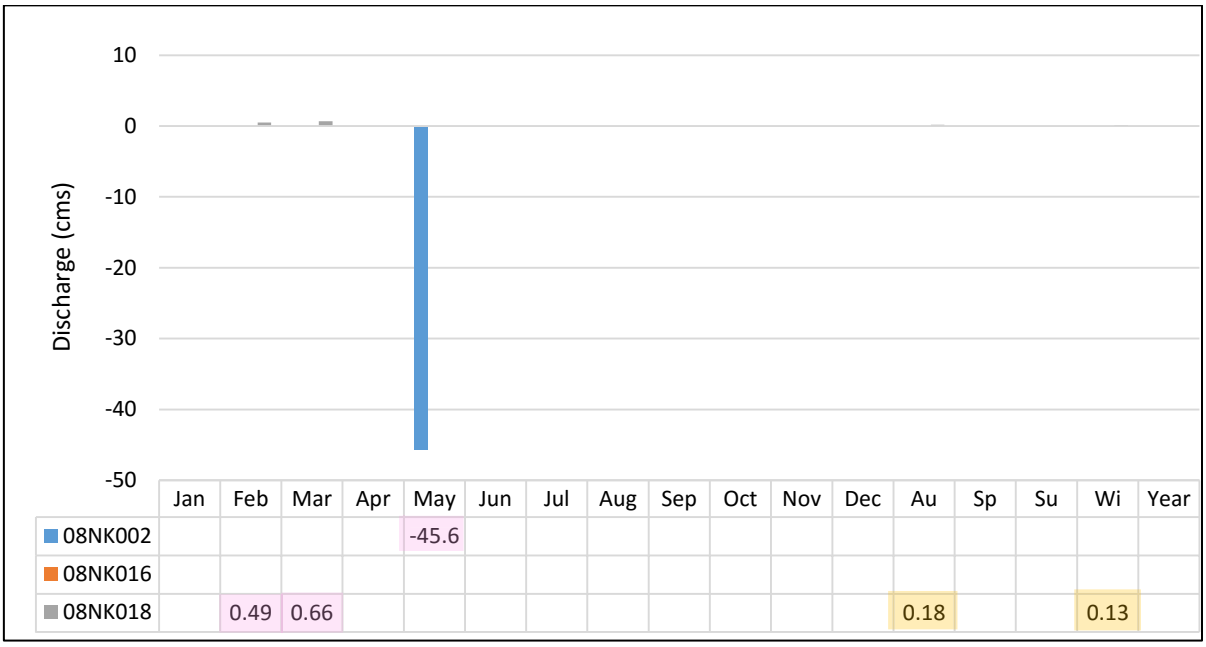

	Jan	Feb	Mar	Apr	May	Jun	Jul	Aug	Sep	Oct	Nov	Dec	Au	Sp	Su	Wi	Year
08NK002					-45.6												
08NK016																	
08NK018		0.49	0.66										0.18			0.13	

Figure 5-7. Monthly and seasonal statistically relevant trends extrapolated to a 40 year period (1970 to 2009). Pink boxes represent α = 0.05, and yellow boxes represent 0.05 < α <0.1. Note Au=autumn, Sp=spring, Su=summer and Wi=winter.

Month: by decade, bi-decade, full period

By performing a trend analysis per month in a mean monthly time-step, the serial correlation is removed from the data. As a result, no pre-whitening was required for analysis reported in Table 5-8. Similar to the seasonal findings above, station 08NK018 demonstrates a higher presence of statistically relevant monotonic trends (α = 0.05) compared to the other two research stations. From 1980-1989 a statistically relevant monotonic negative trend (α = 0.1)

during the summer period was present at all stations; this negative discharge trend was observed again during the summer period from 1970-1989 (Table 5-8). A positive trend of 40 $m^3 s^{-1}$ (over 20 years) was observed from 1970 to 1989 for the month of September, however, only at the southern station, 08NK002. The period from 1990-2009 continued the previously noted negative monotonic trend for the month of July in all three stations. Over the full 40 year period, only station 08NK018 demonstrated a positive monotonic trend during the winter and early spring months.

Table 5-8. Monthly trend analysis (a) per decade and (b) bi-decadal and full research period. Pink boxes represent α = 0.05, yellow boxes represent 0.05 < α <0.1, and results were not recorded if α > 0.1. Note 08NK002=002, 08NK016=016, and 08NK018=018. Units in $m^3 s^{-1}$.

(a)	1970-1979			1980-1989			1990-1999			2000-2009		
	002	016	018	002	016	018	002	016	018	002	016	018
J								-0.80				
F			0.60									
M												
A												
M												
J			-29.90			-15.60						
J				-45.20	-19.10	-5.30			-7.70			
A				-10.20	-7.90	-2.10						
S												
O												
N												
D												

(b)	1970-1989			1990-2009			1970-2009		
	002	016	018	002	016	018	002	016	018
J									4.00
F	-3.60								0.40
M									0.80
A			2.20						
M									
J	-94.40	-45.60	-27.40						
J	-60.00	-28.80	-7.60	-38.20	-24.600	-8.60			
A	-17.60	-11.00	-3.80	-14.40					
S	40.00								
O									
N									
D									

In summary, based on mean monthly discharge, a decrease in discharge was observed during the summer months, with the Fording River station (08NK018) being the only station to show a statistically relevant trend in the winter months, an increase in discharge.

5.3.3 Frequency Analysis

Frequency analysis can offer substantial insight to hydrological changes occurring within a watershed, and potentially thresholds associated with the watershed's natural buffering capabilities. The overlaying annual hydrographs (Figures C-5 and C-6) show the present, yet still uncommon, winter discharge spikes, likely related to rain events, the variation in discharge associated with the autumn rains, with the difference in the peak flows being pronounced. The

MK analysis in conjunction with linear regression was used to determine statistically relevant trends for the instantaneous peak flow, maximum annual flow and minimum annual flow. Smoothing trends and visual observations were used to support findings, as well as to present non-monotonic or non-statistically relevant trends. Only the Fording River station (08NK018) contained a statistically relevant trend for the minimum and maximum annual discharge (Table 5-9).

Table 5-9. Monotonic trends for peak instantaneous, maximum annual and minimum annual flow for 08NK018, 08NK016 and 08NK002. The pink box represents $\alpha = 0.05$, and the yellow box represents $0.05 < \alpha < 0.1$.

Station ID		MK (τ)	2-sided *p* value
08NK002	Peak Inst ($m^3 s^{-1}$)	-0.093	0.466
	Max Annual Flow ($m^3 s^{-1}$)	-0.167	0.133
	Min Annual Flow ($m^3 s^{-1}$)	0.122	0.273
08NK016	Peak Inst ($m^3 s^{-1}$)	-0.057	0.646
	Max Annual Flow ($m^3 s^{-1}$)	-0.130	0.244
	Min Annual Flow ($m^3 s^{-1}$)	-0.042	0.709
08NK018	Peak Inst ($m^3 s^{-1}$)	-0.105	0.367
	Max Annual Flow ($m^3 s^{-1}$)	-0.195	0.078
	Min Annual Flow ($m^3 s^{-1}$)	0.274	0.013

5.3.3.1 Peak Instantaneous Flow

Based on an R^2 value of 0.0 (08NK002) to 0.01 (08NK016) there are no trends to report for the instantaneous peak flow for 08NK002, 08NK016 and 08NK018 from 1970 to 2009 (Figure C-16), with a minimal negative shift observed. A more pronounced cyclic curve is identified; however, a four point polynomial trend curve still shows a low R^2 value: from 0.11 (08NK002)

to 0.12 (08NK016). There is no linear trend identified for the Julian date of the instantaneous peak flow at either of the three stations based on R^2 values of 0 to 0.01 (Figure C-17). Table 5-10 provides a brief overview of trend analysis for the instantaneous peak flows.

Table 5-10. Trend analysis for instantaneous peak flows for the three discharge research stations.

Stn. No.	Volume of Inst. Peak Flow	Timing of Inst. Peak Flow
08NK002	No SR* trend: cyclic (wave) neg. trend	No trend
08NK016	No SR* trend: cyclic (wave) neg. trend	No SR* trend, cyclic (wave) trend
08NK018	No SR* trend: cyclic (wave) neg. trend	No linear trend, concave trend present

SR* = Significantly Relevant

5.3.3.2 Maximum Flows

No statistically relevant trend for the Elk River maximum daily discharge was observed from 1970 to 2009; however, a statistically relevant negative trend ($\alpha = 0.1$) is present at the Fording River station (Table 5-9). However, there is a non-statistically relevant negative shift for the timing of the maximum discharge at all three stations (linear trend R^2=0.01 (08NK01) to 0.04 (08NK018)), which would suggest that the maximum discharge may be starting to shift to an earlier time period (Figure C- 18). The volume of the maximum flow has a non-statistically relevant negative trend (R^2=0.003 (08NK016) to 0.06 (08NK018)) for the three stations (Figure C-19).

5.3.3.3 Probability Density Function

Kernel density estimation (KDE) curves were completed for the three discharge research stations, divided into two and four sections based on an overlapping spread of four to six years.

Additionally, all three stations were analyzed based on the full 40 years. The KDE provides a visual of the discharge frequency; comparing the two and four periods offers insight as to whether changes to the discharge frequency have occurred throughout the watershed, and if the changes are comparable or different by station. The bandwidth was determined based the Sheather and Jones (1991) method.

Assessing at each station separately, the main difference is in the length of the tail (the high discharge events) and the peak frequency value (Figures C-20 to C-22). There is a general increase in the high discharge events in the 1970s and 1990s for all three stations. The maximum volume of similar discharge readings also varies per station, with an increase in the lower discharge values over the first 20 years, and a slight increase in discharge, reducing the peak, over the next 20 years for the Elk River stations. This does not appear to be the case for the Fording River, which keeps a similar volume pattern for the lower end discharge over the 40 years. The difference between the three stations can be seen in the overall increase in discharge for the second half of the research period on the Elk River, shown by a change in the density peak and longer tail in the latter half of the research period; whereas, the Fording River showed a similar density peak between the two periods and shorter tail in the latter half of the research period (Figures 5-8, C-20, to C-22).

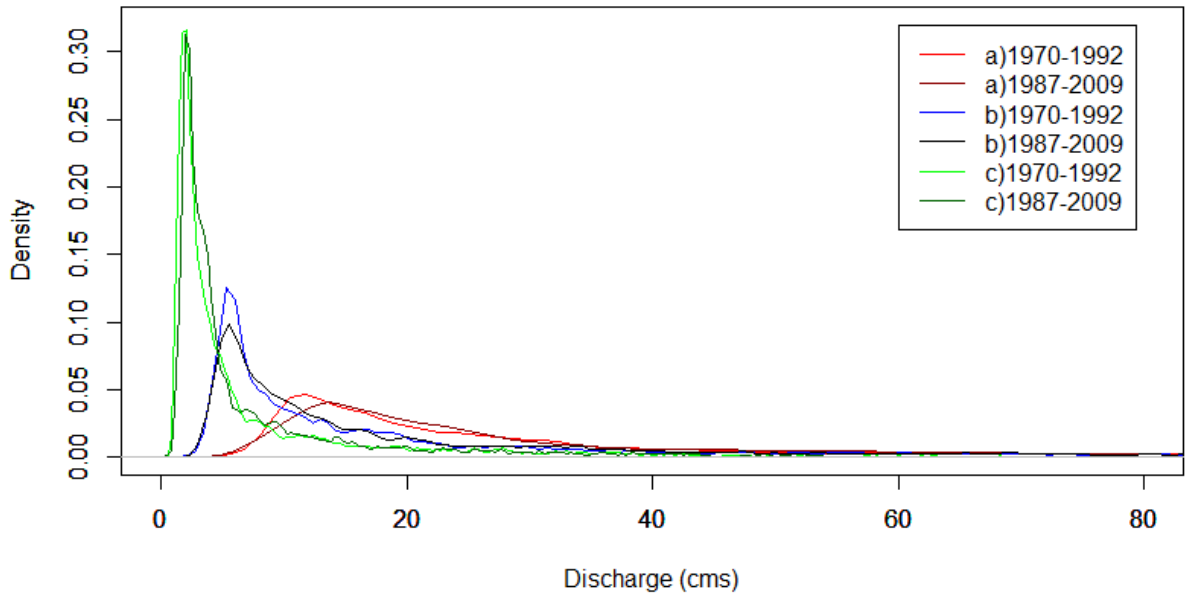

Figure 5-8. Kernel Density estimation for daily discharge stations (a) 08NK002, (b) 08NK016 and (c) 08NK018.

5.3.3.4 Start of Freshet

As described in Chapter 3, two methodologies were used to identify the start of freshet: (1) Zhang et al. (2001), and (2) Burn et al. (2004). There is a non-statistically relevant positive shift (freshet occurring later) when assessing the data based on the Zhang et al. (2001) approach for all three stations (Table 5-11 and Figure C-23[26]). This is contrary to the timing trend shown in the instantaneous peak flow and maximum annual flow, both either showing a negative (non-statistically relevant trend) or no trend at all. The Burn et al. (2004) approach does not adequately describe the start of freshet in the ERW. This method appears to be strongly influenced by the effects of winter rain-on-snow events that can result in a spike in the winter discharge, causing this method to identify the start of freshet in the winter months. As the climate continues to warm, the occurrence of winter period rain-on-snow events will likely

[26] In 2004, there was insufficient comparative rise in the discharge at station 08NK002 to meet this methods requirements to identify freshet, as a result a NA placeholder was added.

continue to increase, which could make this methodology difficult to use in snow-dominated watersheds in BC.

Table 5-11. Summary of findings from change in the start of freshet and the point where 50% of that year's water volume has been reached, based on approaches developed by other researchers.

Stn. No.	Start of Freshet (Zhang et al. 2001)		Annual 50% Volume (Burn 1994)	
	R^2 (linear)	*p* value	R^2 (linear)	*p* value
08NK002	0.02 (positive)	0.365	0.00	0.883
08NK016	0.01 (positive)	0.660	0.00	0.888
08NK018	0.02 (positive)	0.362	0.00	0.835

5.3.3.5 Annual 50% volume

The Burn (1994) method for determining the date when, based on the water year, 50% of the annual volume has been achieved, was developed as a means to incorporate rain-on-snow events but does not let these events determine the outcome (such as change detection methodologies). Neither of the three research stations showed a statistically significant linear trend with regards to the 50% volume timing (Table 5-11). With $R^2 = 0$, there are no trends to report (Figure C-24).

5.3.3.6 Low Flows

Low flow analysis was calculated based on the Water Year (October 1 to September 30) since in the ERW the low flow period often happens at the end of the Calendar Year period (December to January). Over the 40 year research period the date showing the lowest flow for

that year has a non-statistically relevant increase at station 08NK002, more a polynomial trend (R^2=0.14) than linear (R^2=0.04) (Figures C-25 and C-26). Correspondingly, there is a non-statistically relevant increase in the low flow quantity over the past 40 years (Table 5-12). Fitting a LOWESS curve to the data points, shows that the variation is more linear than cyclic.

Table 5-12. Summary of low flow findings for the discharge research stations.

Activity	08NK002	08NK016	08NK018
Date of lowest flow	Non statistically relevant increase (R^2=0.04)	No linear trend, non-monotonic trend with a decrease in the last 15 year (R^2=0.15)	Non statistically relevant decrease (R^2=0.06)
Low flow discharge ($m^3 s^{-1}$)	Non statistically relevant positive shift (R^2=0.06)	Non statistically relevant positive shift (R^2=0.02)	Statistically weak positive shift (R^2=0.17)

These low flow findings, showing a tendency towards an increase in the low flow discharge, corroborates the findings from Section 5.3.3.3 showing an increase in the low flow discharge.

5.4 Climate

Monotonic and non-monotonic temporal trends were analyzed over the 40 years, bi-decade, decade and month time periods. Micro-climates and overall climatic variability is common in the ERW, so analyzes were completed using only observed data. That being the case, micro-climates can occur outside of the monitoring station's recording area, thereby affecting discharge but are not visible in the climate data. Focus was placed on two climate stations,

one located in the northern portion of the watershed (1152899) and the other in the centre of the watershed (1152850), analyzing both for precipitation (total, rain and snow) and temperature (minimum, mean and maximum). Snow data (snow water equivalent) were analyzed from three monitoring stations (2C07, 2C16 and 2C09P/Q) managed by the BC RFC of MFLNRO (Table 3-2).

5.4.1 Precipitation

Precipitation data were used from 10 climate stations throughout the ERW to characterize precipitation variation in the basin, while trend estimation was completed on the two aforementioned climate research stations. A comparatively higher precipitation band was observed through the mid to mid-upper portion of the watershed, with precipitation records both in the north and south sections of the watershed showing similar results. The trend analysis presented a statistically significant reduction in the quantity of winter precipitation at both climate stations, in contrast to the statistically significant precipitation increase revealed during the spring.

5.4.1.1 Descriptive Statistics

Comparing the precipitation IQR (Figure 5-9) from the 10 representative climate stations, the band of higher precipitation is observed just north of Fernie (EC850) to Corbin (EC915). To improve the effectiveness of correlating these stations, the time period for this assessment was reduced from the full research period to 1970 - 1995, with the number of years in the analysis ranging from 7 to 22 (Table D-1). Both stations 690 and 282 are located outside of the ERW boundary; however, due to their proximity to the watershed, and the lack of appropriate climate

stations present in this area, they were included in this comparison. This plot was produced using the average total annual precipitation per station (based on a 95% threshold). With a CV range between 14.4% and 24.4%, there appears to be a negative shift between the CV and station elevation (R^2 = 0.08), although more analysis is required to confirm this tendency. When calculating the precipitation based on a 90% threshold (monthly calculation) and 95% threshold (annual calculation) for five chosen stations, there was approximately a 1-7% reduction in the total reported precipitation when a 90% threshold was used compared to a 95% threshold (Table D-2).

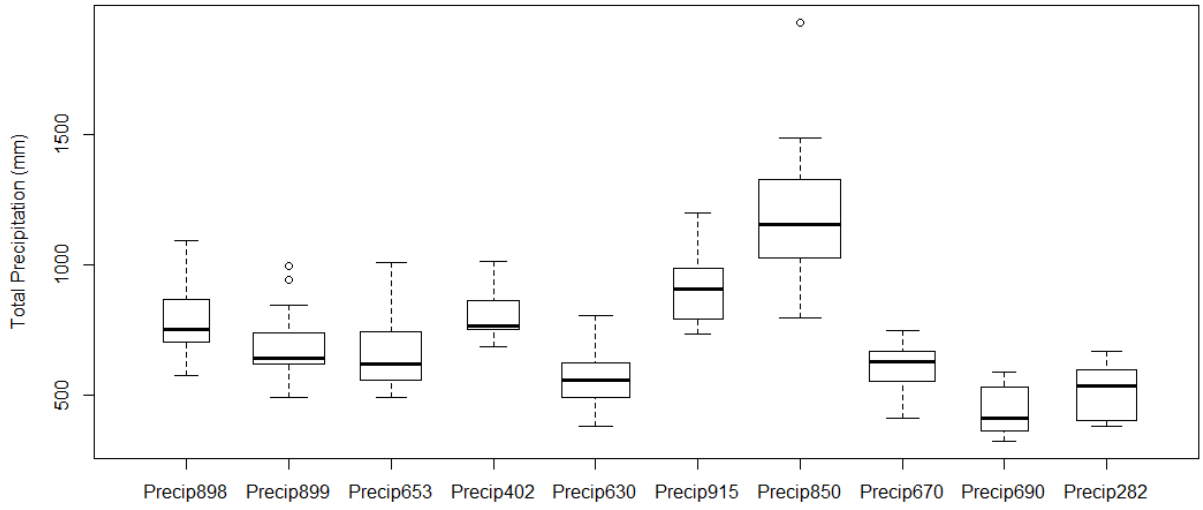

Figure 5-9. Annual precipitation for climate stations in and around the Elk River watershed; 1970 to 1995. Plot interpretation defined in Section 4.5.3.

Incorporating the annual precipitation data from the 10 climate stations, and comparing them based on latitude and elevation, it is possible to identify an increase in the precipitation quantity located in the mid/lower north portion of the watershed. A non-statistically relevant linear relationship is shown between all stations (Figure 5-10), when comparing mean annual precipitation with the station elevation (R^2 = 0.09). However, if the two mid-basin stations

from this regionalization analysis are removed, the linear relationship converts to a strong correlation ($R^2 = 0.85$) (Figure 5-11).

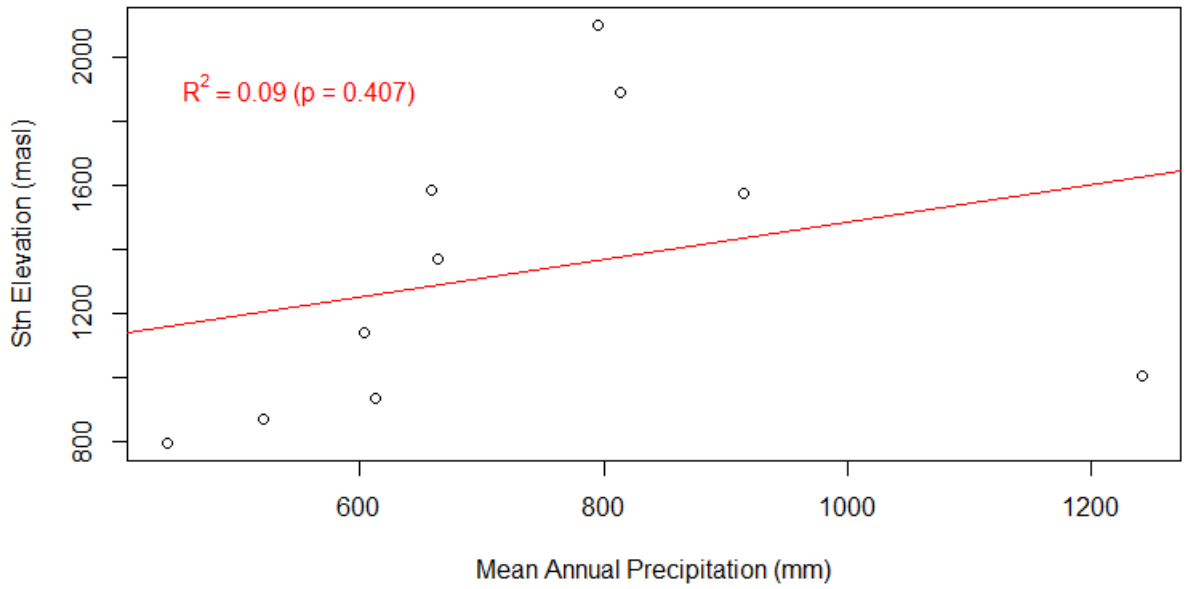

Figure 5-10. Mean total annual precipitation by elevation for the 10 climate stations in the Elk River Watershed (1970-1995).

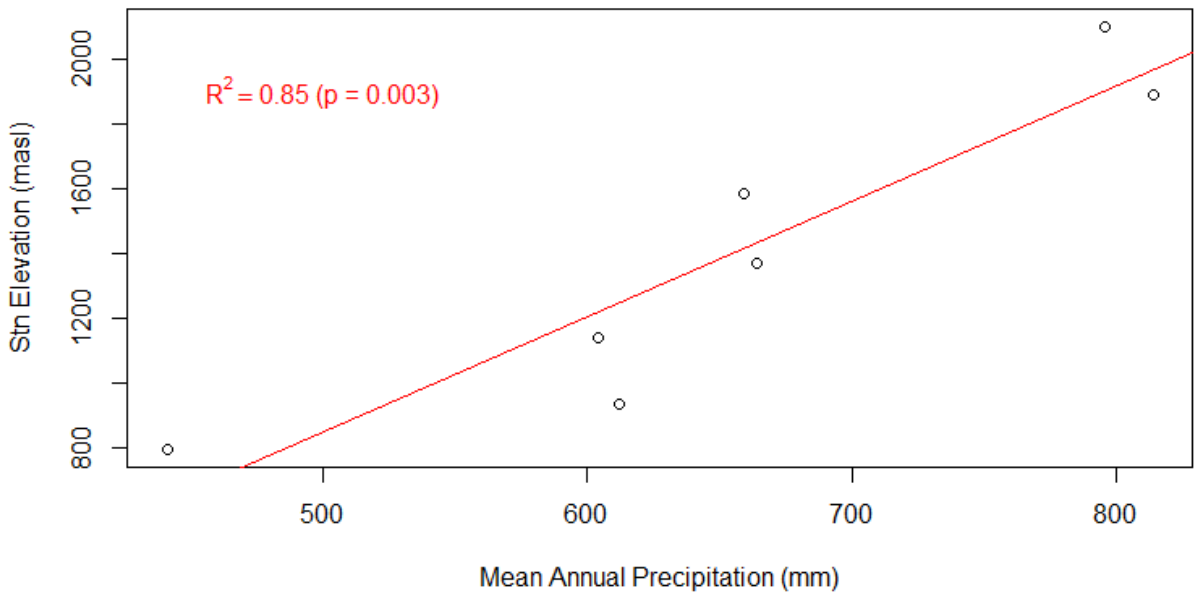

Figure 5-11. Upper northern and lower southern Elk River watershed climate stations, showing linear correlation by elevation with the two mid stations (EC850 and EC915) removed.

There are three snow monitoring stations managed by the RFC located in the ERW (Figure 3-5). Two of the stations are operated manually (2C07 and 2C16) and accessed monthly to record the data. The station 2C09Q (previously 2C09P) is automated and is supported by telemetry allowing for real time data transmitting. The IQR (Figure 5-12) for the snow water equivalent (SWE) data from the RFC stations show the three manual stations[27] containing a much narrower spread of data compared to the information obtained from the automated station. For this analysis, the first of the month was used from station 2C09 rather than taking the mean of the month to improve the ability to compare the automated and manual stations (the comparison between the two methods is shown in Figure D-1). Comparing the RFC snow stations by elevation and latitude, the latitude of the stations appears to have more of an influence on SWE than the elevation of the station as the station the farthest north also shows the highest snow depth. Although this is not the case when one includes the automated station (2C09) as shown in Figure 5-11. The band of higher precipitation is not as prevalent based on the manual RFC snow stations, although the range in the density is greater at the Fernie snow station (2C07) compared to the other two manual stations (Figure D-2).

[27] Station 2C17 has been included in this initial analysis, as it is located just west of the Elk River Watershed (Figure A-1).

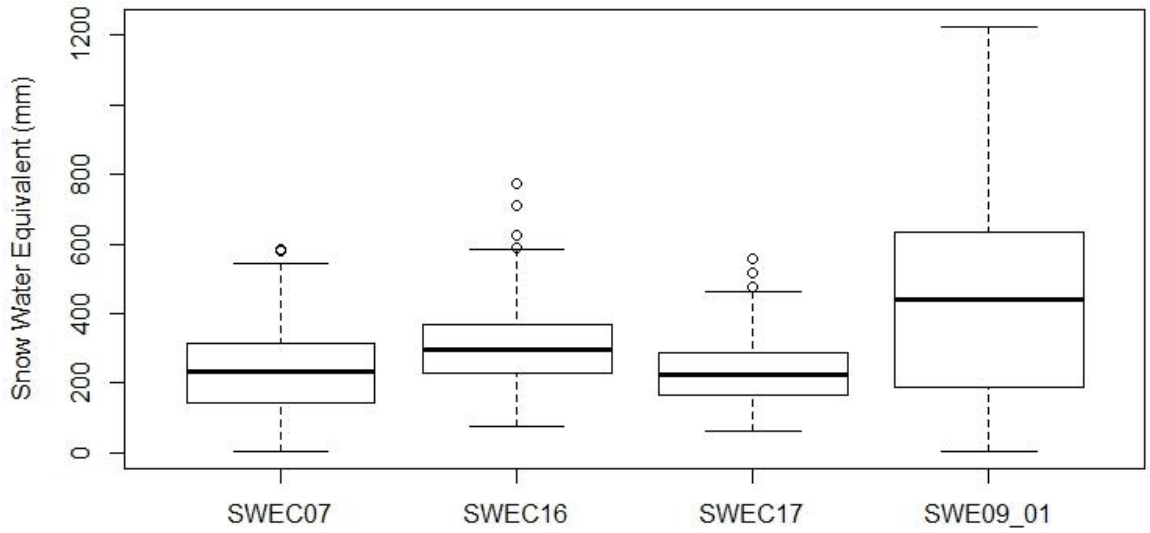

Figure 5-12. Monthly snow water equivalent (SWE) data for the four River Forecast Centre snow monitoring stations in and around the Elk River Watershed. Station 2C17 (SWEC17) is west of the Elk River watershed. Station 2C09P/Q (SWE09_01) results equate to the value from the first of the month. Plot interpretation defined in Section 4.5.3.

Table 5-13 provides the annual peak values, and associated month, for each station. Station 2C07 contains readings until June 1, whereas the other two stations only show readings until May 1. As a result, the May 15 and June 1 readings have been removed from station 2C07 for this analysis.

Table 5-13. Maximum value and associated month for RFC snow monitoring stations 2C07, 2C16 and 2C17.

	2C07	2C16	2C17*
Mean Depth (cm)	100 (March)	112 (April)	103 (April)
Max Depth (cm)	180 (March)	193 (April)	168 (May)
Mean SWE (mm)	309 (April)	375 (April)	300 (May)
Max SWE (mm)	579 (April)	772 (May)	556 (May)
Mean Density (%)	34 (May)	35 (May)	31 (May)
Max Density (%)	45 (May)[28]	44 (May)	37 (May)

* 2C17 (Thunder Creek station) is located west of the ERW

5.4.1.2 Trends

Trend estimates were completed for total precipitation, snow and rain at stations EC899 and EC850, and for SWE from stations 2C07, 2C16 and 2C09P/Q. Analysis was completed using: (i) total monthly sum for total precipitation, rain and snow; (ii) mean monthly for SWE; and (iii) total annual for precipitation, rain and snow. The monthly and annual assessments matched the 90% and 95% thresholds as described in Section 4.4. For the climate stations trend analysis, the time periods included by month, by season, by decade, and the full period of research (40 years). For the RFC snow monitoring stations, the SWE trends were analyzed by month and over the length of the research period (40 years).

There was serial correlation present in the daily and monthly total precipitation data for both stations EC850 and EC899, and as a result pre-whitening was conducted. No serial correlation

[28] A maximum monthly reading of 54% was taken during the reporting period of May15th. This was not reported in this research, as the other two stations do not have readings for May 15 or June 1st.

was present for the annual total precipitation. There were 32 years of precipitation data for station EC899 and 37 years of precipitation data for station EC850 out of a possible 40 years. There are 29 years between 1970 and 2009 where both stations have ≥ 90% of available data. Based on these 29 years, station EC899 has just over half (55%) the amount of precipitation as station EC850, when comparing month by month the difference is almost the same at 54% (Figure D-3). The variation in the precipitation pattern between the two stations can be seen in Figure D-4, showing a statistical difference in precipitation, based on the normalized levels, between the two stations only during the summer and a portion of the autumn months.

Annual sum analysis

Non-monotonic trends show an increase in precipitation, and a stronger increase in rain over the past two decades (Figure D-5). Conversely, the snow levels are showing a linear decline over the 40 year period. Areas where there are no data points represent years where there was ≤ 95% available data. The only statistically significant trends for station EC850, based on the mean annual value, is the snow parameter with an average decrease of -2.7 mm yr^{-1} (p=0.0775) from 1970 to 2009, and a statistically relevant decrease of -27.8 mm yr^{-1} (p=0.0165) from 1970 to 1979 (Table 5-14). Station EC899 has proportionally more statistically significant trends based on the annual mean precipitation data analysis (Table 5-14). A statistically significant trend is observed in the precipitation (i.e. total, rain and snow) over the 40 year period in station EC899; showing a decrease in total precipitation and snow, and an increase in rain. This trend is corroborated with the non-monotonic graph (Figure D-6) showing the strong decline in the snow parameter. The strong decrease in precipitation from 1970 to 1979 could be correlated with the end of the PDO cool phase, which occurred in 1976 (see Section 6.2).

Table 5-14. Statistically relevant trends, based on mean annual values, for climate station 1152899 and 1152850. Pink boxes represent α = 0.05, and yellow boxes represent 0.05 < α <0.1.

Stn. ID.	Variable	Time	Slope (mm yr^{-1})	CI-lower (mm yr^{-1})	CI-upper (mm yr^{-1})	*p*
1152899	Precip	1970-2009	-6.06	-10.51	-2.57	0.004
1152899	Rain	1970-2009	2.95	0.22	5.42	0.030
1152899	Snow	1970-2009	-7.50	-10.65	-4.23	0.000
1152850	Snow	1970-2009	-2.73	-5.84	0.44	0.078
1152899	Precip	1970-1979	-38.36	-69.95	-11.44	0.036
1152899	Snow	1970-1979	-34.15	-81.42	-29.12	0.016
1152850	Snow	1970-1979	-27.83	-49.24	-16.94	0.017
1152899	Precip	1970-1989	-6.10	-26.40	0.80	0.093
1152899	Snow	1980-1989	-25.61	-14.21	-14.21	0.089
1152899	Rain	2000-2009	61.71	-20.99	74.23	0.060

Monthly sum analysis

Similar to the annual mean trends, a stronger trend presence is identified at station 1152899 compared to station 1152850. In general, a decrease in winter precipitation was observed during this period, with an increase in spring precipitation (Figure 5-13). The greatest change of precipitation is observed in December showing a decrease of 89 mm (p = 0.0353) and 79 mm (p = 0.0025) over the 40 year period. Table D-3 provides the Theil Sen slope estimator results for all months, seasons and full year analysis based on the mean monthly discharge.

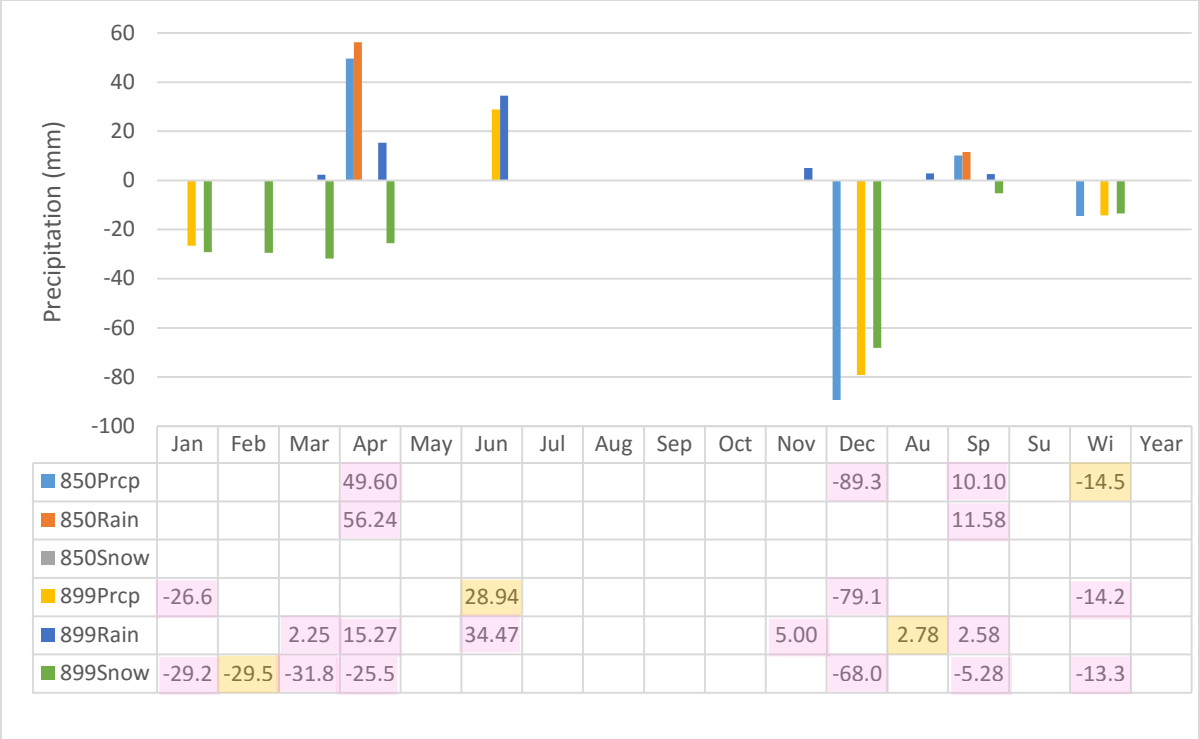

	Jan	Feb	Mar	Apr	May	Jun	Jul	Aug	Sep	Oct	Nov	Dec	Au	Sp	Su	Wi	Year
850Prcp				49.60								-89.3		10.10		-14.5	
850Rain				56.24										11.58			
850Snow																	
899Prcp	-26.6					28.94						-79.1				-14.2	
899Rain			2.25	15.27		34.47					5.00		2.78	2.58			
899Snow	-29.2	-29.5	-31.8	-25.5								-68.0		-5.28		-13.3	

Figure 5-13. Monthly total precipitation trend analysis over 40 years from 1970 to 2009. Pink boxes represent $\alpha = 0.05$, and yellow boxes represent $0.05 < \alpha < 0.1$. Note Au=autumn, Sp=spring, Su=summer and Wi=winter.

Based on a significance level (α) of 0.1, an increase in precipitation during the spring, and inversely a decrease in precipitation over the winter months can be observed in the non-monotonic analysis as well for both stations, with a significantly stronger decline in the northern station. The seasonal trends, based on monthly data totals, match the monotonic results with an increase in the spring and decrease in the winter for station 1152850; and a strong decrease in the winter precipitation for station 1152899 (Figures 5-13, D-7 and D-8). Based on the monthly analysis over the 40 year period, the non-monotonic trends differ somewhat per station. There is a strong increase in the April precipitation and the strong linear decrease in the December precipitation for station 1152850; whereas, station 1152899 shows the strong decrease in precipitation for both January and December (Figures D-9 and D-10). However, the slight increase in the snow and decrease in the rain during the spring months

results in a high variability in the precipitation total. The month of July shows a strong cyclic trend, with a peak in the 1990s and decreasing on either side.

To explore further the reducing winter precipitation, the trend associated with the proportion of snow versus rain was assessed for the 40 year period. Showing an R^2 value of 0.23, both stations demonstrated a statistically relevant decrease in the percentage of snow versus rain from 1970 to 2009 (Figure 5-14). The mean percentage of snow to precipitation for stations EC850 (1152850) and EC899 (1152899) is 23% and 53% respectively.

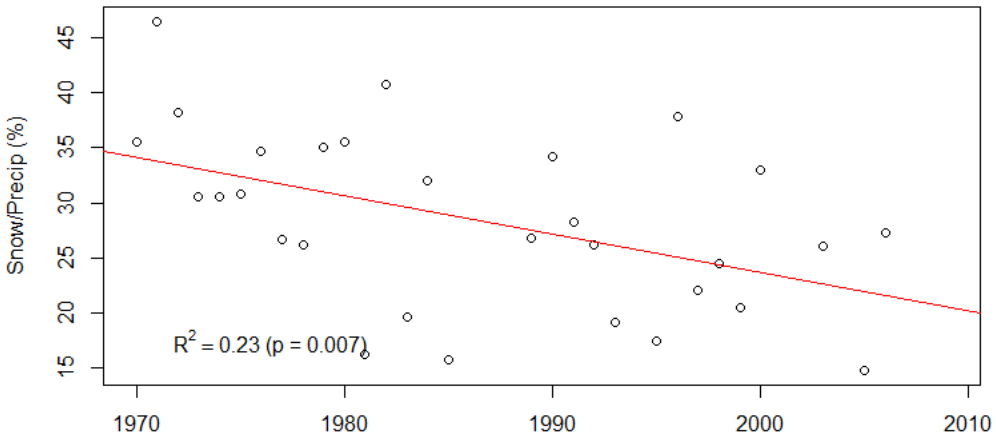

a.

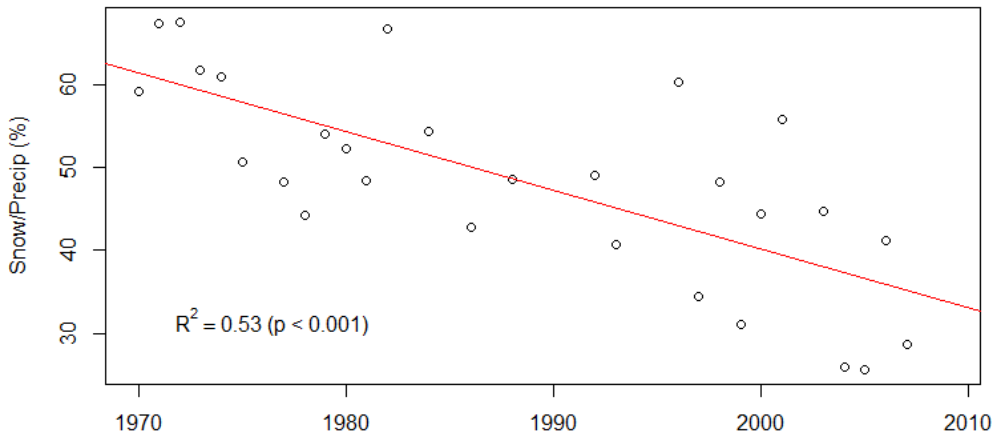

b.

Figure 5-14. Comparison of snow versus rain between 1970 and 2009 for stations (a) 1152850 and (b) 1152899.

An overall decrease in the SWE in the past 40 years can be seen both through graphs and associated linear correlation assessment (Tables 5-15 and 5-16). The SWE data show serial correlation, so prior to completing the trend analysis of the entire period, pre-whitening was required. Trend analysis over the 40 year period demonstrated a strong negative trend in the Fernie snow monitoring station, more so with the manual site than the automated site. This is likely due to the uneven length of record, as the automated site collects data before January and after June, which are the boundaries of the manual site. Based on a monthly trend analysis, site 2C07 shows the strongest trend presence, with the month of May showing a strong negative trend.

Table 5-15. Mann-Kendall analysis on snow water equivalent in the Elk River Watershed. Pink boxes represent $\alpha = 0.05$.

Stn. No.	τ	p	Theil Sen slope (per month)
2C07	-0.16	0.004	-0.34
2C16	-0.06	0.362	-0.14
2C09P/Q	-0.11	0.032	-0.65

Table 5-16. Trend assessment by month for SWE from RFC monitoring stations. 1970 – 2009. Pink boxes represent $\alpha = 0.05$, and the yellow box represents $0.05 < \alpha < 0.1$.

	Jan		Feb		March		April		May	
Stn. No.	τ	p	τ	p	τ	p	τ	p	τ	p
2C07	-0.13	0.29	-0.14	0.23	-0.24	0.03	-0.27	0.01	-0.32	0.01
2C16	-0.20	0.28	-0.11	0.36	-0.18	0.12	-0.14	0.22	-0.11	0.33
2C09P/Q	-0.21	0.14	-0.23	0.09	-0.28	0.04	-0.18	0.19	-0.01	0.93

5.4.2 Air Temperature

5.4.2.1 Descriptive Statistics

There is a fairly consistent temperature median throughout the ERW based on the 10 climate stations studied (Figures 5-15 and 5-16). As expected, the mean values show a comparative increase in temperature when comparing the southern stations to the northern stations in the ERW (Table 5-17). Figure 5-15 identifies station EC282 as having the highest summer temperature reading (18.3°C) out of the group, and station 898 contains the lowest temperature reading during the winter months (-11.8°C).

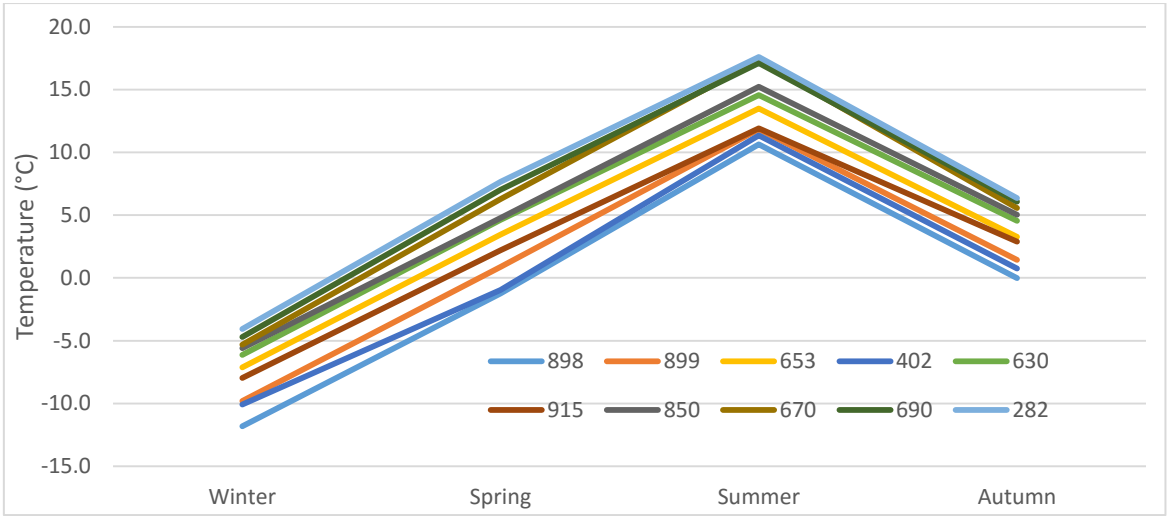

Figure 5-15. Annual mean air temperature by season for climate stations in and around the Elk River Watershed.

Table 5-17. Descriptive statistics for four climate stations in the Elk River Watershed; two in the northern sub region: EC899 and EC630 (station 1157630) and two in the central to southern sub region: EC850 and EC670 (station 1152670) for 1970 to 2013.

	EC899	EC630	EC850	EC670
Elevation (masl)	1585	1138	1001	931
Start Date	1970	1980	1970	1970
End Date	2013	2011	2013	2000
Years of Data (>90% of yr complete)	33	29	36	19

Climate Parameters	EC899	EC630	EC850	EC670
Years of Data (>90% of yr complete)	33	29	36	12
Mean Minimum (°C)	-1.4	2.5	2.9	4.9
Mean (°C)	1.1	4.5	5.0	5.9
Mean Maximum (°C)	3.0	5.8	6.9	7.2
SD (°C)	1.0	0.8	0.9	0.7
Absolute minimum (°C)	-49.0	-39.8	-39.0	-35.0
Absolute maximum (°C)	37.5	36.5	37.0	36.7
Mean Annual Precipitation (mm yr^{-1})	650.7	603.3	1191.7	595.6
Yrs. of Data (>90% of yr. complete)	32.0	29.0	37.0	42.0
SD (°C)	130.4	124.4	250.6	108.2
CV (%)	20.0	20.6	21.0	18.2

Figure 5-16 shows the IQR for the mean annual temperature for the 10 representative climate stations from north (left) to south (right). Even though Stations 402 (1155402) and 630 (1157630) are located within close proximity of each other, there is a 750 m elevation difference between the two stations, 1889.8 m and 1136.7 m respectively, resulting in the large

difference in mean annual temperature. Station 915 is located farther away from the other stations, on the eastern border of the watershed, with an elevation of 1572 m. The number of available years in this calculation ranges from 7 to 17. Based on the mean annual temperature compared to the station's elevation, there is a strong linear correlation with an R^2 of 0.97 (Figure E-1).

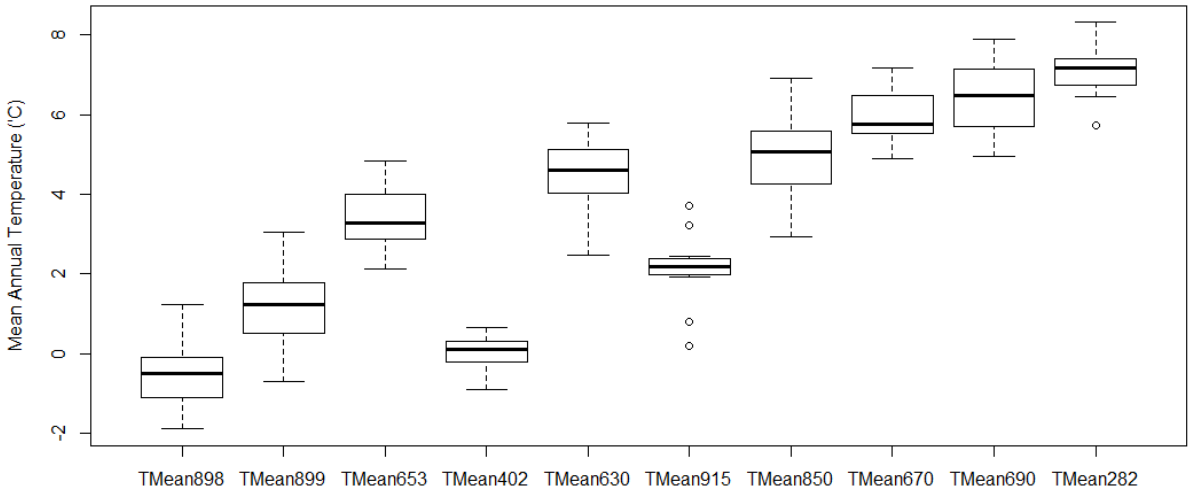

Figure 5-16. Mean annual temperature for climate stations in the Elk River Watershed for the period 1975-1995.

5.4.2.2 Trends

There is a strong serial correlation in the daily data and the calculated monthly mean, so pre-whitening was used prior to trend analysis; similar to the other parameters, when comparing individual months or using the annual mean values, serial correlation was not present.

The annual temperature trend analysis was completed for the maximum, mean and minimum temperature datasets. An overall increase in the maximum temperatures for both stations (α = 0.1), and increase in the mean southern station occurred over the 40 year period (Table 5-18).

Assessments were completed per decade, with statistically relevant negative trends present between 1980 and 1989 for the northern station.

Table 5-18. Statistically significant temperature trends for climate station 1152899 and 1152850 from 1970 to 2009. Pink boxes represent α = 0.05, and the yellow box represents 0.05 < α <0.1.

Stn No.	Parameter	Time Period	Slope (°C)	CI lower (°C)	CI upper (°C)	*p*
1152899	Max Temp	1970-2009	0.04	-0.00	0.09	0.062
1152850	Max Temp	1970-2009	0.04	0.01	0.06	0.005
1152850	Mean Temp	1970-2009	0.05	0.01	0.08	0.022
1152899	Min Temp	1980-1989	-0.56	-0.89	-0.40	0.035

Monthly mean trend analysis was completed on the minimum, mean and maximum temperature data. The southern station displayed statistically relevant positive temperature trends (α = 0.1) for five out of 12 months, spread fairly evenly throughout the year (Figure 5-17 and Table E-1). The northern station did not show a significantly positive temperature trend based on monthly total analysis; on the contrary, statistically relevant negative trends were observed for the month of June (α = 0.1). Table E-1 provides the Theil Sen slope estimator results for all months, seasons and full year analysis based on the mean monthly discharge.

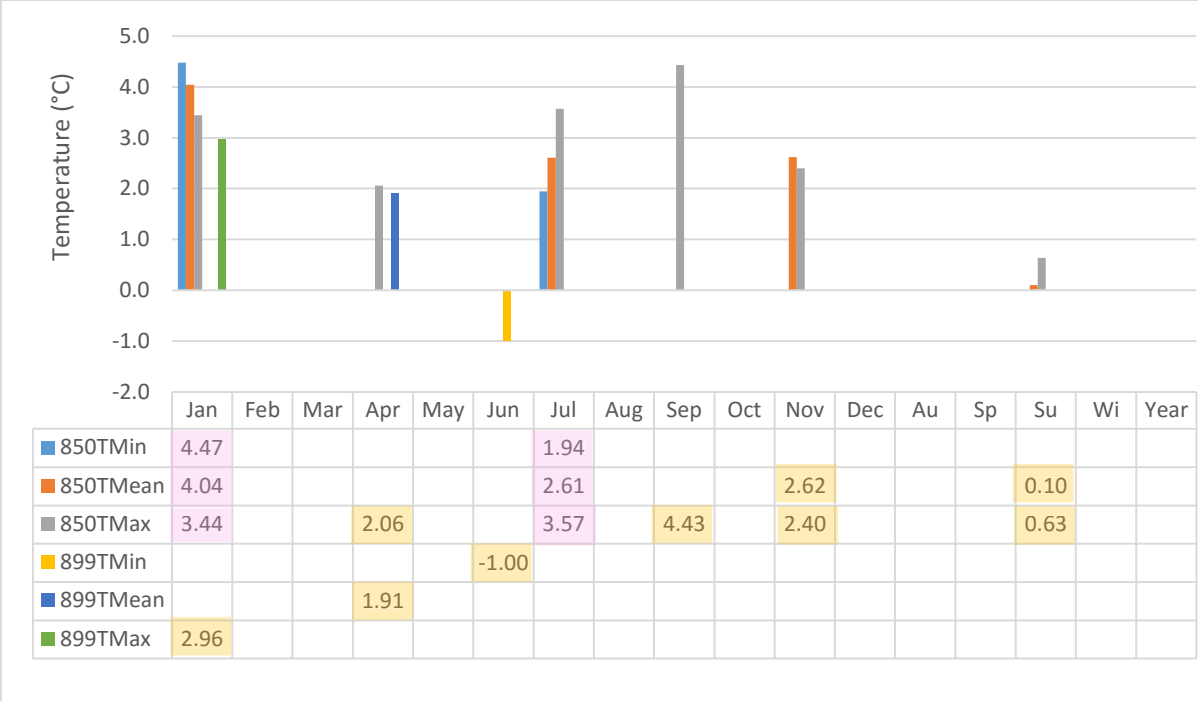

	Jan	Feb	Mar	Apr	May	Jun	Jul	Aug	Sep	Oct	Nov	Dec	Au	Sp	Su	Wi	Year
850TMin	4.47						1.94										
850TMean	4.04						2.61				2.62				0.10		
850TMax	3.44			2.06			3.57		4.43		2.40				0.63		
899TMin						-1.00											
899TMean				1.91													
899TMax	2.96																

Figure 5-17. Estimated monotonic trends over the 40 year research period. Analysis was completed using monthly mean data. Pink boxes represent $\alpha = 0.05$, and yellow boxes represent $0.05 < \alpha < 0.1$. Note Au=autumn, Sp=spring, Su=summer and Wi=winter.

The non-monotonic trends show a general linear increase with the annual mean data for minimum, mean and maximum temperature from station 1152850 (Figure E-2). Conversely, the trends do not follow the same pattern for station 1152899 with a concave trend for maximum temperature, a positive linear trend for mean temperature and a convex trend for the minimum temperature (Figure E-3). The flex point for the minimum and maximum temperature trends appears to be in the 1990s, the same period where a shift in the PDO from a warm phase to a cool phase occurred. The seasonal smoothing trend lines (Figures E-4 and E-5) show a weak to no trend present at station 1152850 for the spring and autumn periods, a slight upwards trend in the summer period and a more defined upward trend in the winter period. Station 1152899 has a similar response to the spring and autumn period, however the summer and winter periods exhibit concave trends for the maximum temperature, a convex

pattern from 1975 to 1985 for the minimum temperature during the summer followed by no change and minimal to no change for the mean and minimum temperature during the winter period.

The monthly analysis shows an increase in temperature during January, February, July, September and November, and a cyclic trend in April, June and December (Figures E-6 and E-7). The monthly analysis does not show a steady pattern between the two climate stations (Figure 5-18), outlining the variations in temperature patterns that are prevalent throughout the watershed. Station 1152899 does not demonstrate the strong increase in temperature for the winter months as observed in the southern station, with the maximum temperature showing the concave pattern for February, March, July, August, November and December. The non-monotonic graphs help explain why there were so few trends present for station 1152899 in the monotonic analysis.

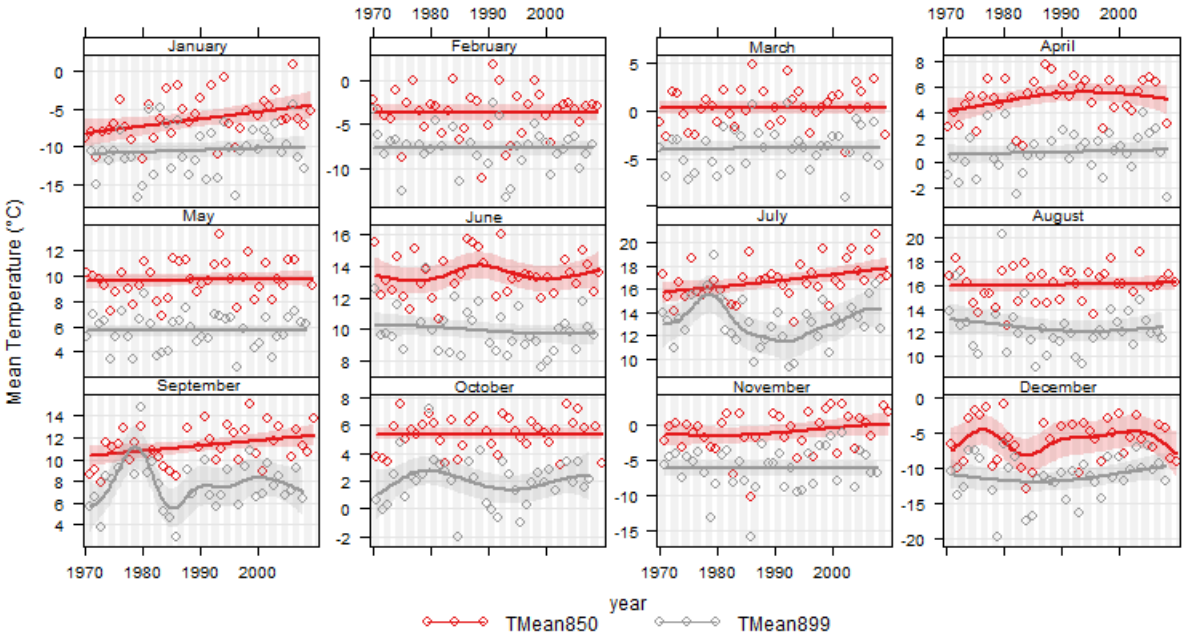

Figure 5-18. Trend comparison for mean temperature at station 1152850 and 1152899, from 1970 to 2009.

5.5 Discussion

The climatological trends in the ERW display a northern/central area split showing a higher percentage of precipitation trends (both positive and negative) in the northern portion (Figure 5-13) compared to a higher percentage of temperature trends (positive) in the central portion of the ERW (Figure 5-17). The percentage of statistically relevant discharge trends throughout the watershed is low over the 40 year period, with the Fording River station showing the strongest presence of a trend. When the trends are investigated by decade and bi-decade, a decrease in the summer discharge is apparent.

Discharge at the Fording River (station 08NK018), which has the smallest drainage basin of the three discharge research stations and the highest percentage of surface mining activities, demonstrated the highest presence of trends, showing a decrease in discharge during the summer months, and an increase during the latter winter months. The decrease in discharge matches the findings by Brahney (2014) who observed that 95-98% of streams assessed in the CRB showed a decrease in late summer discharge. Brahney (2014) reports a general decrease in discharge in all seasons across the East Columbia region[29], although none that proved to be statistically significant. This finding differs to the increase in discharge observed at the Fording River station for both the autumn and winter periods.

The BC population has increased significantly from 1905 to 2005, from 0.26 million to 4.26 million people, respectively (Ministry of Forests and Range, 2006). The Columbia River Basin (CRB) population consists of 3.7% of the total 2006 BC population (Columbia Basin Trust,

[29] The East Columbia region includes the ERW.

2008), so the urban expansion is less than would be observed in other regions in BC. From 2000-2013 there was a loss of 8% of cumulative forest cover in the ERW (Figure A-7); however, this time period does not take into account the surficial disturbance from mine shafts to open-pit coal mining that occurred in the late 1960s (Katay, 2014).

The earlier onset of freshet reported in many hydrological studies does not match the timing of the peak flow in the ERW (which showed no change), but does coincide with the maximum annual discharge, which appears to be occurring (not statistically relevant) earlier in the year. However, based on the Zhang et al. (2001) approach for determining the start of freshet, there is a non-statistically relevant positive shift (freshet starting later) in the ERW. These results match the Brahney (2014) findings that show the CRB freshet happening later in the year.

The literature review is fairly consistent with an increase in temperature throughout BC over the past century; while showing an increase in overall precipitation, however a decrease in the quantity of snow. In the ERW a positive trend in temperature is identified; with a reduction in the annual precipitation in the northern portion tied to the decrease in the snow percentage. However, this increase in the central temperature and an overall reduction of northern precipitation (with an increase in the percentage of rain) does not provide a direct correlation to the increase in Fording River discharge and overall decrease in summer discharge based on the bi-decade assessment.

Table 5-19. Summary of hydro-climatological trend results for the Elk River Watershed compared to other research in the Columbia River Basin (CBR) and British Columbia (BC).

Results	Literature Review
Discharge	
Later freshet shift (not statistically relevant) based on methodology by Zhang et al. (2001).	Generally earlier freshet expected; but CBR has shown a later freshet (Brahney, 2014).
Increase in winter discharge at Fording River (08NK018).	Both increases and decreases have been reported, region specific.
Increase in the maximum and minimum discharge levels for Fording River (08NK018).	Both increases and decreases have been reported, region specific.
Decrease in summer discharge during first 20 years (all stations).	Both increases and decreases have been reported, region specific.
Decrease in discharge in July for all stations based on bi-decade periods.	Both increases and decreases have been reported, region specific.
Climate - Precipitation	
Based on annual mean: decrease in snow at both stations.	Decrease in snow levels in the CBR and many areas in BC; Zhang and Wei (2012) found the same response in their study area.
Based on annual mean: decrease in precipitation at northern station (EC899) from 1970-2009.	Shows a wetter climate over BC, with a shift showing less snow and more rain.
Based on annual mean: no statistical change in precipitation at the southern (EC850) station.	Shows a wetter climate over BC, increase in BC and CBR.
Based on monthly total: decrease in winter precipitation, for northern (EC899) station.	Decrease in snow levels in the CBR and many areas in BC.
Based on monthly total: increase in spring precipitation (rain) for southern (EC850) station.	Increase in rain is being observed in the CBR.

Results	Literature Review
Climate - Temperature	
Temperature is highly correlated based on elevation.	Temperature decreases with elevation.
Based on annual mean: maximum temperatures increased for both stations over the 40 years.	Reporting an increase in temperature across BC.
Based on annual mean: general increase in temperature for the southern station.	Reporting an increase in temperature across BC.
Based on monthly mean: positive temperature trend in southern station for 5 out of 12 months spread throughout the year.	Reporting an increase in temperature across BC; although some areas showing decrease in last 50 years due to atmospheric teleconnection patterns.
Less significantly relevant positive trends (2 out of 12 months) in the northern station, plus a negative trend in June.	Reporting an increase in temperature across BC; although some areas showing decrease in last 50 years due to atmospheric teleconnection patterns. Brahney (2014) found an overall increase in temperature for the CBR over past 100 years.

The southern ERW temperature trends were overall consistent with those for BC generally with an increase in temperature; however, this was not the case for the northern station. Based on the annual mean temperature, both stations showed a statistical increase in the maximum annual temperature over the 40 years ($\alpha = 0.1$), with the southern station also showing a statistical positive trend in the mean temperature over the 40 years. Interestingly, the northern station is not showing the temperature increase compared to its southern counterpart; however, it is the northern station that is showing the stronger, statistically relevant negative trend in snow levels. Findings throughout BC have noted that some regions experienced a negative temperature trend over the past 50 years likely due to the influence of atmospheric teleconnection patterns.

5.6 Summary

This chapter has used the Mann-Kendall trend analysis with the associated Theil Sen slope estimator to investigate trends in discharge, precipitation and temperature in the ERW, thereby addressing all three parts of research question 1 (see Section 1.4):

(i) The trend analysis displayed an infrequent decrease in discharge over the 40 year period during the summer months present at all stations; and, an increase in discharge over the winter months on the Fording River (08NK018). Overall, there were few statistically relevant discharge trends over the 40 year period, with the highest percentage of discharge trends present on the Fording River (08NK018).

(ii) An overall reduction in winter precipitation was observed throughout the ERW. The northern climate station (1152899) showed a higher percentage of trends over the 40 year period, showing both a decrease in overall precipitation and increase in total rain. The southern climate station (1152850) showed minimal trends, with the exception of the decrease in winter precipitation and increase in spring rains.

(iii) An overall increase in the maximum temperature was observed at both climate stations, with the southern station (1152850) displaying a higher percentage of seasonal and monthly trends over the 40 year period, including an increase in annual mean temperature. Contrary to the precipitation trend distribution, there were no monthly or seasonal temperature trends (α =0.05) at station 1152899.

Further investigation is required to determine if the lack of northern temperature trends, decrease in precipitation yet an increase in winter discharge on Fording River can be correlated or if the increase in discharge is a result from another variable. This will be investigated further in Chapter 6.

6 Results and Discussion: correlating hydro-climatological trends in the Elk River Watershed

6.1 Introduction

Chapter 5 revealed some irregularities between the climate and hydrological trends; such as an increase in precipitation, when no corresponding increase in discharge was observed. Chapter 6 will assess these findings to answer research question 2: can the climatological trends be correlated to the hydrological trends; and if not, what might be the other variable(s) involved?

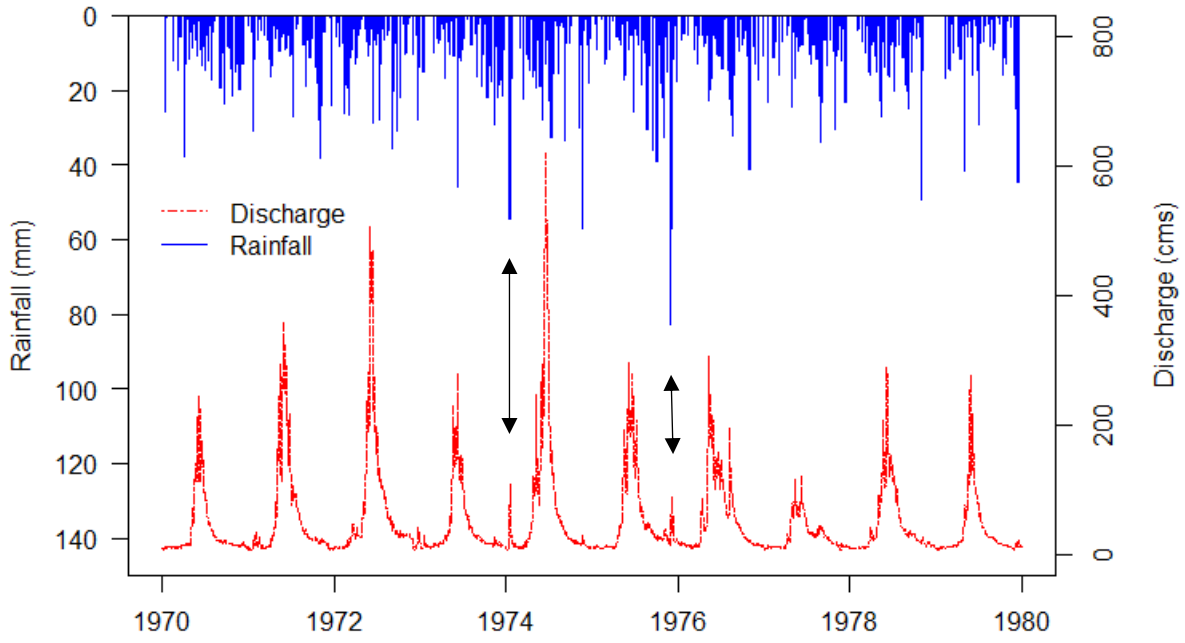

Figure 6-1. Comparison between the daily precipitation (rain) at the Fernie climate station (1152850) and the daily discharge from the Fernie WSC station (08NK002). The two black arrows show a correlation between precipitation and discharge.

Many processes within a watershed influence the response characteristics and timing associated with how precipitation may enter a stream. The response is not always immediate, as it is influenced by space and time. For instance, Figure 6-1 illustrates that precipitation

spikes for the Fernie climate station do not necessarily correspond with either the timing and/or discharge magnitude for the Fernie discharge monitoring station; the same can be observed between the northern climate station 1152899 and WSC station 08NK016 (Figure F-1). To address this, the correlation between the discharge and the climate parameters was undertaken.

The total monthly discharge was compared with the total monthly rainfall from 1970 to 2009 based on the Kendall rank correlation test (Table 6-1). A strong relationship between the northern climate station (1152899) and the discharge stations (τ ranges from 0.56 to 0.59) was identified, with a moderate strength relationship between the southern climate station (1152850) and the southern discharge station (08NK002).

Table 6-1. Kendall correlation test (α =0.05) between monthly mean discharge and climate parameters from 1970 to 2009. Note: Climate station 1152850 does not affect the northern discharge stations: 08NK018 and 08NK016.

	Rain899	Rain850	Precip899	Precip850	TMean899	TMean850
Disch002 (τ)	0.57	0.29	0.16	-0.07	0.57	0.58
Disch016 (τ)	0.59	------	0.15	------	0.61	------
Disch018 (τ)	0.56	------	0.14	------	0.57	------

The relationship reduces in strength significantly when looking at the correlation between the discharge and the precipitation (τ range between -0.07 to 0.16). This is likely due to the nival regime characteristics where the winter precipitation does not enter the stream channel until the spring melt (freshet). The relationship between the mean monthly temperature and mean monthly discharge is strong (τ range between 0.57 and 0.61).

The correlation between the precipitation and rain parameter displays a moderately strong relationship throughout the watershed, with the exception of the correlation between the rain and total precipitation from the southern climate station (1152850) that shows a strong relationship ($\tau = 0.55$). The snow parameters at the two climate stations display a strong ($\tau = 0.66$) relationship (Table 6-2). The correlation between the snow parameters is shown in Figure D-4. The changing weather patterns during the summer months, including the presence of micro-climates, reduce the strength of the summer and autumn precipitation correlation.

Table 6-2. Kendall correlation test ($\alpha = 0.05$) between precipitation parameters for stations 1152850 and 1152899 from 1970 to 2009.

	Rain899	Rain850	Snow899	Snow850	Precip899	Precip850
Rain899 (τ)	1					
Rain850 (τ)	0.38	1				
Snow899 (τ)	-0.43	-----	1			
Snow850 (τ)	-----	-0.15	0.66	1		
Precip899 (τ)	0.37	0.31	NSR	-----	1	
Precip850 (τ)	-----	0.55	-----	0.35	0.36	1

NSR: not statistically relevant

Based on this assessment, there is a statistically relevant correlation between the climate variables (precipitation and temperature) and the discharge based on the Kendall rank correlation test (Table 6-1).

6.2 Atmospheric Teleconnection Patterns

There are four atmospheric teleconnection patterns that are considered in this research: Pacific Decadal Oscillation (PDO), El Niño/Southern Oscillation (ENSO), North Pacific pattern (NP), and Arctic Oscillation (AO). The effects from these atmospheric patterns vary based on location and time of year. At different regions within the CRB, Brahney (2014) found areas where positive, negative and no relationship exists between the atmospheric teleconnection patterns (PDO, ENSO and NOI[30]) and the stream discharge. Within the ERW, there is a statistically relevant relationship between the three discharge research stations and NP, a very weak relationship between the discharge from the Fording River station (08NK018) and PDO, and no statistically relevant relationships between the discharge and either ENSO or AO (Table 6-3).

Table 6-3. Mann-Kendall correlation test between discharge and the atmospheric teleconnection patterns from 1970 to 2009. Pink boxes represent $\alpha = 0.05$, and the yellow box represents $0.05 < \alpha < 0.1$.

Stn No.	NP τ	NP p	PDO τ	PDO p	ENSO τ	ENSO p	AO τ	AO p
08NK018	0.45	< 0.001	0.05	0.09	0.03	0.27	0.03	0.41
08NK016	0.46	< 0.001	0.04	0.23	0.03	0.43	0.02	0.55
08NK002	0.45	< 0.001	0.05	0.14	0.02	0.64	0.02	0.48

With the influence of the PDO and ENSO most apparent during the winter months, it may not be surprising that there was a stronger relationship between the atmospheric patterns (NP, PDO and ENSO) with the snow levels compared to stream discharge. The atmospheric index AO

[30] NOI: Northern Oscillation Index

did not show a statistically significant relationship with discharge or SWE in either of these periods.

Table 6-4. Atmospheric Indices compared with the SWE data from the Fernie (2C07 and 2C09P/Q) and Mt Joffre (2C16) River Forecast Centre stations between 1970 and 2009. Pink boxes represent α = 0.05, and the yellow box represents 0.05 < α <0.1.

Stn No.	NP τ	NP p	PDO τ	PDO p	ENSO τ	ENSO p	AO τ	AO p
2C07	0.17	< 0.001	-0.16	0.00	-0.11	0.03	0.01	0.79
2C16	0.27	< 0.001	-0.14	0.01	-0.07	0.17	0.05	0.35
2C09P/Q	0.15	0.001	0.09	0.05	-0.05	0.34	-0.02	0.69

The shifting of the PDO can fluctuate between a few years to >30 years (Schoennagel, Veblen, Romme, Sibold, & Cook, 2005; Brahney, 2014) causing the forecasting of this index to be difficult. The following PDO historical shifts have been identified: 1946-1976 (cool phase), 1977-1998 (warm phase), 1998-2002 (cool phase), 2002-2005 (warm phase), 2005-2007 (neutral phase) and 2007-2013 (cool phase) (Wei & Zhang, 2010; Zhang & Wei, 2012; National Oceanic and Atmospheric Administration, 2016). The PDO's influence on temperature has been more consistent across large areas than its influence on the region's precipitation (Rodenhuis, Bennett, Werner, Murdock, & Bronaugh, 2007). The ENSO varies every two to six years showing a weak, moderate, strong and very strong presence of either El Niño (warming period) or La Niña (cooling period) (Figure 6-2). In North America, the main effects from ENSO can be felt between October and March, translating to milder winters and springs for Canada during an El Niño period. The relationship between the PDO and ENSO can be seen in Figure 6-3, showing similarities in their pattern.

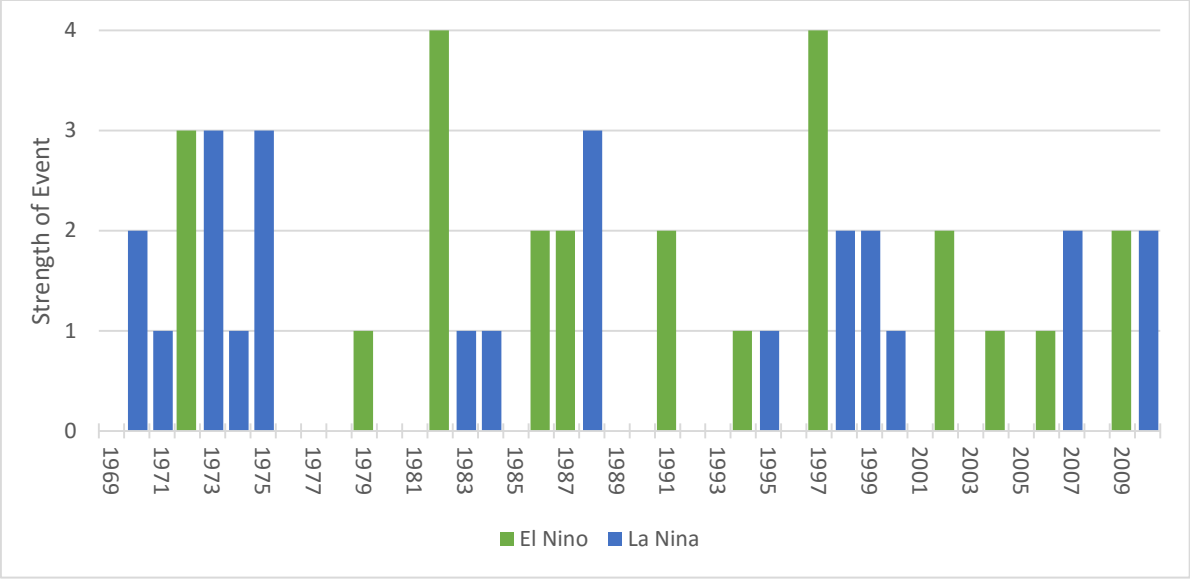

Figure 6-2. Historical ENSO shifts between the El Niño (warm) and El Niña (cool) phase. The y axis represents the strength of the event from (1) weak, (2) moderate (3) strong (4) very strong (Null, 2016).

The NP is most influential between March and July (Figure 6-4). In 1992 and 1993 there was a stronger than normal (dominant) positive NP phase that helped intensified the Pacific jet stream, increasing the frequency and magnitude of the spring storms and, it has been suspected, was a large contributor to the Midwest flooding in 1993 (Bell & Janowiak, 1995).

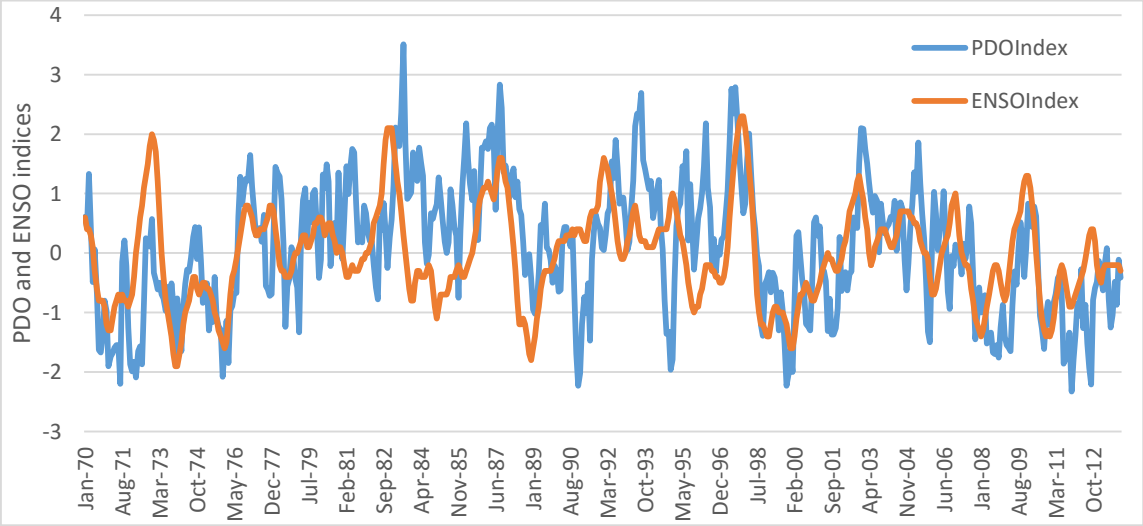

Figure 6-3. The monthly Pacific Decadal Oscillation and El Nino/Southern Oscillation indices from 1970 to 2013 (National Oceanic and Atmospheric Administration, 2016).

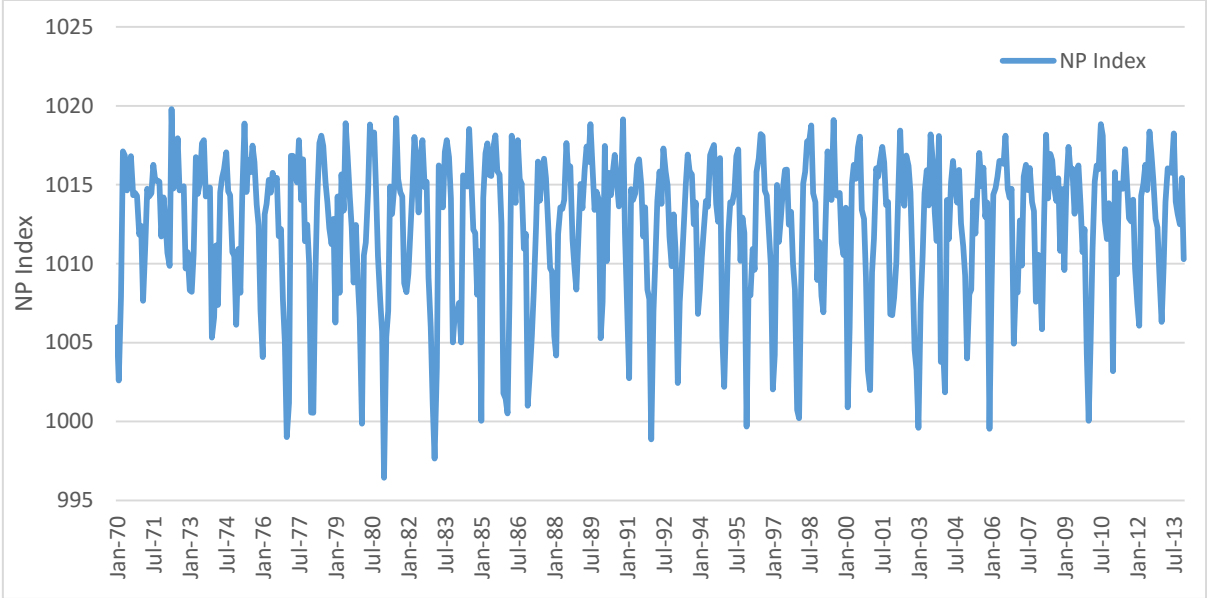

Figure 6-4. The monthly Northern Pacific index from 1970 to 2013 (National Oceanic and Atmospheric Administration, 2016).

The AO varies over time, however, no set time period has been identified for this teleconnection pattern. A positive AO results in the cold Arctic air staying in the polar region. When the AO is negative, the cold Arctic air is shifted to the mid latitudes due to a high pressure present in the polar regions (National Oceanic and Atmospheric Administration, 2016).

6.3 Generalized Linear Models

To investigate which explanatory variable(s) (i.e. precipitation, temperature, etc.) may have the most influence on the discharge (response variable), a generalized least square (GLS) model was used. Analysis was completed for two months, August and October, and assessed over the 40 year research period from 1970 to 2009. The months of August and October were selected as they provide one month representation for the two snow-free seasons of the year: summer and autumn, respectively. There are two discharge stations that were assessed,

stations 08NK016 and 08NK018, resulting in separate models for each station. The climate station located closest to the discharge stations was used for the precipitation and temperature variables; hence, climate station 1152899 was modelled with 08NK018 and 08NK016. The atmospheric teleconnection patterns (PDO, ENSO, AO and NP) were also incorporated into the models.

6.3.1 Model Interpretation for August

The discharge from stations 08NK018 and 08NK016 demonstrated a Gaussian distribution type, with outliers present outside of the 95% CI in both cases. For the month of August, the explanatory variables containing outliers included: temperature, precipitation, discharge, baseflow, PDO and ENSO. Upon verification, it was determined that the outliers were the result of extreme events for each variable. A second dataset was produced where these outliers had been removed. Models were developed both with and without the baseflow variable. Only the models derived from the dataset where the outliers had been removed were able to meet the required linear assumptions. The outliers for temperature, discharge, precipitation and baseflow were removed leaving a total of 27 and 22 (out of 40) full years of record for the analysis for discharge station 08NK018 and 08NK016, respectively. It is assumed that by removing the outliers from the equation, the model depicts the influences based on average conditions; consequently, this model cannot be used to explain the variable influences when any of the variables are experienced extreme events.

The best model for the discharge station 08NK018 explains 83% of the variation in the response variable, whereas the model where the baseflow was not included explains only 28%

of the variation (Table 6-5). Removing the baseflow variable from the model decreases the strength of the model by 55%; however, this supports increasing the information available from the model regarding the other parameters. For the discharge station 08NK016, the best model explains 87% of the variation on the response variable. When the baseflow variable was removed from the model for station 08NK016, the model was no longer able to meet the homogeneity of variance assumption so this model was not reported. It has been shown that NP teleconnection pattern offers a strong influence during the summer period for the Fording River discharge (08NK018). The Elk River station appears to be more influenced by ENSO than the NP teleconnection pattern. Further investigation is recommended into whether another form of linear or additive model would be preferred for this period to improve the model's ability to meet the linear assumptions.

Table 6-5. Model outputs for stations 08NK018 and 08NK016 for August from 1970 to 2009.

Model No.	Model
A1	Discharge 08NK018 ~ Baseflow + Temperature + NP +PDO + Year
A2	Discharge 08NK018 ~ NP + Precipitation + Temperature
A3	Discharge 08NK016 ~ Baseflow + Precipitation + ENSO

Model No.	Goodness of fit	Explanatory Variable (p value)
A1	0.825 (83%)	Baseflow ($p < 0.001$), NP ($p = 0.046$)
A2	0.286 (29%)	NP ($p = 0.010$), Precipitation ($p = 0.043$)
A3	0.866 (87%)	Precipitation ($p = 0.027$), Baseflow ($p < 0.001$)

6.3.2 Model Interpretation for October

The discharge from stations 08NK018 and 08NK016 demonstrated a gamma distribution type, with outliers present outside of the 95% CI in both cases. Outliers were identified in the temperature, discharge and baseflow data sets. A second dataset was developed that had the outliers removed, this produced a dataset of 30 years with which to model with. Due to the presence of the outliers, only the models derived from the dataset where the outliers had been removed were able to meet the required linear assumptions. As a result, it is recommended that the interpretation of these findings can be attributed only to an average discharge event and not be extrapolated to explain any extreme events.

Table 6-6. Model outputs for stations 08NK018 and 08NK016 for October from 1970 to 2009.

Model No.	Model
O1	Discharge 08NK018 ~ Year + Baseflow + NP + AO + ENSO
O2	Discharge 08NK018 ~ Precipitation + ENSO
O3	Discharge 08NK016 ~ Year + Baseflow + Temperature + NP + ENSO
O4	Discharge 08NK016 ~ Year + Precipitation + Temperature + AO + ENSO

Model No.	Goodness of fit	Explanatory Variable (p value)
O1	0.849 (85%)	Year ($p = 0.043$), Baseflow ($p < 0.001$), ENSO ($p = 0.012$)
O2	0.185 (18%)	Precipitation ($p = 0.021$), ENSO ($p = 0.047$)
O3	0.843 (84%)	Baseflow ($p < 0.001$), NP ($p = 0.018$), ENSO ($p = 0.003$)
O4	0.173 (17%)	Precipitation ($p = 0.031$), ENSO ($p = 0.052$)

Incorporating the baseflow into the model calculation increased the model's goodness of fit from 18% to 85% for the discharge at 08NK018 and 17% to 84% for the discharge at 08NK016; while leaving approximately 15% of the influence on the discharge unaccounted for. This is a higher increase than was observed during the month of August. ENSO is prominent in all of the October models, with the NP index influencing the discharge from 08NK016 when the baseflow is included in the calculation.

As there were outliers present in both the August and October datasets, four model varieties were developed as described in Section 3.5.6. When the outliers were present in the dataset, the model was unable to meet the linear assumptions, specifically the requirement for homogeneity of variance. As mentioned above, the information acquired from these models should be considered relevant only to average conditions, and not to be used to interpolate any extreme events observed by any of the variables. Further research is recommended to analyze the explanatory variable influence on the discharge during extreme events.

The models chosen (Tables 6-5 and 6-6) represent the model with the highest R^2 value that met the linear assumptions. As outlined, the strength of the model is increased when the baseflow variable is included for both the August and October periods. By removing the influence of the baseflow, the strength of the other variables can be detected. The baseflow is derived from a calculation that includes station discharge (see Section 4.7.1), due to the high correlation between the discharge and baseflow, including the baseflow in the model may increase uncertainty. Re-evaluating the model strength using baseflow information that has been derived from tracer or field observations is strongly recommended. The influence of the

atmospheric indices varies, based on the month, with the two indices NP and ENSO showing the strongest influence on the discharge. The strength of the atmospheric index ENSO on the discharge was not identified in Section 6.1 when using the Mann-Kendall non-parametric test. This may be a result of the difference in the analysis time period. Thus, Section 6.1 assessed the correlation of the atmospheric indices on the full year of discharge; whereas, the GLMs were assessing the influence of the atmospheric indices on individual months.

6.4 Double Mass Curve

A double mass curve (DMC) analysis was conducted by correlating cumulative precipitation and cumulative discharge from 1970 to 2013. Analysis was completed between the northern precipitation (1152899) and central precipitation (1152850) stations and the discharge stations (08NK018, 08NK016 and 08NK002). To reduce potential errors, the observed data were calculated based on daily information. This allowed the removal of any pairs where missing data were present. The DMC using precipitation from ClimateBC was based on a mean monthly discharge as the ClimateBC output is in monthly time periods. By assessing the mean monthly discharge against the cumulative precipitation a more noticeable deviation from the main trend line is observed. The outputs are divided based on the precipitation station they are associated with: stations 1152899, 1152850 and ClimateBC (Fording station) entitled CBC899.

6.4.1 Climate Station 1152899

All three discharge stations show a deviation from the trend line at the beginning of the correlation, as well as at end of the correlation (Figure 6-5). Stations 08NK018 and 08NK002

also show a deviation from the trend line during the middle of the time period. The associated dates with the shifts from the trend line are based on a visual assessment so are to be interpreted as estimates (Table 6-7). To reduce some of the estimation errors, the daily data have been converted to seasonal dates: winter (December of previous year to February), spring (March to May), and autumn (September to November).

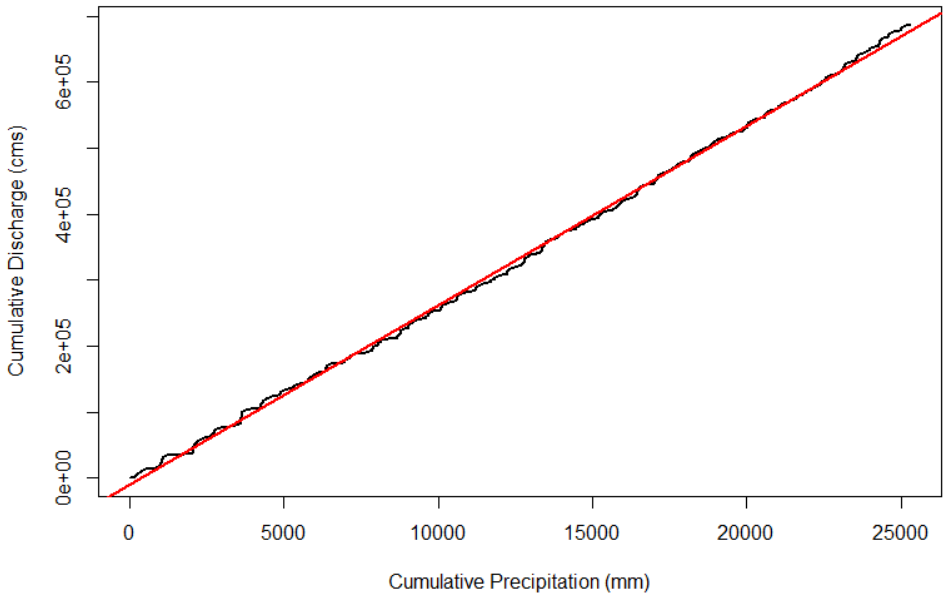

a.

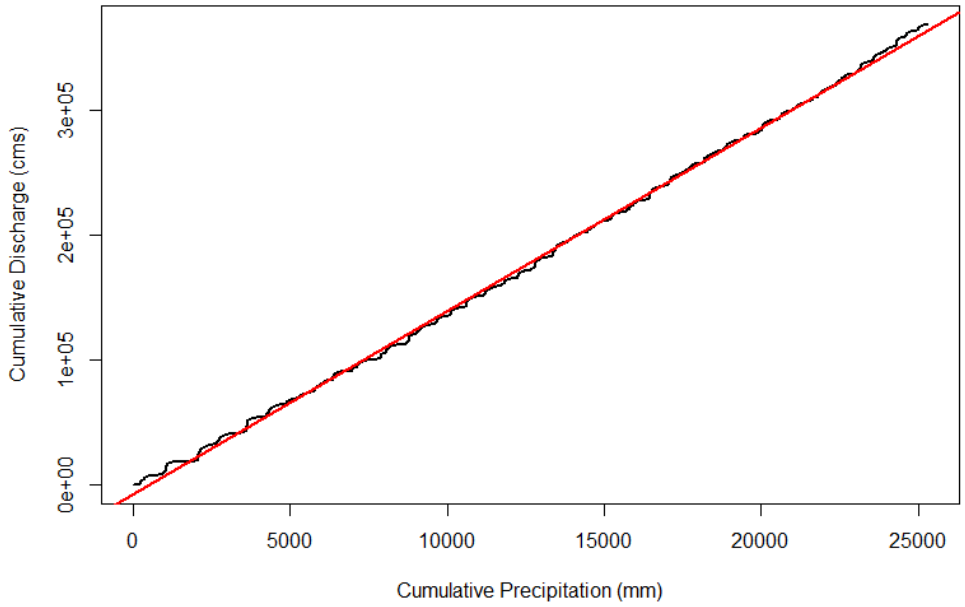

b.

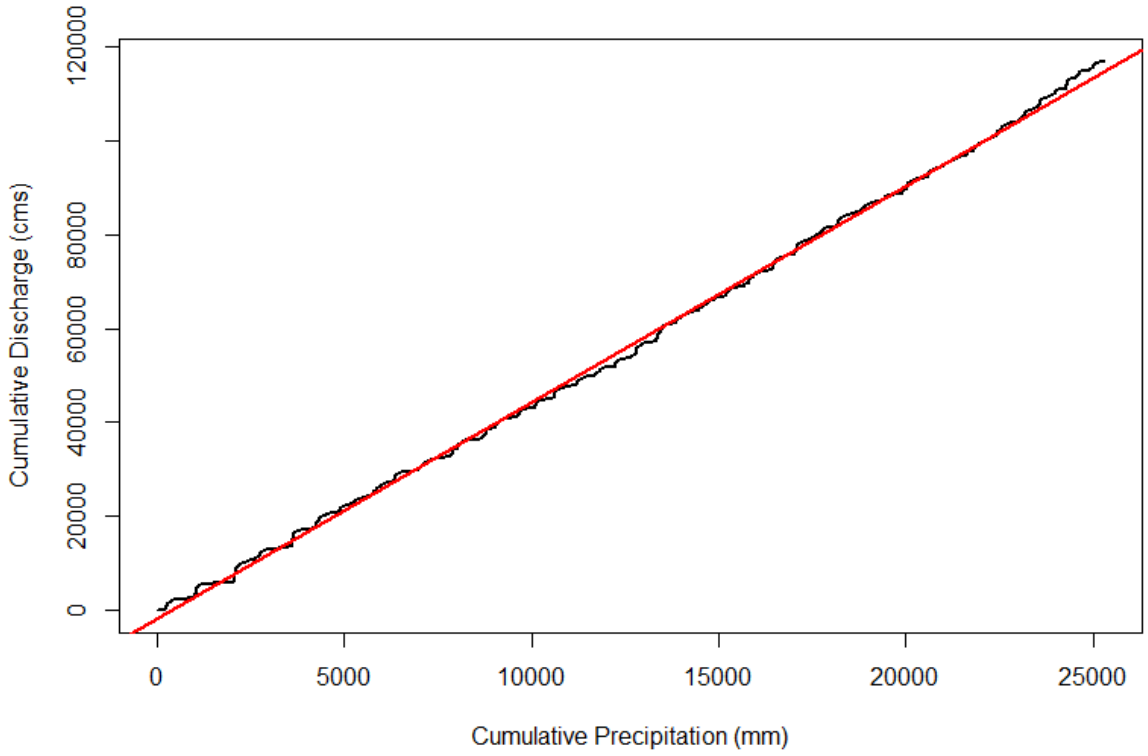

c.

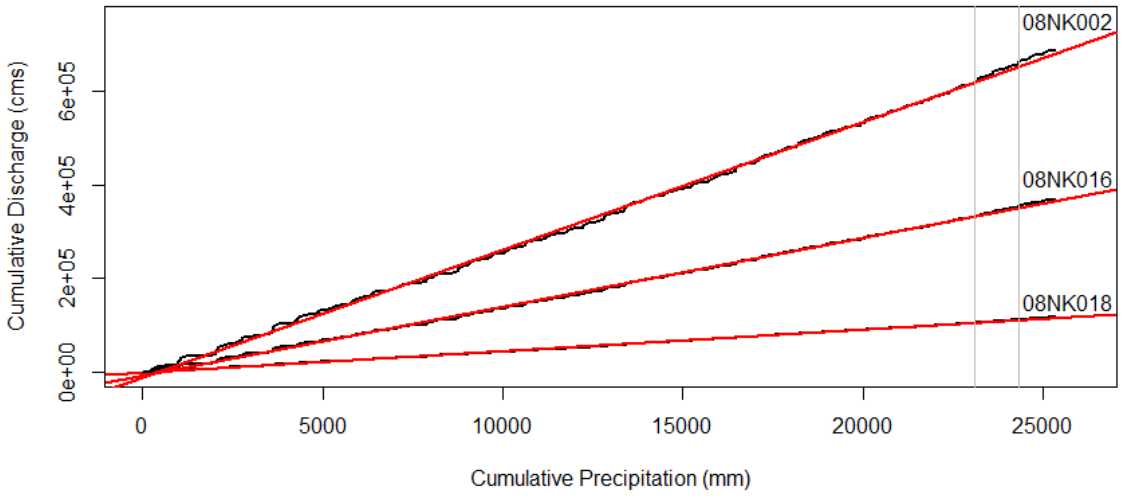

d.

Figure 6-5. Double mass curve correlating cumulative daily precipitation from climate station 1152899 with cumulative daily discharge from three discharge stations: (a) 08NK002; (b) 08NK016; (c) 08NK018 (d) all three discharge stations together (grey lines representing estimated point of deviation from the trend line). Analysis is between 1970 and 2013. The red line represents the correlation trend line.

Table 6-7. Dates correlating to the points (based on cumulative daily data) where the observed data deviate from the trend line in plots. Dates have been determined based on visual assessment, so must be treated as estimates.

Precipitation Stn. 1152899	Date of deviation at end of correlation
08NK002	Summer 2008
08NK016	Spring 2011
08NK018	Winter 2011

At the start of the study period the slight deviation from the trend line is fairly consistent for all three discharge stations (occurring in winter 1971/1972). There is also a shift of the curve off of the trend line near the end of the analysis period, showing the shift occurring first at 08NK002, followed by 08NK016 and 08NK018 (Table 6-7). There is a deviation from the trend line in the middle of the period, late 1980/early 1990s, that coincides with the change in discharge observed in Section 5.3.1.

When the double mass curve is calculated using total monthly values for both the discharge and precipitation, the deviation from the trend line at the end of the analysis is more pronounced, while the deviation from the trend line at the middle of the analysis has been muted (Figure F-2). There is a larger percentage of missing observed precipitation data from the northern climate station 1152899 between August 2008 and February 2009. From January 1, 2007 to December 31, 2013 there is a total of 73 out of 84 months (87%) that contain precipitation data at station 1152899.

6.4.2 Climate Station 1152850

Comparing these findings by using the cumulative precipitation from the southern climate station 1152850, there is a similar shift from the trend line at the beginning of the analysis, but not at the end of the analysis (Figures F-3 to F-5). There are only two months of missing precipitation data from station 1152850 from 2007 to 2013.

6.4.3 ClimateBC

To assess whether the deviation from the pattern in these two northern stations was a result from the missing precipitation data or possibly a landscape change, the precipitation data from ClimateBC, matching the coordinates from station 1152899, were used for comparison; referred to as ClimateBC (CBC899). The ClimateBC precipitation data are based on a monthly total, so the total monthly discharge was used as a comparison.

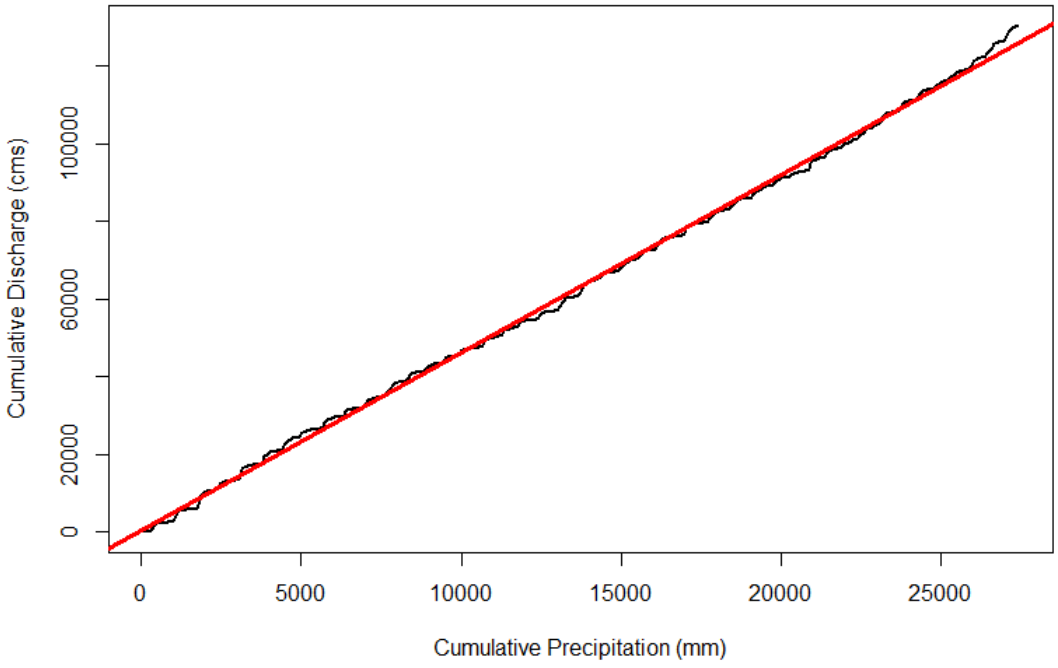

Figure 6-6. Double mass curve between cumulative total monthly precipitation (from ClimateBC (CBC899)) and cumulative total monthly discharge (08NK018) with trend line shown in red; from 1970 to 2013.

The deviation from the trend line observed in the beginning of the analysis period is not visible when using the ClimateBC precipitation data at any of the discharge stations (Figures 6-6, F-6 and F-7). However, this is not the case for the findings at the end of the analysis period. The deviation from the trend line is more pronounced using the ClimateBC precipitation data at all three discharge stations for the time period at the end of the analysis (Figures 6-6, F-6 and F-7). Based on a visual evaluation, the shift away from the trend line occurs at a later date (approximately one year later) when comparing the DMC using the precipitation from the ClimateBC model versus the observed precipitation data (Tables 6-7 and 6-8). Furthermore, the order of the shift has changed, showing the discharge at station 08NK018 occurring first, followed by the discharge at station 08NK016 and 08NK002. Further exploration into why the two analysis types, daily mean observed data and monthly modelled data, indicate a different deviation date from the trend line.

Table 6-8. Dates corresponding to the points where the observed data deviates from the trend line in Figures 6-6, F-6 and F-7. Dates have been determined based on a visual assessment, so are estimates only.

ClimateBC (CBC899)	Date of deviation at end of correlation
08NK002	Summer 2012
08NK016	Summer 2012
08NK018	Spring 2012

Showing the consistency of the shift of the curve from the trend line when using both the observed and modelled precipitation data helps provide support regarding the accuracy of the findings. Further analysis is required to determine the basis for why a deviation has been

observed when comparing the discharge against both the observed and modelled precipitation data.

6.5 Discussion

The purpose of Chapter 6 was to determine if the discharge trends could be correlated to the climatic trends, which climatic parameters exhibited the strongest influence on the discharge, and whether there were additional factors influencing the ERW discharge.

Statistically relevant correlations exist between the discharge and both the precipitation and temperature. There is a stronger correlation between the rain variable and discharge at all three stations compared to total precipitation. In addition, there is a strong correlation between the discharge and the mean monthly temperature (Table 6-1). The correlation findings suggest that there is a relationship between hydro-climatic parameters.

However, based on the trend analysis from Chapter 5 there are not many statistically relevant trends in the discharge, whereas during the same period there are statistically relevant precipitation trends. So, further analysis was conducted into what were the main influences on the discharge. The atmospheric teleconnection patterns can have a strong influence on many areas within Canada. The findings (see Section 6.2) outlined that, over the full year, the NP was the most influential teleconnection pattern ($\alpha = 0.05$) on the discharge at all three research discharge stations, followed by a possible influence from the PDO on the discharge at station 08NK018 ($\alpha = 0.1$) (Table 6-3). Focusing on the winter period, the most influential teleconnection patterns on the SWE within the ERW included NP, PDO and possibly ENSO

(Table 6-4). Some of the teleconnection patterns show more of an influence based on the time of year, such that ENSO has a stronger influence from October to March, and NP has a stronger influence from March to July. The PDO does not show a seasonal fluctuation, but rather an annual to multi-decadal period fluctuation. Similarly, the AO does not have a seasonal pattern.

The influences from these climatic variables on the stream discharge was assessed for one month out of each snow free season, August and October. A GLS was used to describe the influence on the response variable discharge on two separate systems, Elk River (08NK016) and the Fording River (08NK018). The explanatory variables assessed included: precipitation, temperature, baseflow, PDO, ENSO, AO and NP. To ensure accuracy of the findings, the residuals from the GLS models must meet the linear assumptions (see Section 4.6.6). Only the datasets with the outliers removed were able to meet these assumptions. The baseflow was a strong influence in both August and October, and the models were able to explain approximately 85% of the variation in the discharge at both stations (Tables 6-5 and 6-6). With the baseflow removed from the model, the strength of the model decreased to representing 28% in August and ~17% in October of the variation in the discharge. Precipitation tends to be the strong climatic variable influencing the discharge in both August and October, with the influence from the teleconnection patterns shifting from NP in August to ENSO in October. This influence matches the seasonal strengths of both of these teleconnection patterns. Neither the PDO nor the AO showed a significant influence on the discharge in either August or October; however, this may be more a factor of these teleconnection patterns periods of influence. The PDO and AO influence can vary throughout the year so it would be more difficult to define a monthly effect. Ultimately, the linear model provides another means to

support our understanding of which variables most significantly influences the streamflow in the ERW.

Finally, the DMC analysis helps to determine if there have been any changes to the discharge in relation to the different station precipitation patterns over the research period. For this analysis, the period was extended by four years, from 1970 to 2013, as a change was detected very close to the end of the research period of 2009. There are three PDO periods that may help to identify some of the variation observed in the DMC: 1946-1976 (cool phase), 1977-1998 (warm phase) and 2007 to 2013 (cool phase). There is a deviation from the trend line in all of the observed data plots occurring between early to mid-1970s. This would coincide with the end of the PDO cool phase (Table 6-7). There was another deviation from the trend line observed in the middle of the analysis period for two of the three discharge stations, occurring in the late 1980s to early 1990s. This does not coincide as strongly with the dates of the PDO warm phase, but it does coincide with the discharge shift observed in the late 1980s - early 1990s as described in Chapter 5 (Figure 5-5). It was suspected that this change in discharge was occurring over a full decade; however, based on the DMC findings, it is now proposed that this change in discharge is instead occurring for a shorter period of time. Near the end of the analysis, there is another deviation from the trend line ranging from 2008 to 2011 based on observed versus modelled data. A PDO cool phase was reported to have occurred between 2007 and 2013 that coincides with the timing of this variation. The shift of the DMC observed on either end is in the same direction; showing an increase in discharge in relation to precipitation (corresponding with the PDO cool phase), whereas the shift observed in the middle of the analysis is opposite, showing a decrease in discharge in relation to precipitation

(corresponding with the PDO warm phase). Completing the same analysis using observed monthly total discharge compared with observed monthly total precipitation showed a stronger shift from the trend line at the end of the research period compared to other deviations from the trend line.

Due to the presence of missing observed data near the end of the analysis period, the DMC was conducted using the ClimateBC modelled data as a comparison. The early shift from the trend line was not observed in the DMC when the modelled precipitation data were used; however, the strength of the shift near the end of the analysis period is significantly stronger than seen with the observed data. The strong deviation from the trend line observed both in the modelled dataset and the total monthly observed dataset would not likely be explained solely by the influence of the PDO. Further research is required to determine the reason behind the strength of this correlation shift near the end of the research period.

6.6 Summary

Correlation tests, generalized linear models and double mass curves were used to address the three-part research question 2 (see Section 1.4):

(i) There was a significant correlation between the precipitation and temperature variables in the ERW compared with the discharge from the three research discharge stations. The correlation is statistically stronger between the temperature and the discharge, compared to the precipitation and the discharge.

(ii) The influence of the baseflow, precipitation and teleconnection patterns (NP for August and ENSO for October) on the northern discharge stations has shown to be statistically relevant.

(iii) Based on an initial assessment using the DMC analysis, it appears that there is an influence from the PDO on the discharge at all three discharge stations. When comparing the modelled precipitation data against the discharge, a strong shift is observed away from the trend line near the end of the research period. This is not easily explained by the presence of the PDO as an equal shift is not observed in this analysis at the beginning of the research period.

Further research is required to help identify the influences associated with this change in the cumulative precipitation/discharge relationship.

7 Results and Discussion: hydrological forecasting in response to land use and land cover, and climate changes in the Elk River Watershed

7.1 Introduction

This chapter addresses research question 3: What will be the effect on the Elk River discharge of anticipated climate change and/or LULC over the next 80 years? Is there a threshold for land cover change given a set climate scenario? Does this differ based on the location within the watershed?

The SWAT (Soil Water Assessment Tool) model is an internationally used model designed to support the forecasting of hydrological response as a reaction to LULC change; built for hydrological assessments in agricultural environments, and successfully used in many different environments. Due to the LULC detail that this model supports, the fact that it is open source software, plus the international and local support for this model, the SWAT model was selected to address the research question identified above (for details see Section 2.2).

7.2 Results and Discussion

Running the SWAT model in the ERW unfortunately proved to be unsuccessful. Based on preliminary findings, it appears that the problem of using this model on the ERW is its limited inclusion of the many different processes occurring in a snow-dominated, mountainous and forested environment. Modelling the simulated versus observed data showed an inability to predict the start of freshet or provide an accurate representation of the volume of discharge during the test years (Figure 7-1). It was first suspected that this was due to precipitation gaps

in the observed data, so the system was run using the incorporated Global Weather Data (GWD), removing the observed climate data; however, the change in climate information did not prove to be the solution. Location of GWD points in relation to existing climate stations around the Fording River watershed are shown in Figure G-1. Following discussions with other SWAT users, as well as additional literature review, it became apparent that the SWAT model may not be able to effectively model the hydrological system in the ERW.

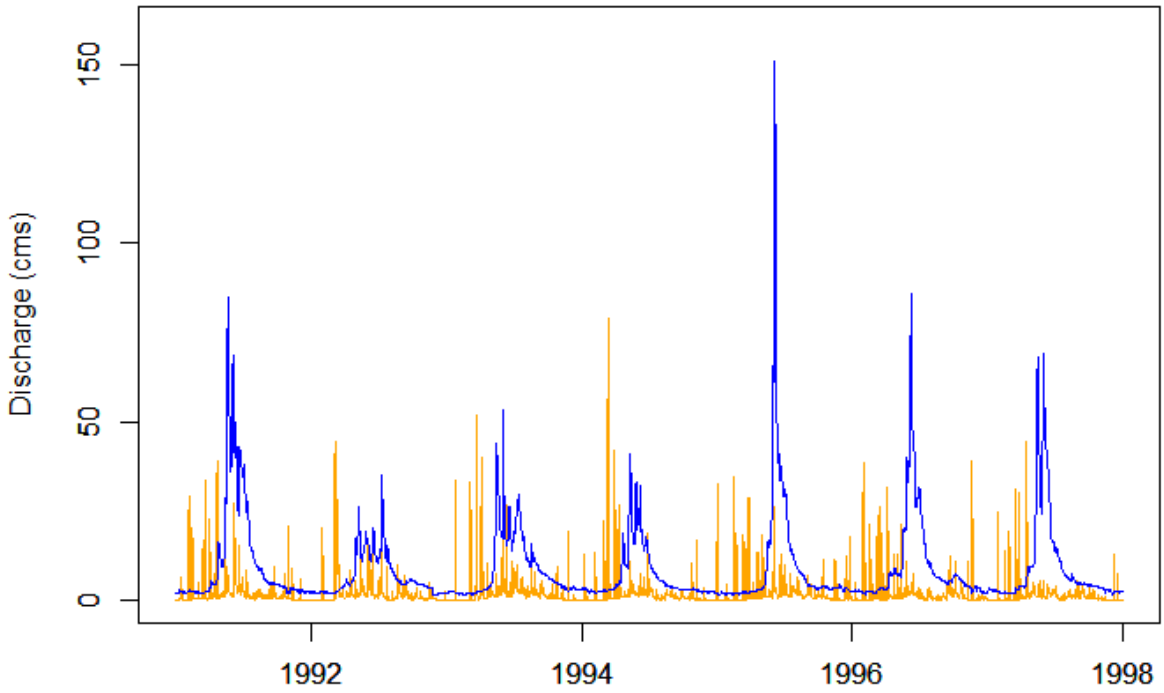

Figure 7-1. Modelled (yellow) versus observed (blue) data using the SWAT model for station 08NK018 from 1991 to 1997.

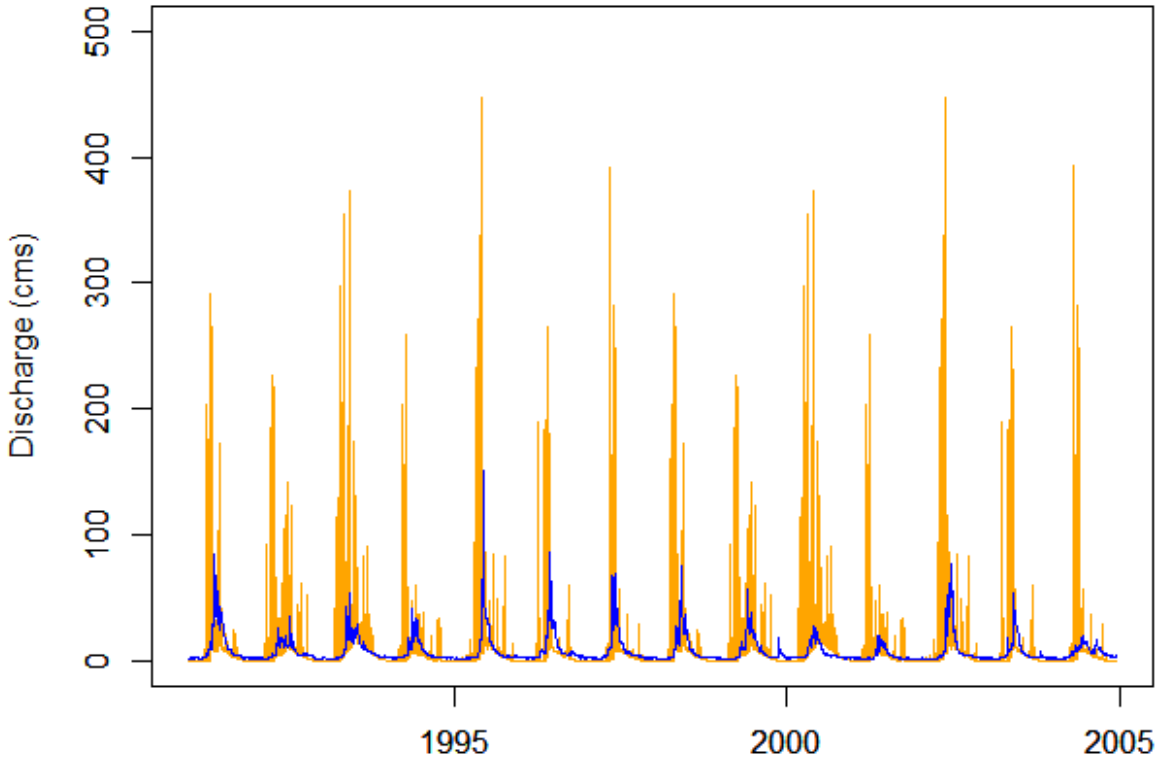

Figure 7-2. SWAT model output discharge (yellow) using the Global Weather data climate information, compared against the observed discharge from station 08NK018 from 1991 to 2004.

When running the model using the Global Weather climate information, the outputs showed a significantly higher than normal discharge (Figure 7-2). This concern of the modelled climate data was also raised in the ARCSWAT help forum identifying that the Global Weather model was overestimating precipitation. When comparing modelled (Global Weather) data with the observed data there was a very weak (R^2 = 0.01) linear precipitation correlation with the strongest correlation shown between the modelled maximum temperature values and observed values (R^2 = 0.66) (Figures G-2 and G-3). The location and elevation of the sites are not the same (Figure G-1), so some difference between the two outputs is expected; however, such variation between the observed and modelled precipitation values provided unrealistic outputs. The Global Weather model stations on the east of the ERW are located on the other side of the

Rocky Mountains, so these stations were not included in the analysis as the modelled climate would be substantially different then observed meteorological information within the watershed. Even with the over-estimating of the discharge, which is assumed to be associated with the over-estimation of the precipitation, the start of the freshet is still occurring significantly earlier than the observed data.

Moving through the calibration stage of the modelling setup, it was not possible to effectively adjust the outputs using realistic parameters to better characterize the true discharge. Watson et al. (2008) determined that the effectiveness of the SWAT model in its original state is poor when looking at landscapes dominated by forest cover. In response to this, they developed a modified SWAT model built to address some of these deficiencies (Watson, McKeown, Putz, & MacDonald, 2008). Dr. Green, P.Geo. (adjunct professor at the University of British Columbia, Department of Forest Resources Management, personal communication, 2016) also described concerns with the SWAT model's ability to replicate runoff from a snow-dominated forested watershed. Based on an initial review of the SWAT algorithms, Dr. Green found that the influence of the forest canopy was not accounted for with either snow interception or the snowmelt energy balance.

7.3 Summary

With the SWAT model proving to be ineffective at modelling the hydrological response in the ERW, it was not possible to realistically predict future trends in discharge due to changes in LULC and/or climate in the ERW (i.e. research question 3). It is proposed that the aforementioned modified SWAT model (Watson, McKeown, Putz, & MacDonald, 2008) be

used to determine if this is more appropriate. Further research may be required to ensure that the SWAT model can be effectively used in snow-dominated mountainous forested environments.

8 Conclusion

Long-term data availability is essential for the analysis of trends and patterns within hydro-climatological data. Brahney (2014) states that the means of interpreting these data are equally, if not more important, as data alone cannot tell the story. This research offers a component of the groundwork needed for developing a proactive approach towards water and resource management in and around the Elk River watershed. Understanding the interaction between the hydro-climatological variables and LULC supports the development of a sustainable and defensible outcome.

The first two research questions from Section 1.4 (repeated below) were addressed through the use of trend analysis, linear models and a double mass curve (DMC). The third research question was unable to be answered due to problems associated with using the SWAT model on the ERW.

Research questions:

1) Is there a trend in discharge, precipitation and temperature over the past 40 years in the mid to upper portion of the ERW?

2) If there is a trend in discharge, can this trend be correlated to the climatic trends? Which climatic parameters have the most influence on the discharge, temperature or precipitation? What might be the other factors influencing the discharge in the ERW?

3) What will be the effect on the Elk River discharge of anticipated LULC change and/or climate change over the next 80 years? Is there a threshold for land cover change given a set climate scenarios? Does this differ based on the location within the watershed?

8.1 Response to Research Question 1

The research findings show minimal full period trends in the stream discharge, with the exception of the monitoring station located on the Fording River where a statistically relevant increase in discharge during autumn and winter was observed. There is a statistically relevant decrease in the summer discharge from all three stations from 1970 to 1989. The discharge frequency analysis provided insight to the (not statistically relevant) decrease in peak and maximum flow volumes, whereas there were statistically relevant decrease in the maximum and increase in the minimum flows for the Fording River (08NK018). No statistically relevant change was observed with regards to the start of freshet, central discharge volume or occurrence of the peak flows. Non-statistically relevant shifts are identified in Section 5.3.2.3.

A statistically relevant decrease in the winter precipitation (snow) is observed throughout the region, identified through the ECCC climate stations as well as the RFC snow monitoring stations. Overall, the northern station shows a stronger trend towards a declining winter precipitation, with both stations showing a trend towards an increase in rain (Table 5-14 and Figure 5-13). The northern station has experienced a statistically relevant decrease in total precipitation and snow over the 40 year research period, while also experiencing a statistically relevant increase in the quantity of rain. The southern station did not show a statistically

relevant precipitation or rain trend over this 40 year period, but did experience a decrease in the quantity of snow (Table 5-14). Contrary to the strength of the precipitation trends, the northern climate station did not experience many statistically relevant temperature trends over the research period. A statistically relevant increase in the maximum temperature was observed at both climate stations, with the southern climate station also showing an increase in the mean temperature (Table 5-18). The southern climate station experienced a general increase in temperature during the spring and summer periods, whereas no seasonal temperature trends were found at the northern climate station (Figure 5-17).

8.2 Response to Research Question 2

The strength of the atmospheric teleconnection patterns can be observed over the 40 year research period, as identified through Kendall rank correlation, linear modelling and double mass curves. Understanding the influences of these patterns on the ERW discharge supports the communities' ability to prepare for upcoming conditions. Due to the strength of influence from the baseflow on the stream discharge, the GLS model is able to explain ~ 85% of the variability in the stream discharge. By removing the baseflow variable, the influence from the precipitation and atmospheric teleconnection patterns becomes more pronounced yet reduces the model's strength to explaining ~20% of the discharge variability. Using the different methods to analyze the data on different time periods allows for a better understanding of the varying influences on the stream discharge. The DMC showed a strong divergence from the main trend near the end of the research period at all discharge stations based on northern climate information. When comparing the discharge with the modelled precipitation data, there was a much stronger shift from the trend line near the end of the analysis period. An 8%

overall decrease in the upper ERW forest cover has been identified (Figure A-7) from 2000 to 2013, which, based on Stednick's (1996) evaluation, is considered to be below the threshold identified when a loss of vegetation (LULC change) will affect the watershed's discharge. However, more research is required to determine if the cumulative LULC change in the Fording River watershed is resulting in the change in the Fording River discharge observed both during the winter months and in the latter half of the research period. As Blösch et al. (2007) have identified that the effect from LULC change[31] on the site discharge is negatively correlated to the site's catchment size. At this time, it is unclear all of the influences that may have contributed to this divergence from the trend at the end of the research period; the strength of the PDO, a response to LULC change, or the cumulative effects from many variables.

8.3 Looking Forward

There are a number of opportunities available to build from this research and further dissect the hydro-climatological historical patterns and future projections in the ERW. To support the overall climatological findings, trend analysis completed on additional climate stations both in and outside the ERW would be encouraged. Including the analysis of discharge monitoring stations with smaller drainage basins would be beneficial as this could provide additional information on the buffering capacity of the watersheds, plus provide the ability to focus on the hydrological response based on drainage size. Increasing the linear model discharge analysis to include a review of each month would supply additional insight on the annual changes occurring within the ERW. Incorporating the modified DMC (Zhang & Wei, 2012) to single out the potential influences of the LULC change would offer necessary information

[31] When the LULC does not change in size or intensity between different catchment sizes.

on the hydrological effects from the anthropogenic and natural disturbance within the ERW. This information could then be used in support of developing sustainable land management decisions. Collecting, analyzing and incorporating observed baseflow, groundwater and glacial data would increase the comprehensiveness of the hydrological analysis. The inclusion of detailed information on the anthropogenic water inputs and withdrawals within the ERW would be necessary to provide a full understanding of the current and projected hydrological yields.

8.4 Summary

Concluding this research with the opportunity to forecast the hydrological response in the ERW incorporating the proposed LULC and projected climate change, was not possible in this study; however, further research in this area is encouraged as it still remains an important part of the hydro-climatological analysis. The lack of statistically relevant trends in the discharge, in light of the presence of statistically relevant precipitation trends, indicates that a factor other than climate is also influencing the discharge; this could include the watershed's natural buffering capacity or the influence of LULC change. Further investigation is recommended to determine whether the shift, or a component of the shift, observed in the DMC can be attributed to having identified the natural watershed buffering capacity threshold within the northern portion of the ERW.

Bibliography

Arnold, J., Kiniry, J., Srinivasan, R., Williams, J., Haney, E., & Neitsch, S. (2012). *Soil and Water Assessment Tool; Input/Output Documentation.* Houston: Texas Water Resources Institute.

Bayazit, M., & Onoz, B. (2007). To Prewhiten or Not to Prewhiten in Trend Analysis? *Hydrological Sciences Journal des Sciences Hydrologiques, 52*(4), 611-624.

Beckers, J., Smerdon, B., & Wilson, M. (2009). *Review of Hydrologic Models for Forest Management and Climate Change Applications in British Columbia and Alberta.* Kamloops: Forrex Forum for Research and Extension in Natural Resources Society.

Beckers, J., Smerdon, B., Redding, T., Anderson, A., Pike, R., & Werner, A. (2009). Hydrologic Models for Forest Management Applications: Part 1: Model Selection. *Streamline, 13*, 35-44.

Bell, G. D., & Janowiak, J. E. (1995). Atmospheric Circulation Associated with the Midwest Floods of 1993. *Bulletin of the American Meterological Society*, 681-695.

Blain, G. C. (2013). The Mann-Kendall Test: The Need to Consider the Interaction Between Serial Correlation and Trend. *Acta Scientiarum Agronomy, 35*(4), 393-402. doi:http://dx.doi.org/10.4025/actasciagron.v35i4.16006

Blöschl, G., et al. (2007). At What Scale Do Climate Variability and Land Cover Change Impact on Flooding and Low Flows? *Hydrological Processes, 21*, 1241-1247.

Bond, N. (2015). hydrostats: Hydrologic Indices for Daily Time Series Data. R package version 0.2.4. Retrieved from https://CRAN.R-project.org/package=hydrostats

Brahney, J. (2014). *Water Quantity and Quality in the Columbia Basin Trust Region.* University of British Columbia, Okanagan. Columbia Basin Trust.

Bronaugh, D., & Werner, A. (2013). zyp: Zhang + Yue-Pilon trends. Pacific Climate Impacts Consortium. Retrieved from https://CRAN.R-project.org/package=zyp

Burford, J. E., Dery, S. J., & Holmes, R. D. (2009). Some Aspects of the Hydroclimatology of the Quesnel River Basin, British Columbia, Canada. *Hydrological Processes, 23*, 1529-1536.

Burn, D. H. (1994). Hydrologic Effects of Climatic Change in West-Central Canada. *Journal of Hydrology, 160*, 53-70.

Burn, D. H., & Hag Elnur, M. A. (2002). Detection of Hydrologic Trends and Variability. *Journal of Hydrology, 255*, 107-122.

Burn, D. H., Abdul Aziz, O. I., & Pietroniro, A. (2004). A Comparison of Trends in Hydrological Variables for Two Watersheds in the Mackenzie River Basin. *Canadian Water Resources Journal/Revue canadienne des ressources hydriques, 29*(4), 283-298.

Canada, N. (2010). *Changing Currents: Water Sustainability and the Future of Canada's Natural Resource Sectors.* Ottawa: National Round Table on the Environment and the Economy.

Carpenter, T., & Georgakakos, K. (2006). Intercomparison of Lumped Versus Distributed Hydrologic Model Ensemble Simulations on Operational Forest Scales. *Journal of Hydrology, 329*, 174-185.

Carslaw, D. C., & Ropkins, K. (2012). openair - An R Package for Air Quality Data Analysis. *Environmental Modelling & Software, 27-28*, 53-61. doi:10.1016/j.envsoft.2011.09.008

Carslaw, D. C., & Ropkins, K. (2016). openair: Open-Source Tools for the Analysis of Air Pollution Data. R package version 1.8-6. Retrieved from http://CRAN.R-project.org/package=openair

Carver, M. (2013). From Creeks to Rivers: Watershed Functions and Issues in the Columbia Basin. *Watershed Governance Symposium.* Fairmont Hotsprings.

Centre for Ecology and Hydrology. (2016). *National River Flow Archive*. Retrieved June 1, 2016, from http://nrfa.ceh.ac.uk/derived-data-series

Chhabr, A., & Geist, H. (2006). Multiple Impacts of Land-Use/Cover Change. In E. F. Lambin, & H. Geist (Eds.), *Land-Use and Land-Cover Change* (pp. 71-113). Berline: Springer.

Chilton, R. R. (1981). *A Summary of Climatic Regimes of British Columbia.* Victoria: BC Ministry of Environment.

Columbia Basin Trust. (2008). *2008 State of the Basin Report.* Castlegar: Columbia Basin Trust.

Columbia Basin Trust. (2013). *Columbia River Basin*. Retrieved March 5, 2014, from http://www.cbt.org/powerandwater/

Coulson, C. H., & Obedkoff, W. (1998). *British Columbia Streamflow Inventory.* Province of British Columbia Ministry of Environment, Water Inventory Section. Victoria: Resource Inventory Branch.

Coulthard, B., Smith, D. J., & Meko, D. M. (2016). Is Worst-Case Scenario Streamflow Drought Underestimated in British Columbia? A Multi-Century Perspective for the South Coast, Derived from Tree-Rings. *Journal of Hydrology, 534*, 205-218.

DeFries, R., & Eshleman, K. N. (2004). Land-Use Change and Hydrologic Processes: A Major Focus for the Future. *Hydrological Processes, 18*, 2183-2186. doi:10.1002/hyp.5584

Déry, S., Hernandez-Henriquez, M., Owens, P., Parkes, M., & Petticrew, E. (2012). A Century of Hydrological Variability and Trends in the Fraser River Basin. *Environmental Research Letters, 7*, 1-10.

Dingman, S. L. (2002). *Physical Hydrology* (2nd ed.). Long Grove, Il: Waveland Press Inc.

Eaton , B., & Moore, R. (2010). Regional Hydrology. In R. G. Pike, T. E. Redding, R. D. Moore, R. D. Winkler, & K. D. Bladon, *Compendium of forest hydrology and geomorphology in British Columbia* (pp. 85-110). Victoria: Ministry of Forests and Range Forest Science Program.

Fernie Museum. (nd). *Fernie History - an Overview*. Retrieved February 10, 2014, from Fernie Museum: http://www.ferniemuseum.com/content/fernies-history-overview

Fleckenstein, J., Anderson, M., Fogg, G., & Mount, J. (2004). Managing Surface Water - Groundwater to Restore Fall Flows in the Cosumnes River. *Journal of Water Resources Planning and Management, 4*(130), 301-310.

Floury, M., Delattre, C., Ormerod, S. J., & Souchon, Y. (2012). Global Versus Local Change Effects on a Large European River. *Science of the Total Environment, 441*, 220-229. Retrieved from http://dx.doi.org/10.1016/j.scitotenv.2012.09.051

Fox, J., & Weisberg, S. (2011). *An {R} Companion to Applied Regression* (2nd ed.). Thousand Oaks, California, USA: Sage.

Gassman, P., Reyes, M., Green, C., & Arnold, J. (2007). The Soil and Water Assessment Tool: Historical Development, Applications, and Future Research Directions. *American Society of Agricultural and Biological Engineers, 50*(4), 1211-1250.

Godkin, D. (2015, January 1). *Tough Slugging for BC's Coal Miners; BC's Coal Mining Industry Has Always Had More Heroes Than Villains Over Its Tumultuous 150-Year History*. (R. Noble, Editor) Retrieved January 2016, from Canadian Mining Journal: http://www.canadianminingjournal.com/features/tough-slugging-for-bcs-coal-miners/

Green, K. C., & Alila, Y. (2012). A Paradigm Shift in Understanding and Quantifying the Effects of Forest Harvesting on Floods in Snow Environments. *Water Resources Research, 48*, 1-21. doi:doi:10.1029/2012WR012449

Griffis, V. W., & Stedinger, J. R. (2007). The Use of GLS Regression in Regional Hydrologic Analyses. *Journal of Hydrology, 344*, 82-95.

Hamann, A., & Wang, T. (2006). Potential Effects of Climate Change on Ecosystem and Tree Species Distribution in British Columbia. *Ecology, 87*(11), 2773-2786.

Hansen, M. C., et al. (2013). High Resolution Global Maps of 21st Century Forest Cover Change. *Science, 342*(6160), 850-853. doi:10.1126/science.1244693

Harrell Jr, F., & Dupont, C. (n.d.). Hmisc: Harrell Miscellaneous. R package version 3.17-4. Retrieved from https://CRAN.R-project.org/package=Hmisc

Hatcher, K. L., & Jones, J. A. (2013). Climate and Streamflow Trends in the Columbia River Basin: Evidence for Ecological and Engineering Resilience to Climate Change. *Atmosphere-Ocean*, 2-20. doi:10.1080/07055900.2013.808167

Hatfield, T. A., Lewis, A., & Ohlson, D. (2003). Development of Instream Flow Thresholds as Guidelines for Reviewing Proposed Water Uses. Victoria: prepared for British Columbia Ministry of Sustainable Resource Management, and British Columbia Ministry of Water,Land, and Air Protection.

Helsel, D. R., & Hirsch, R. M. (2002). *Statsitical Methods in Water Resources.* U.S. Geological Survey.

Hundecha, Y., & Bardossy, A. (2004). Modeling of the Effects of Land Use Changes on the Runoff Generation of a River Basin Through Parameter Regionalization of a Watershed Model. *Journal of Hydrology, 292*, 281-295.

Jones, J. A. (2011). Hydrologic Response to Climate Change: Considering Geographic Context and Alternative Hypotheses. *Hydrological Processes, 25*, 1996-2000. doi:10.1002/hyp.8004

Jost, G., & Weber, F. (2012). *Potential Impacts of Climate Change on BC Hydro's Water Resources.* BC Hydro.

Katay, F. (2014). *Exploration and Mining in the Kootenay-Boundary Region, British Columbia.* Victoria: British Columbia Ministry of Energy and Mines, British Columbia Geological Survey.

Katz, R. W. (1993). Towards a Statistical Paradigm for Climate Change. *Climate Research, 2*, 167-175.

Katz, R. W., & Brown, B. G. (1992). Exreme Events in a Changing Climate: Variabilty is More Important than Averages. *Climatic Change, 21*, 289-302.

Keggenhoff, I., Elizbarashvili, M., Amiri-Farahani, A., & King, L. (2014). Trends in Daily Temperature and Precipitation Extremes over Georgia, 1971 - 2010. *Weather and Climate Extremes, 4*, 75-85.

Koffler, D., Gauster, T., & Laaha, G. (2015). lfstat: Calculation of Low Flow Statistics for Daily Stream Flow Data. R package version 0.8.0. Retrieved from https://CRAN.R-project.org/package=lfstat

Krysanova, V., & Arnold, J. (2008). Advances in Ecohydrological Modelling with SWAT - A Review. *Hydrological Sciences Journal des Sciences Hydrologiques, 53*(5), 939-947. doi:10.1623/hysj.53.5.939

Lake, T. (2013). *Province of British Columbia; Order of the Minister of Environment Section 89; Environment Management Act.* Victoria.

Lemly, D. A. (2014). *Review of Environment Canada's Teck Coal Environmental Assessment and Evaluation of Selenium Toxicology Tests on Westslope Cutthroat Trout in the Elk and Fording Rivers in Southeast British Columbia.* Ottawa: Environment Canada.

Lyne, V., & Hollick, M. (1979). Stochastic Time Variable Rainfall-Runoff Modelling. *Proceedings of the Hydrology and Water Resources Symposium. 79*, pp. 89-92. Perth: Institution of Engineers National Conference Publication.

Machiwal, D., & Jha, M. K. (2012). *Hydrologic Time Series Analysis: Theory and Practice.* New Delhi, India: Springer.

Maidment, D. R. (1993). *Handbook of Hydrology.* (D. R. Maidment, Ed.) New York, Unites States: McGraw-Hill.

Matheussen, B., Kirschbaum, R. L., Goodman, I. A., O'Donnell, G. M., & Lettenmaier, D. P. (2000). Effects of Land Cover Change on Streamflow in the Interior Columbia River Basin (USA and Canada). *Hydrological Processes, 14*, 867-885.

McLeod, A. I. (2011). Kendall: Kendall Rank Correlation and Mann-Kendall Trend. R package version 2.2. Retrieved from https://CRAN.R-project.org/package=Kendall

Ministry of Forests and Range. (2006). *The State of British Columbia's Forests.* Victoria: Crown Publications.

Murdock, T. Q., & Spittlehouse, D. L. (2011). *Selecting and Using Climate Change Scenarios for British Columbia.* Victoria: Pacific Climate Impacts Consortium; University of Victoria.

Murdock, T., & Soble, S. (2013). *Climate Extremes in the Canadian Columbia Basin: A Preliminary Assessment.* Victoria: Pacific Climate Impact Consortium.

National Oceanic and Atmospheric Administration. (2016, June 01). *Teleconnections*. Retrieved from NOAA National Centers For Environmental Information: http://www.ncdc.noaa.gov/teleconnections/

Neitsch, S., Arnold, J., Kiniry, J., Williams, J., & King, K. (2005). *SWAT Theoretical Documentation.* Temple, TX: Blackland Research Center.

Northwest Hydraulic Consultants Ltd. (2006). *City of Fernie Elk River Flood Hazard Assessment.* North Vancouver: Northwest Hydraulics Consultants Ltd.

Null, J. (2016, June 4). *El Nino and La Nina Years and Intensities*. Retrieved June 6, 2016, from http://ggweather.com/enso/oni.htm

Obedkoff, W. (1985). *Elk River Study Hydrology Overview.* Province of British Columbia Ministry of Environment, Hydrology Section. Victoria: Water Management Branch.

Owrangi, A. M., Lannigan, R., & Simonovic, S. P. (2014). Interaction Between Land-Use Change, Flooding and Human Health in Metro Vancouver, Canada. *Natural Hazards, 72*(2), 1219-1230.

Palmer, M. A., Reidy Liermann, C. A., Nilsson, C., Florke, M., Alcamo, J., Lake, P. S., & Bond, N. (2008). Climate Change and the World's River Basins: Anticipating Management Options. *Frontiers in Ecology and the Environment, 6*(2), 81-89.

Pineiro, J., Bates, D., DebRoy, S., Sarkar, D., & Team, R. C. (2016). nlme: Linear and Nonlinear Mixed Effects Models. R package version 3.1-127. Retrieved from http://CRAN.R-project.org/package=nlme

Poff, N. L., et al. (1997). The Natural Flow Regime: A Paradigm for River Conservation and Restoration. *BioScience, 47*(11), 769-784.

Prasch, M., Mauser, W., & Weber, M. (2013). Quantifying Present and Future Glacier Melt-Water Contribution to Runoff in a Central Himalayan River Basin. *The Cryosphere, 7*, 889-904.

R Core Team. (2015). R: A Language and Environment for Statistical Computing. Vienna, Austria: R Foundation for Statistical Computing. Retrieved from https://www.R-project.org/

Rahman, K., Maringanti, C., Beniston, M., Widmer, F., Abbaspour, K., & Lehmann, A. (2012). Streamflow Modeling in a High Managed Mountainous Glacier Watershed Using SWAT: The Upper Rhone River Watershed Case in Switzerland. *Water Resources Management*. doi:10.1007/s11269-012-0188-9

Regonda, S. K., Rajagopalan, B., Clark, M., & Pitlick, J. (2005). Seasonal Cycle Shifts in Hydroclimatology over the Western United States. *Journal of Climate, 18*, 372-384.

Robson, A., Bardossy, A., Jones, D., & Kundzewicz, Z. (2000). Statistical Methods for Testing for Change. In Z. Kundzewicz, & A. Robson (Eds.), *Detecting Trend and Other Changes in Hydrological Data* (pp. 49-88). Geneva: World Meterological Organization.

Rodenhuis, D., Bennett, K. E., Werner, A. T., Murdock, T. Q., & Bronaugh, D. (2007). *Climate Overview 2007: Hydro-climatology and Future Climate Impacts in British Columbia.* University of Victoria. Victoria: Pacific Climate Impacts Consortium.

Rumsey, C. A., Miller, M. P., Susong, D. D., Tillman, F. D., & Anning, D. W. (2015). Regional Scale Estimates of Baseflow and Factors Influencing Baseflow in the Upper Colorado River Basin. *Journal of Hydrology: Regional Studies, 4*, 91-107.

Ryan, J. A., & Ulrich, J. M. (2014). xts: eXtensible Time Series. R package version 0.9-. Retrieved from https://CRAN.R-project.org/package=xts

Schaeffer, M., Selten, F. M., & Opsteegh, J. D. (2005). Shifts of Means Are Not a Proxy for Changes in Extreme Winter Temperatures in Climate Projections. *Climate Dynamics, 25*, 51-63. doi:DOI 10.1007/s00382-004-0495-9

Schilling, K., Gassman, P., Kling, C., Campbell, T., Jha, M., Wolter, C., & Arnold, J. (2013). The Potential for Agricultural Land Use Change to Reduce Flood Risk in a Large Watershed. *Hydrological Processes, 28*(8), 3314-3325. doi:10.1002/hyp

Schindler, D. (2001). The Cumulative Effects on Climate Warming and other Human Stresses on Canadian Freshwaters in the New Millennium. *Canadian Journal of Fisheries and Aquatic Sciences, 58*(1), 18-29.

Schnorbus, M., & Rodenhuis, D. (2010). *Assessing Hydrologic Impacts on Water Resources in BC.* Victoria: Pacific Climate Impacts Consortium.

Schoennagel, T., Veblen, T. T., Romme, W. H., Sibold, J. S., & Cook, E. R. (2005). ENSO and PDO Variability Affect Drought-Induced Fire Occurrence in Rocky Mountain Subalpine Forests. *Ecological Applications, 15*(6), 2000-2014.

Schreier, H. (2012). Water Management Adaptation Strategies for Land Use Changes and Increased Climate Variaility in Mountain Communities in Western Canada. In J. Krecek, M. J. Haigh, T. Hoger, & E. Kubin, *Management of Mountain Watersheds* (pp. 17-30). India: Springer and Capital Publishing Company.

Sebok, S. (2014, January 28). Describing Distributions and Relationships (Part II). *EDUC 602: Education Research Design and Data Analysis* . Prince George, B.C., Canada: University of Northern British Columbia.

Shatilla, N. J. (2013). *The Influence of Surface Mining on Runoff Timing and Flow Pathways in Elk Valley, British Columbia.* Hamilton: McMaster University.

Shope, C., et al. (2014). Using the SWAT Model to Improve Process Descriptions and Define Hydrologic Partitioning in South Korea. *Hydrological Earth Systems Science, 18*, 539-557.

Stednick, J. D. (1996). Monitoring the Effects of Timber Harvest on Annual Water Yield. *Journal of Hydrology, 176*, 79-95.

Teck Coal Ltd. (2013). *Area Based Management Plan: The Elk Valley Water Quality Plan.* Terms of Reference.

Templ, M., Alfons, A., Kowarik, A., & Prantner, B. (2015). VIM: Visualization and Imputation of Missing Values. R package version 4.4.1. Retrieved from https://CRAN.R-project.org/package=VIM

Tong, S. T., Sun, Y., Ranatunga, T., He, J., & Yang, Y. J. (2012). Predicting Plausible Impacts of Sets of Climate and Land Use Change Scenarios on Water Resoures. *Applied Geography, 32*, 477-489.

VanShaar, J. R., Haddeland, I., & Lettenmaier, D. P. (2002). Effects of Land-Cover Changes on the Hydrological Response of Interior Columbia River Basin Forested Catchments. *Hydrological Processes, 16*, 2499-2520.

Wang, G., Yang, H., Wang, L., Xu, Z., & Xue, B. (2014). Using the SWAT Model to Assess Impacts of Land Use Changes on Runoff Generation in Headwaters. *Hydrological Processes, 28*, 1032-1042.

Wang, T., Hamann, A., Spittlehouse, D. L., & Carroll, C. (2016). Locally Downscaled and Spatially Customizable Climate Data for Historical and Future Periods for North America. *PLoS ONE*, 1-17.

Ward, A., & Trimble, S. (2004). *Environmental Hydrology* (2nd ed.). London: CRC Press LLC.

Watson, B. M., McKeown, R. A., Putz, G., & MacDonald, D. J. (2008). Modification of SWAT for Modelling Streamflow from Forested Watersheds on the Canadian Boreal Plain. *Journal of Environmental Engineering and Science, 7*(S1), 145-159.

Wei, X., & Zhang, M. (2010). Quantifying Streamflow Change Caused by Forest Disturbance at a Large Spatial Scale: A Single Watershed Study. *Water Resources Research, 46*(12), 1-15.

Wellen, C. C., Shatilla, N. J., & Carey, S. K. (2015). Regional Scale Selenium Loading Associated with Surface Coal Mining, Elk Valley British Columbia, Canada. *Science of the Total Environment, 532*, 791-802.

Wickham, H., & Francois, R. (2015). dplyr: A Grammar of Data Manipulation. R package version 0.4.3. Retrieved from https://CRAN.R-project.org/package=dplyr

Winkler, R. D., Moore, R. D., Redding, T. E., Spittlehouse, D. L., Carlyle-Moses, D. E., & Smerdon, B. D. (2010). Hydrologic Processes and Watershed Response. In R. G. Pike, T. E. Redding, R. D. Moore, R. D. Winkler, & K. D. Bladon, *Compendium of Forest Hydrology and Geomorphology in British Columbia* (Vol. 1, pp. 133-177). Victoria, BC: Government Publications Services.

Wuerthner, G. (2001). *Rocky Mountain: A Visitor's Companion.* Mechanicsburg: Stackpole Books.

Yue, S., & Wang, C. Y. (2002). Applicability of Prewhitening to Eliminate the Influence of Serial Correlation on the Mann-Kendall Test. *Water Resources Research, 38*(6), 1-.

Yue, S., Pilon, P., Phinney, B., & Cavadias, G. (2002). The Influence of Autocorrelation on the Ability to Detect Trend in Hydrological Series. *Hydrological Processes, 16*, 1807-1829.

Zambrano-Bigiarini, M. (2014). hydroTSM: Time Series Management, Analysis. R package version 0.4-2-1. Retrieved from https://CRAN.R-project.org/package=hydroTSM

Zhang, M., & Wei, X. (2012). The Effects of Cumulative Forest Disturbance on Streamflow in a Large Watershed in the Central Interior of British Columbia, Canada. *Hydrology and Earth System Sciences, 16*, 2021-2034.

Zhang, X., & Yang, F. (2004). *RClimDex(1.0) User's Manual.* Downsview: Climate Research Branch; Environment Canada.

Zhang, X., & Zwiers, F. W. (2004). Comment on "Applicability of Prewhitening to Eliminate the Influence of Serial Correlation on the Mann-Kendall Test" by Sheng Yue and Chun Yuan Wang. *Water Resources Research, 40*(3), 1-5.

Zhang, X., Harvey, D., Hogg, W. D., & Yuzyk, T. R. (2001). Trends in Canadian Streamflow. *Water Resources Research, 37*(4), 987-998.

Zhang, X., Vincent, L., Hogg, W. D., & Niitsoo, A. (2000). Temperature and Precipitation Trends in Canada During the 20th Century. *Atmosphere Ocean, 38*(3), 395-429.

Zomlot, Z., Verbeiren, B., Huysmans, M., & Batelaan, O. (2015). Spatial Distribution of Groundwater Recharge and Base Flow: Assessment of Controlling Factors. *Journal of Hydrology: Regional Studies, 4*, 349-368.

Zuur, A. F., Ieno, E. N., & Smith, G. M. (2007). *Analysing Ecological Data.* New York: Springer.

Zuur, A. F., Ieno, E. N., Walker, N. J., Saveliev, A. A., & Smith, G. M. (2009). *Mixed Effects Models and Extensions in Ecology with R.* New York: Springer Science and Business Media.

Zwiers, F. W., Schnorbus, M. A., & Maruszeczka, G. D. (2011). *Hydrologic Impacts of Climate Change on BC Water Resources.* University of Victoria. Victoria: Pacific Climate Impacts Consortium.

Appendix

A. Watershed Maps

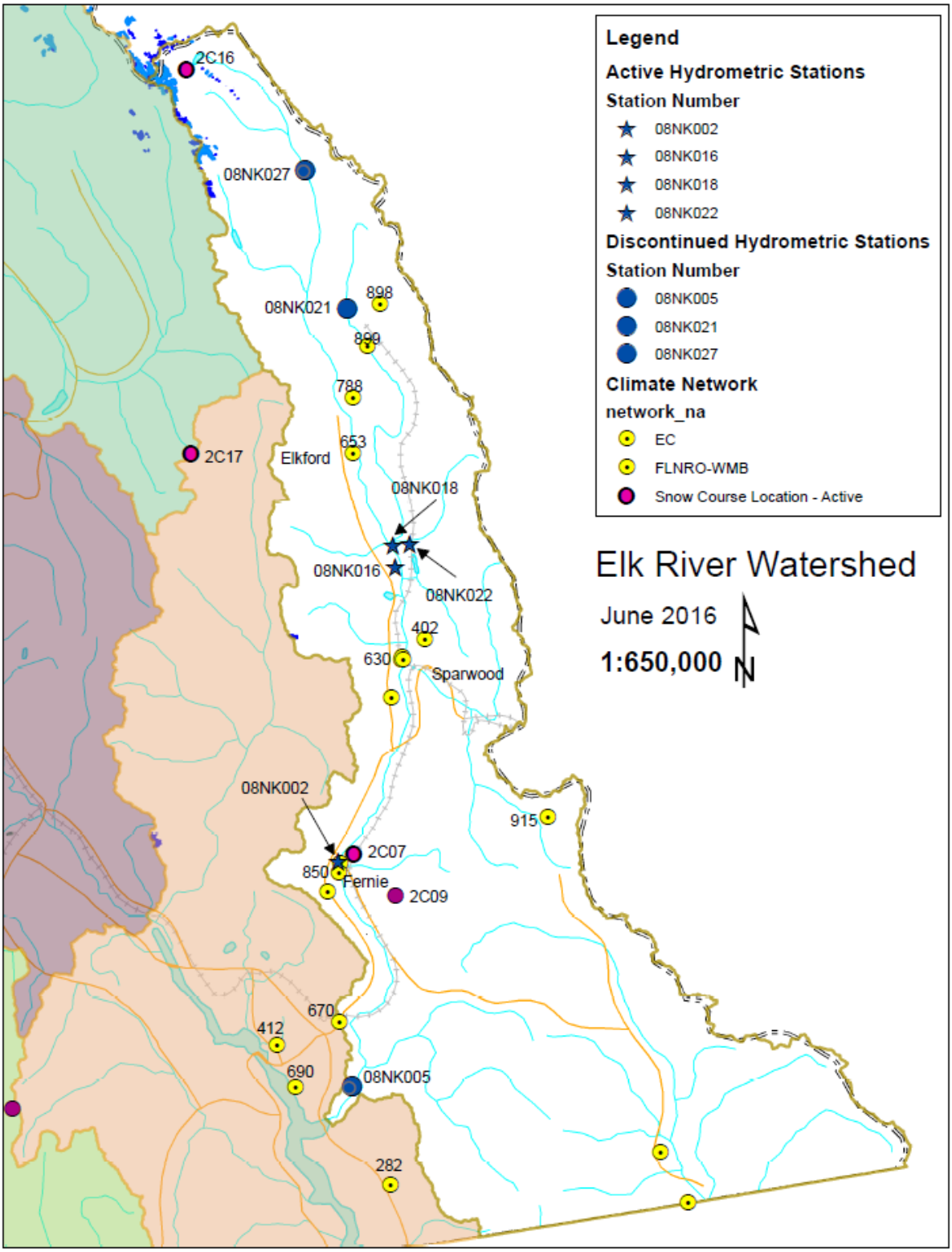

Figure A-1. Map of the Elk River Watershed displaying climate and discharge stations used in this research.

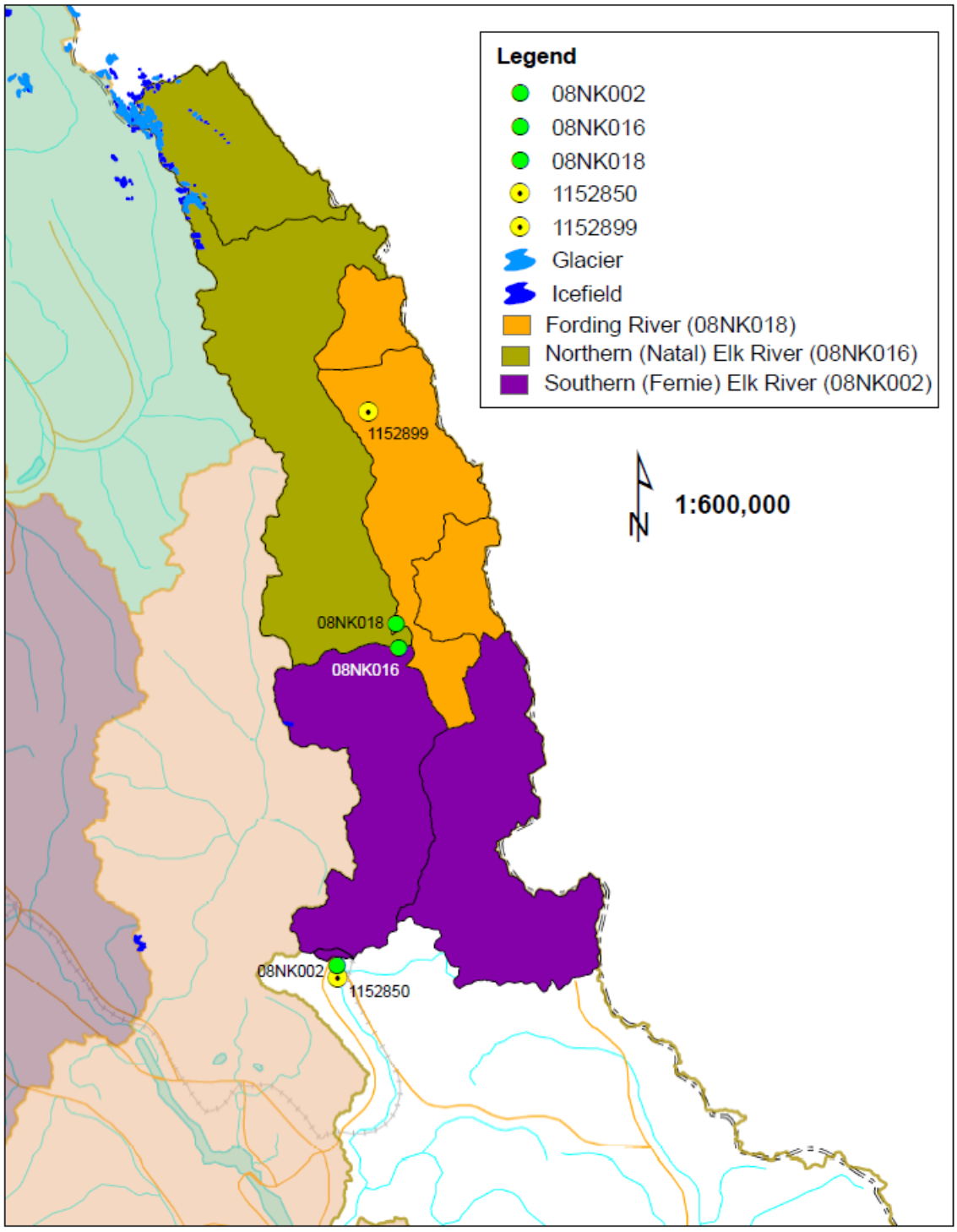

Figure A-2. Map of the Elk River Watershed showing the location of the three discharge and two climate stations used for the inferential statistics. Note that the Southern Elk River station basin (08NK002) incorporates the purple, green and orange identified areas; and the Northern Elk River basin (08NK016) incorporates the green and orange identified areas. The two climate stations 1152850 (EC850) and 1152899 (EC899).

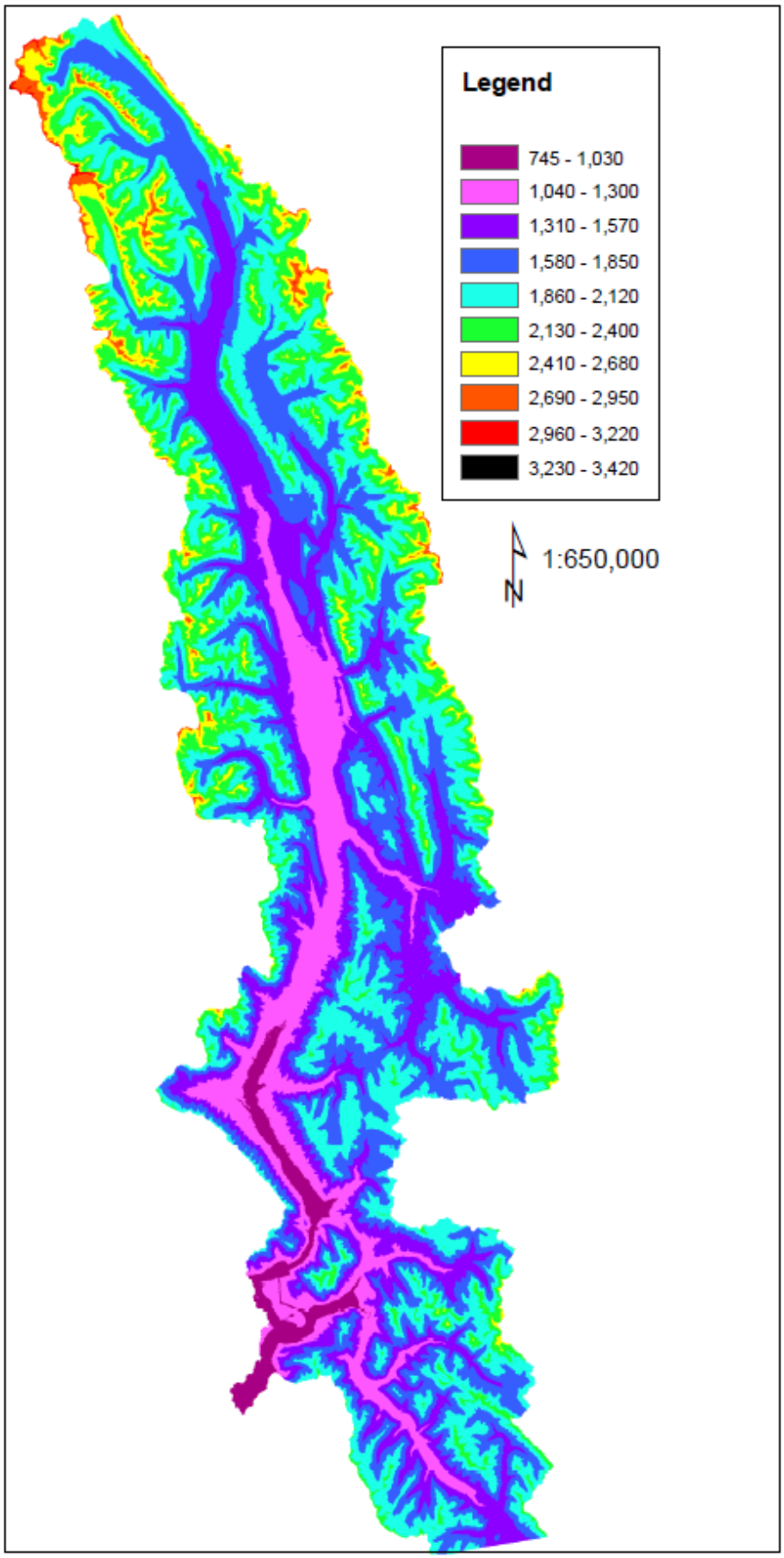
Legend
745 - 1,030
1,040 - 1,300
1,310 - 1,570
1,580 - 1,850
1,860 - 2,120
2,130 - 2,400
2,410 - 2,680
2,690 - 2,950
2,960 - 3,220
3,230 - 3,420
N
1:650,000

a.

b.

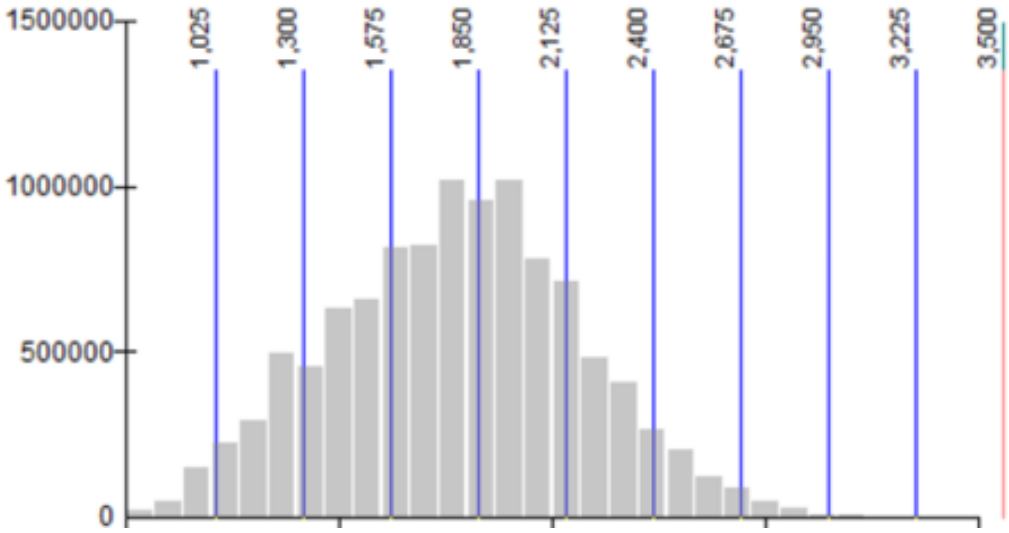

Figure A-3. Elevation for the Elk River Watershed; (a) map of the watershed (meters above sea level) and (b) histogram of the elevation ranges identified in the map.

a.

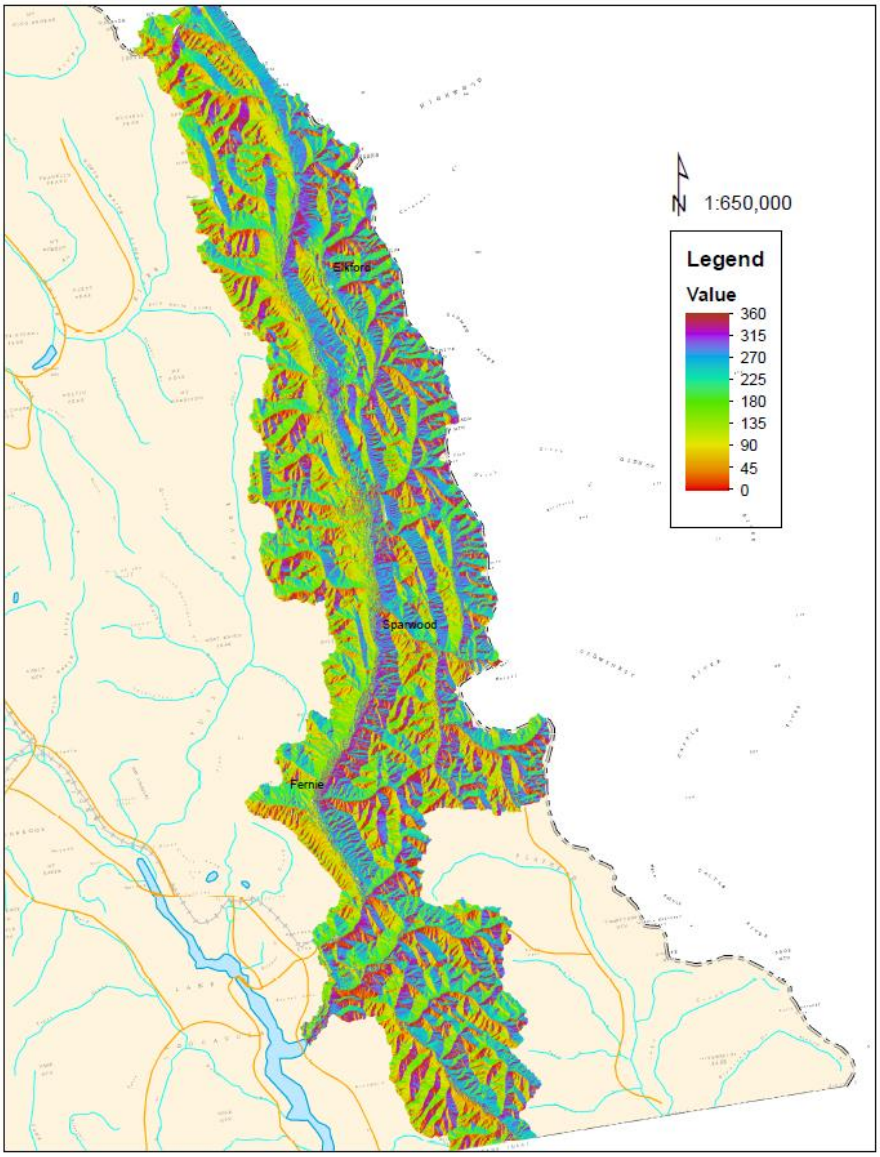

b.

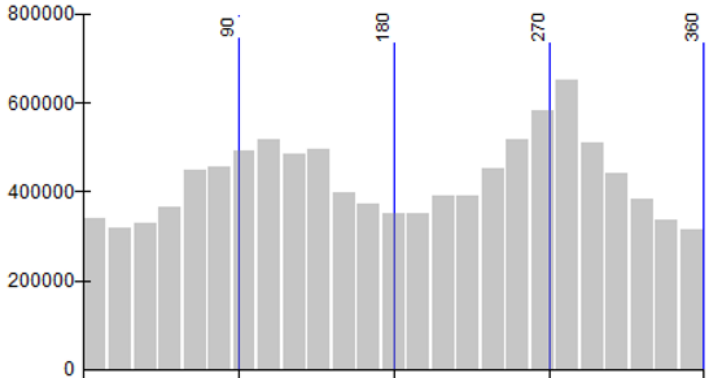

Figure A-4. Aspect (°) for the Elk River Watershed; (a) map of watershed and (b) associated density (y axis) and aspect (°) histogram (x axis). Note east=90°, south=180°, west=270°, and north =360°/0°.

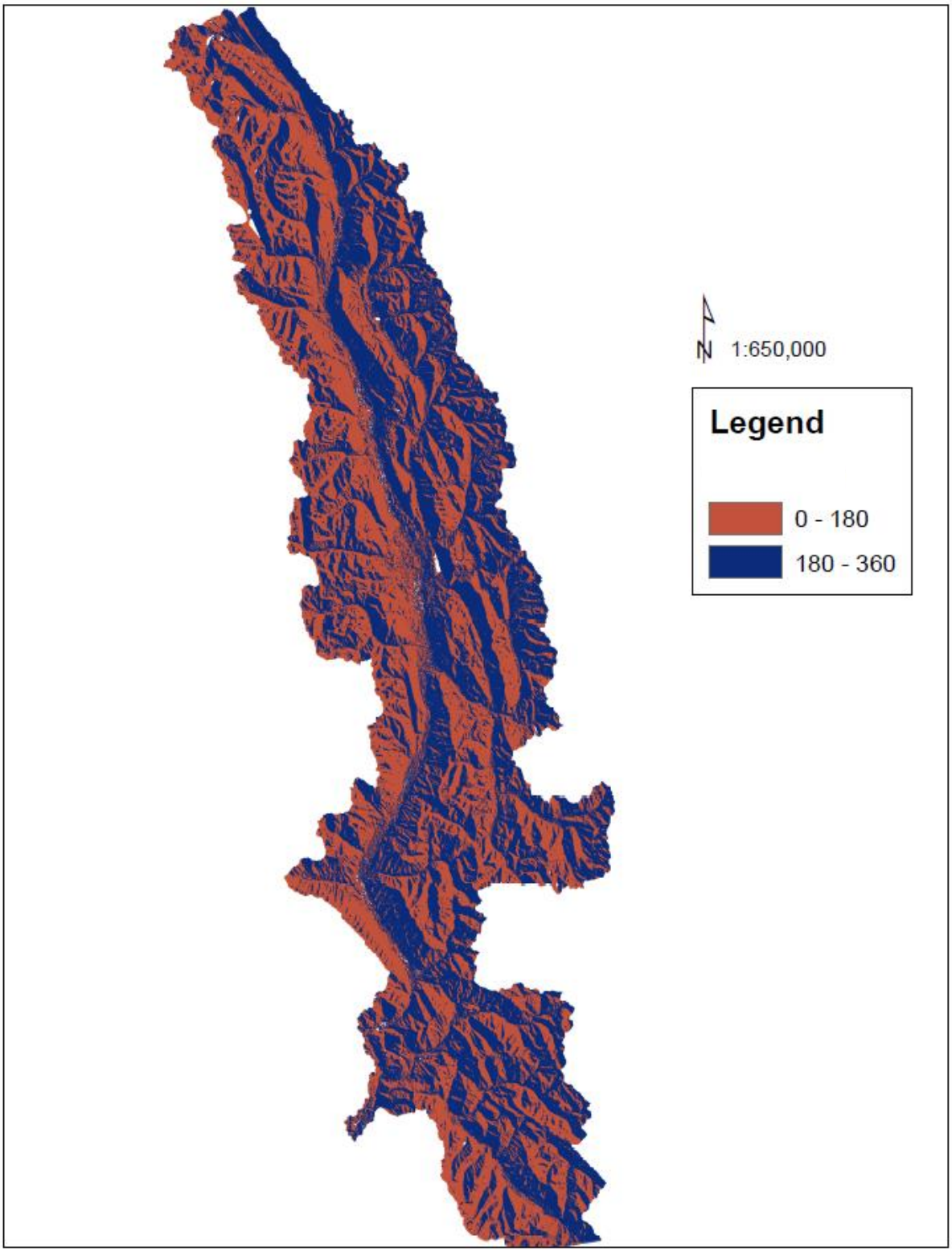

Figure A-5. Aspect (°) for the Elk River Watershed showing 0°-180° (north-east-south) and 180°-360° (south-west-north).

a.

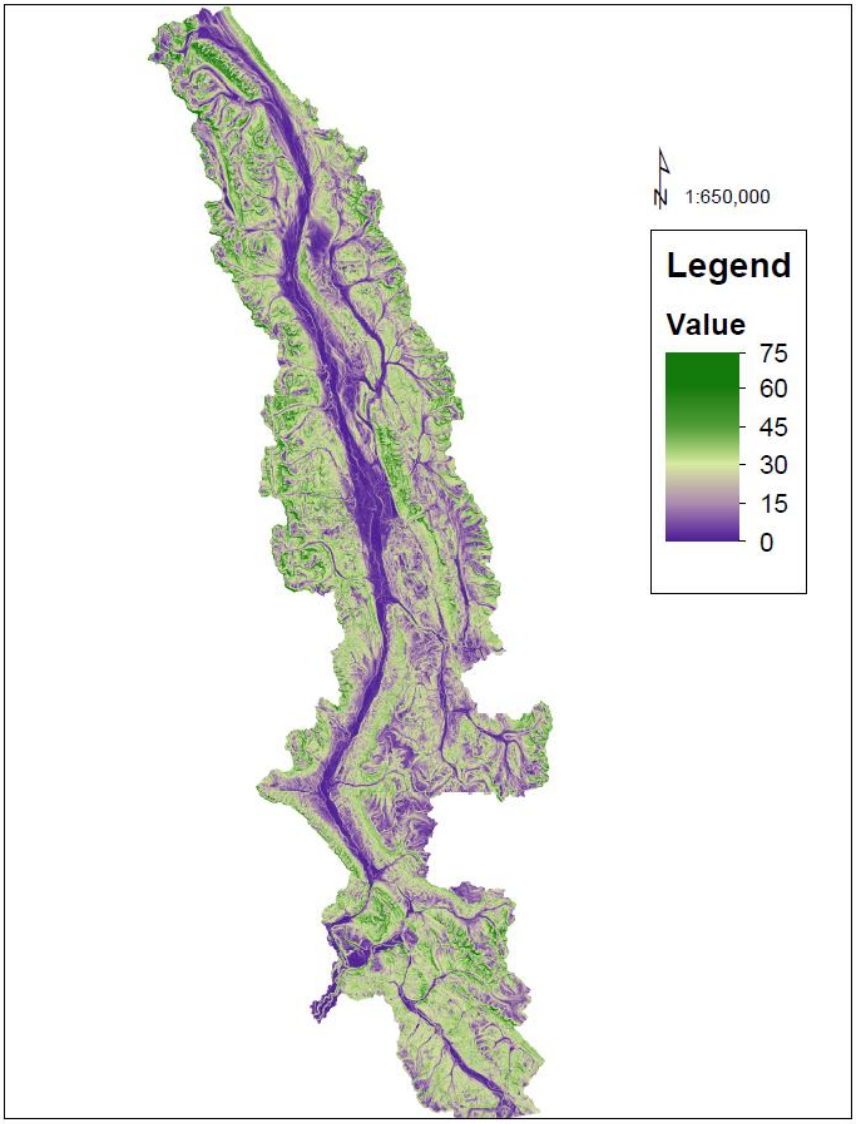

b.

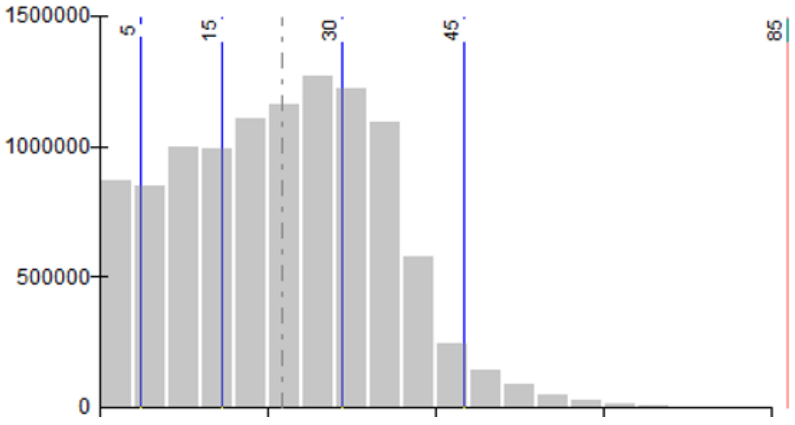

Figure A-6. Slope (°) distribution in the Elk River Watershed; (a) map showing slope values (°), and (b) histogram comparing density (y axis) and slope (°) (x axis). Dotted vertical line identifies mean slope of 22.5°.

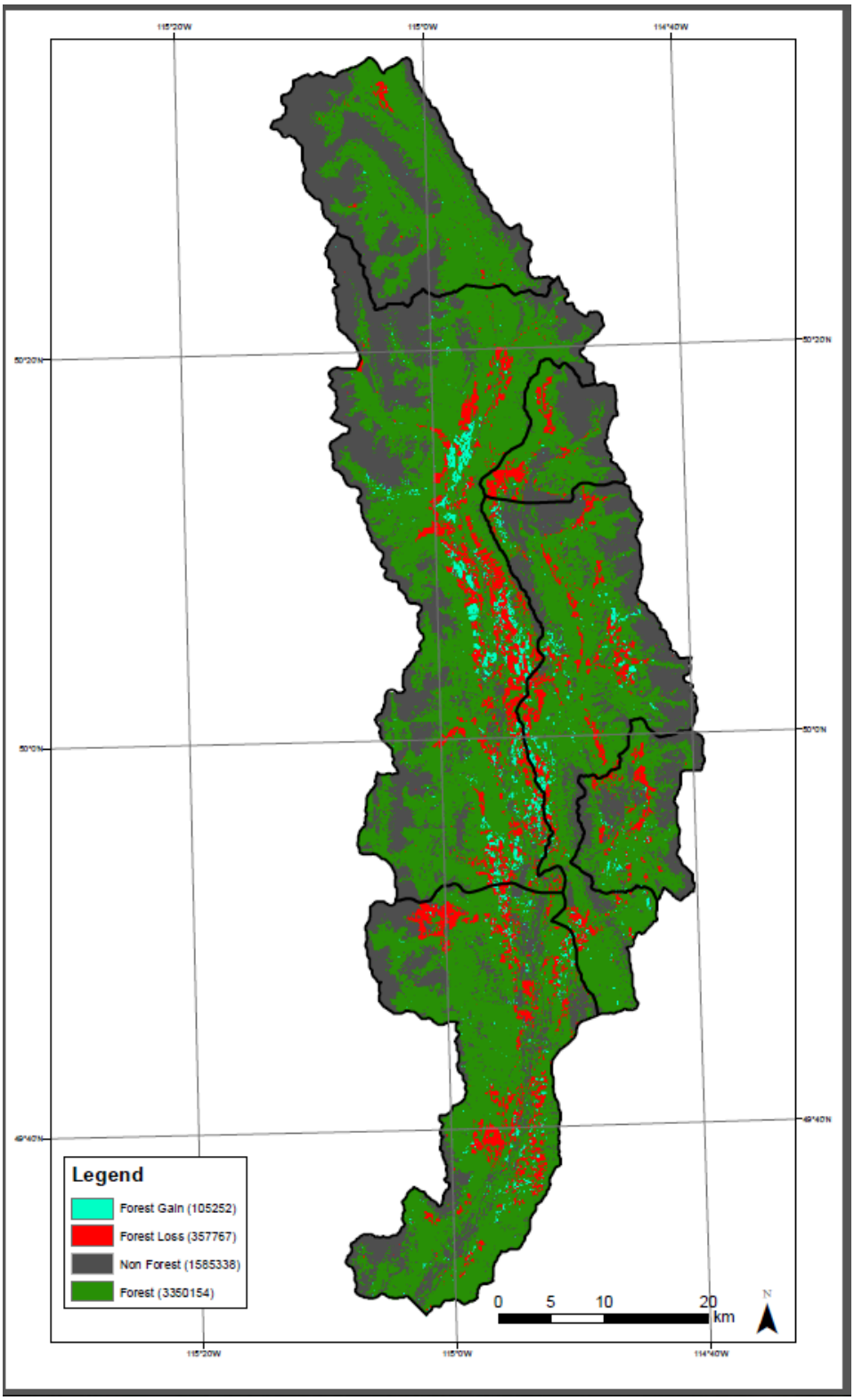

Figure A-7. Land cover change upstream of Fernie (08NK002) from 2000 to 2013. Supplied by Alexandre Bevington; Research Earth Scientist, MFLNRO.

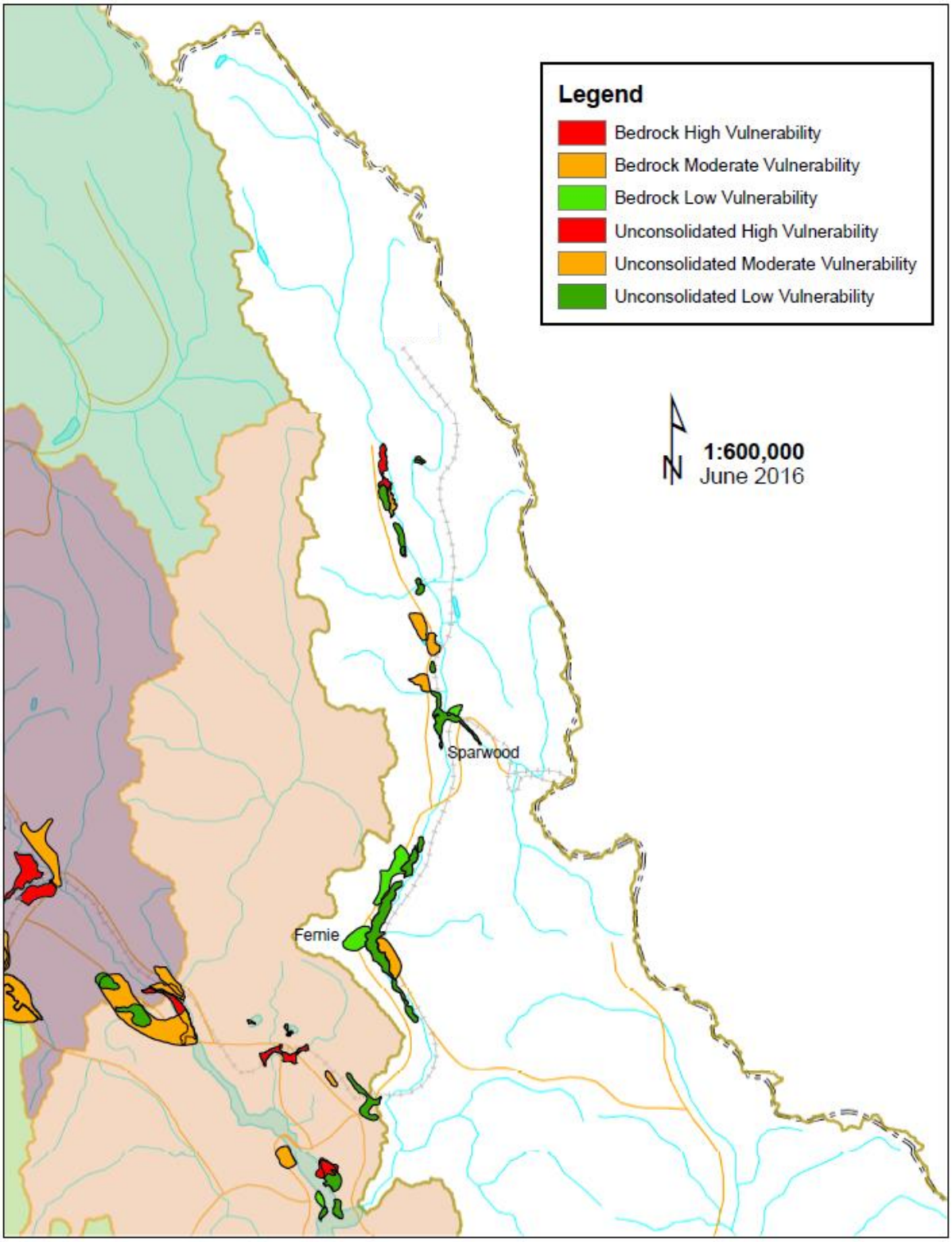

Figure A-8. Aquifers located within the Elk River Watershed based on information from the British Columbia provincial government database.

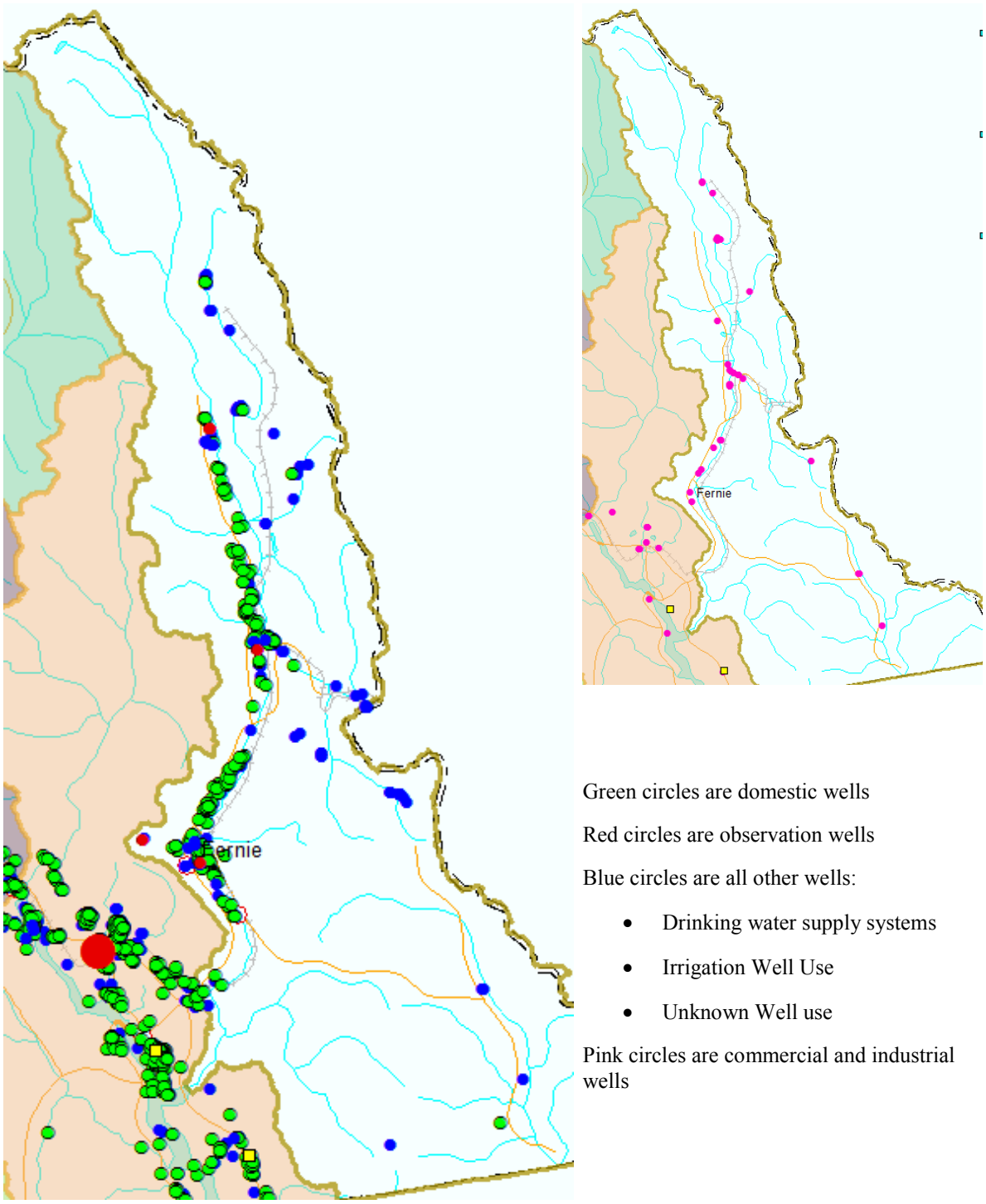

Figure A-9. Groundwater well use and presence in the Elk River Watershed based on information from the British Columbia provincial government database.

B. Missing Data

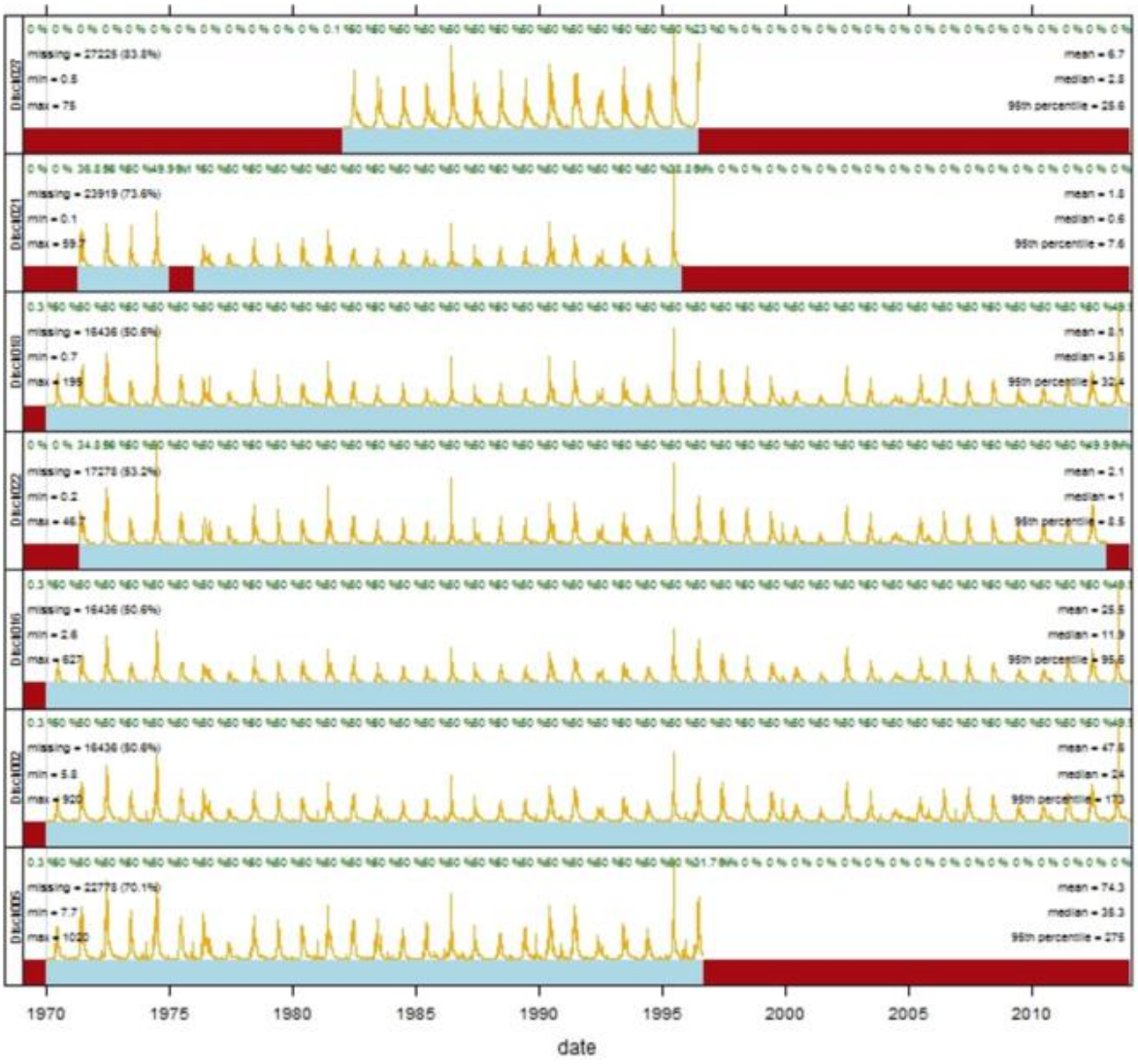

Figure B-1. Hydrograph of the seven discharge stations in the Elk River Watershed from 1970 to 2013. Blue shows periods of available discharge data, red shows periods of missing discharge data. The stations are shown from north (top) to south (bottom) and include: 08NK027, 08NK021, 08NK018, 08NK022, 08NK016, 08NK002, and 08NK005.

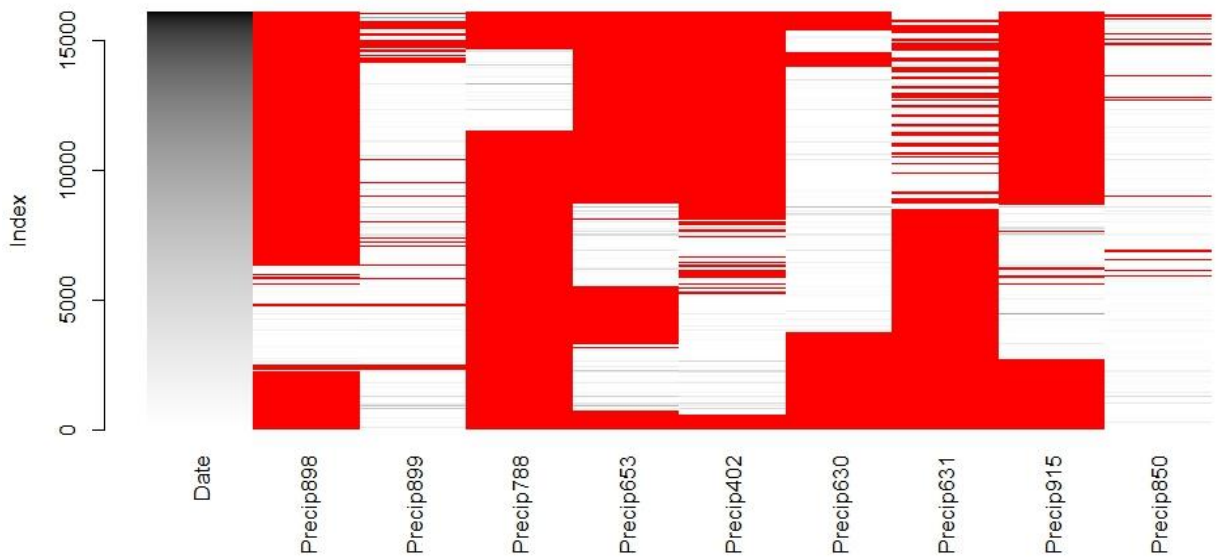

Figure B-2. Map of missing precipitation data in climate station outputs from the northern half of the Elk River watershed. The areas in red represent missing data. This graph is for the time period between January 1, 1970 and December 31, 2013. The y axis is time, with 1 representing January 1, 1970

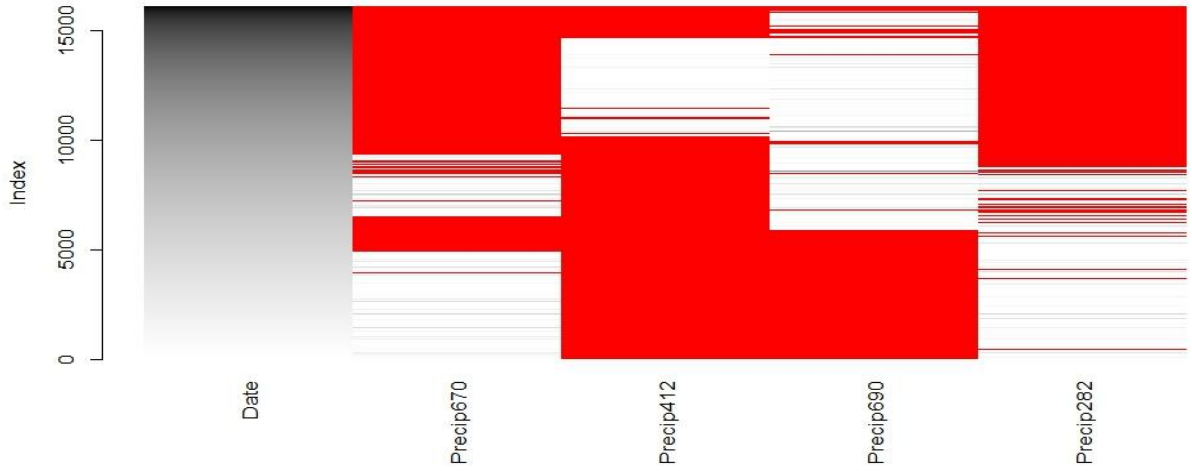

Figure B-3. Map of missing precipitation data in climate station outputs for the southern half of the Elk River watershed. The areas in red represent missing data. This graph is for the time period between January 1, 1970 and December 31, 2013. The y axis is time, with 1 representing January 1, 1970.

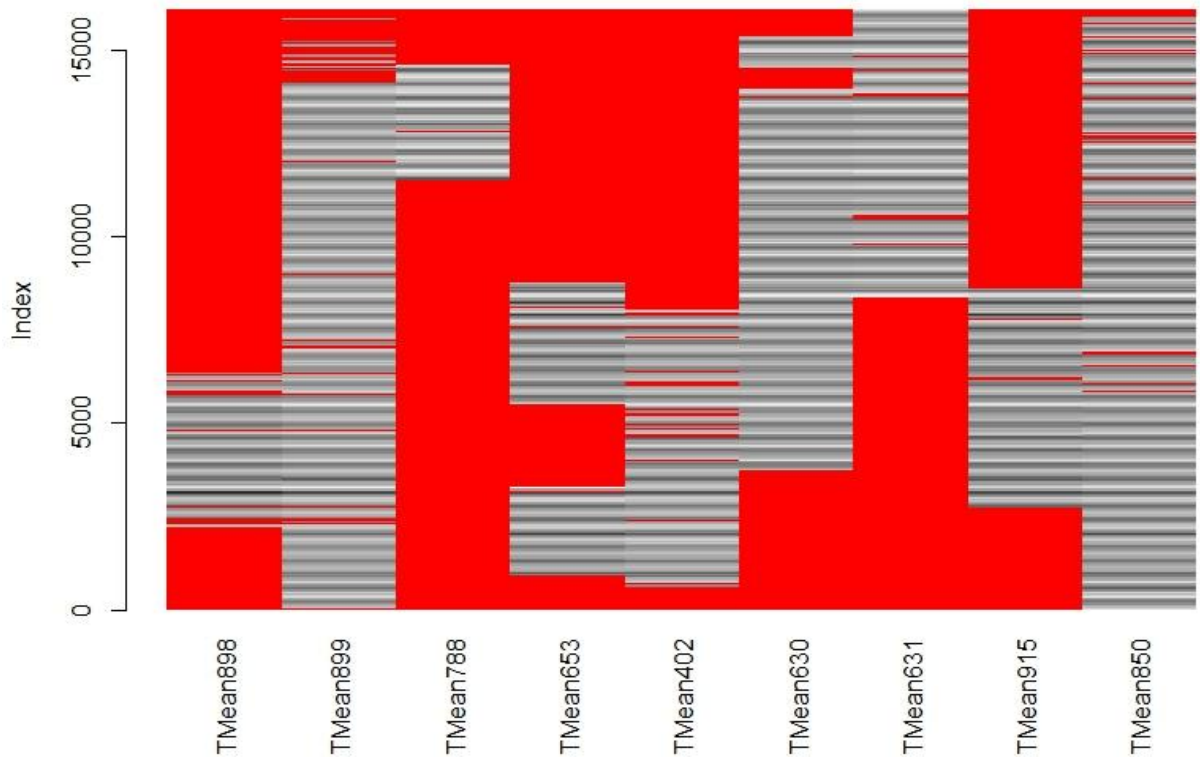

Figure B-4. Missing temperature data, represented in red, from the climate monitoring stations in the northern half of the Elk River watershed. The y axis is the date with 1 equal to January 1, 1970. Available data shown from January 1, 1970 to December 31, 2013.

Climate BC data

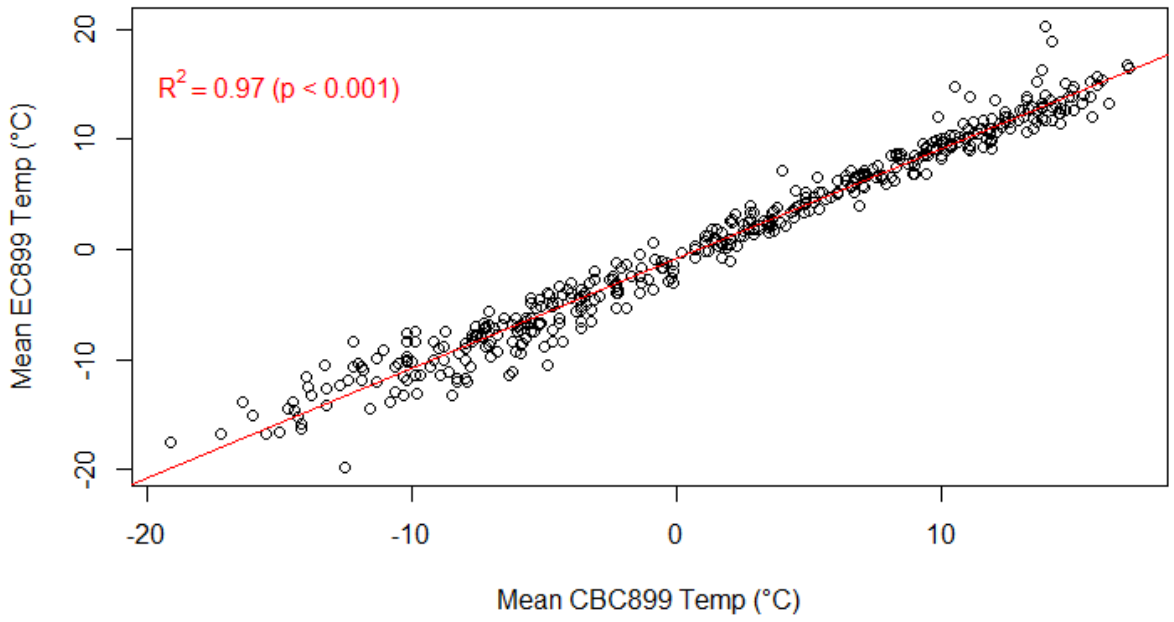

a.

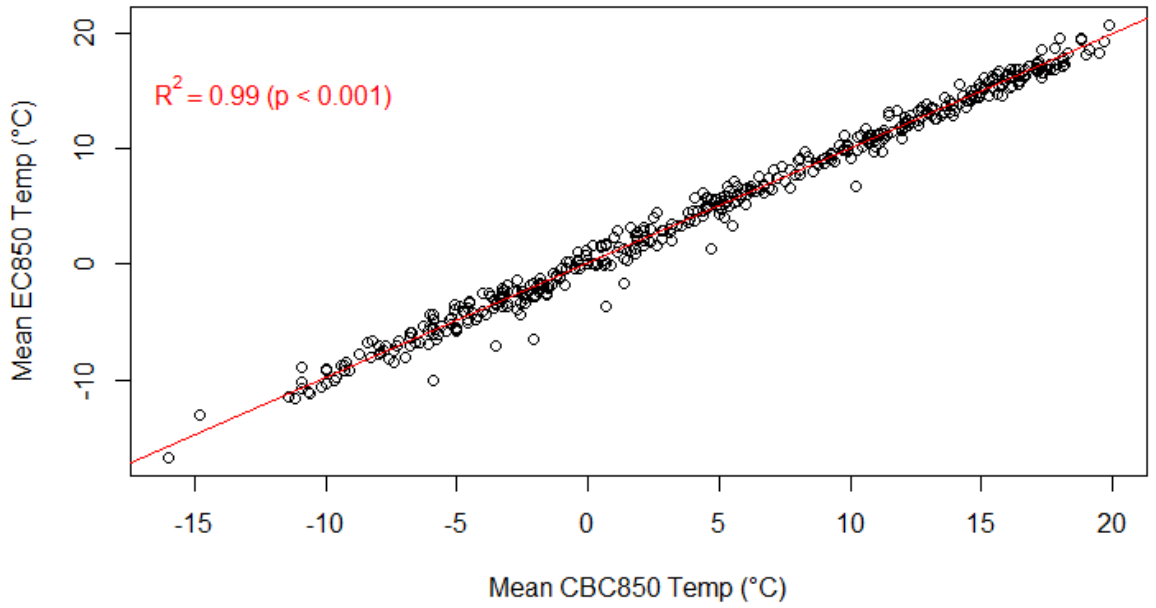

b.

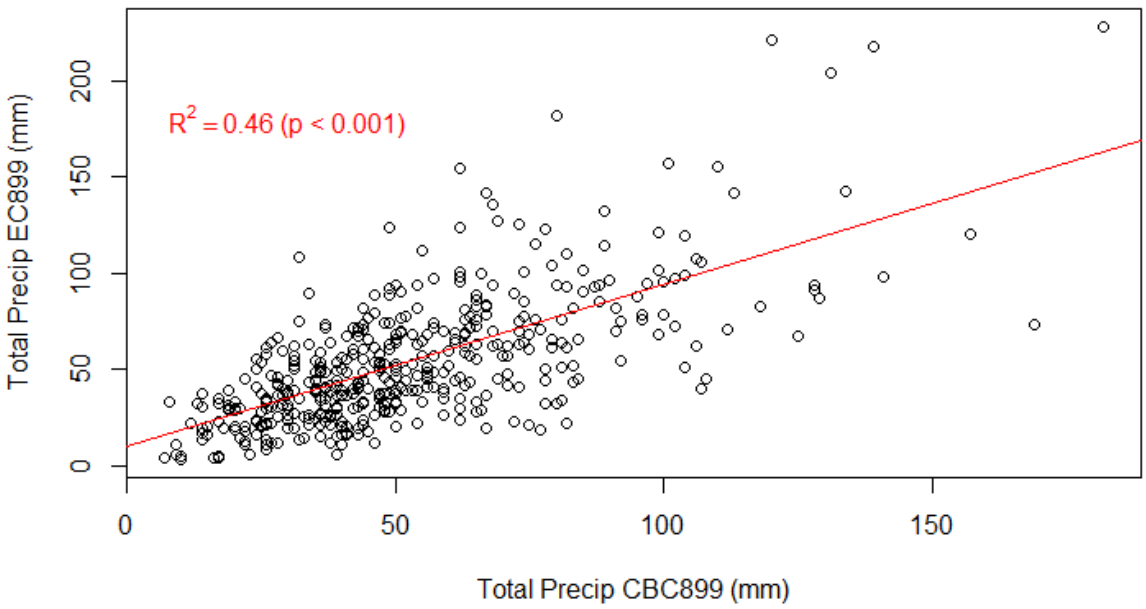

c.

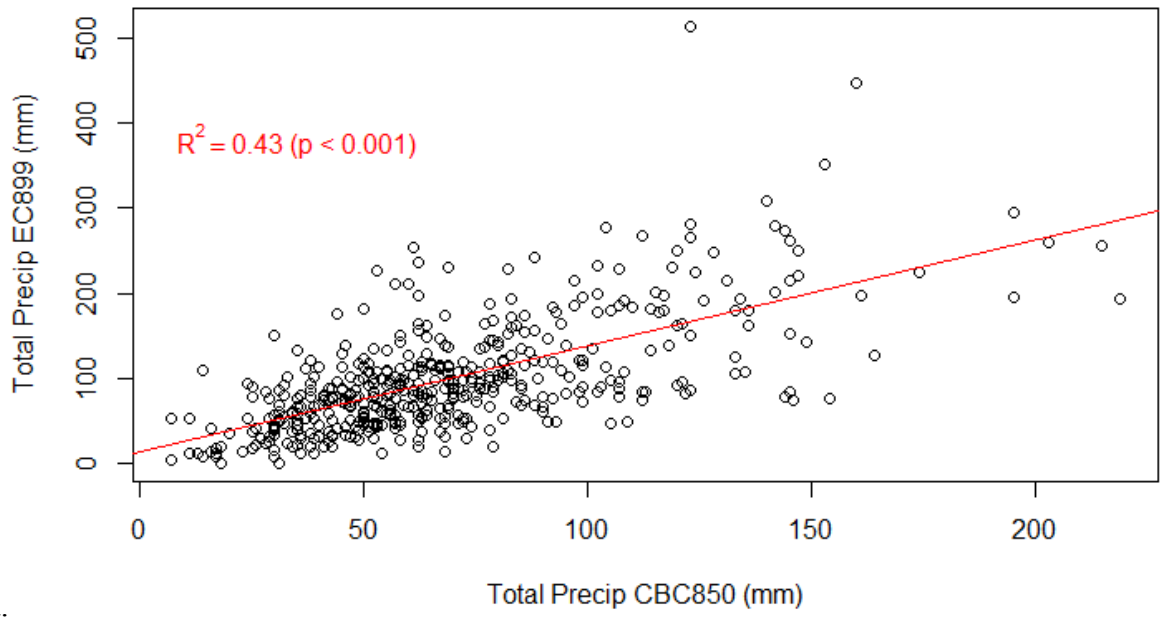

d.

Figure B-5. Comparison of monthly observed and modelled (ClimateBC), with associated R^2, temperature (a & b) and precipitation (c & d) data from 1970 to 2013.

C. Discharge

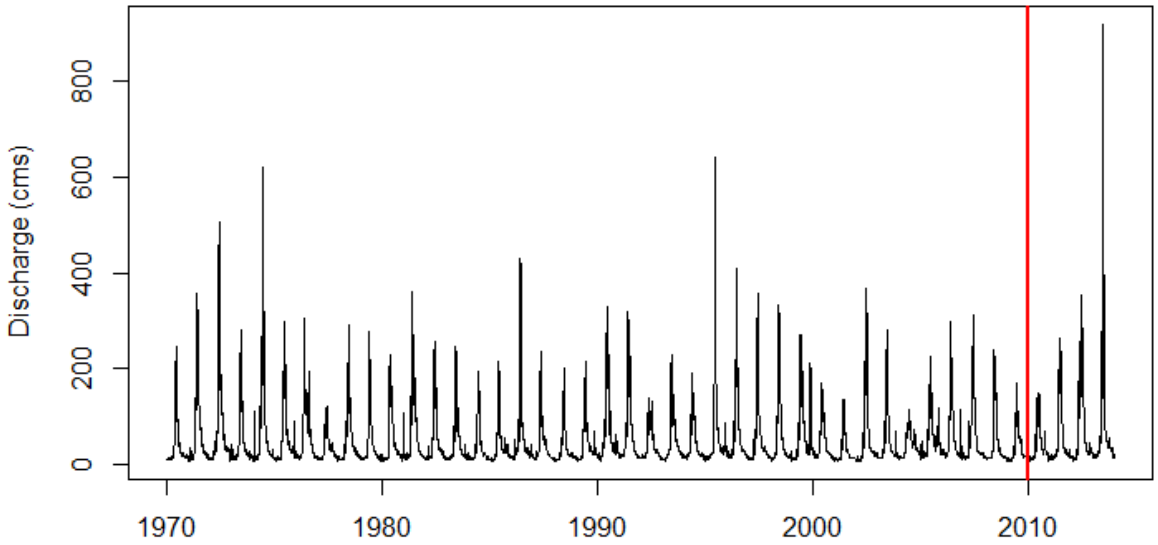

a.

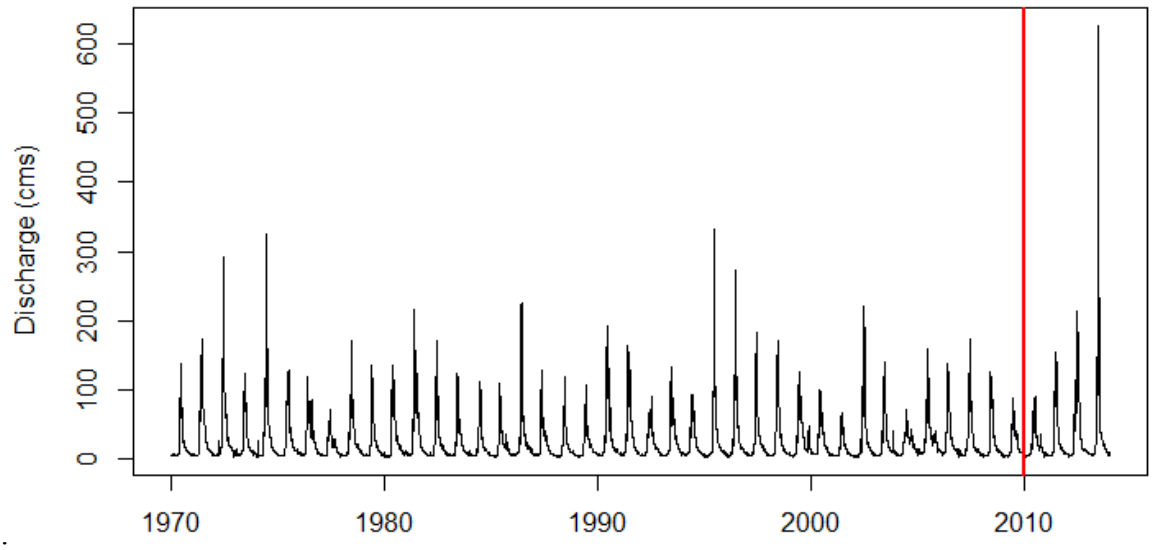

b.

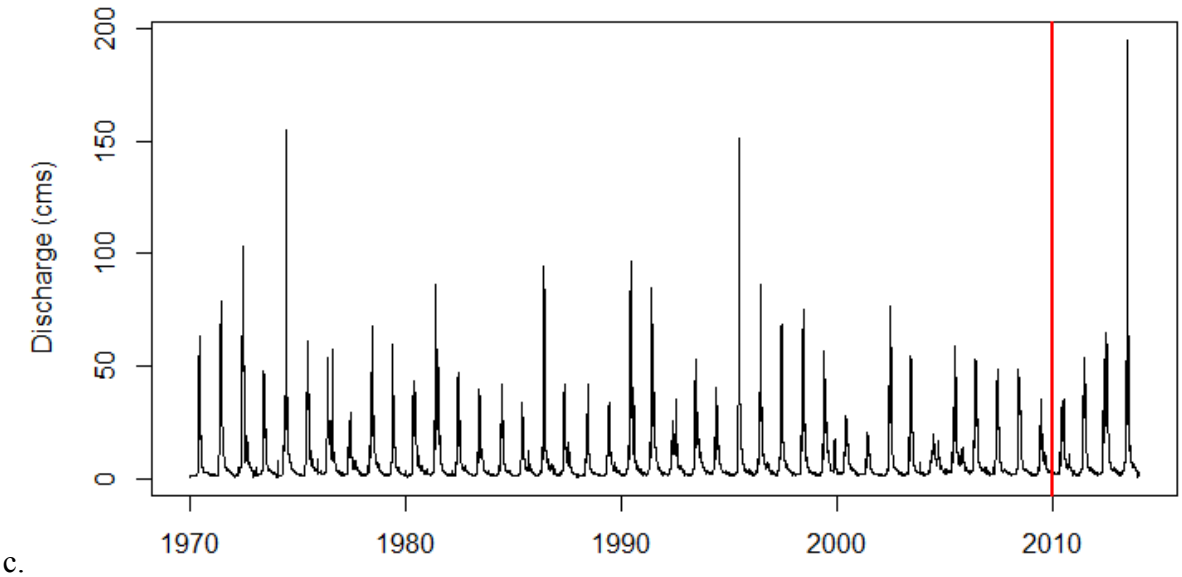

c.

Figure C-1. Hydrograph for Water Survey of Canada stations (a) 08NK002, (b) 08NK016 and (c) 08NK018 from 1970 to 2013. A vertical red line has been placed at December 31, 2009; hydrograph left of the red line represents 1970 to 2009.

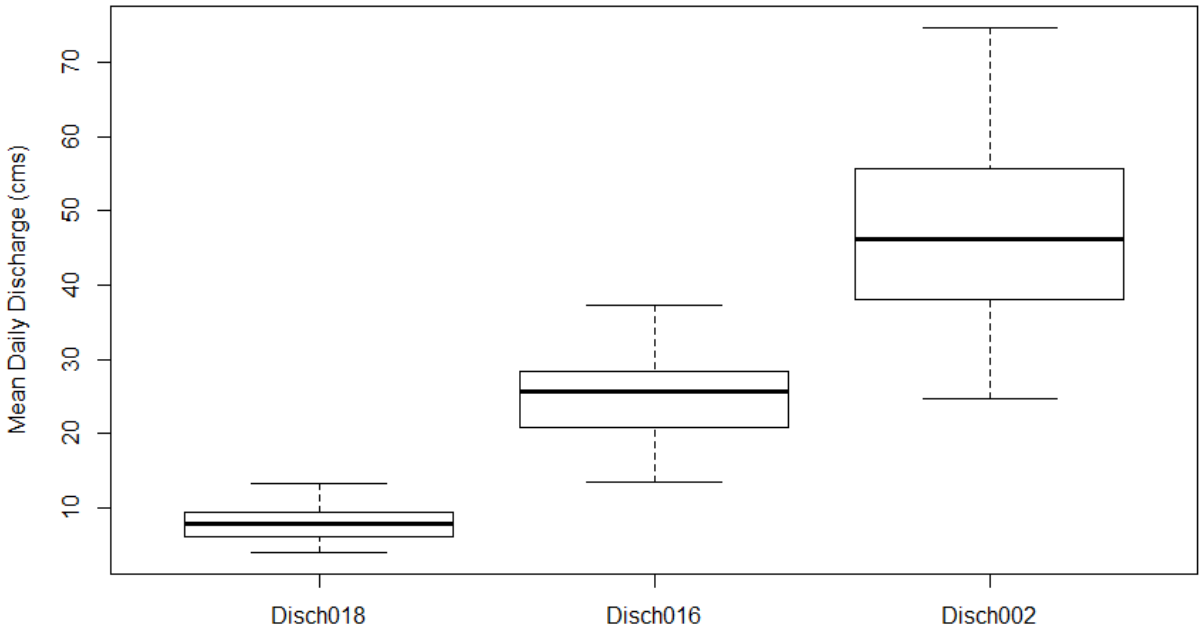

Figure C-2. Mean annual discharge for the three focused stations from 1970 to 2009. Available data must exceed 95% for the year to be counted.

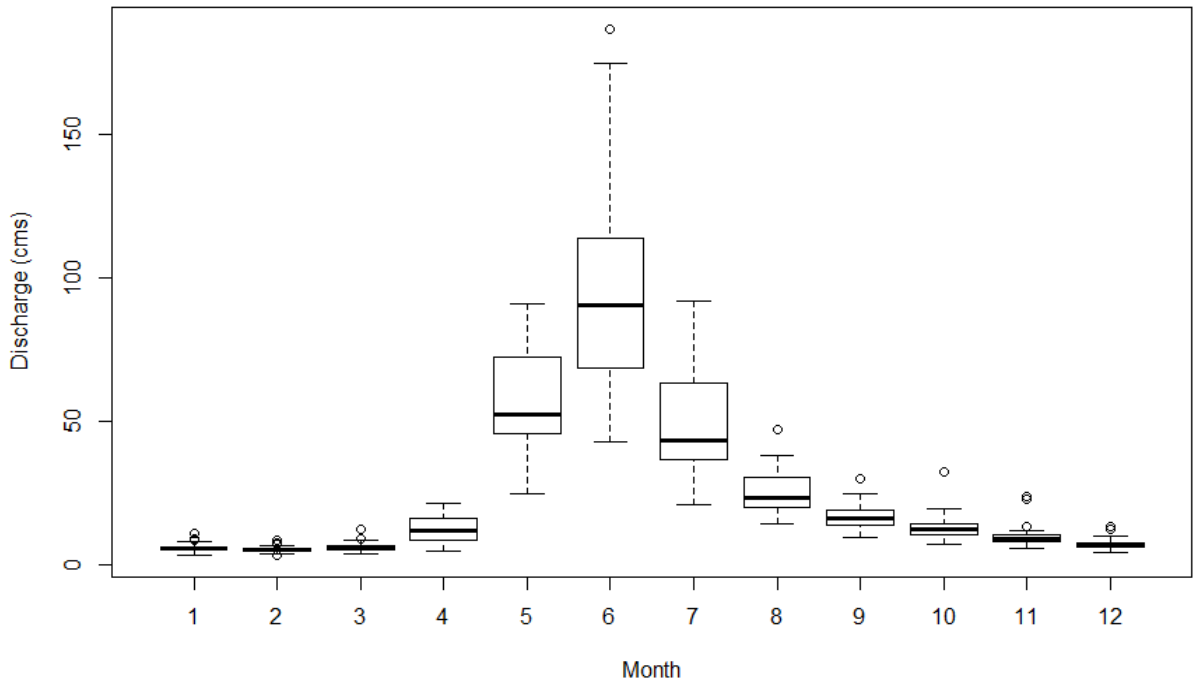

Figure C-3. Interquartile range by monthly mean discharge for station 08NK016 from 1970 to 2009. Graph is based on calendar months: January = 1 and December = 12.

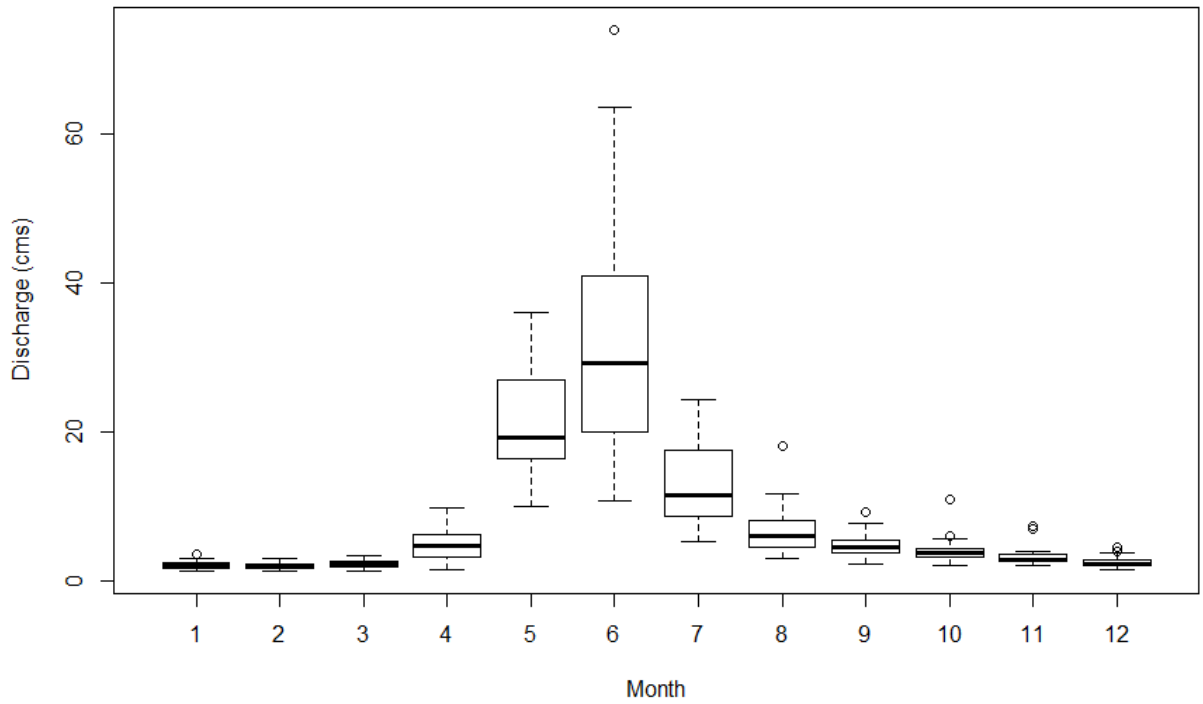

Figure C-4. Interquartile range by monthly mean discharge for station 08NK018 from 1970 to 2009. Graph is based on calendar months: January = 1 and December = 12.

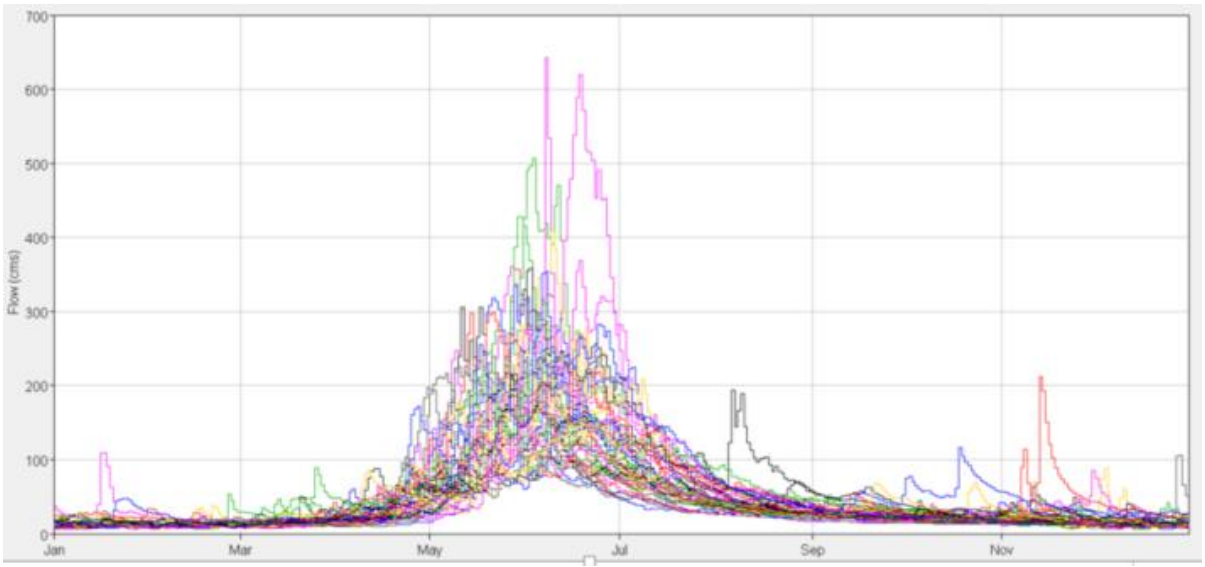

Figure C-5. Hydrograph showing all years from 1970 to 2009 for station 08NK002.

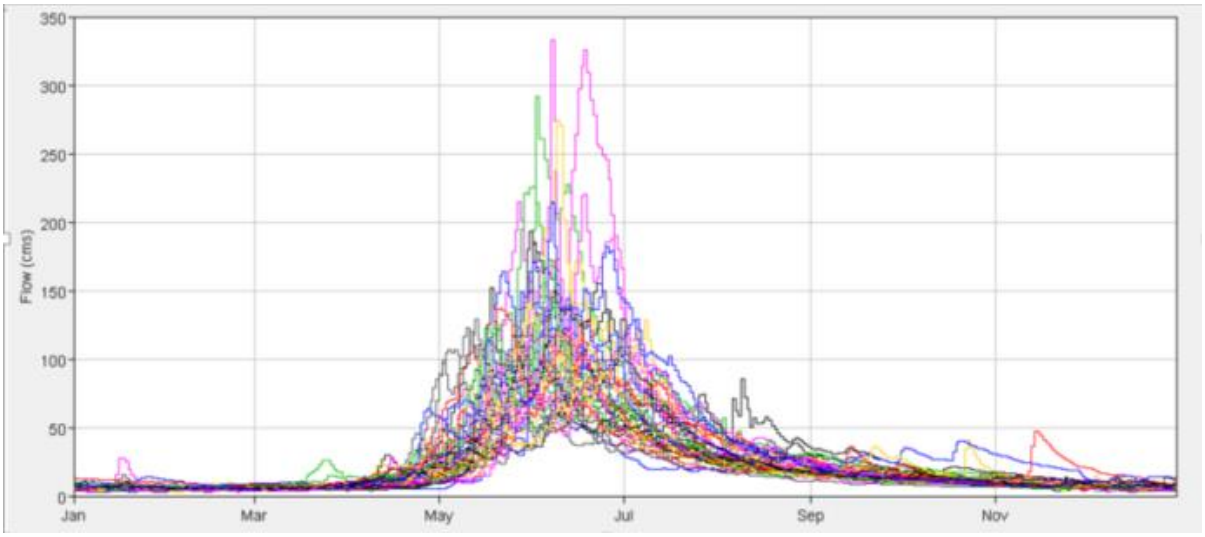

Figure C-6. Hydrograph showing all years from 1970 to 2009 for station 08NK016.

Table C-1. Mean annual discharge (m3s-1) by decade for Water Survey of Canada stations 08NK018, 08NK016 and 08NK002.

	08NK018			08NK016			08NK002		
Decade	μ	SD	±CI 95%	μ	SD	±CI 95%	μ	SD	±CI 95%
1970	8.69	13.52	0.44	26.66	35.60	1.15	51.17	68.13	2.21
1980	6.85	9.42	0.31	22.92	28.47	0.92	41.90	49.79	1.62
1990	8.81	11.85	0.38	27.25	33.81	1.10	51.30	60.09	1.95
2000	7.41	9.44	0.31	23.54	28.12	0.91	43.35	49.41	1.60

Hydrometric regionalization

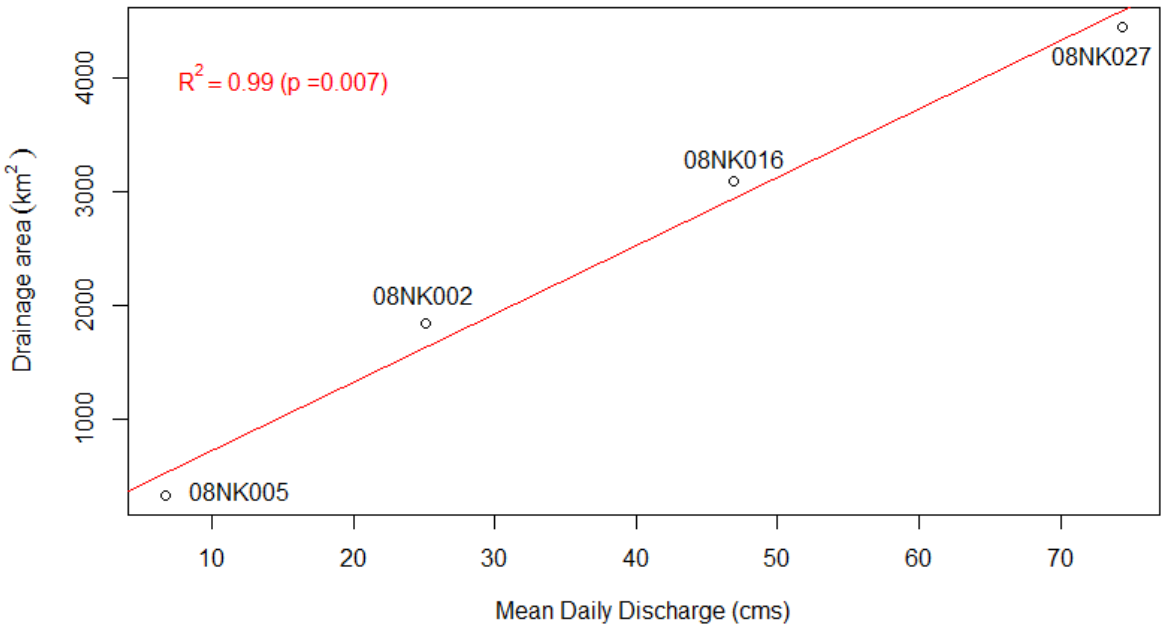

Figure C-7. Station's mean daily discharge (m^3s^{-1}) correlated with watershed drainage area (km^2).

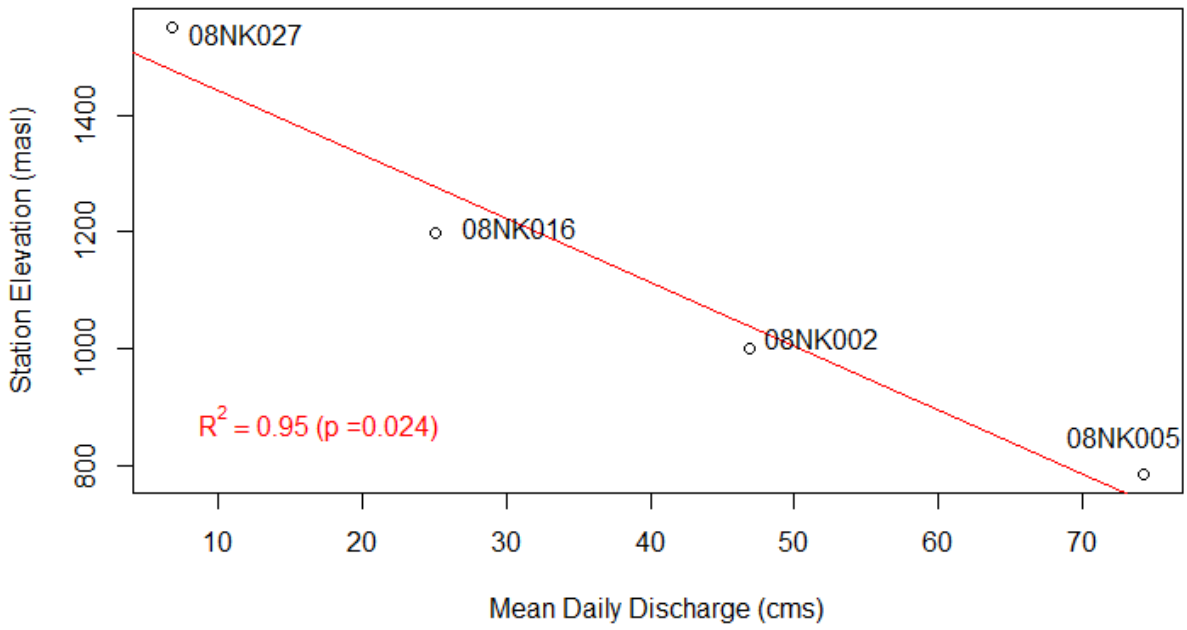

Figure C-8. Regionalized assessment of the different stations on the Elk River. Station 08NK005 (elevation 784 m) is regulated.

Trends

a.

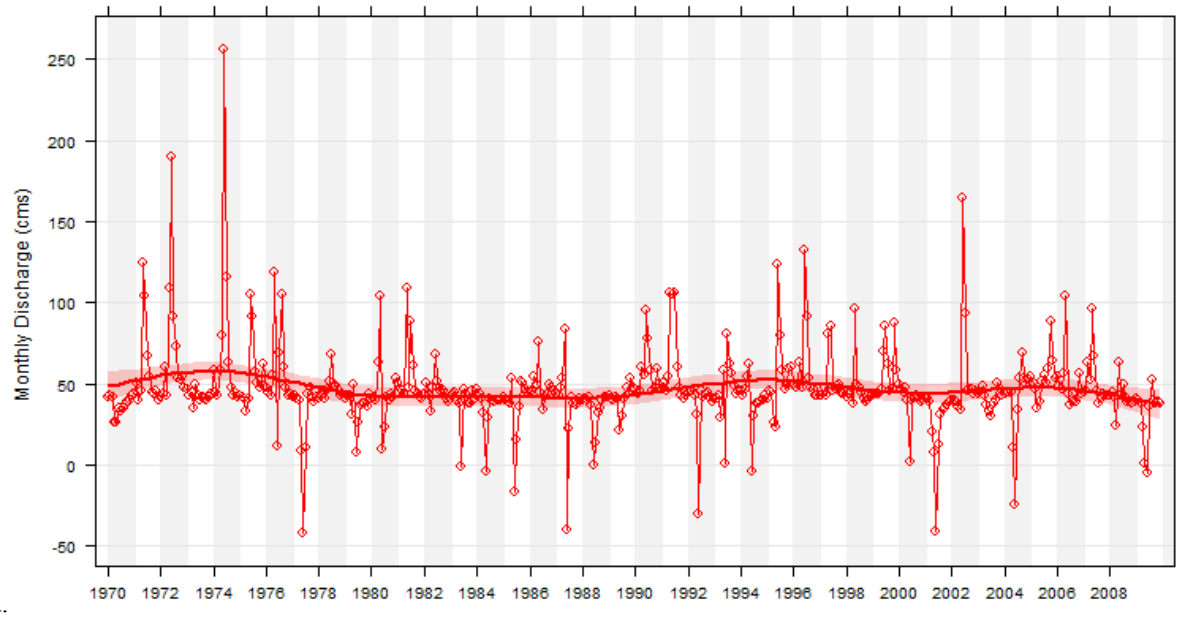

b.

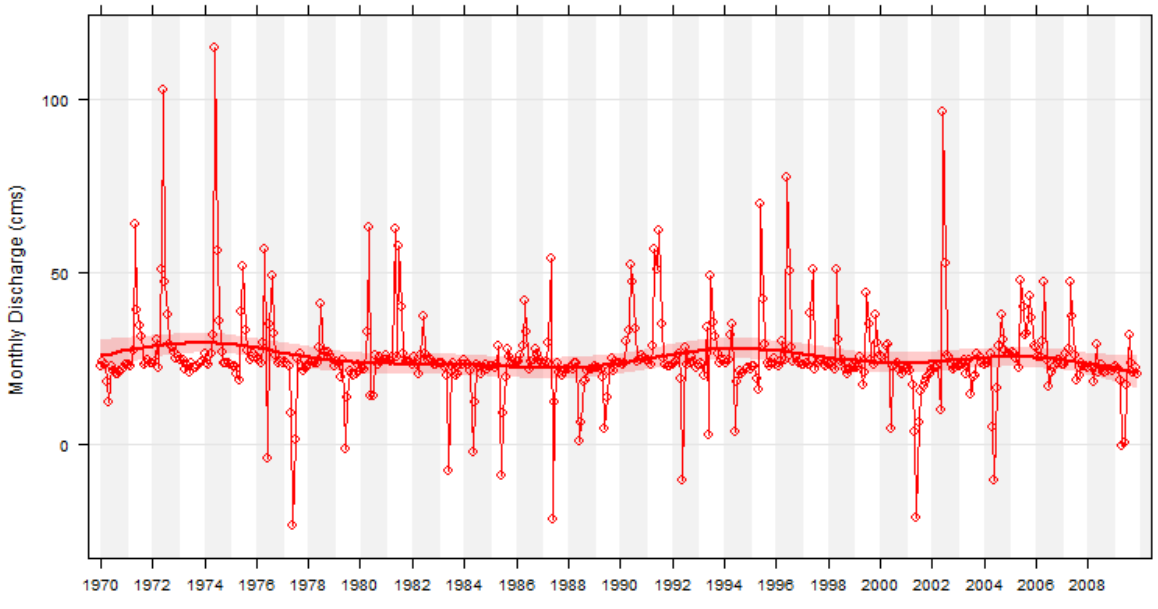

c.

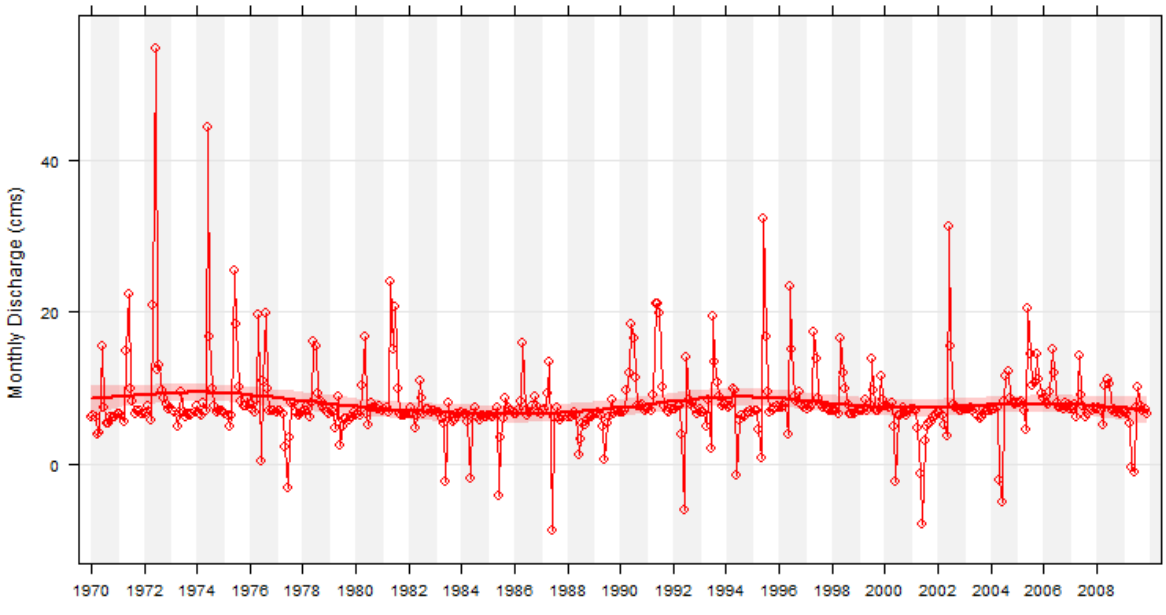

Figure C-9. Smoothing trend for the monthly mean discharge at stations (a) 08NK002, (b) 08NK016 and (c) 08NK018 from 1970 to 2009. 95% Confidence level is shown in light red on either side of trend line. Seasonal trend has been removed.

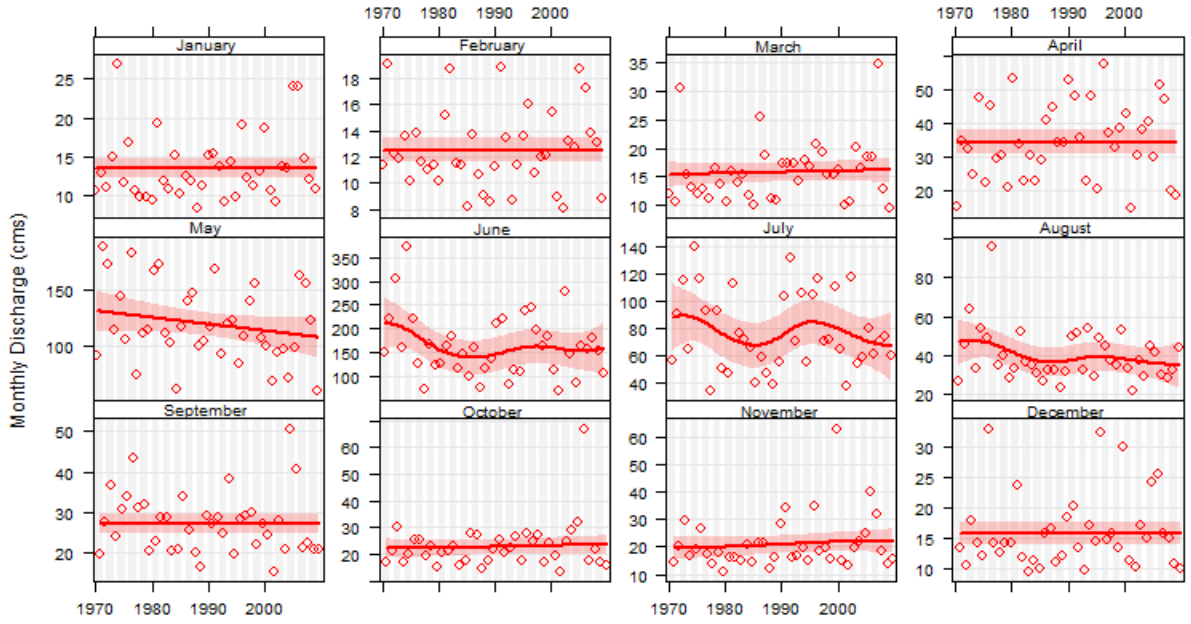

Figure C-10. Mean monthly discharge analysis for 08NK002 from 1970 to 2009. 95% Confidence level is shown in light red on either side of trend line.

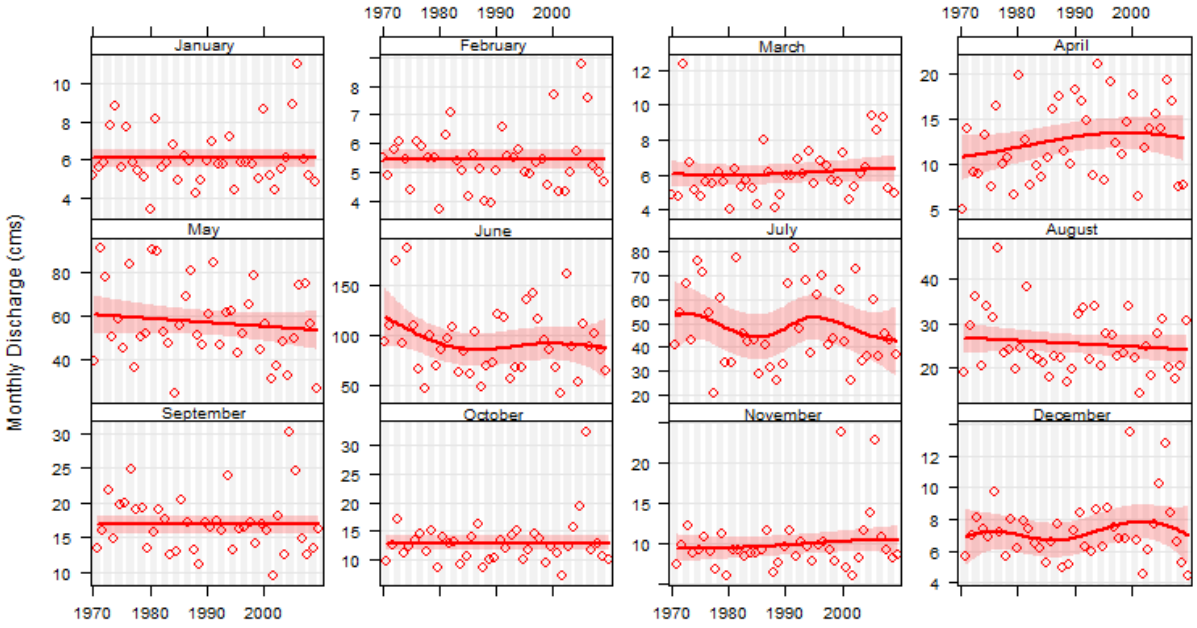

Figure C-11. Mean monthly discharge analysis for 08NK016 – smoothing trend. 95% Confidence level is shown in light red on either side of trend line.

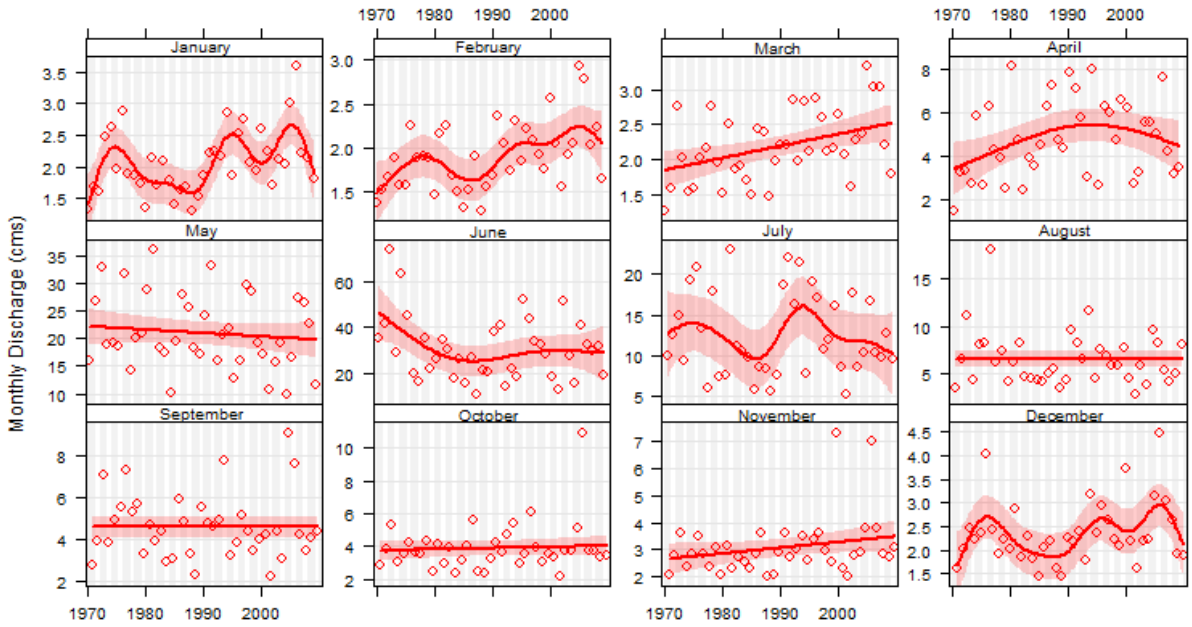

Figure C-12. Mean monthly discharge analysis for 08NK018 – smoothing trend. 95% Confidence level is shown in light red on either side of trend line.

a.

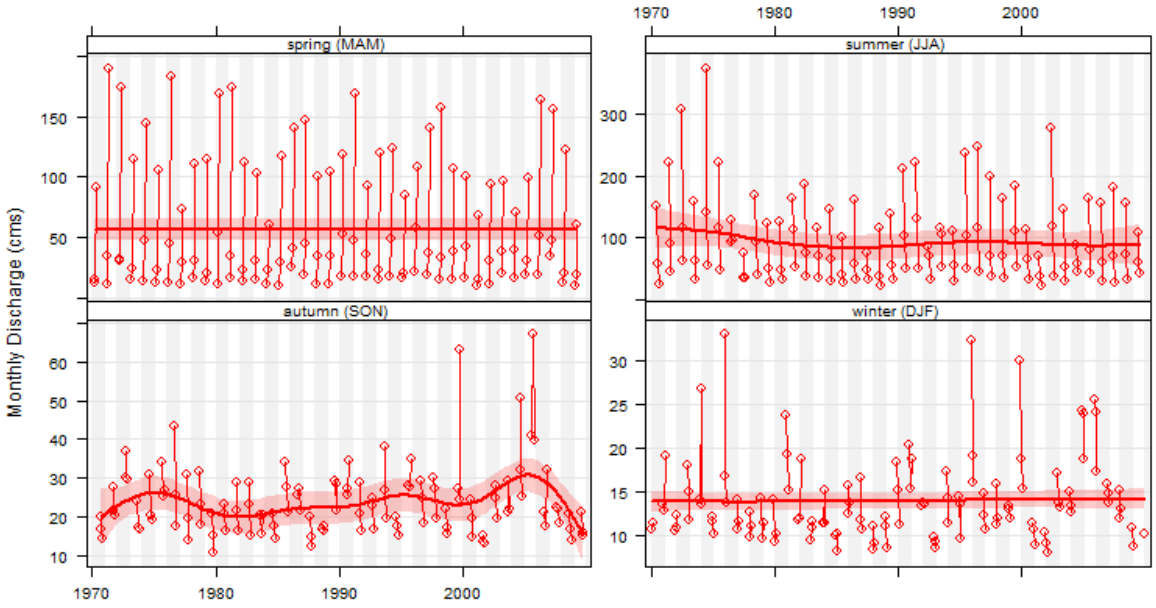

b.

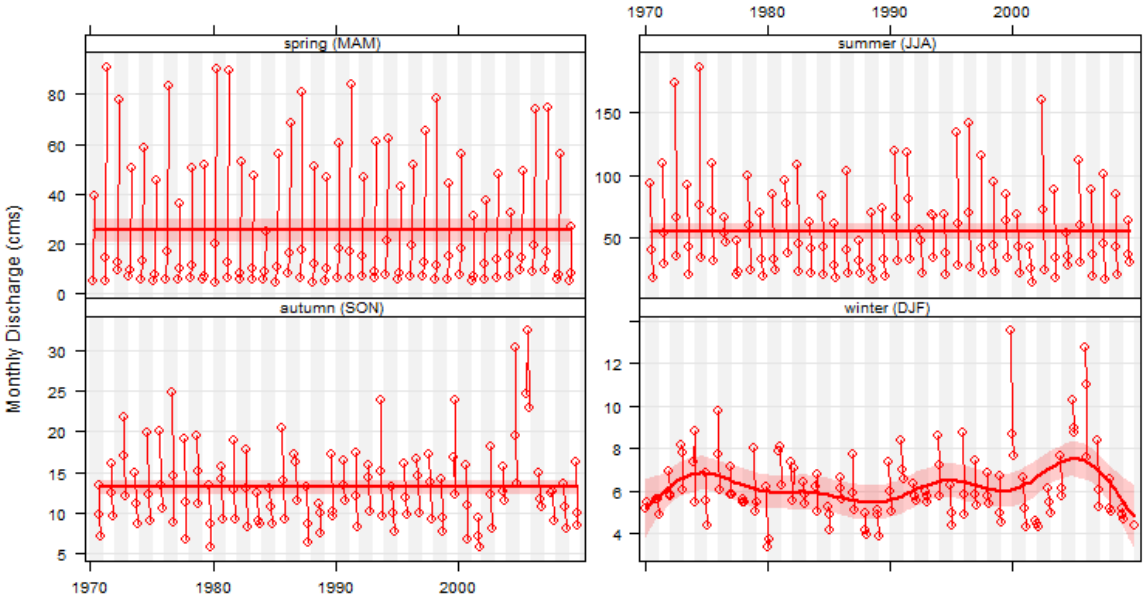

c.

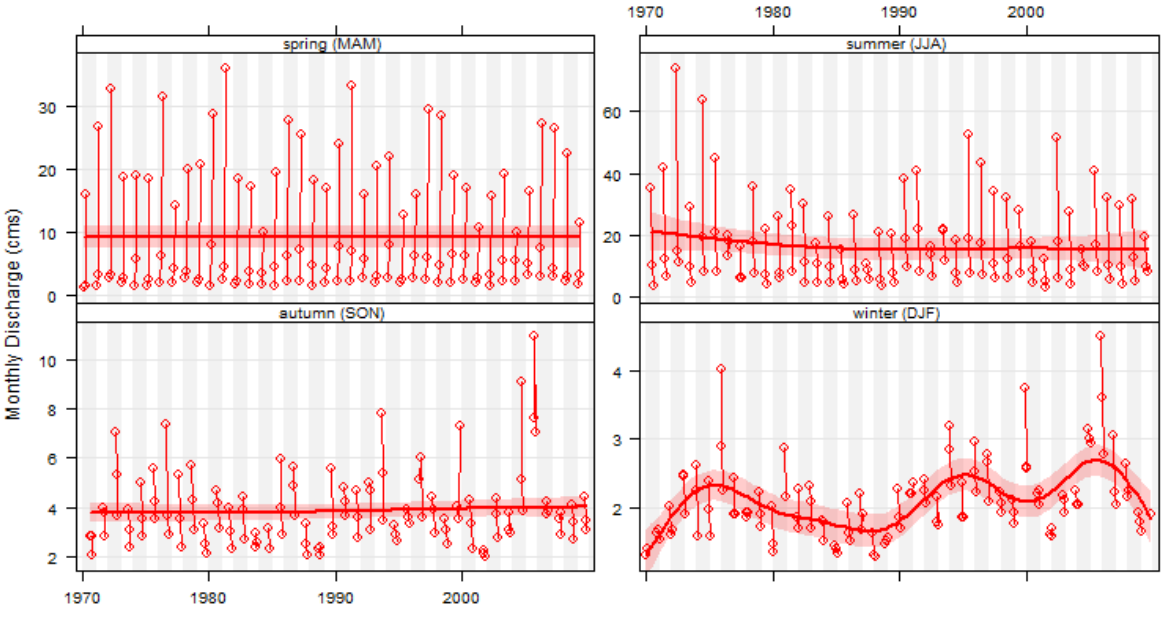

Figure C-13. Seasonal trends based on the monthly discharge means for (a) 08NK002, (b) 08NK016 and (c) 08NK018, from 1970 to 2009. 95% Confidence level is shown in light red on either side of trend line.

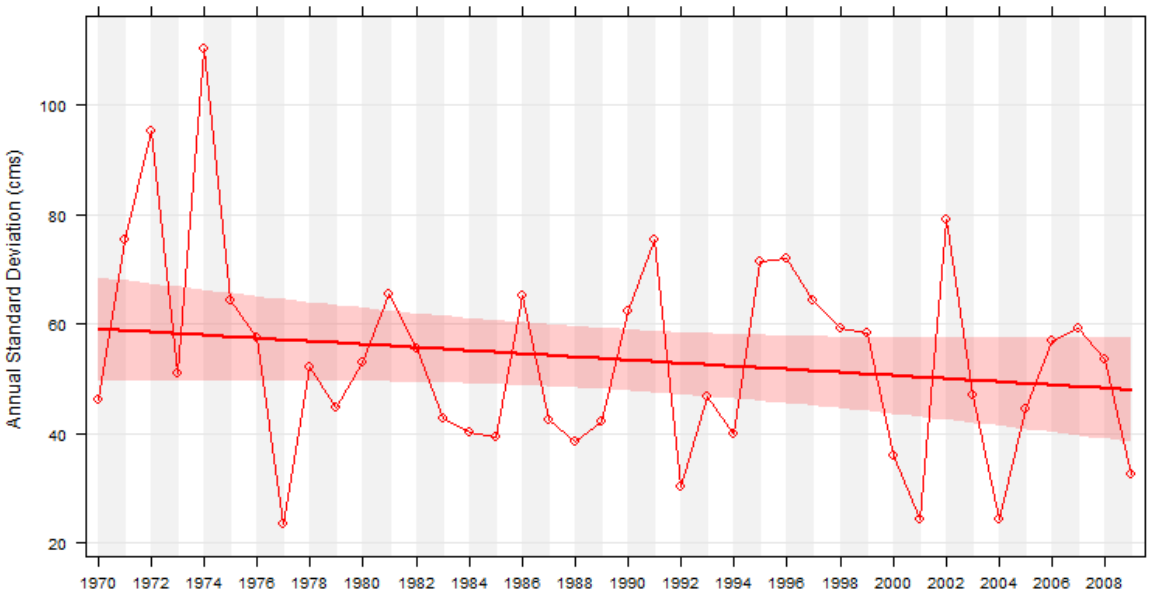
Annual Standard Deviation (cms)
100
80
60
40
20
1970 1972 1974 1976 1978 1980 1982 1984 1986 1988 1990 1992 1994 1996 1998 2000 2002 2004 2006 2008

a.

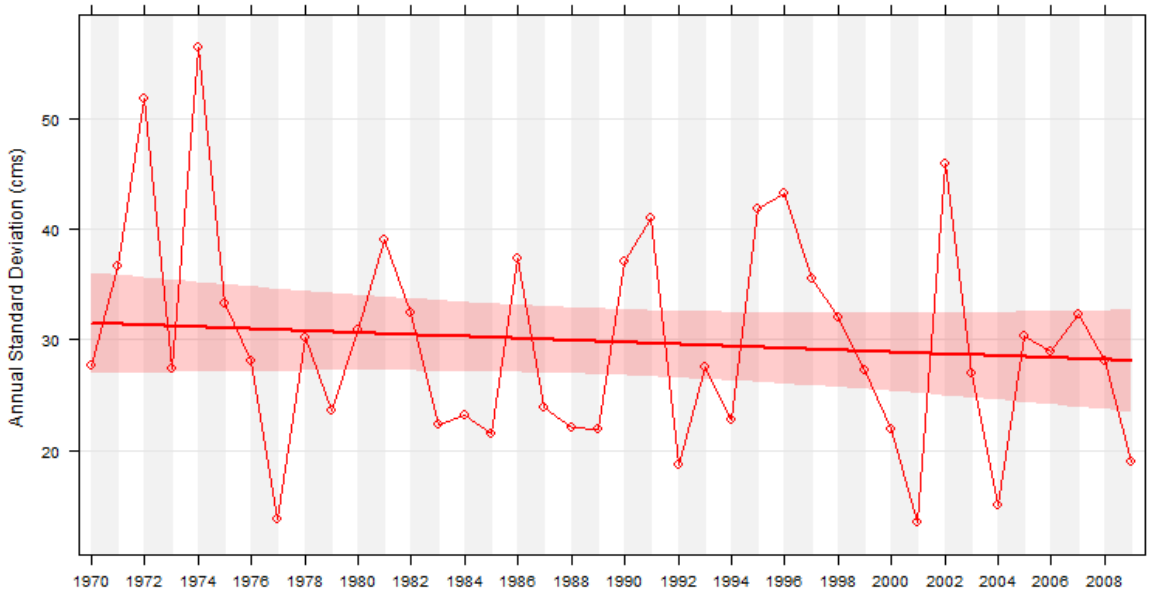
Annual Standard Deviation (cms)
50
40
30
20
1970 1972 1974 1976 1978 1980 1982 1984 1986 1988 1990 1992 1994 1996 1998 2000 2002 2004 2006 2008

b.

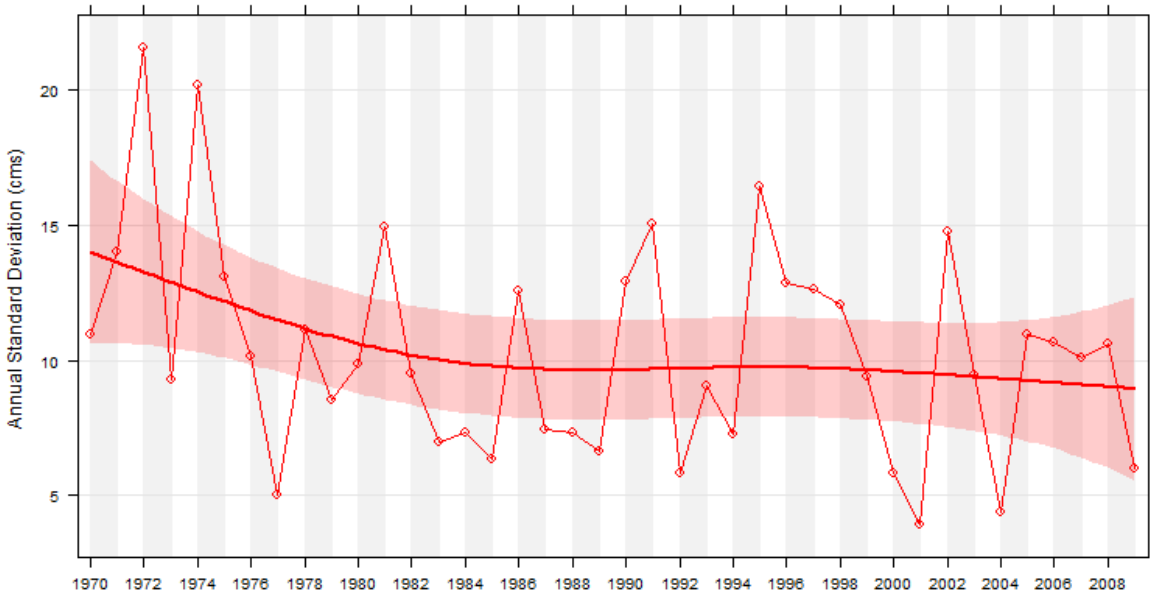

c.

Figure C-14. Annual discharge standard deviation for (a) 08NK002, (b) 08NK016 and (c) 08NK018 from 1970 to 2009. 95% Confidence level is shown in light red on either side of trend line.

Table C-2. Mean monthly and mean annual discharge trends for seven stations in the Elk River Watershed, the pink boxes represent $\alpha = 0.05$.

Mean Monthly				
1970 - 2009	slope ($m^3 s^{-1}$)	CI lower ($m^3 s^{-1}$)	CI upper ($m^3 s^{-1}$)	*p* value
08NK027	0.002	-0.007	0.011	0.671
08NK016	0.001	-0.004	0.006	0.611
08NK002	0.003	-0.011	0.017	0.683
08NK005	0.003	-0.041	0.055	0.881
08NK022	0.000	0.000	0.001	0.043
08NK018	0.001	-0.001	0.003	0.198
08NK021	0.000	-0.001	0.001	0.799
Mean Annual				
1970 - 2009	slope ($m^3 s^{-1}$)	CI lower ($m^3 s^{-1}$)	CI upper ($m^3 s^{-1}$)	*p* value
08NK027	0.111	0.020	0.211	0.033
08NK016	-0.050	-0.240	0.101	0.584
08NK002	-0.181	-0.559	0.188	0.397
08NK005	-0.554	-1.654	0.456	0.311
08NK022	-0.005	-0.024	0.012	0.580
08NK018	-0.020	-0.098	0.041	0.514
08NK021	0.005	-0.026	0.044	0.770

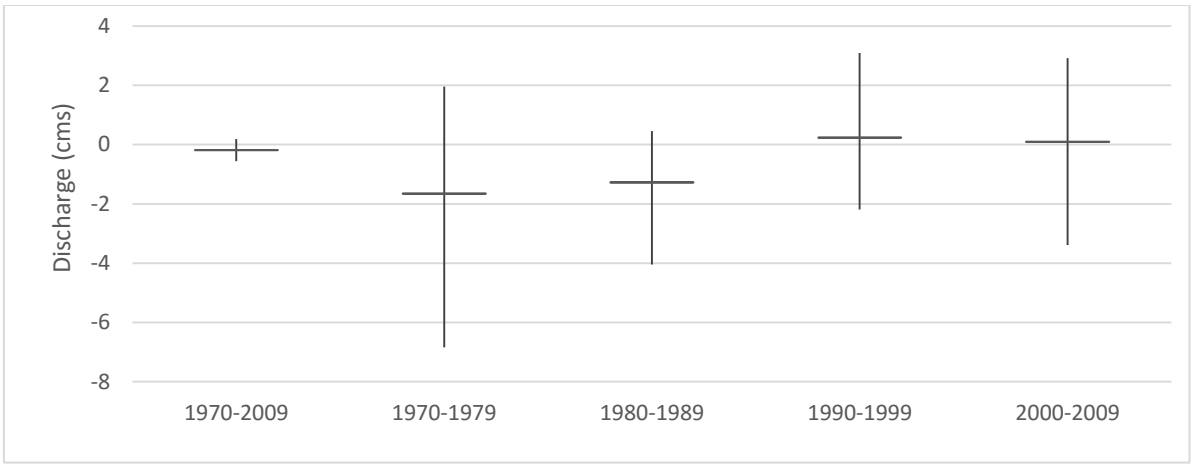

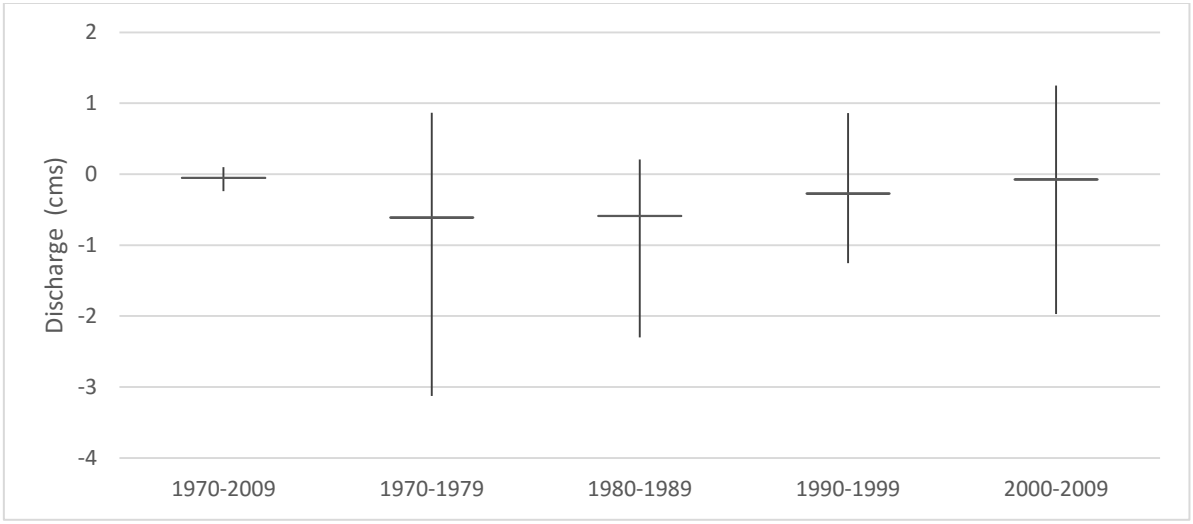

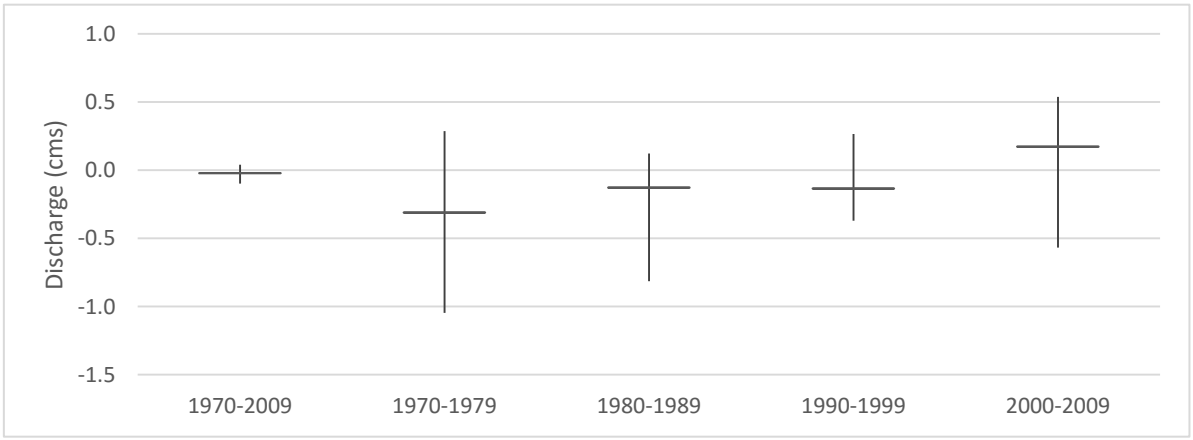

Figure C-15. Trend analysis based on annual mean discharge for (a) 08NK002, (b) 08NK016 and (c) 08NK018 from 1970 to 2009. The vertical bars represent the 95% Cl associated with the Theil Sen slope estimator, which is shown as the horizontal line.

Table C-3. Trend assessment based on mean monthly discharge for the three discharge research stations from 1970 to 2009. The Theil Sen slope results represent the percentage of change per month. Pink boxes represent $\alpha = 0.05$, yellow boxes represent $0.05 < \alpha < 0.1$, all other results are at $\alpha > 0.1$.

	08NK002	08NK016	08NK018
January	0.028	-0.008	0.011
February	0.019	-0.007	0.012
March	0.099	0.032	0.017
April	0.163	0.115	0.039
May	-1.141	-0.523	-0.145
June	-0.751	-0.357	-0.165
July	-0.174	-0.149	-0.030
August	-0.197	-0.128	-0.026
September	-0.179	-0.101	-0.026
October	0.028	-0.023	0.001
November	0.060	0.019	0.013
December	0.032	-0.024	0.005
Autumn	0.007	0.002	0.001
Spring	0.006	0.004	0.002
Summer	-0.011	-0.008	-0.001
Winter	0.000	-0.001	0.001
Full year	0.003	0.001	0.001

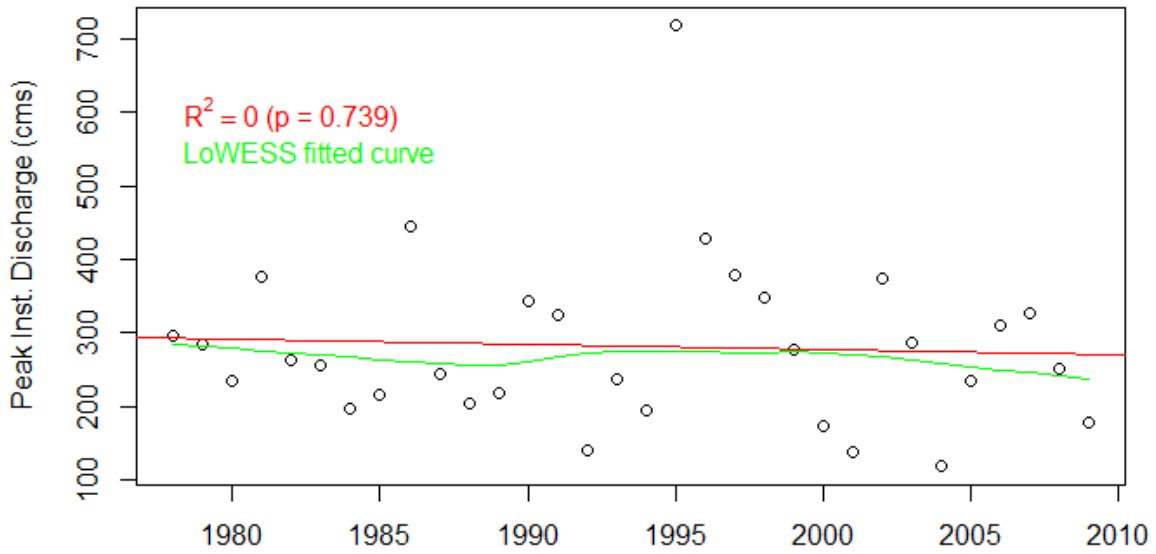
Peak Inst. Discharge (cms)
100
200
300
400
500
600
700
1980
1985
1990
1995
2000
2005
2010
R2 = 0 (p = 0.739)
LoWESS fitted curve

a.

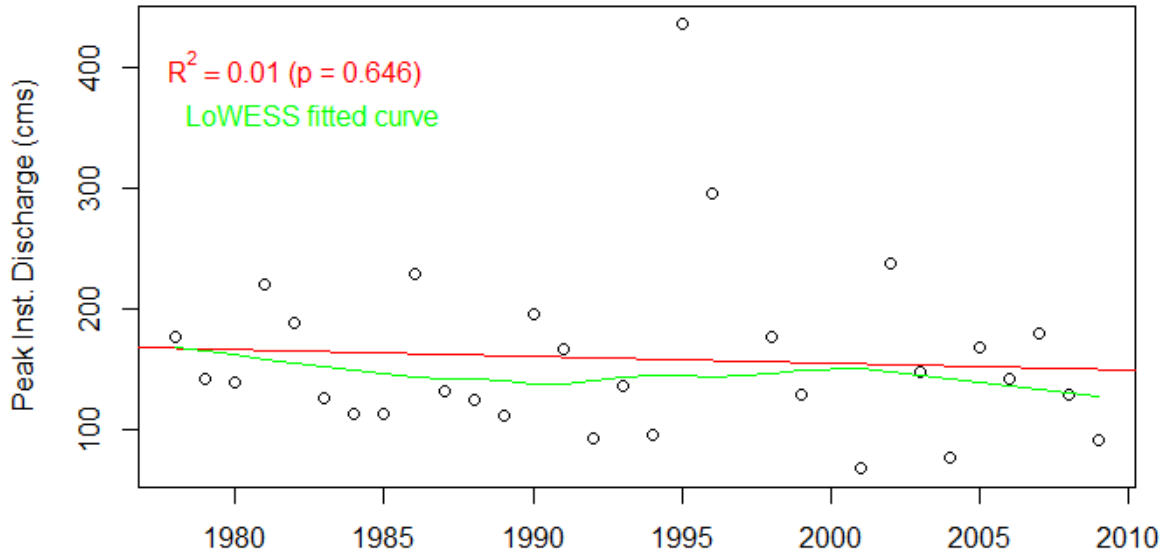
Peak Inst. Discharge (cms)
100
200
300
400
1980
1985
1990
1995
2000
2005
2010
R2 = 0.01 (p = 0.646)
LoWESS fitted curve

b.

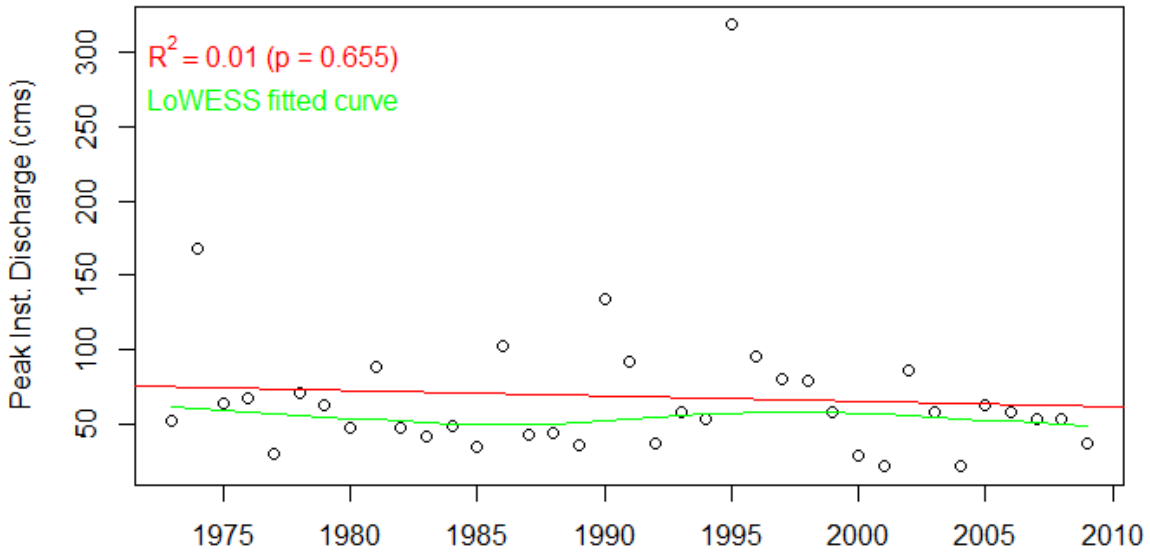

c.

Figure C-16. Instantaneous peak flow volume for all three discharge research stations from 1970 to 2009. Both linear trend line (with associated R^2) and smoothing curve LOWESS are shown. (a) 08NK002, (b) 08NK016 and (c) 08NK018.

Timing of Instantaneous Peak Flow Discharge

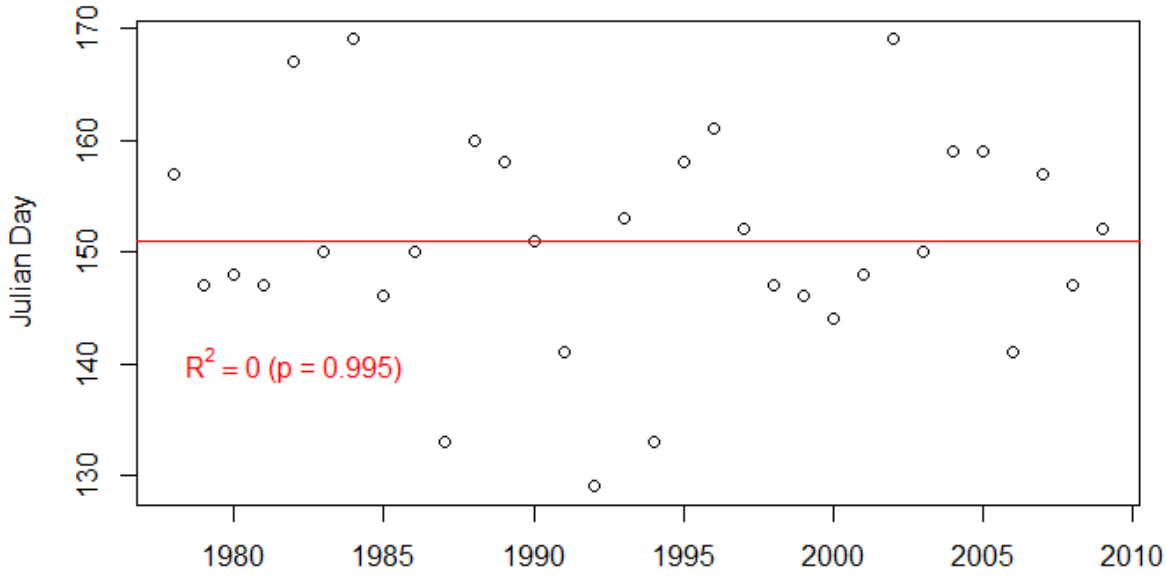

a.

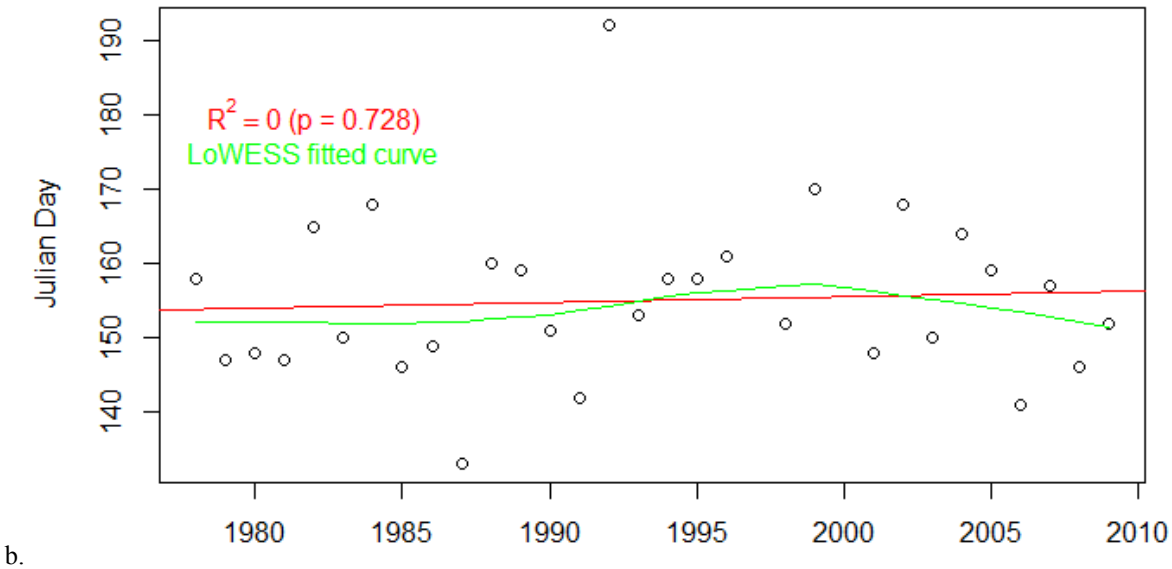

b.

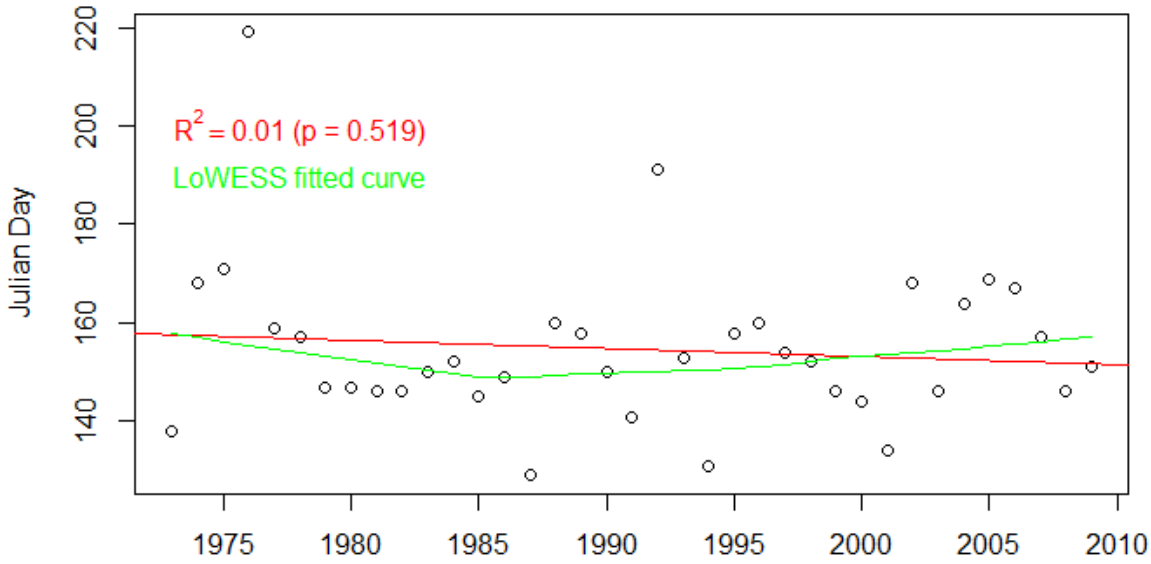

c.

Figure C-17. Timing of instantaneous peak flows for the discharge research stations from 1970 to 2009. Both linear and polynomial (four point) trend line are shown, with associated R^2 value. (a) 08NK002; (b) 08NK016 and (c) 08NK018.

Maximum Daily Discharge (High Flow Events)

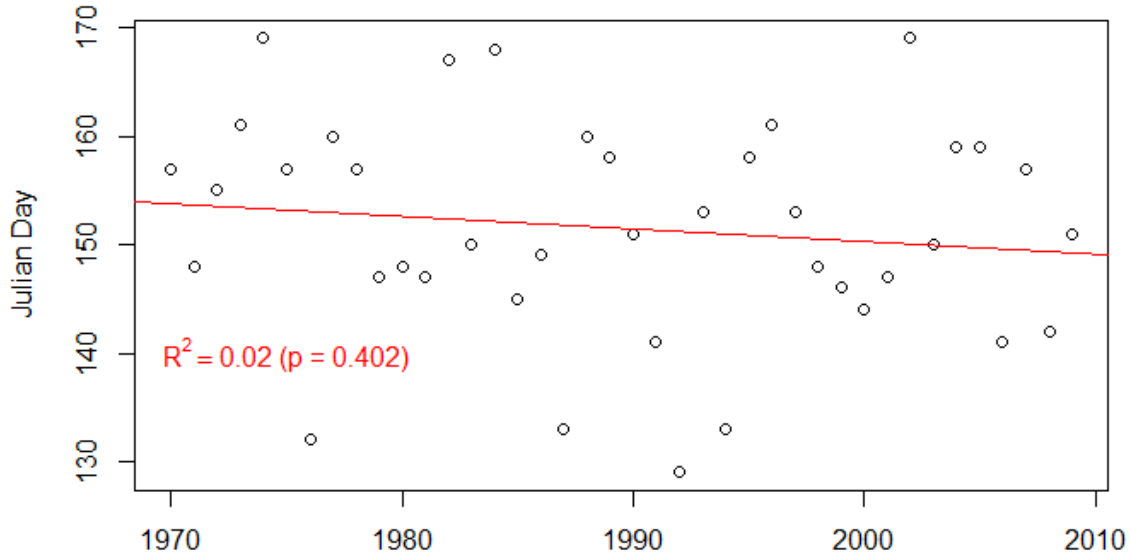

a.

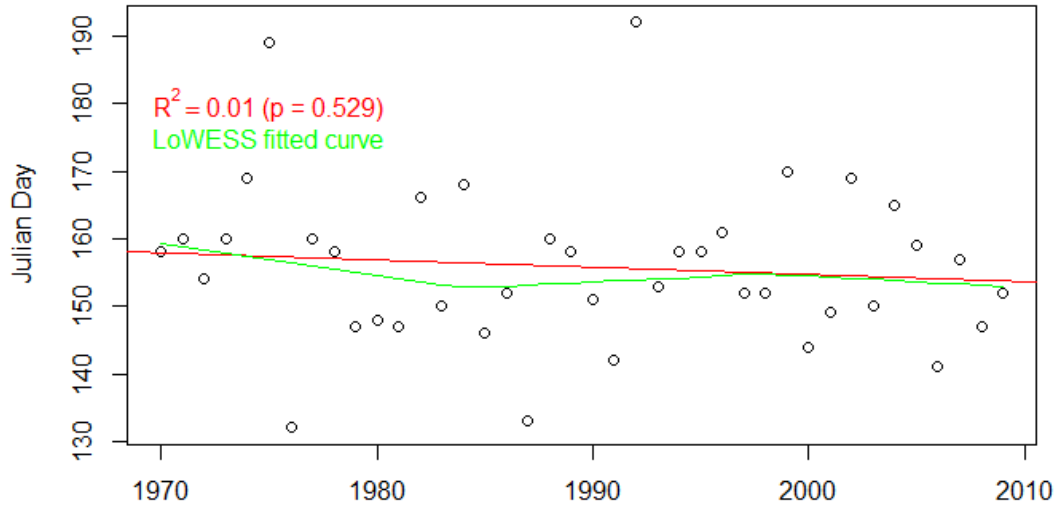

b.

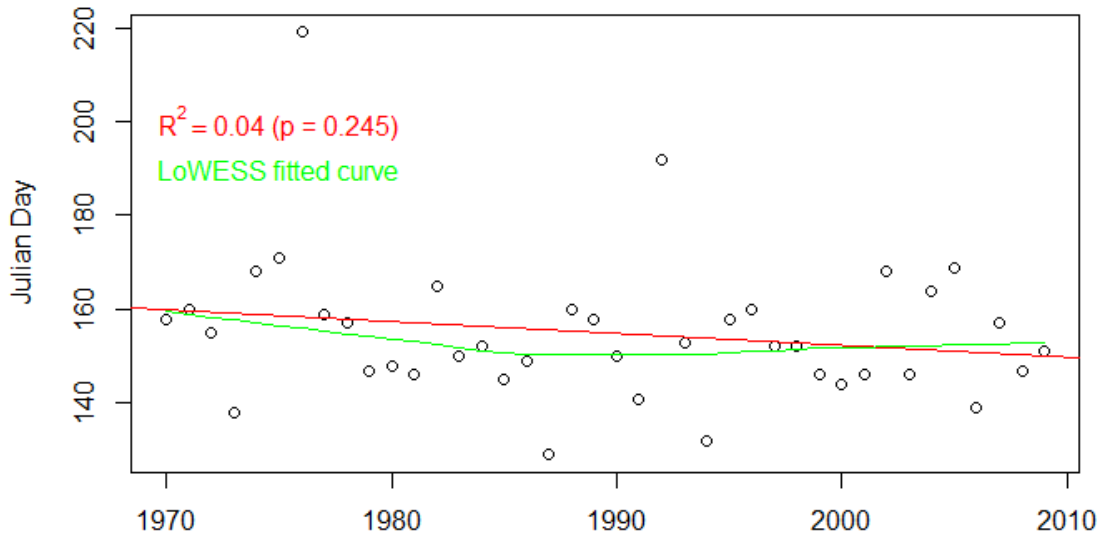

c.

Figure C-18. Timing of the maximum annual discharge for all three discharge research stations from 1970 – 2009. (a) 08NK002; (b) 08NK016 and (c) 08NK018.

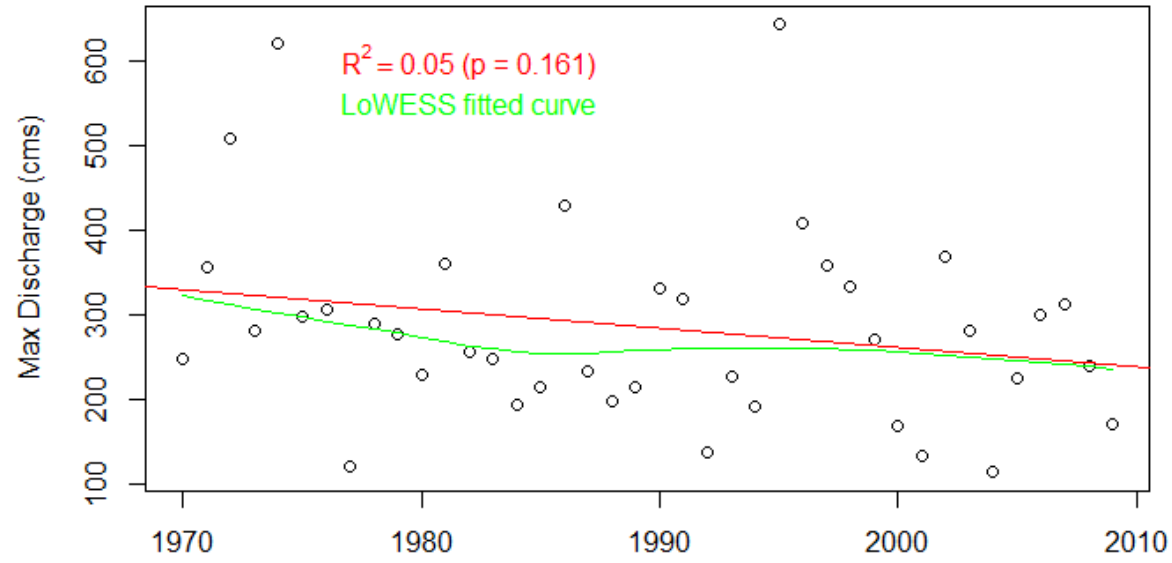

a.

b.

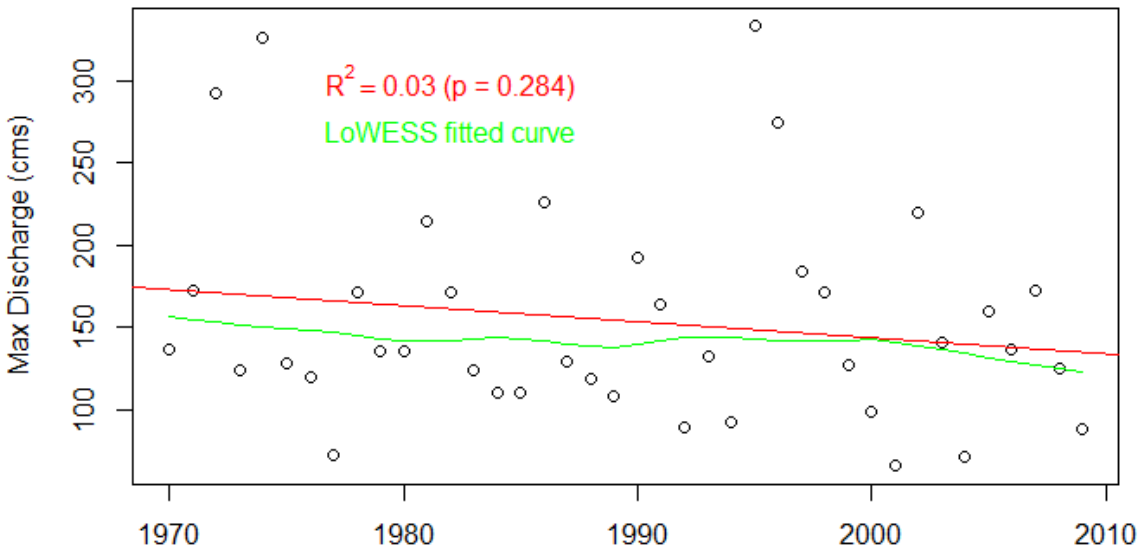

c.

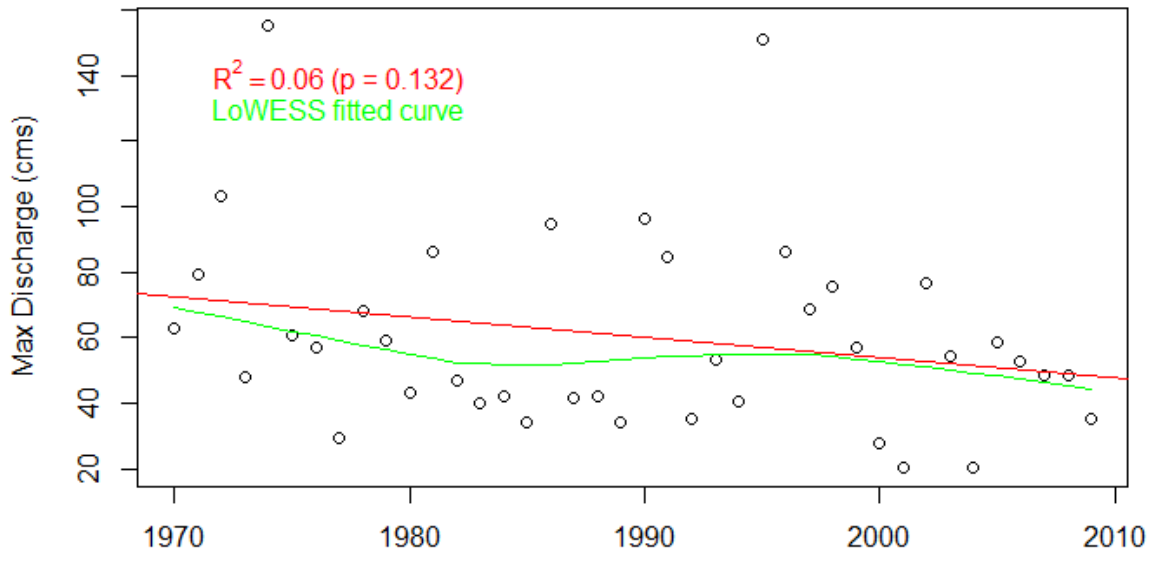

Figure C-19. Maximum annual discharge volume for all three discharge research stations from 1970 – 2009: (a) 08N002; (b) 08NK016 and (c) 08NK018.

Probability Density Function

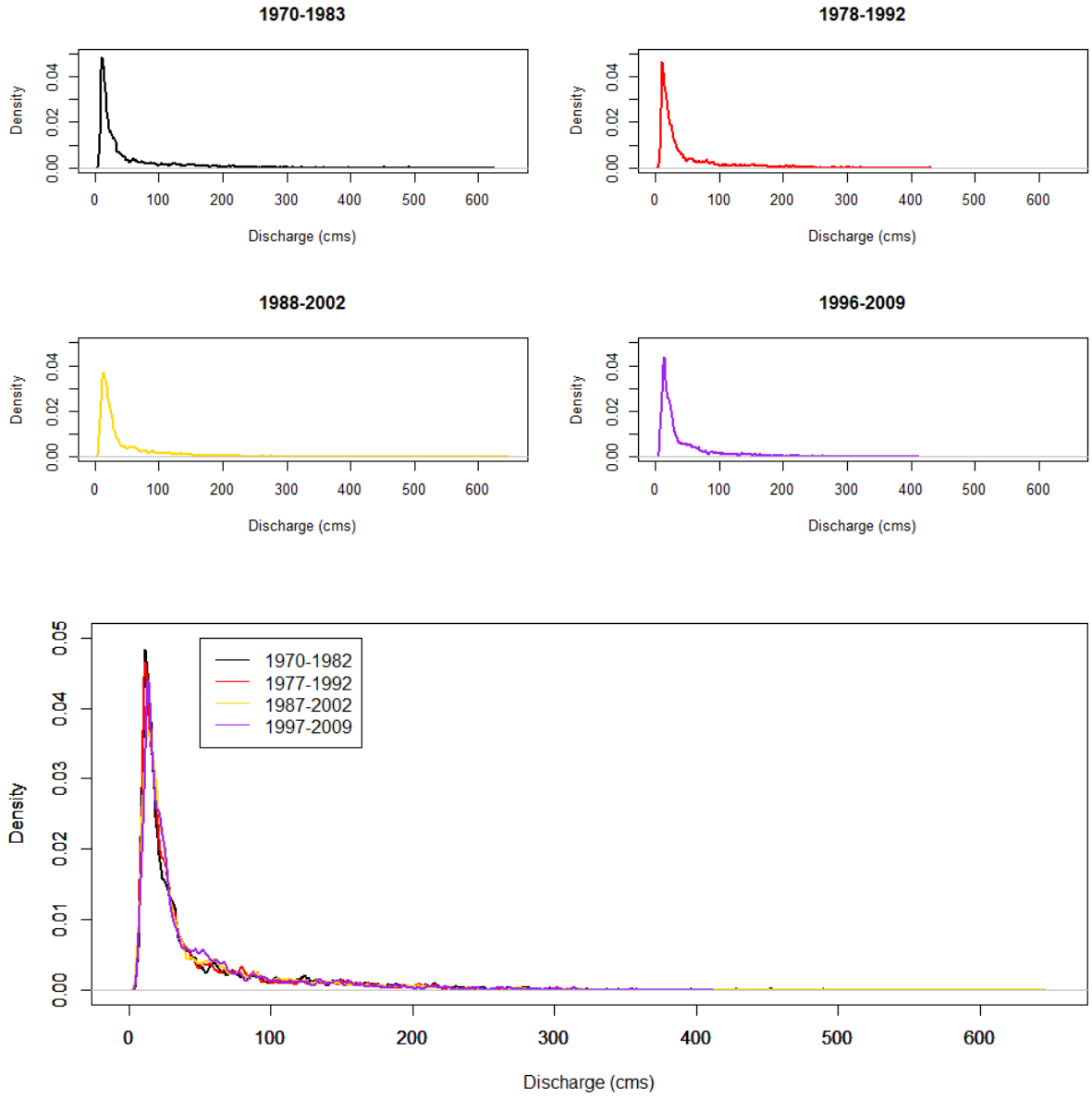

Figure C-20. Kernel density estimation for daily mean discharge from station 08NK002.

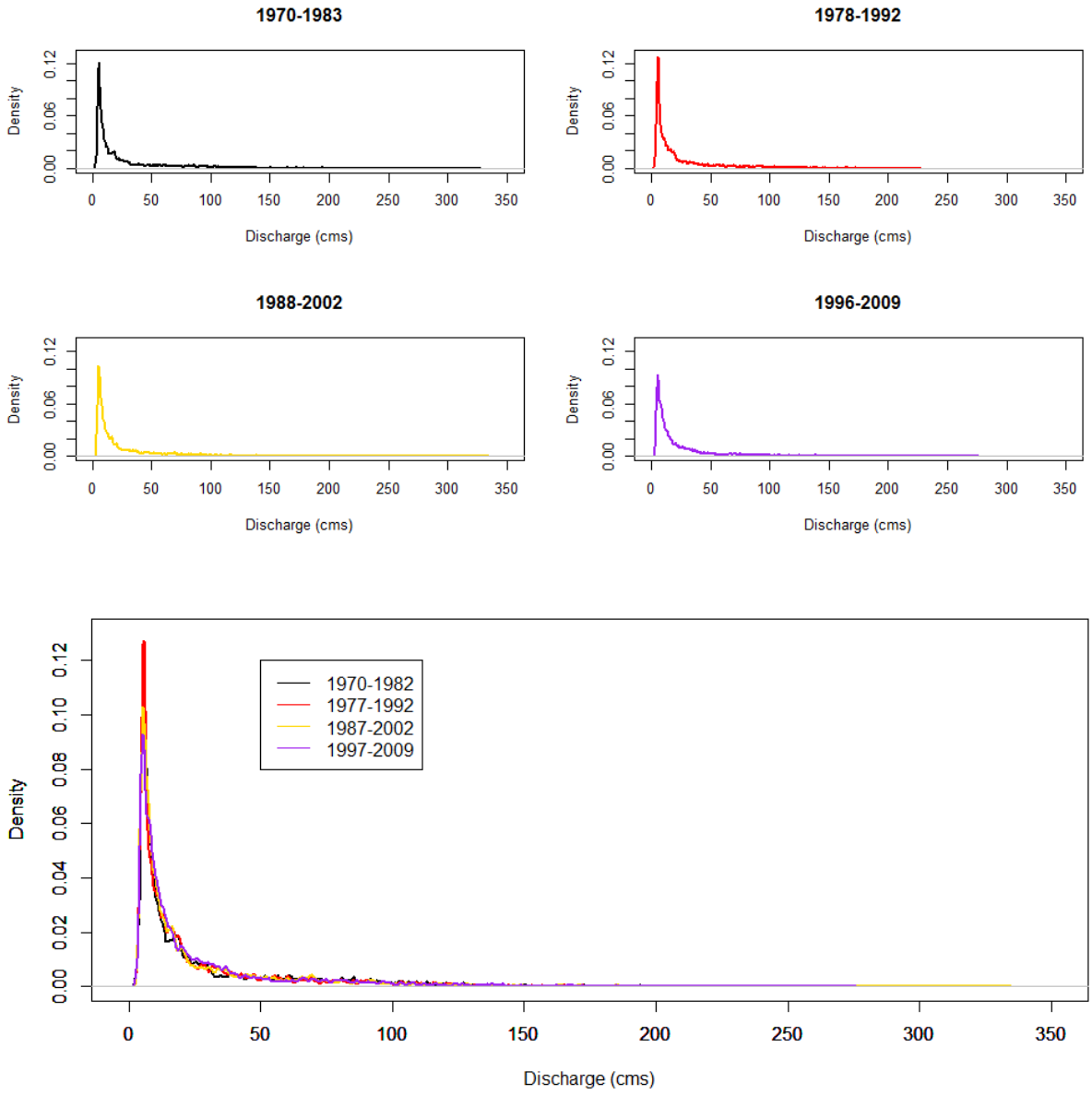

Figure C-21. Kernel density estimation for daily mean discharge from station 08NK016.

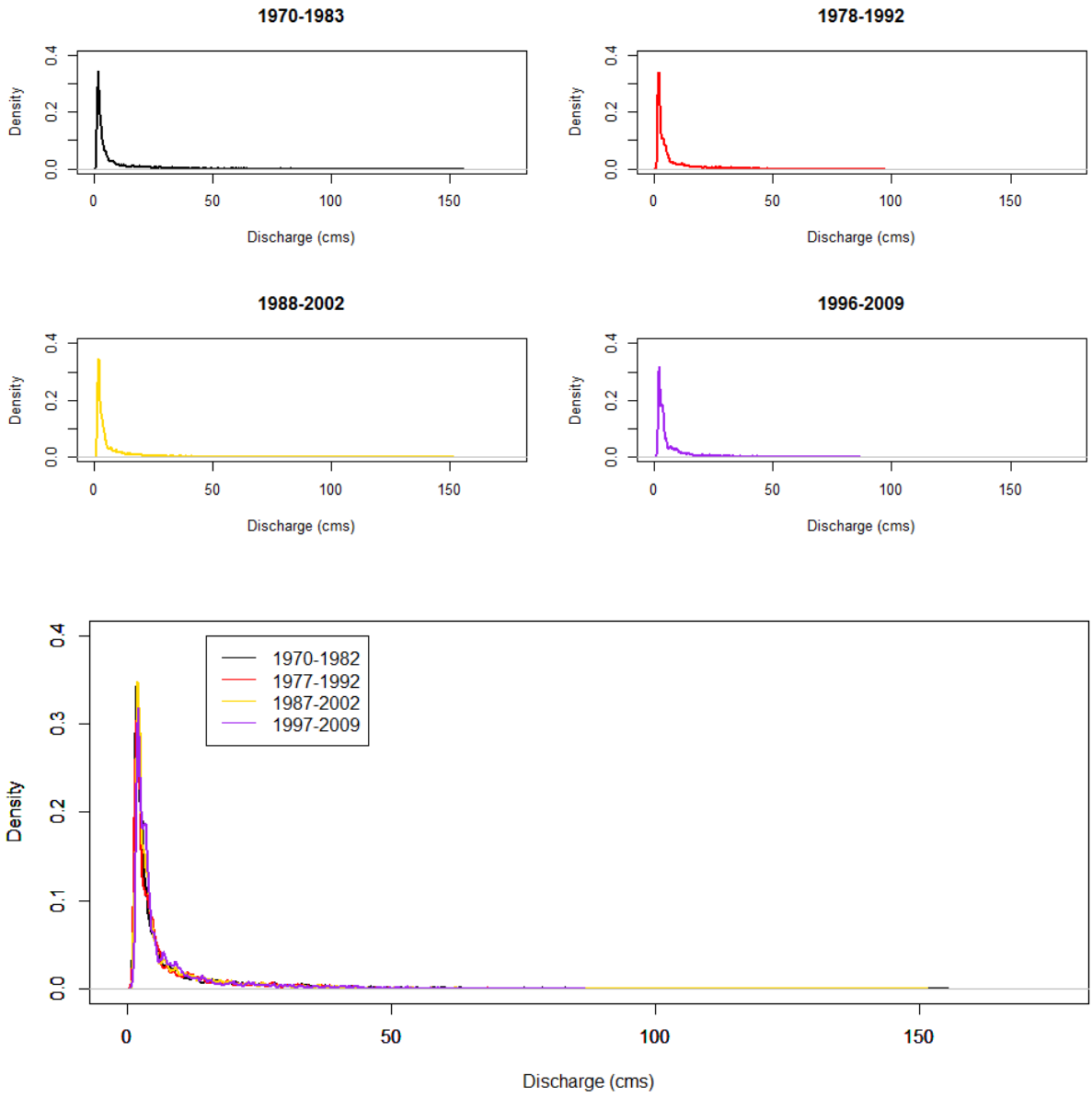

Figure C-22. Kernel density estimation for daily mean discharge from station 08NK018.

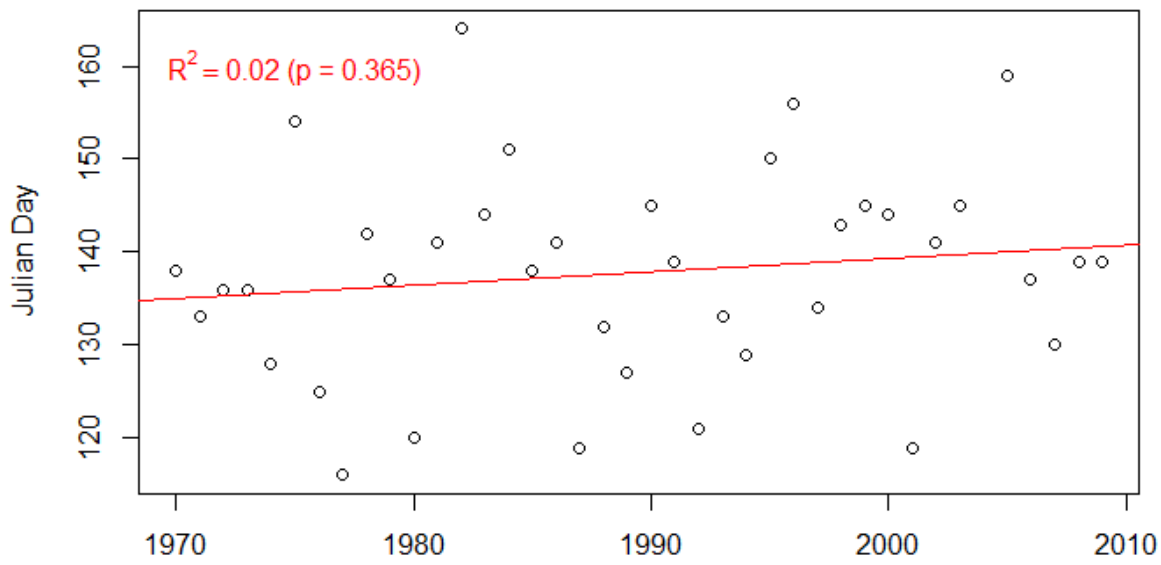
$R^2 = 0.02$ (p = 0.365)
Julian Day
120
130
140
150
160
1970
1980
1990
2000
2010

a.

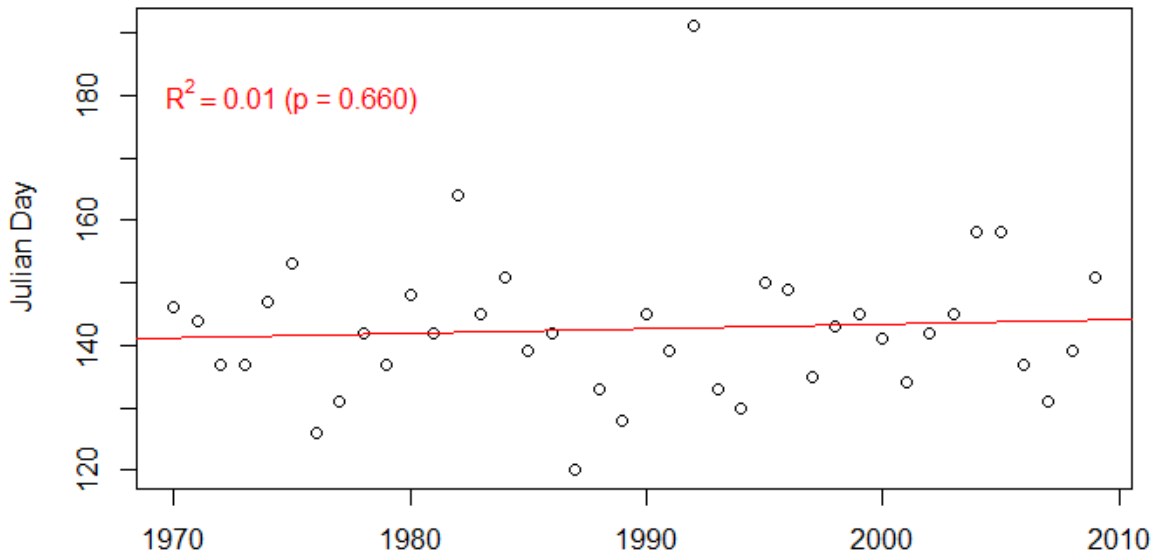
$R^2 = 0.01$ (p = 0.660)
Julian Day
120
140
160
180
1970
1980
1990
2000
2010

b.

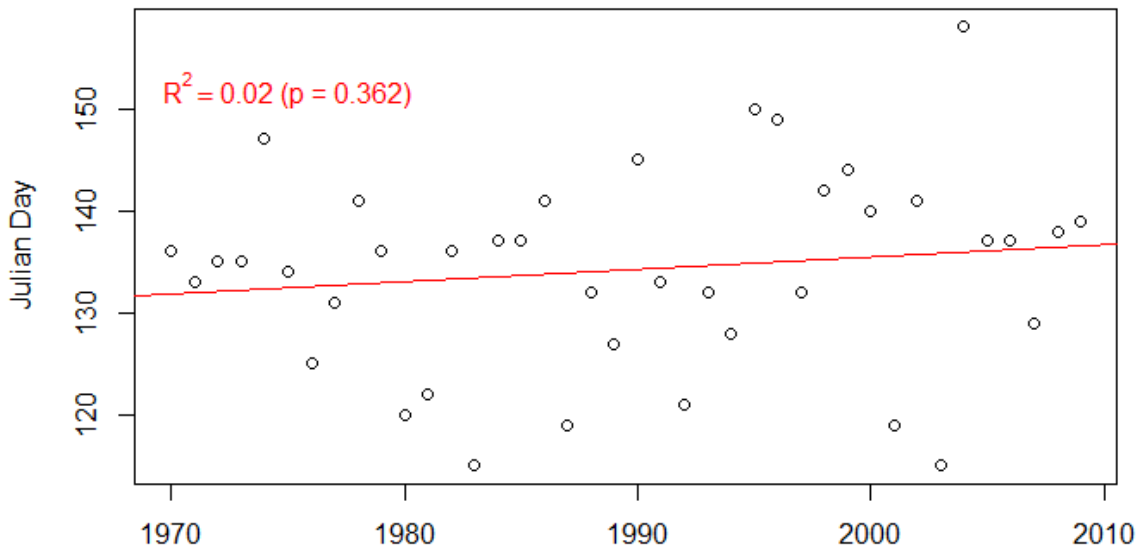

c.

Figure C-23. Start of freshet based on the methodology by Zhang, Harvey, Hogg and Yuzyk (2001): (a) 08NK002; (b) 08NK016 and (c) 08NK018.

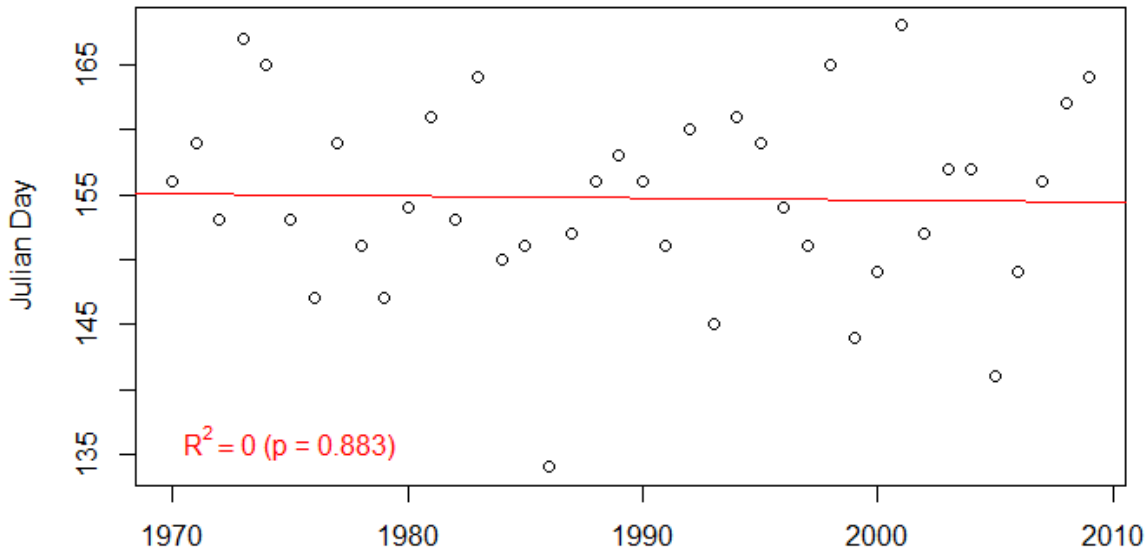

a.

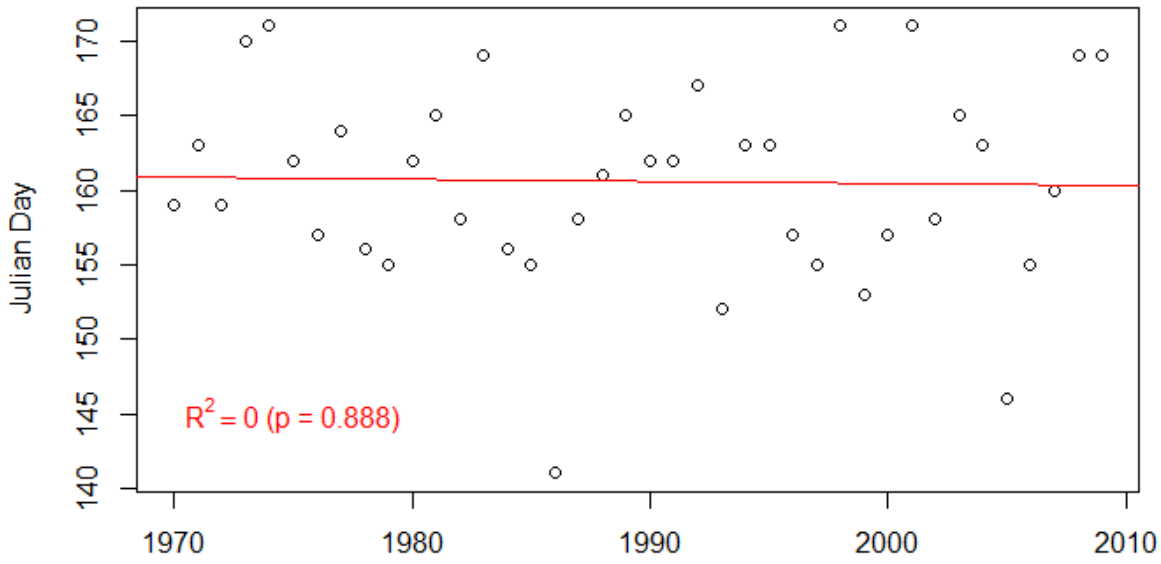

b.

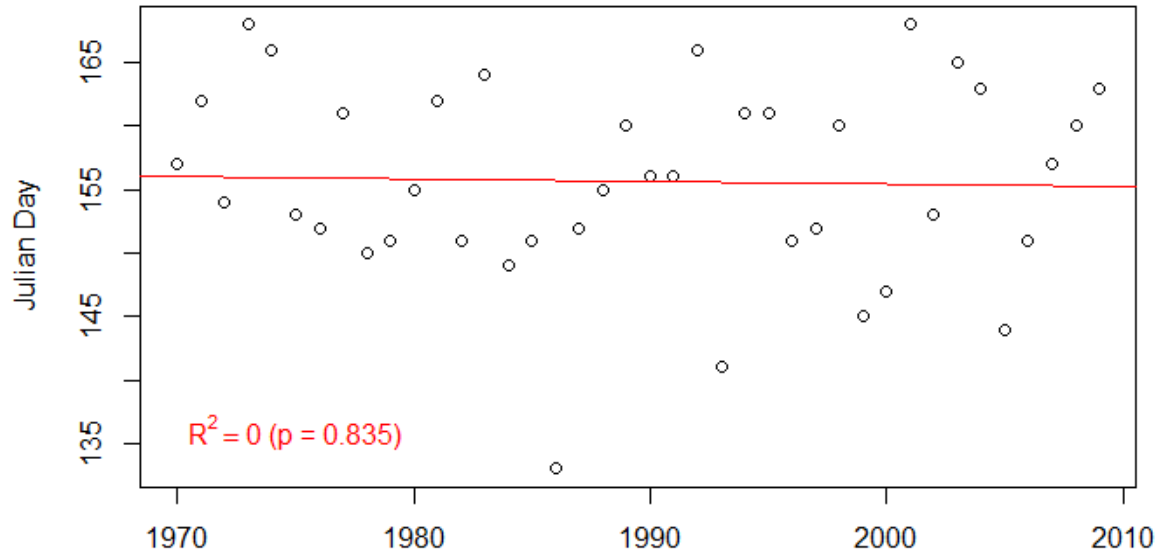

c.

Figure C-24. Timing when 50% of that water year's total volume has been achieved (Burn 1994). Graphs include all three discharge research stations from 1970 to 2009: (a) 08NK002; (b) 08NK016 and (c) 08NK018.

a.

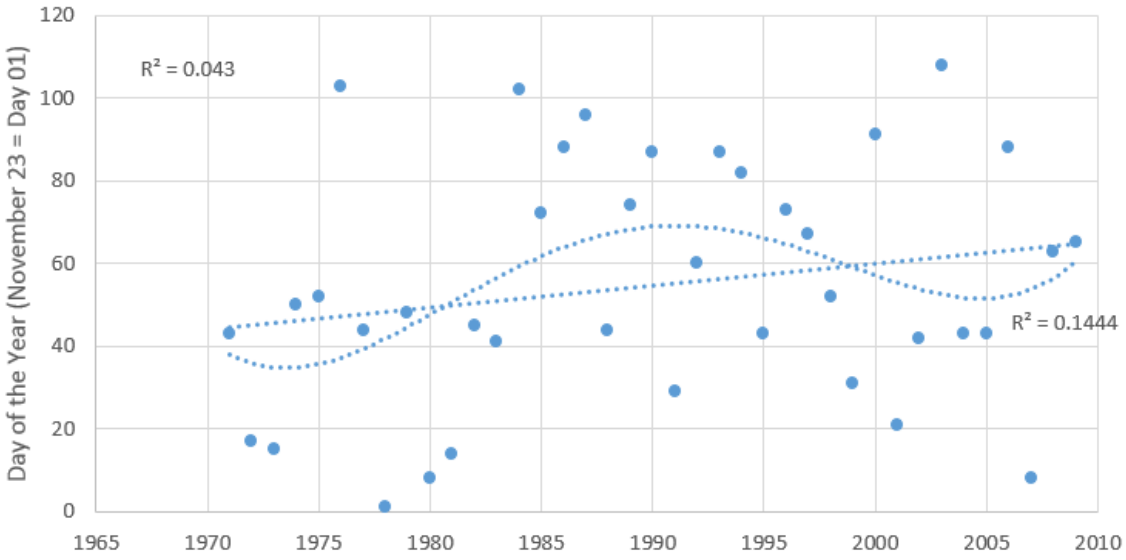
Day of the Year (November 23 = Day 01)
R² = 0.043
R² = 0.1444
120
100
80
60
40
20
0
1965
1970
1975
1980
1985
1990
1995
2000
2005
2010

b.

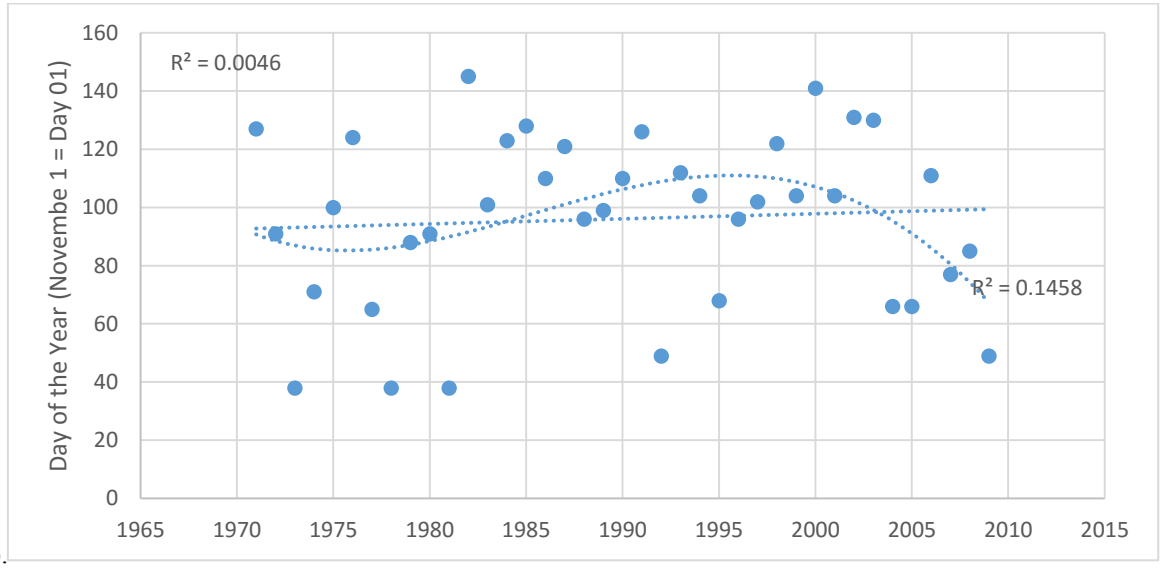
Day of the Year (Novembe 1 = Day 01)
R² = 0.0046
R² = 0.1458
160
140
120
100
80
60
40
20
0
1965
1970
1975
1980
1985
1990
1995
2000
2005
2010
2015

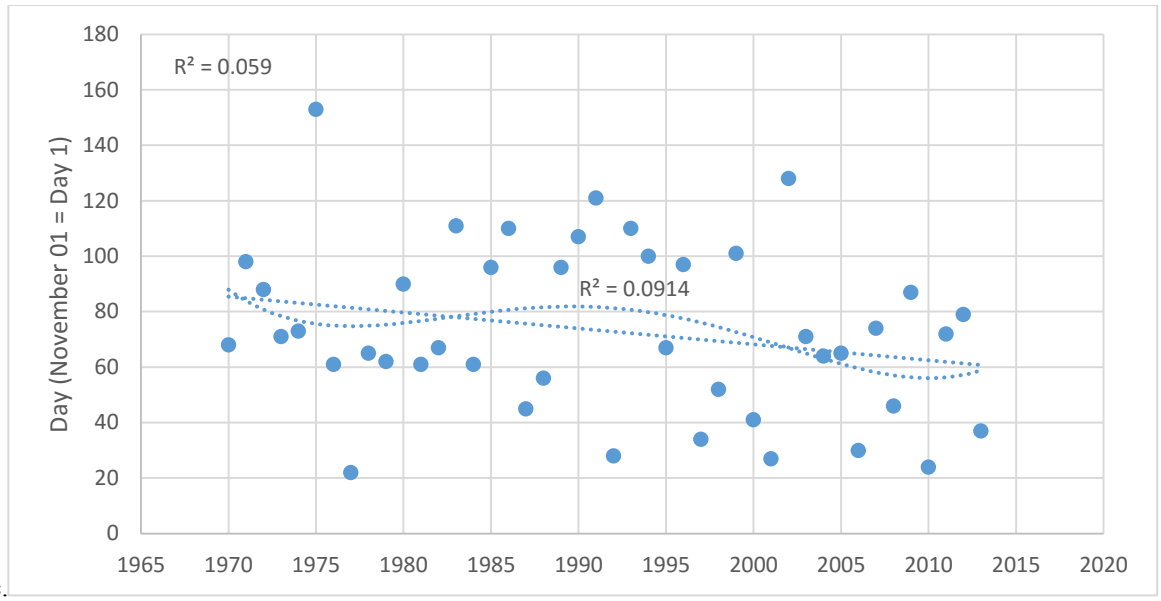

c.

Figure C-25. Timing of the minimum annual flow for all three discharge research stations from 1970 to 2009: (a) 08NK002; (b) 08NK016 and (c) 08NK018. The linear trend line R^2 value is located in the top left hand corner.

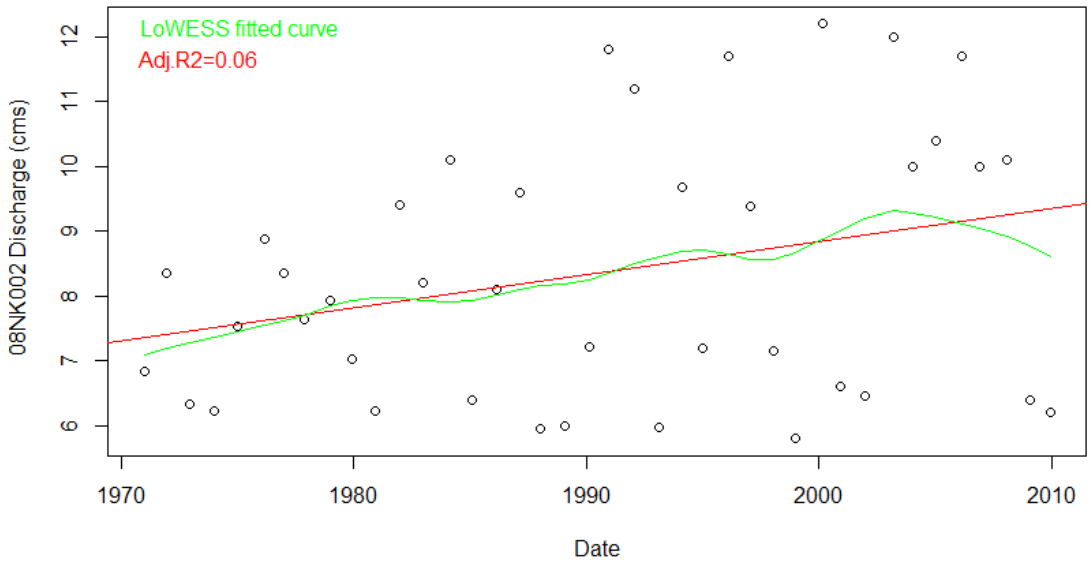

a.

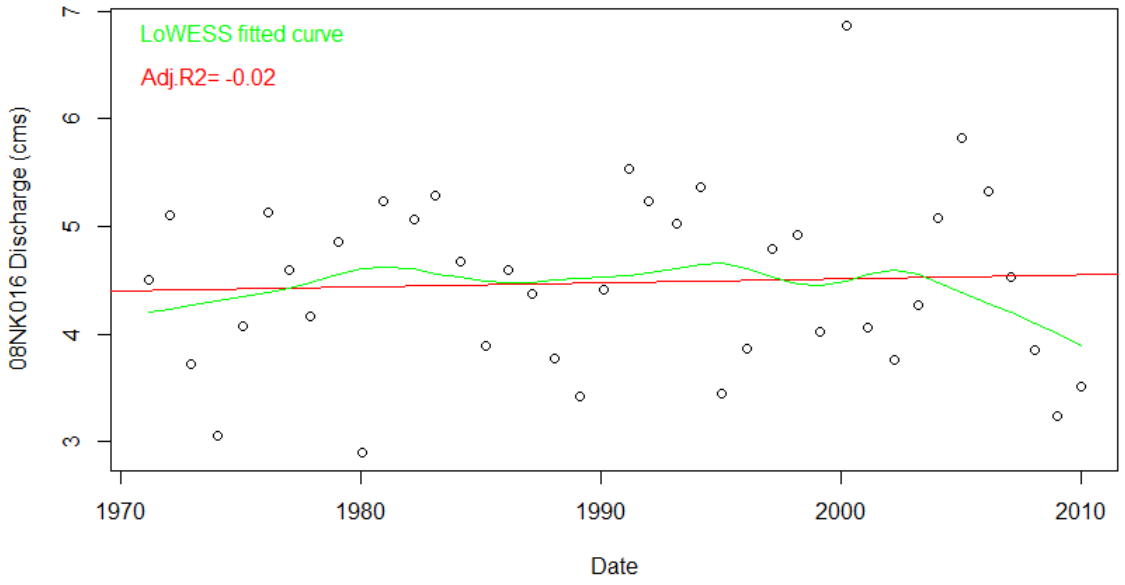

b.

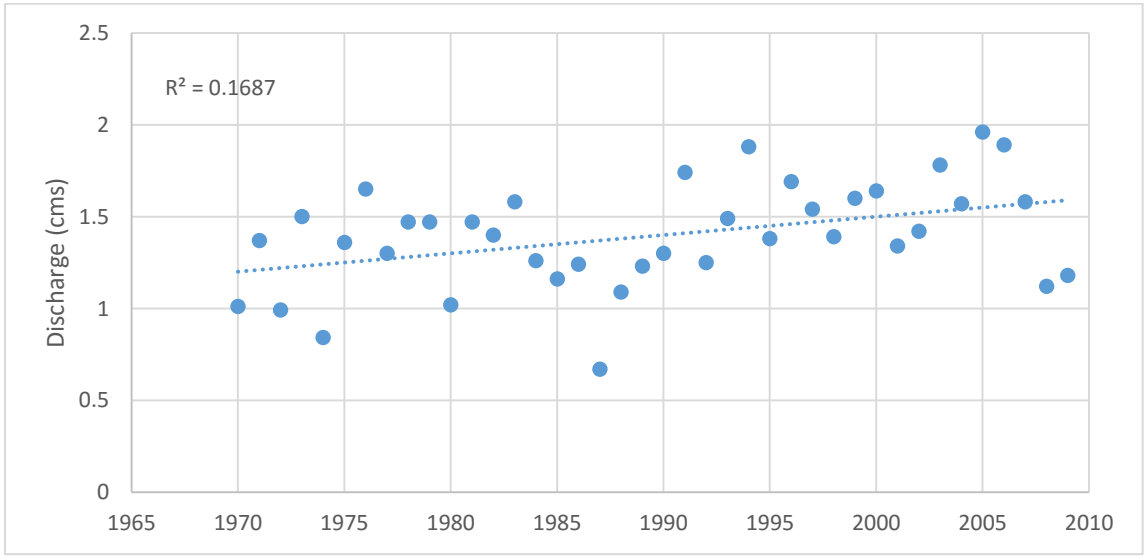

c.

Figure C-26. Minimum annual flow volume for all three discharge research stations from 1970 to 2009: (a) 08NK002; (b) 08NK016 and (c) 08NK018.

D. Precipitation

Table D-1. Annual total precipitation for 10 climate stations in the Elk River Watershed shown from north (left) to south (right). Threshold set at 95%.

	Prcp 898	Prcp 899	Prcp 653	Prcp 402	Prcp 630	Prcp 915	Prcp 850	Prcp 670	Prcp 690	Prcp 282
μ ($m^3 yr^{-1}$)	796	700	664	814	576	915	1202	612	446	521
SD ($m^3 yr^{-1}$)	172	138	154	117	122	149	242	102	109	100
CV (%)	21.6	19.7	23.2	14.4	21.2	16.3	20.1	16.7	24.4	19.2
Yrs	7	17	12	9	15	8	22	14	7	12
% of yrs	27%	65%	46%	35%	58%	31%	85%	54%	27%	46%

Table D-2. Comparing outputs based on 90% available data versus 95% available data for five climate stations.

Station	Annual Prcp (mm) (95% avail.)	No. of years (95% avail.)	Annual Prcp (mm) (90% avail.)	No. years (90% avail.)
898	795.6	7	795.6	7
899	659.0	28	650.7	32
630	603.3	29	603.3	29
402	813.7	9	758.1	12
850	1242.0	30	1191.7	37

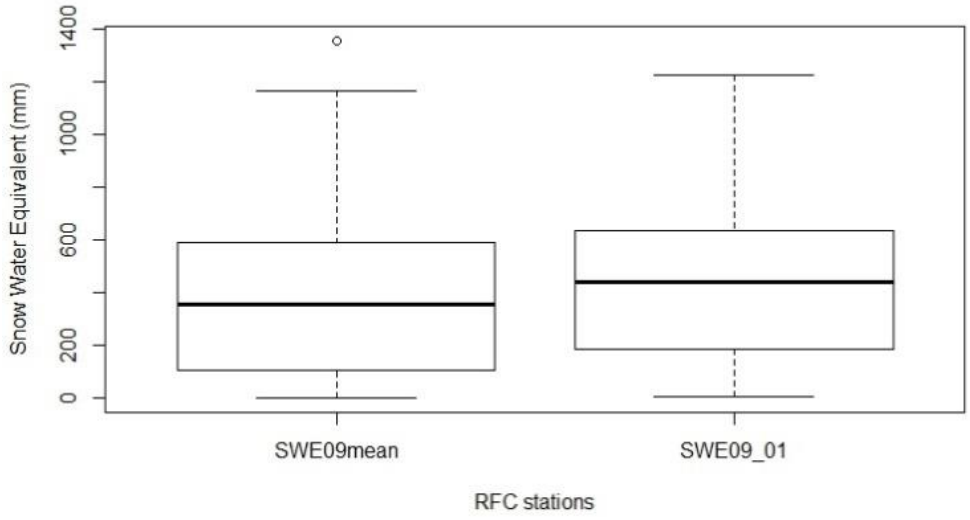

Figure D-1. Interquartile range comparison between using mean values (left) and value recorded on the first of each month (right).

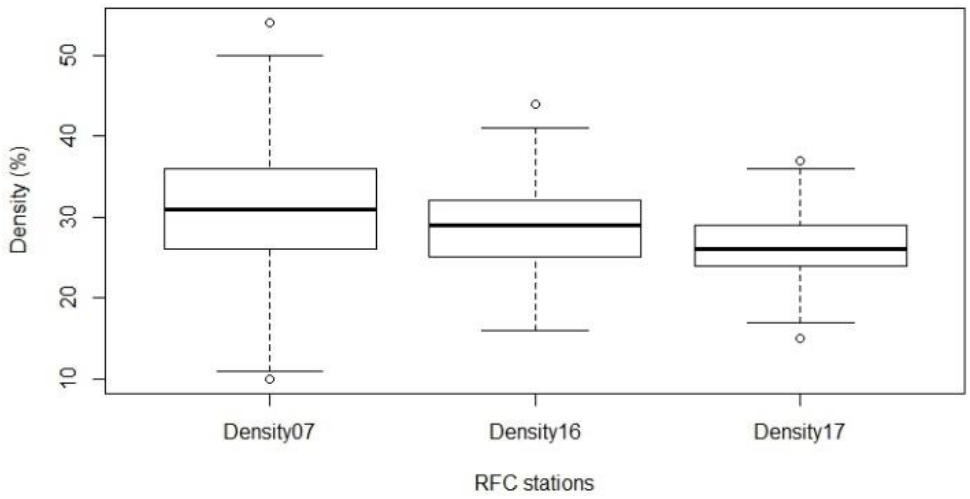

Figure D-2. Monthly snow density from the three manually monitored stations in and around the Elk River basin. Stations C016 and C017 only take measurements until May 1 of each year.

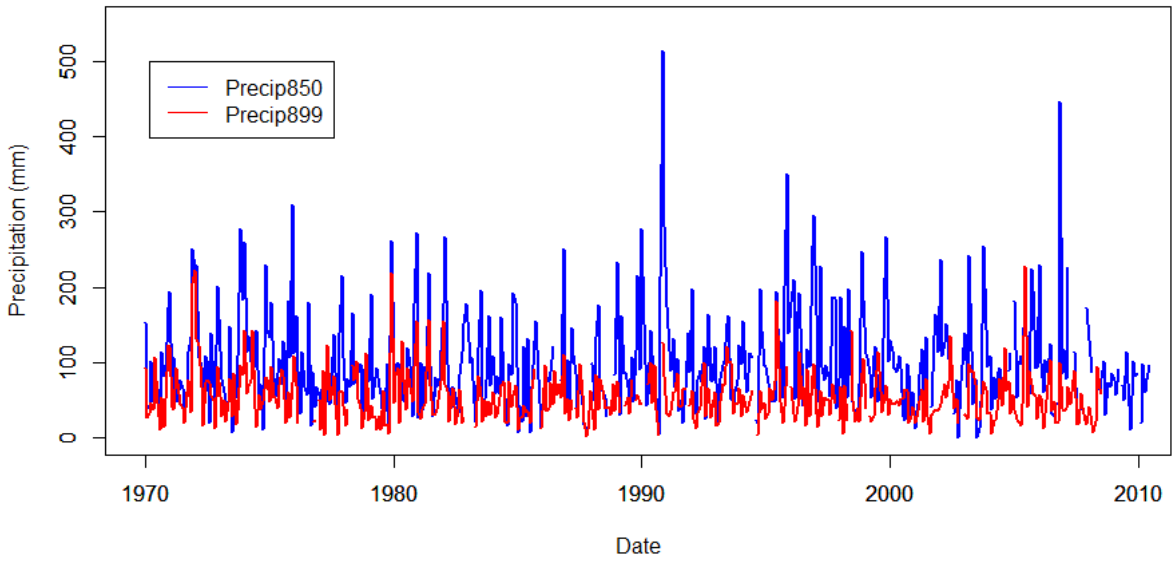

Figure D-3. Total monthly precipitation from 1970 – 2009 for climate station 1152899 and 1152850.

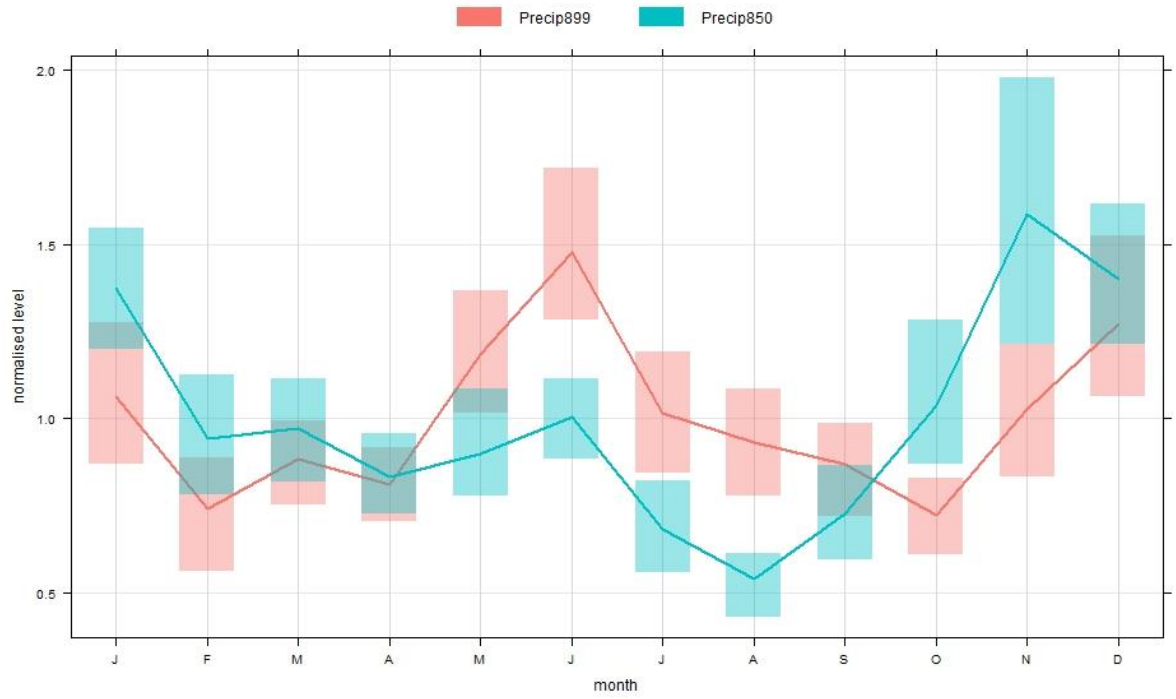

Figure D-4. Monthly total precipitation normalized for climate stations 1152850 and 1152899 from 1970 to 2009.

Trends

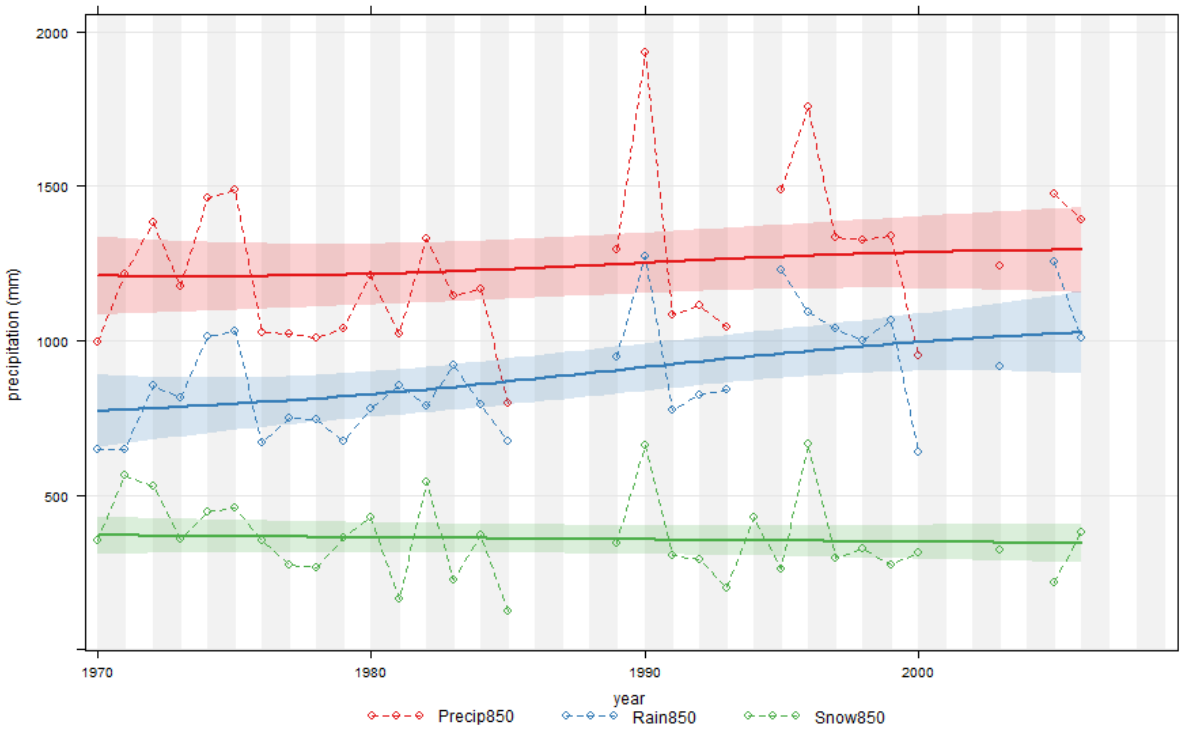

Figure D-5. Annual sum precipitation for climate station 1152850 from 1970 to 2009.

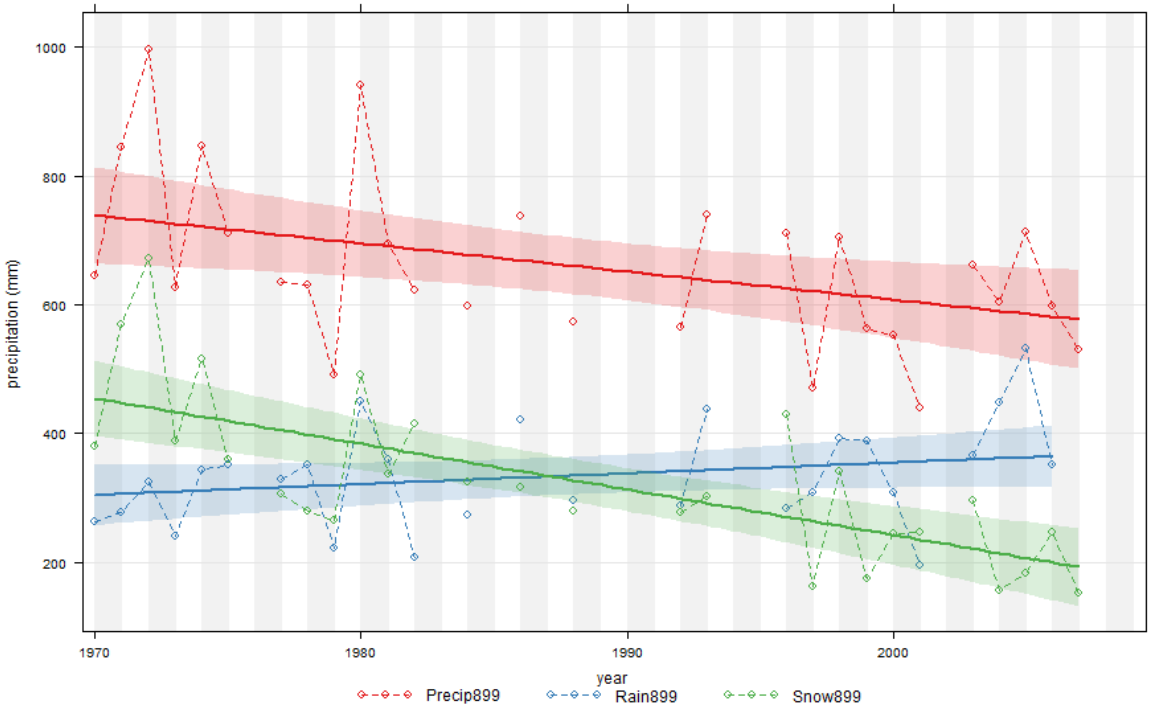

Figure D-6. Annual mean precipitation for station 115899 from 1970 to 2009.

Table D-3. Trend assessment based on total monthly precipitation for stations 1152850 and 1152899 from 1970 to 2009. The Theil Sen slope results represent the percentage of change per month. Pink boxes represent α = 0.05, yellow boxes represent 0.05 < α <0.1, all other results are at α > 0.1.

	850Prcp	850Rain	850Snow	899Prcp	899Rain	899Snow
Jan	-0.119	0.995	-0.833	-0.666	0.000	-0.731
Feb	-0.609	-0.375	-0.245	-0.468	0.000	-0.738
Mar	0.570	0.564	0.106	-0.355	0.056	-0.797
Apr	1.240	1.406	-0.174	-0.686	0.382	-0.639
May	0.574	0.458	0.000	0.180	0.062	0.029
Jun	0.441	0.441	NA	0.724	0.862	0.000
Jul	-0.700	-0.700	NA	0.112	0.123	NA
Aug	-0.572	-0.572	NA	-0.671	-0.482	NA
Sep	-0.652	-0.649	0.000	0.138	0.093	0.000
Oct	0.943	1.336	-0.003	0.193	0.270	0.009
Nov	0.287	0.389	-0.123	0.330	0.125	-0.014
Dec	-2.233	-0.660	-0.555	-1.979	0.000	-1.702
Au	0.059	0.067	0.000	0.088	0.069	0.000
Sp	0.252	0.289	-0.251	-0.045	0.064	-0.132
Su	-0.080	-0.081	NA	0.055	0.105	NA
Wi	-0.363	-0.017	-0.186	-0.356	NA	-0.335
Year	0.004	0.009	0.000	-0.018	0.006	0.000

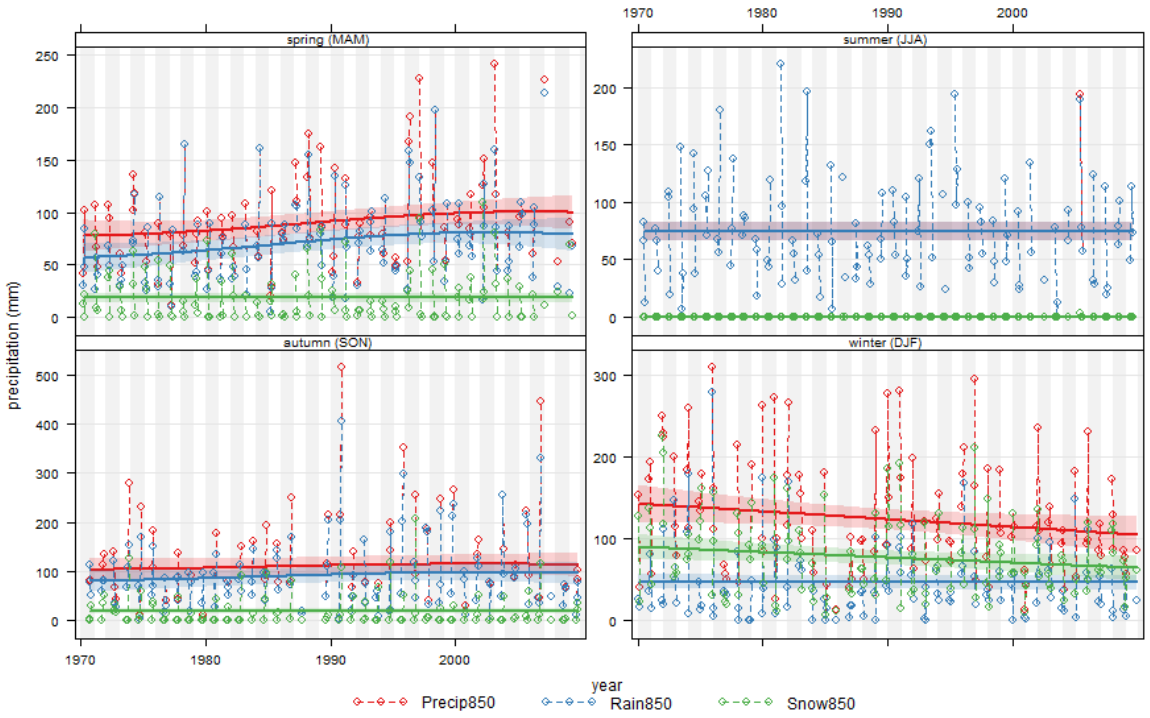

Figure D-7. Total monthly precipitation separated by season for station 1152850 from 1970 to 2009.

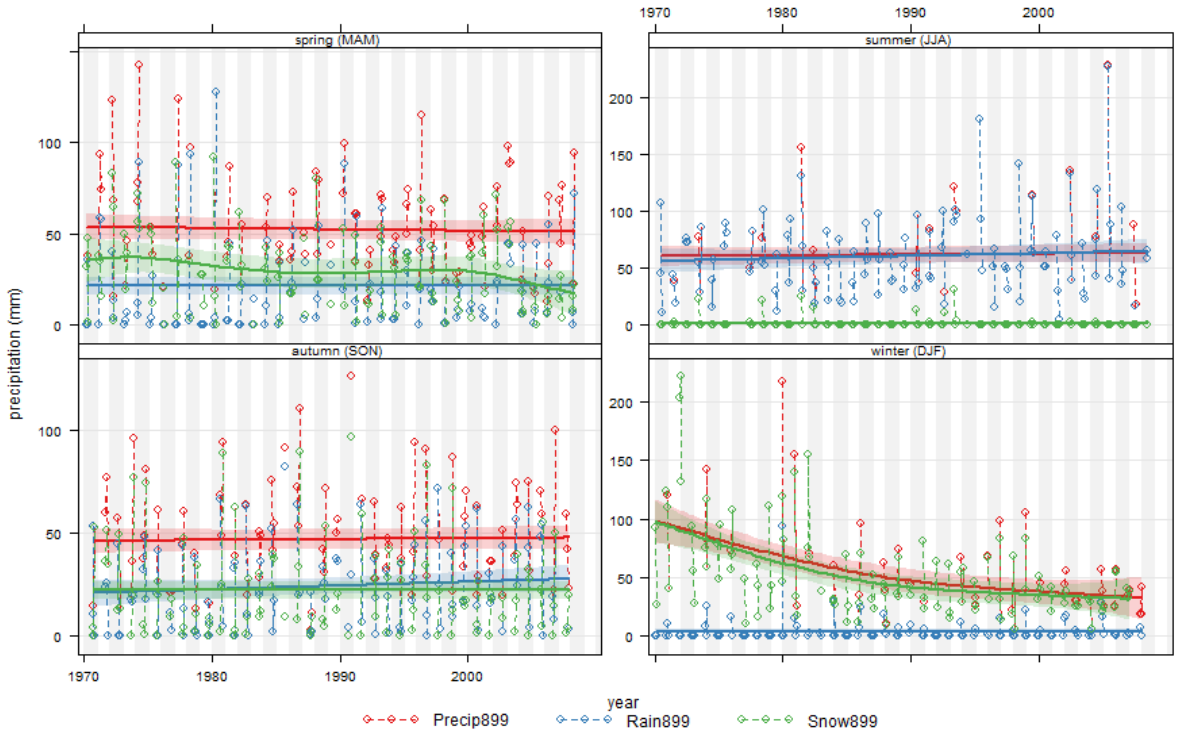

Figure D-8. Total monthly precipitation separated by season for station 1152899 from 1970 to 2009.

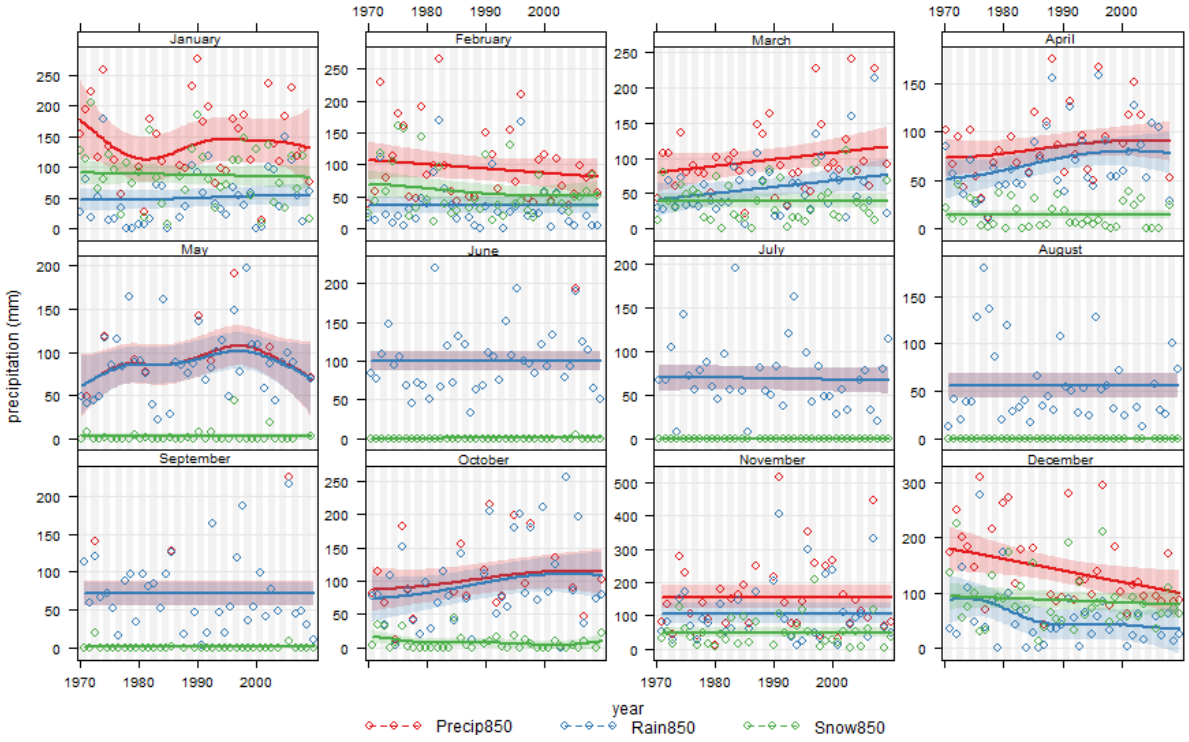

Figure D-9. Monthly total precipitation for station 1152850 from 1970 to 2009.

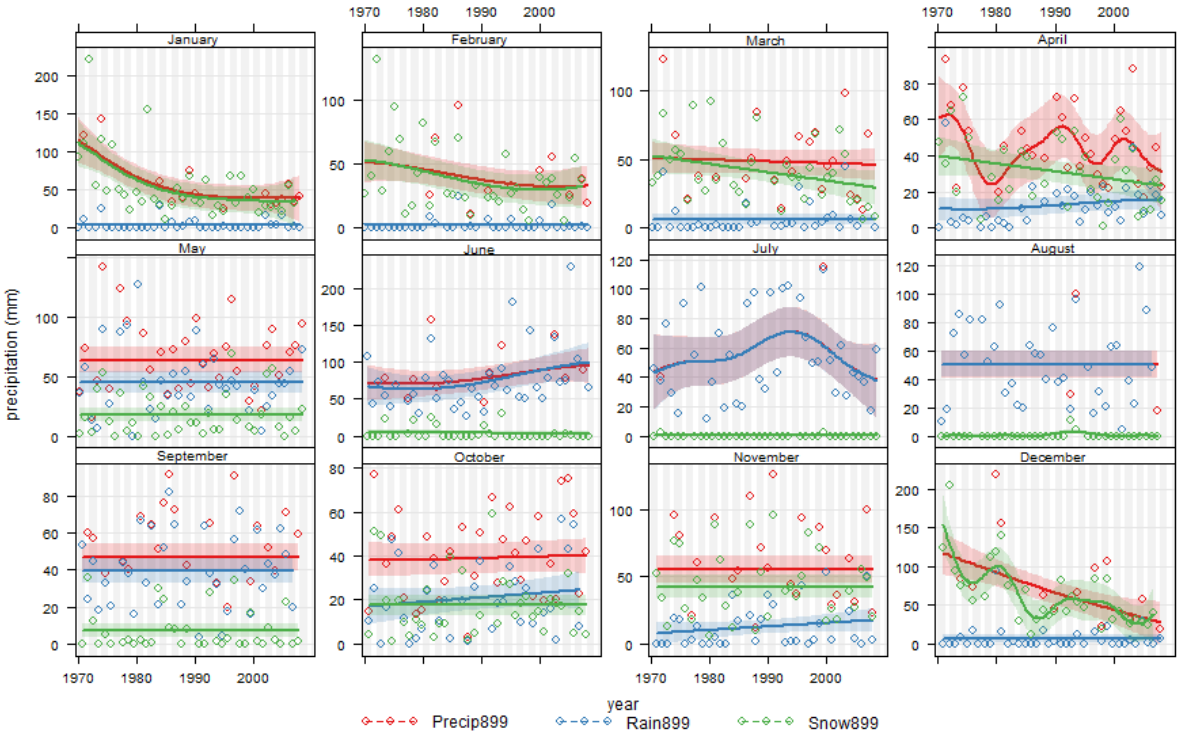

Figure D-10. Monthly total precipitation for station 1152899 from 1970 to 2009.

E. Temperature

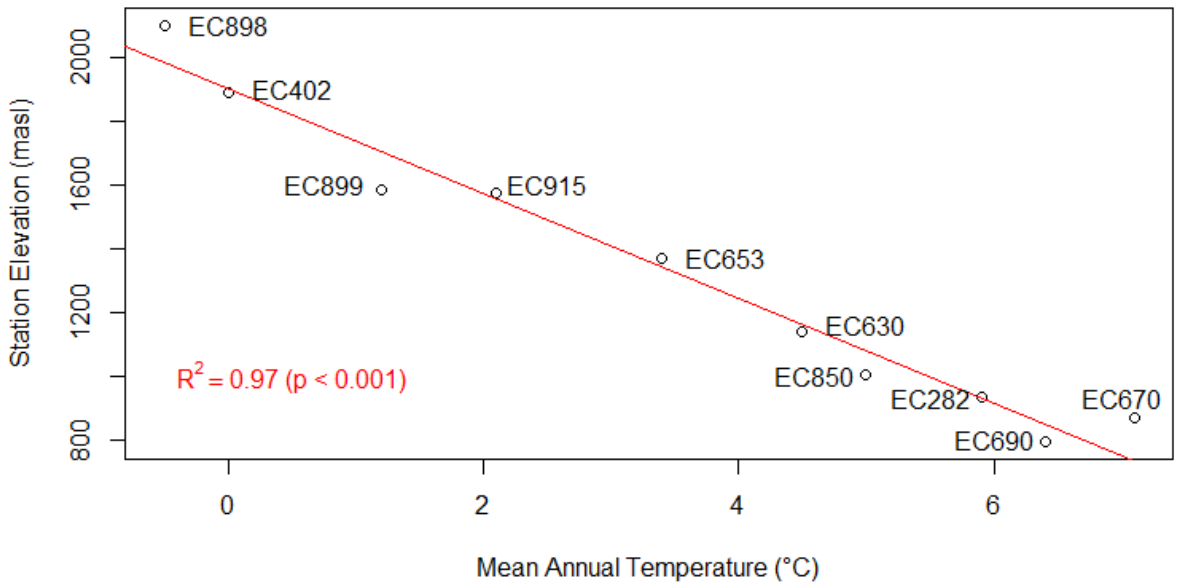

Figure E-1. Mean annual temperature regionalization, incorporates both the northern and southern portion of the watershed.

Trends

Table E-1. Trend assessment based on mean monthly discharge for the three discharge research stations from 1970 to 2009. The Theil Sen slope results represent the percentage of change per month. Pink boxes represent $\alpha = 0.05$, yellow boxes represent $0.05 < \alpha < 0.1$, all other results are at $\alpha > 0.1$.

	850TMin	850TMean	850TMax	899TMin	899TMean	899TMax
Jan	0.112	0.101	0.086	0.037	0.056	0.074
Feb	-0.015	0.002	0.019	-0.041	-0.026	0.033
Mar	0.041	0.040	0.045	0.056	0.040	0.040
Apr	0.027	0.037	0.052	0.023	0.048	0.042
May	0.029	0.039	0.013	-0.001	0.004	0.000
Jun	0.019	0.009	0.009	-0.025	-0.027	-0.032
Jul	0.049	0.065	0.089	-0.042	0.004	0.052
Aug	-0.005	0.012	0.023	-0.054	-0.017	0.017

Sep	0.041	0.050	0.111	-0.021	0.016	0.027
Oct	0.024	0.009	0.005	-0.003	-0.013	0.001
Nov	0.065	0.065	0.060	0.022	0.038	0.042
Dec	0.033	0.019	-0.005	0.025	0.029	0.042
Autumn	0.008	0.003	0.014	0.005	0.001	0.005
Spring	0.011	0.003	0.012	0.008	0.002	0.010
Summer	0.005	0.002	0.016	-0.010	-0.001	-0.001
Winter	0.011	0.004	0.012	0.003	0.001	0.012
Full Year	-0.002	0.004	-0.003	0.000	0.004	0.006

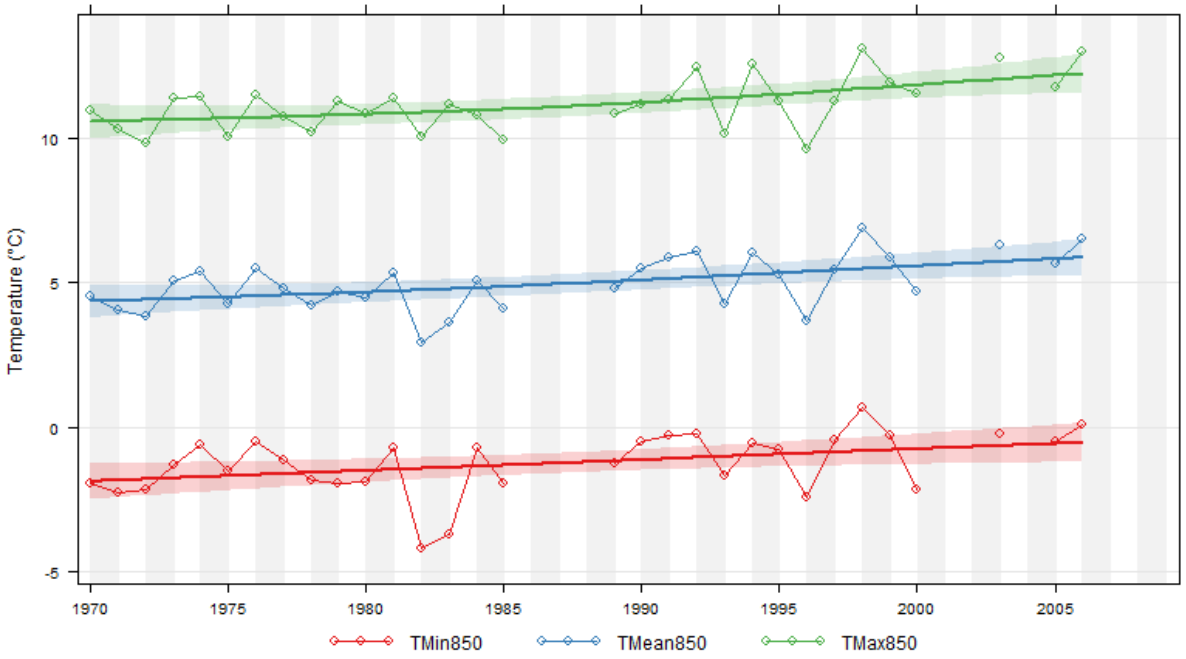

Figure E-2. Annual mean temperature trends for station 1152850 from 1970 to 2009.

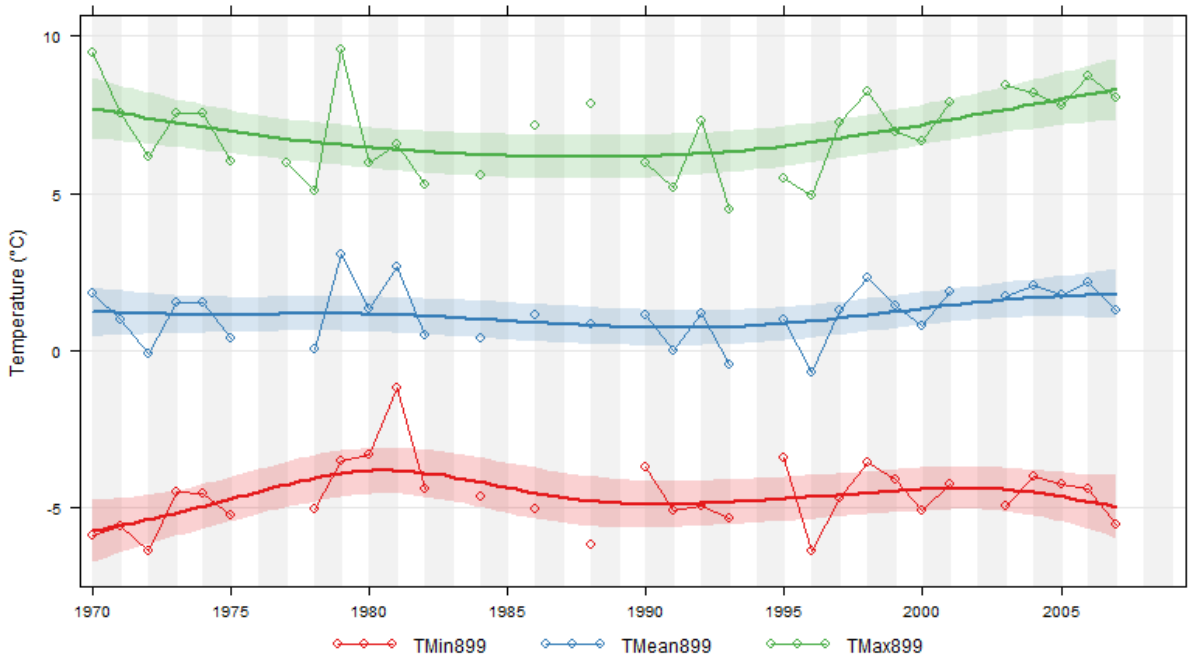

Figure E-3. Annual mean temperature trends for station 1152899 from 1970 to 2009.

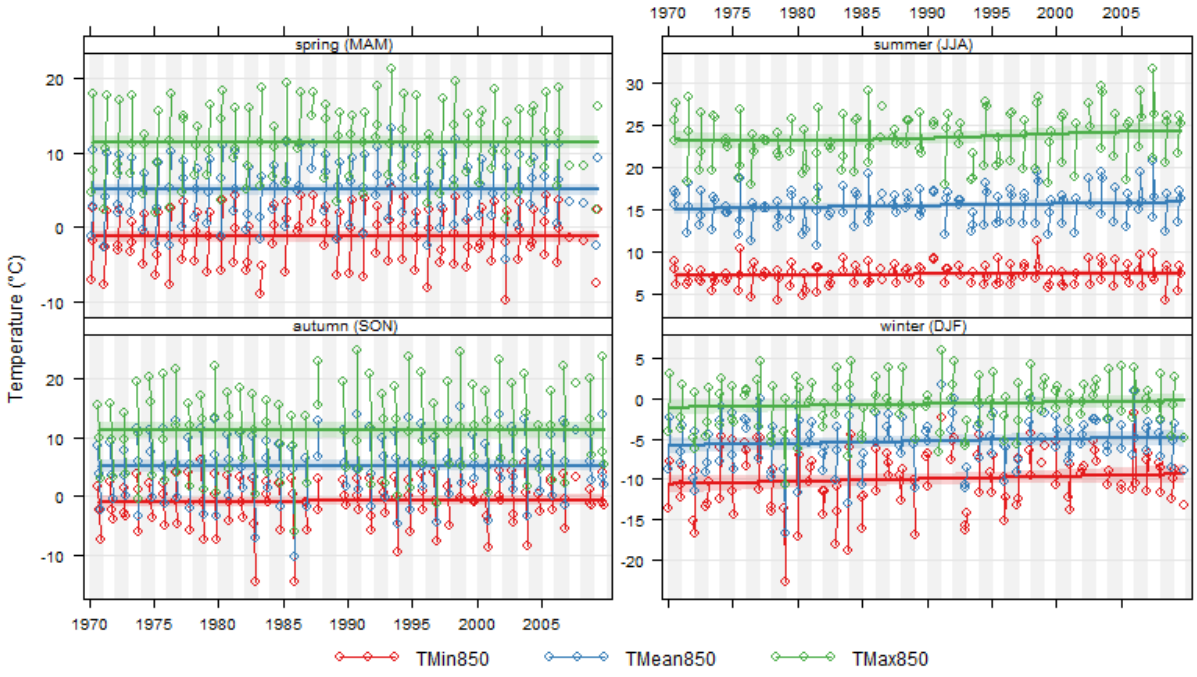

Figure E-4. Seasonal temperature trends for station 1152850 from 1970-2009.

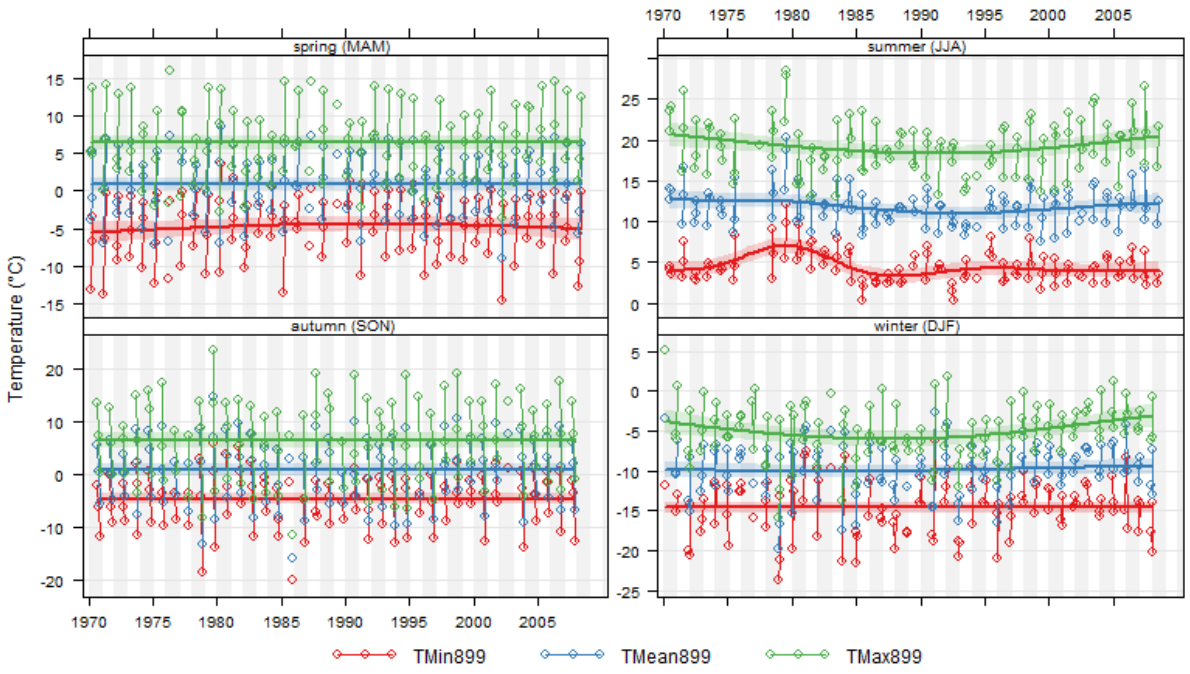

Figure E-5. Seasonal temperature trends for station 1152899 from 1970-2009.

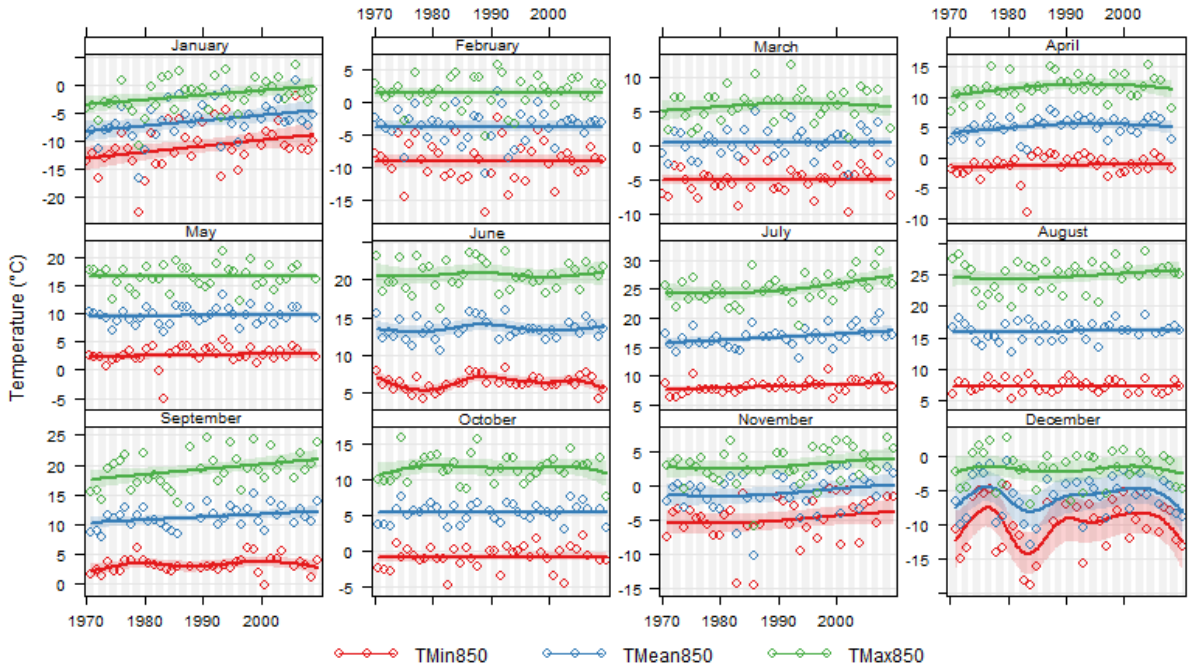

Figure E-6. Monthly mean temperature from 1970 to 2009 for station 1152850.

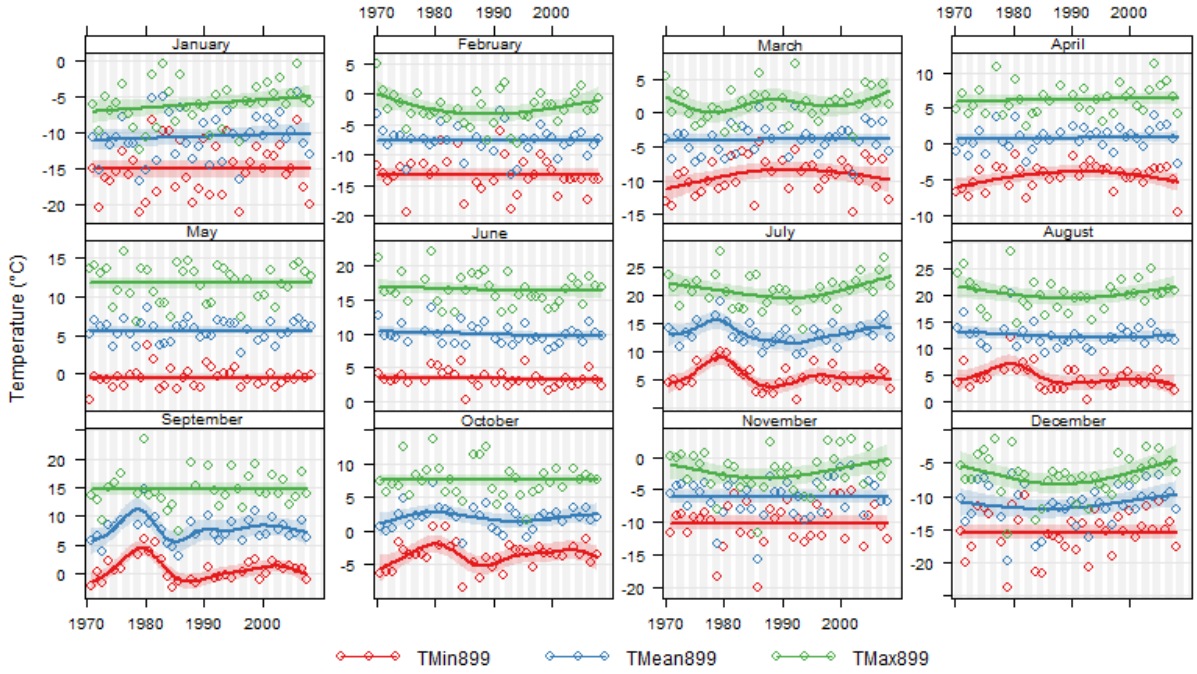

Figure E-7. Monthly mean temperature from 1970 to 2009 for station 1152850.

F. Correlating Hydro-Climatological Trends

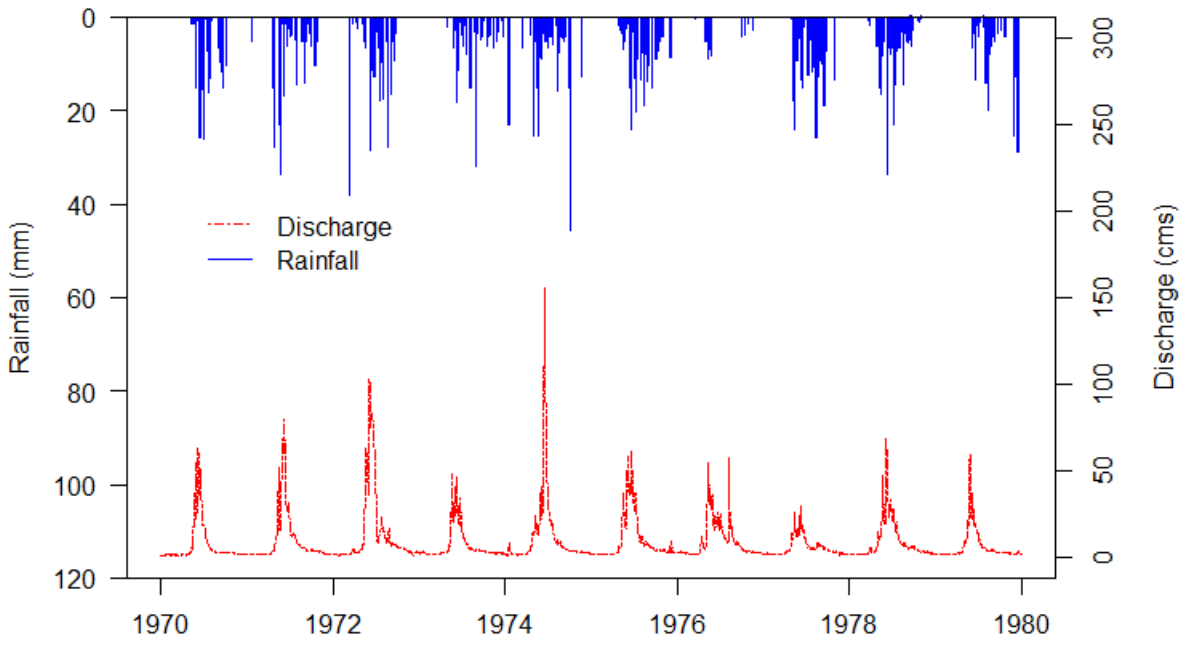

Figure F-1. Comparison between the daily rainfall at climate station 1152899 and the daily discharge at discharge station 08NK016 from 1970 to 1980.

Double Mass Curve

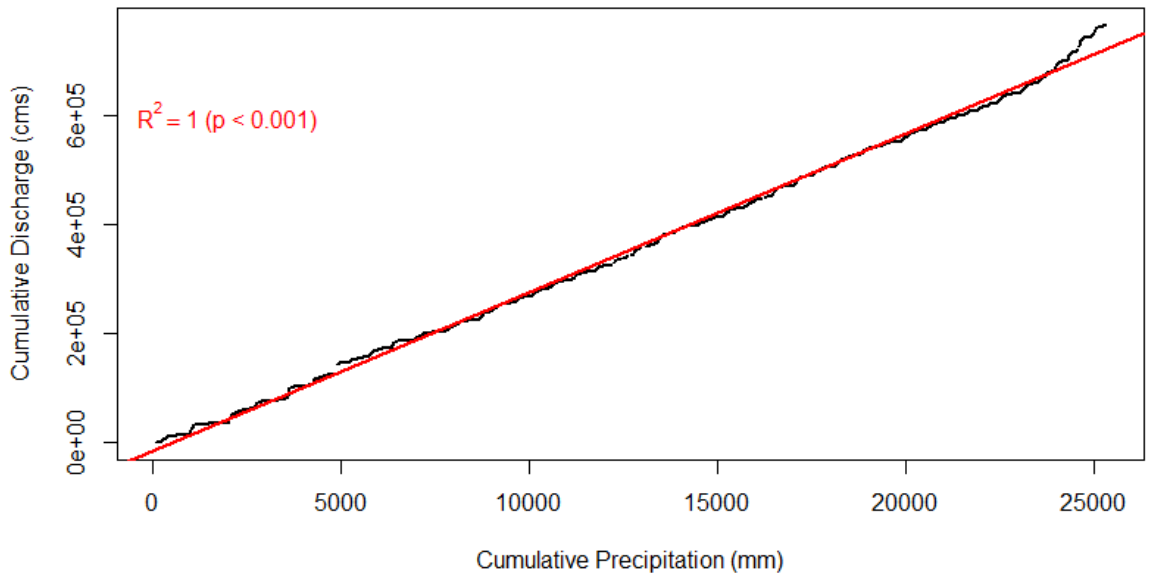

a.

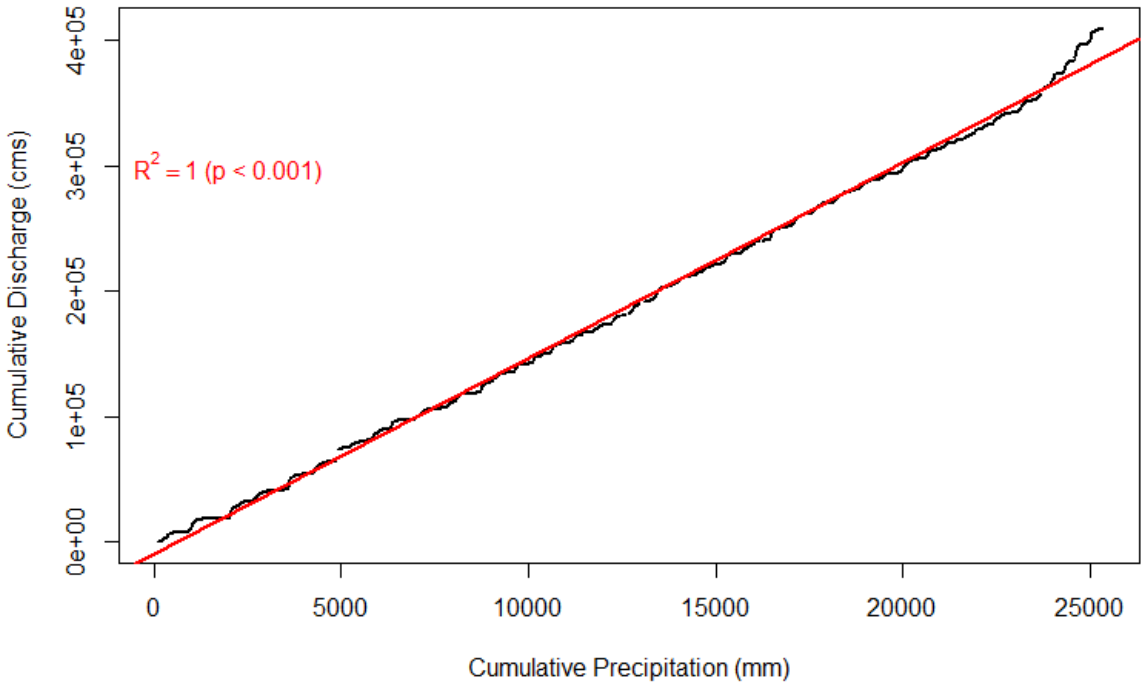

b.

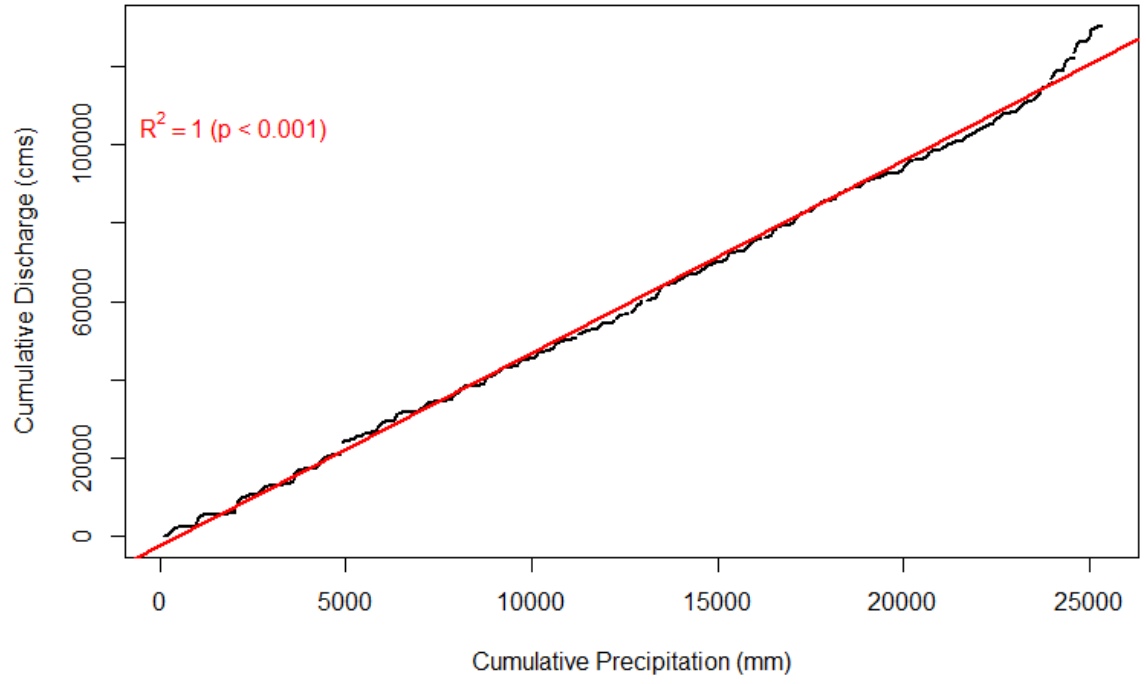

c.

Figure F-2. Monthly total precipitation from station 1152899 and monthly total discharge from stations (a) 08NK002, (b) 08NK016 and (c) 08NK018 with trend line shown in red. Analysis is from 1970 to 2013. The breaks in the line represent periods of missing data.

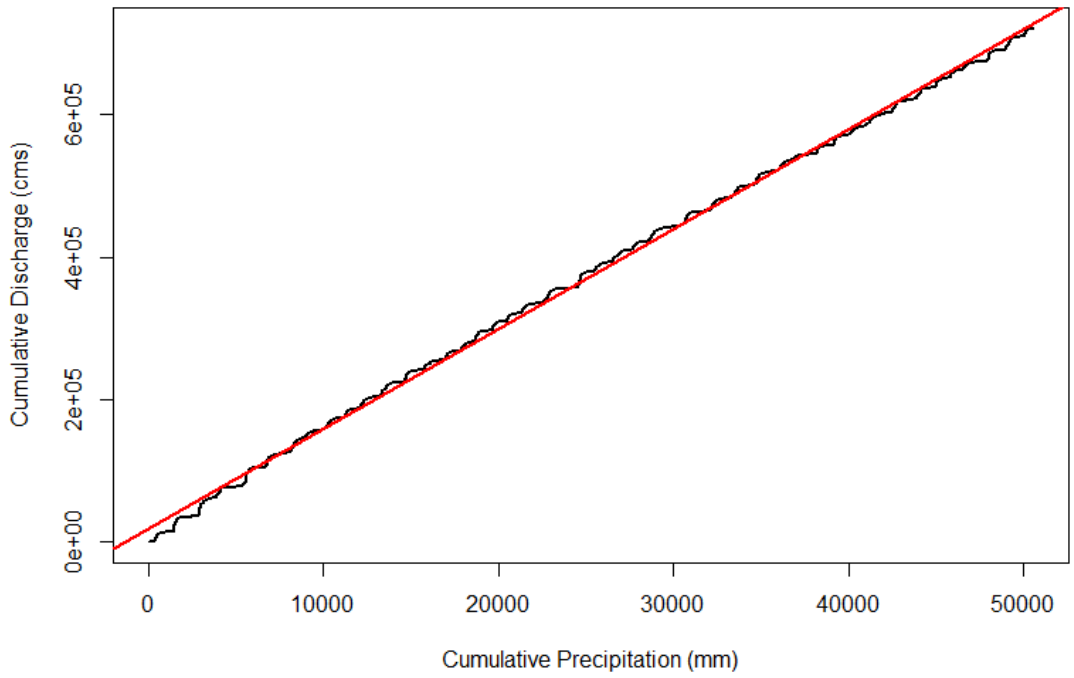

Figure F-3. Daily total precipitation from station 1152850 and daily mean discharge from station 08NK002 with trend line shown in red. Analysis is from 1970 to 2013.

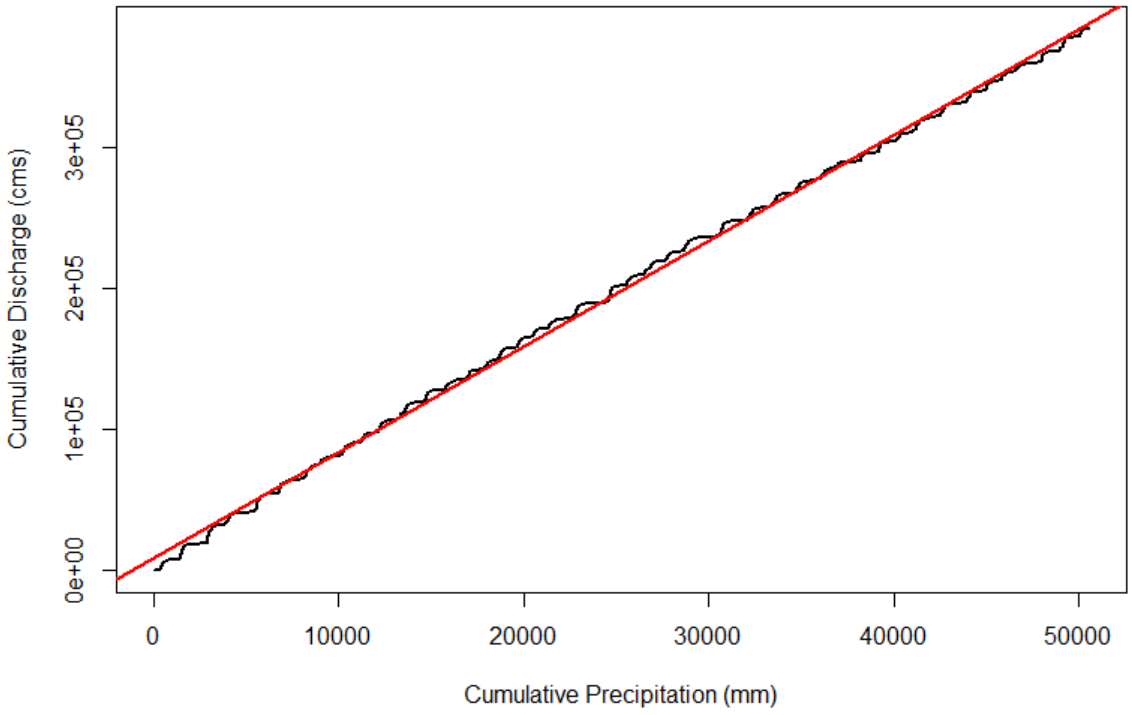

Figure F-4. Daily total precipitation from station 1152850 and daily mean discharge from station 08NK016 with trend line shown in red. Analysis is from 1970 to 2013.

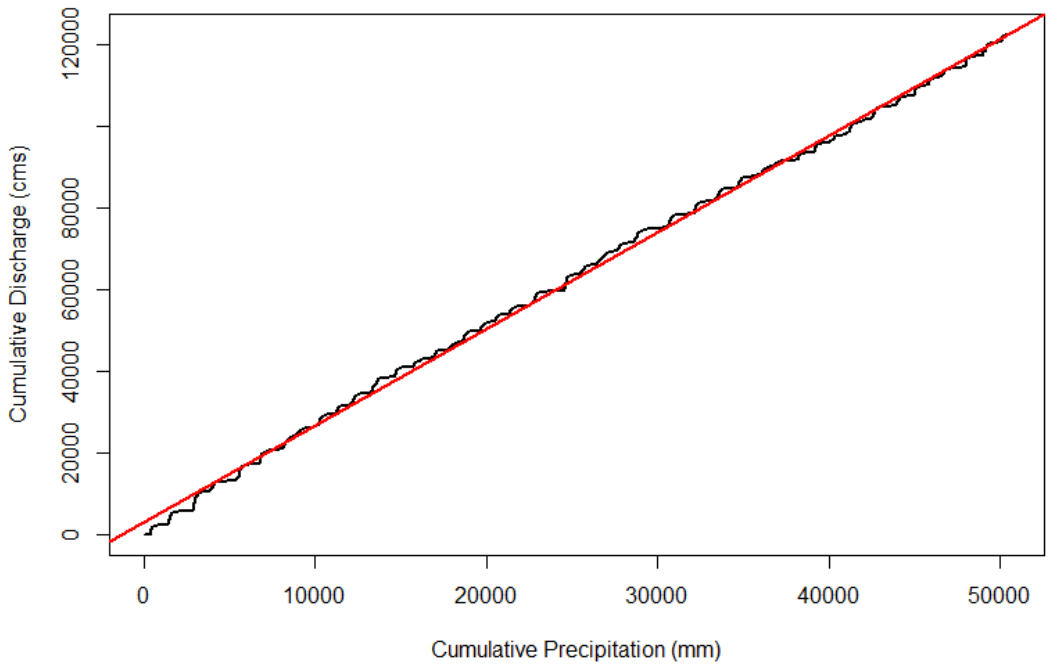

Figure F-5. Daily total precipitation from station 1152850 and daily mean discharge from station 08NK018 with trend line shown in red. Analysis is from 1970 to 2013.

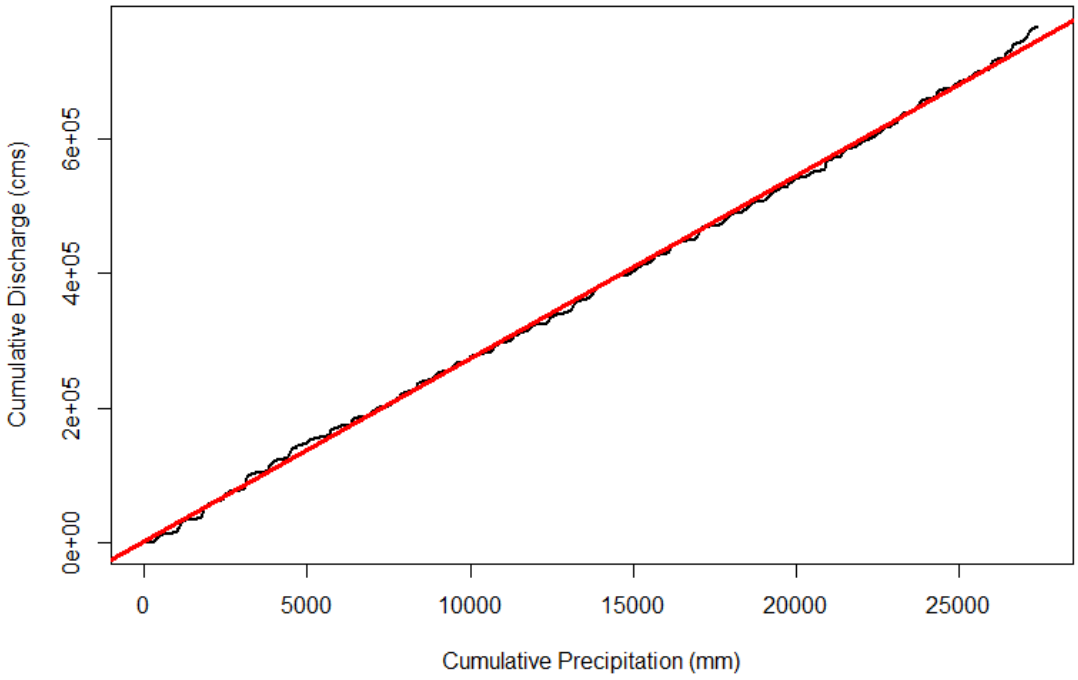

Figure F-6. Monthly total precipitation from ClimateBC (Fording) and monthly total discharge from station 08NK002 with trend line shown in red. Analysis is from 1970 to 2013.

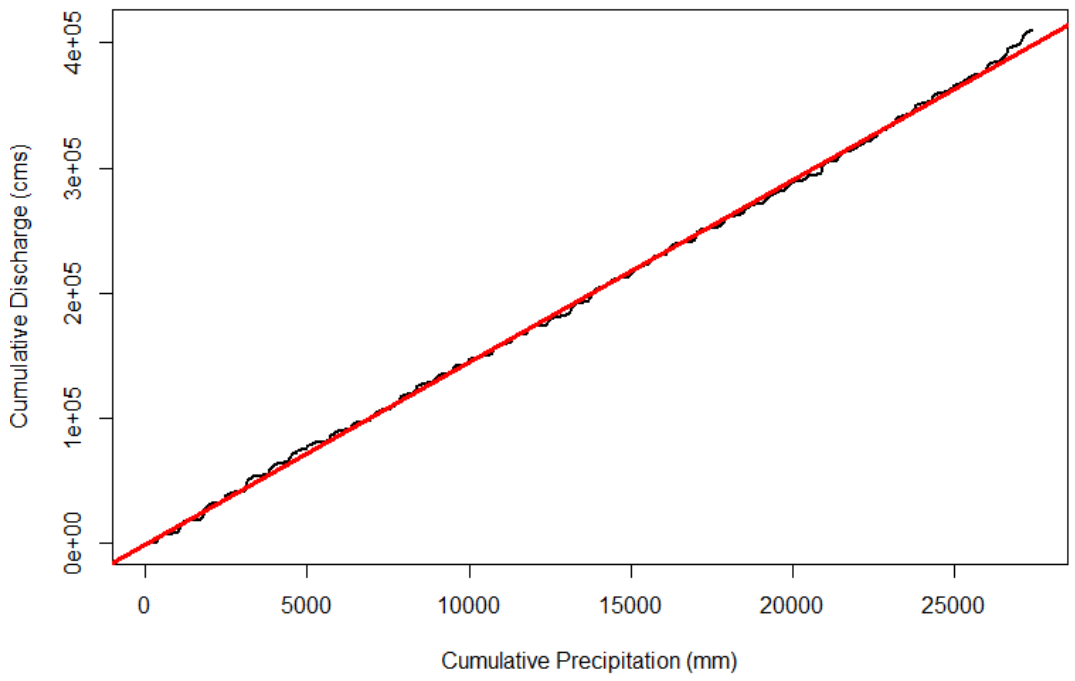

Figure F-7. Monthly total precipitation from ClimateBC (Fording) and monthly total discharge from station 08NK016 with trend line shown in red. Analysis is from 1970 to 2013.

G. SWAT Model

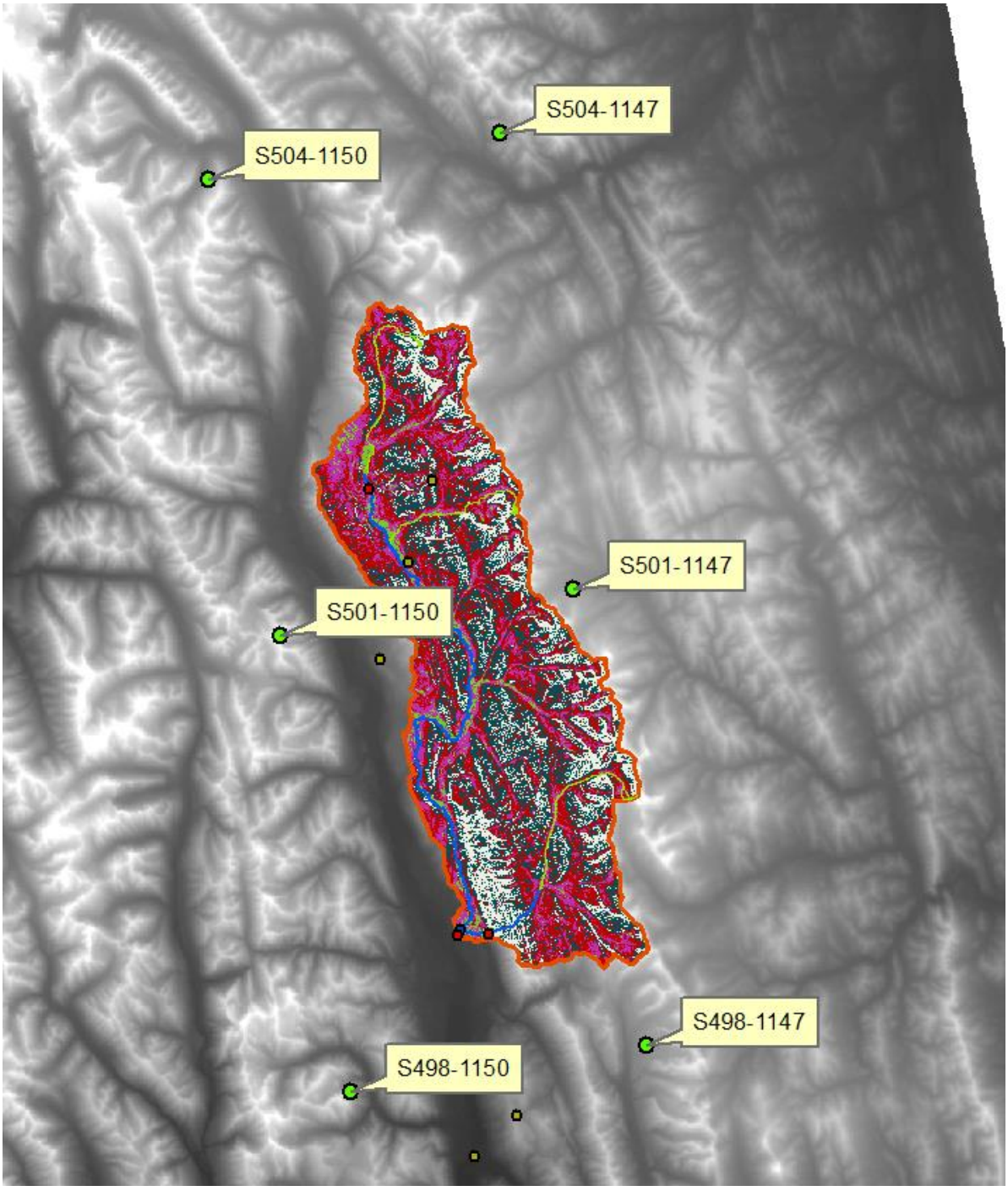

Figure G-1. Green dots showing the grid format for the Global Weather Data for the SWAT program. None of these locations are within the boundaries of the Fording River Watershed.

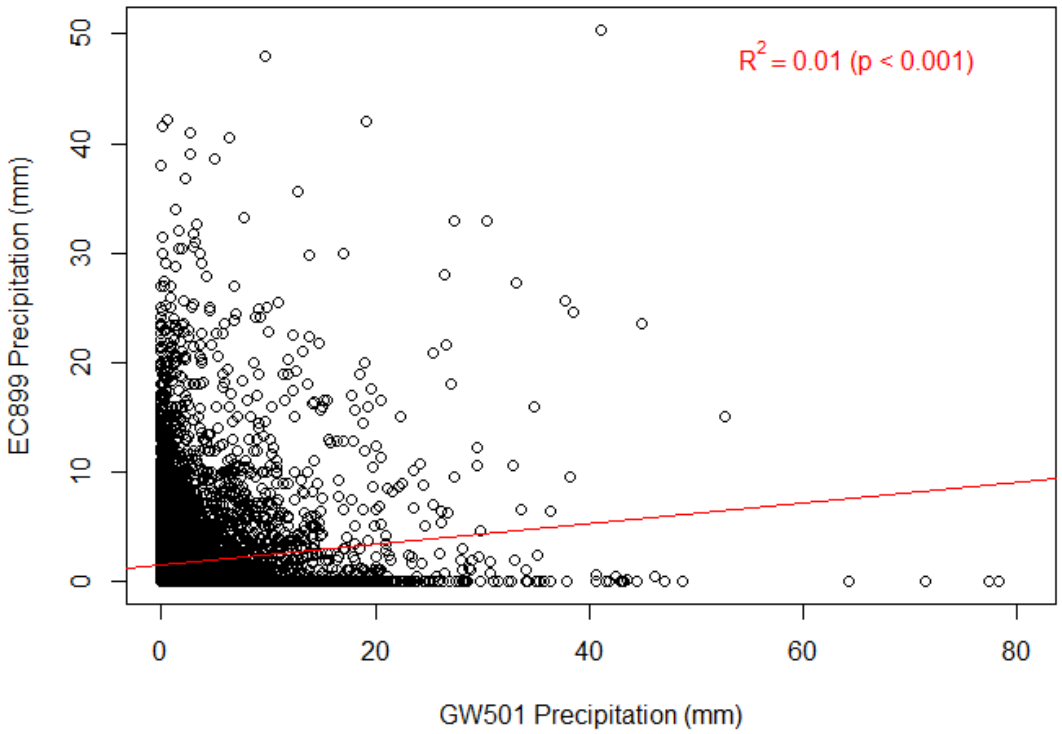

Figure G-2. Comparison of the precipitation from the observed climate station 1152899 and modelled precipitation at a nearby location using the Global Weather Model between 1970 and 2013.

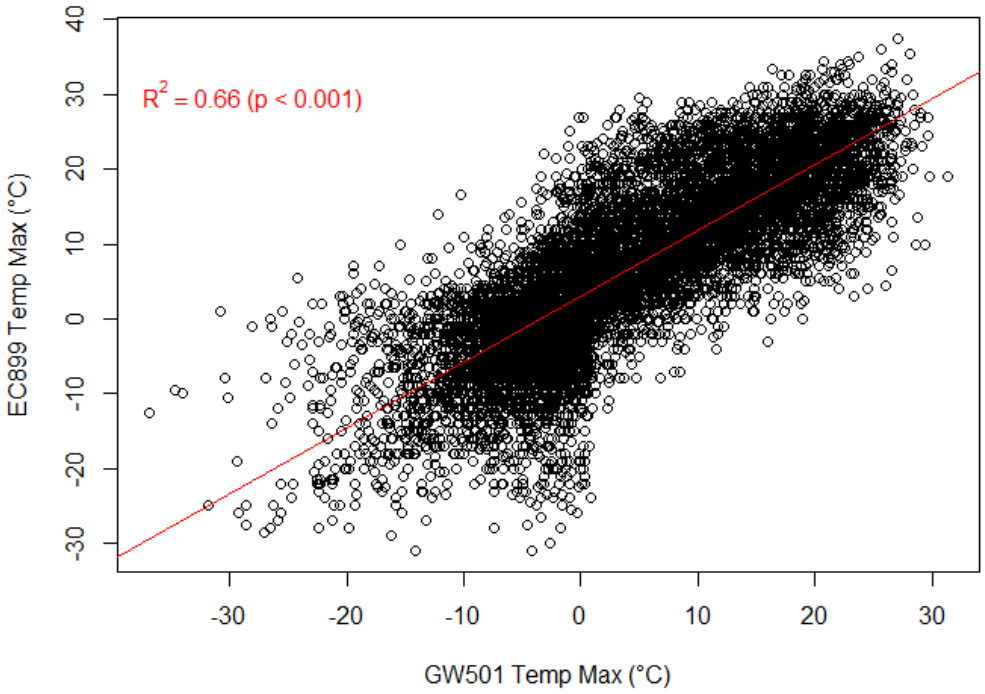

a.

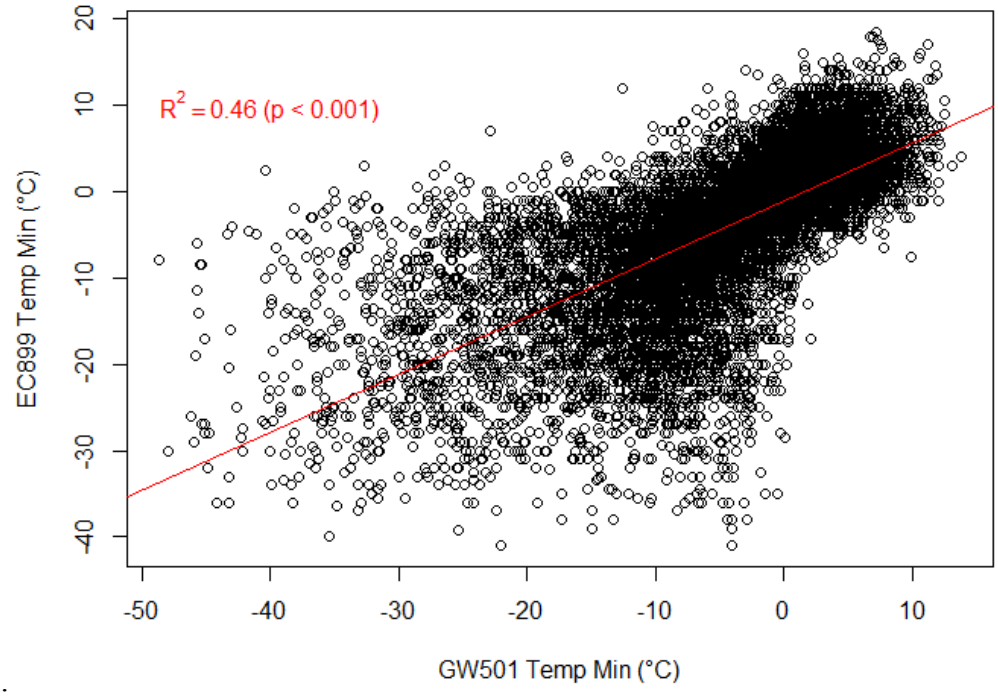

b.

Figure G-3. Comparison of the temperature from the observed climate station 1152899 and Global Weather Modelled output from point S501-1150. Note (a) maximum temperature comparison and (b) minimum temperature comparison from 1979 to 2013.